

**FUZZY CONTROLLED ENERGY STORAGE SYSTEM FOR LOW-
VOLTAGE DISTRIBUTION NETWORKS WITH PHOTOVOLTAIC
SYSTEMS**

WONG JIANHUI

DOCTOR OF PHILOSOPHY IN ENGINEERING

**FACULTY OF ENGINEERING AND SCIENCE
UNIVERSITI TUNKU ABDUL RAHMAN
DECEMBER 2014**

**FUZZY CONTROLLED ENERGY STORAGE SYSTEM FOR LOW-
VOLTAGE DISTRIBUTION NETWORKS WITH PHOTOVOLTAIC
SYSTEMS**

By

WONG JIANHUI

A thesis submitted to the Department of Electrical and Electronics Engineering,
Faculty of Engineering and Science,
Universiti Tunku Abdul Rahman,
in partial fulfillment of the requirements for the degree of
Doctor of Philosophy in Engineering
December 2014

ABSTRACT

FUZZY CONTROLLED ENERGY STORAGE SYSTEM FOR LOW-VOLTAGE DISTRIBUTION NETWORKS WITH PHOTOVOLTAIC SYSTEMS

Wong Jianhui

The development of renewable energy generation helps reduce the amount of CO₂ emission and the fossil fuel dependency. The amount of renewable energy sources is anticipated to increase on the low-voltage distribution networks for the improvement of energy security and reduction of greenhouse gas emission. Malaysia has a high solar irradiance level which is ideal for photovoltaic (PV) systems. The growth of the PV systems on the low-voltage distribution networks can create several technical issues such as voltage rise, voltage unbalance issues, unnecessary neutral current circulation and reverse power flow. Usually, these happen with little fluctuation. However, these issues tend to fluctuate seriously due to the low clear sky index in Malaysia. These issues become more severe when the installation and distribution of the single-phase renewable energy sources are rather arbitrary and not monitored by any utility companies. To ensure an effective operation of the distribution networks with PV systems, an energy storage system consisting of bi-directional inverters coupled with lead acid batteries is developed. A control algorithm utilising fuzzy logic is implemented to govern the operation of the energy storage system. The fuzzy controlled energy storage system is able to mitigate the fluctuating voltage rises and voltage unbalances on the networks by actively manipulating the flow of real power between the networks and the

batteries. The fuzzy logic control algorithm has a rapid response to address the voltage fluctuation due to the intermittent PV power output that fluctuating substantially. Furthermore, this work has the advantage to maximize the use of renewable energies without limiting the generation. The proposed fuzzy control algorithm is able to regulate the voltage and voltage unbalance factor by maintaining the generation and balance of the network. Hence, the proposed work can improve the power quality, increase stability, reliability and efficiency. As a result, the low-voltage distribution networks can operate within its tolerance without limiting the amount of renewable energy sources. To verify the effectiveness of this fuzzy control method, an experimental low-voltage distribution network with two units of 3.6 kW_p PV systems is set up. A number of case studies under various generation and demand scenarios are performed to evaluate the performance of the fuzzy controlled energy storage systems. The results show that the proposed fuzzy control algorithm can effectively govern the energy storage systems to reduce the voltage unbalance factor and maintain the voltage level of the low-voltage distribution networks with PV systems.

ACKNOWLEDGEMENTS

The author would like to extend her gratitude to the supervisor, Prof. Ir. Dr. Lim Yun Seng, and co-supervisor, Dr. Ezra Morris, for their support and encouragement throughout the research and preparation of the thesis. The author would also like to thank her colleagues, particularly Chua Kein Huat, Tang Jun Huat, Yong Wui Kian and Lim Khim Yan who have worked together for developing the experimental laboratory.

This work was funded in part by the Ministry of Energy, Green Technology and Water through the scheme of AAIBE (Akaun Amanah Industri Bekalan Elektrik). The development of PV panel, wind turbines, wind emulator and data acquisition system were carried out by the contractor.

APPROVAL SHEET

This dissertation/thesis entitled “**Fuzzy Controlled Energy Storage System for Low-Voltage Distribution Networks with Photovoltaic Systems**” was prepared by WONG JIANHUI and submitted as partial fulfillment of the requirements for the degree of Doctor of Philosophy in Engineering at Universiti Tunku Abdul Rahman.

Approved by:

(Prof. Ir. Dr. LIM YUN SENG)
Supervisor
Department of Electrical and Electronics Engineering
Faculty of Engineering and Science
Universiti Tunku Abdul Rahman

Date:

(Dr. Ezra Morris)
Co-supervisor
Department of Electrical and Electronics Engineering
Faculty of Engineering and Science
Universiti Tunku Abdul Rahman

Date:

FACULTY OF ENGINEERING AND SCIENCE

UNIVERSITI TUNKU ABDUL RAHMAN

Date:

SUBMISSION OF DISSERTATION

It is hereby certified that **WONG JIANHUI** (ID No: **12UED02199**) has completed this thesis entitled “**Fuzzy Controlled Energy Storage System on Low-Voltage Distribution Networks with Photovoltaic Systems**” under the supervision of Prof. Ir. Dr. Lim Yun Seng (Supervisor) from the Department of Electrical and Electronics Engineering, Faculty of Engineering and Science, and Dr. Ezra Morris (Co-Supervisor) from the Department of Electrical and Electronics Engineering, Faculty of Engineering and Science.

I understand that University will upload softcopy of my thesis in pdf format into UTAR Institutional Repository, which may be made accessible to UTAR community and public.

Yours truly,

(Wong Jianhui)

DECLARATION

I (WONG JIANHUI) hereby declare that the thesis is based on my original work except for quotations and citations which have been duly acknowledged. I also declare that it has not been previously or concurrently submitted for any other degree at UTAR or other institutions.

Name: Wong Jianhui

Date: December 2014

TABLE OF CONTENTS

	Page
ABSTRACT	ii
ACKNOWLEDGEMENT	v
APPROVAL SHEET	vii
SUBMISSION SHEET	viii
DECLARATION	ix
LIST OF TABLES	xvi
LIST OF FIGURES	xvii
LIST OF SYMBOL/ ABBREVIATIONS	xxv
1 INTRODUCTION	1
1.1 Research Background	1
1.2 Objectives	5
1.3 Research Methodology	6
1.4 Research Outline	9
1.5 Publications & Patent	11
2 LITERATURE REVIEW	13
2.1 Introduction	13
2.2 Regulatory Frameworks in Malaysia	14
2.3 Current Prospect of Renewable Energy in Malaysia	20
2.3.1 Photovoltaic (PV) system in Malaysia	22
2.3.2 Wind Energy	24
2.3.3 Small Hydro	26
2.4 Potential Power Quality Issues Caused by Photovoltaic System	27
2.4.1 Voltage Issues: Voltage Regulation and Voltage Rise	30
2.4.2 Voltage Unbalance	32
2.4.3 Voltage Flickers and Fluctuation	33

2.4.4	Reversed Power Flow	35
2.5	Existing Methods for Power Quality Improvement	36
2.5.1	Renewable Energy Curtailment	37
2.5.2	Flexible AC Transmission System (FACTS) Devices: Static Synchronous Compensator (STATCOM)	39
2.5.3	Energy Storage	40
2.5.4	On-Load Tap Changer (OLTC) Control	41
2.5.5	Load Management	42
2.6	Energy Storage System for Low-Voltage Distribution Networks	43
2.6.1	Revolution of Energy Storage System	44
2.6.2	Advantages and Limitations of Different Storage Technologies	45
2.7	Summary	46
3	ARCHITECTURE OF THE EXPERIMENTAL LOW-VOLTAGE DISTRIBUTION NETWORK	49
3.1	Introduction	49
3.2	Review of the Malaysian Low-Voltage Distribution Network Topology	49
3.3	Experimental Low-Voltage Distribution Network	51
3.3.1	Network Emulator	52
3.3.2	Photovoltaic System	54
3.3.3	Wind Turbine Emulator	55
3.3.4	Load Emulator	56
3.3.5	Data Acquisition System	58
3.3.6	Data Taker, DT82	60
3.3.7	Setting Up Data Acquisition Program Using LabVIEW™	63
3.4	Evaluation of Experimental Low-Voltage Distribution Network	65
3.5	Summary	71

4	IMPACT OF GRID-CONNECTED PV SYSTEMS ON THE LOW-VOLTAGE DISTRIBUTION NETWORK	73
4.1	Introduction	73
4.2	Characterization of Photovoltaic Power Output	75
4.3	Voltage Quality Issues	76
4.3.1	Characteristic of Voltage Rises	77
4.3.2	Characteristic of Voltage Unbalance	79
4.3.3	Quantification of Voltage Fluctuation and Flicker	81
4.4	Impacts of Voltage Issues on the low-voltage Distribution Networks	82
4.5	Discussion	84
5	DESIGN AND DEVELOPMENT OF THE ENERGY STORAGE SYSTEM	87
5.1	Introduction	87
5.2	Energy Storage System	90
5.2.1	Step 1: Setting Up the Bi-directional Inverter, namely Sunny Island 5048	91
5.2.2	Step 2: Connecting to the Battery Bank	94
5.2.3	Step 3: Configure the Sunny Island 5048	96
5.2.4	Step 4: Configure the Communication Module	97
5.2.5	Step 5: Communication Link with Supervisory Computer	97
5.3	Step 6: Stage I Simple Controller	102
5.4	Step 7: Stage II Simple Automated Control	105
5.4.1	Control Strategy	106
5.4.2	Operation of the System	108
5.4.3	Case Study I: Voltage Variation under Balanced and Unbalanced Load Condition without Controller	109

5.4.4	Case Study II: Simple Controlled Energy Storage System under Unbalance Load Variation	110
5.4.5	Case Study III: Simple Automated Controlled Energy Storage System under Intermittency PV Power Output	112
5.5	Step 8: Stage III Fuzzy Control	114
5.5.1	The Reasons for Using Fuzzy Control	115
5.5.2	Control Strategy of Fuzzy System	118
5.5.3	Fuzzy System in LabVIEW™	120
5.6	Final Step: Operation of the System	128
5.6.1	Case Study IV: Effects on Voltage Level during High Penetration from PV System without Fuzzy Controlled Energy Storage System	129
5.6.2	Case Study V: Fuzzy Controlled Energy Storage System under Unbalance Load Condition	130
5.6.3	Case Study VI: Fuzzy Control with Intermittency of PV Power Output	132
5.6.4	Case Study VII: Effect on Voltage using Fuzzy Controlled Energy Storage under Sudden Changes of Generation and Loading Conditions	134
5.7	Discussion	139
6	IMPLEMENTATION OF THE SYSTEM	142
6.1	Introduction	142
6.2	Conceptual Design	143
6.3	Strategy of Improving Voltage Quality	145
6.4	Operation of the System	150
6.4.1	Case Study I: Network Condition with High Penetration of PV	151

6.4.2	Case Study II: Performance of the ESS under Intermittent PV Power Output with Balance Load Condition	155
6.4.3	Case Study III: Effectiveness of the Fuzzy Controlled Energy Storage System with PV under Unbalance Load Condition	160
6.5	Discussion	163
7	EXPERIMENTAL VALIDATION OF FUZZY CONTROL ALGORITHM	166
7.1	Introduction	166
7.2	Experimental Setup	167
7.3	Energy Storage System	168
7.3.1	Step 1: Setting Up the Bi-directional Inverter	169
7.3.2	Step 2: Control and monitoring in LabVIEW	171
7.4	Step 3: Evaluation	175
7.4.1	Case Study I: Effects on Voltage Level under Load Variation without Energy Storage System	177
7.4.2	Case Study II: Effects on the Voltage Unbalance Factor under Load Variation with Fuzzy Controlled Energy Storage System	178
7.4.3	Case Study III: Performance of the Fuzzy Controlled Energy Storage System with Single-phase PV System under Balanced Load Condition	179
7.4.4	Case Study IV: Performance of the Fuzzy controlled energy storage system with Single-phase PV under Unbalanced Load Condition	182

7.4.5	Case Study V: Responses of the Fuzzy controlled energy storage system under Different Generation and Loading Condition	184
7.5	Discussion	186
8	CONCLUSION & FUTURE WORK	189
8.1	Conclusions	189
8.2	Limitation & Future Work	193
9	LIST OF REFERENCES	195

LIST OF TABLES

Table		Page
2.1	Feed-in tariff (FiT) rate for solar in Malaysia	18
2.2	Summary of energy storage technologies that market available for low-voltage distribution networks	46
2.3	Application of energy storage system for different levels	48
3.1	Technical specification of PV module	55
3.2	List of voltage and voltage unbalance tests under different scenarios	65
3.3	Load conditions for voltage & voltage unbalance test	66
4.1	Parameters of the underground cables	74
4.2	Voltage unbalance effects on a typical electric motor (Basso, 2008; Thomas, 2008)	83
5.1	YASDI initialisation file formed with three sections.	98
5.2	List of parameters readable in Sunny Island	100
5.3	Definition of the instruction from the output variable	123
7.1	Description of the command line written in the command prompt	172
7.2	List of parameters to be read/ write from/to the bi-directional inverter	174
7.3	Comparison between Sunny Island 5048 and Studer Xtender XTM 4000-48	187

LIST OF FIGURES

Figure		Page
1.1	Global temperature anomaly from year 1880 to 2013 (NASA GISS, 2014)	2
1.2	Conventional structure of the Malaysian electrical power system	3
1.3	Structure of the electrical power system with the deployment of renewable energy sources on the Malaysian low-voltage distribution network	3
1.4	Flow chart of the methodology	9
2.1	Timeline of the initiative taken by the Malaysian government	16
2.2	Electricity consumption and renewable energy generation in Malaysia from year 1971 – 2012 (The World Bank Data, 2014)	17
2.3	Feed-in tariff prices and retail electricity prices for different countries	20
2.4	Cumulative installed capacity of commissioned renewable energy sources under the feed-in tariff as of May 2014 (SEDA, 2014a)	21
2.5	Power generations using PV system	22
2.6	The annual average solar radiation on various regions in Malaysia	23
2.7	Global module price index, annual installed and cumulative installed grid connected PV capacity in Malaysia (SEDA, 2014a; NREL and LBNL, 2014)	24
2.8	Wind generation	25
2.9	Wind speed study location in Malaysia	26
2.10	Average wind speeds at different locations in Malaysia (Chiang et al., 2003)	26
2.11	Major sources of Carbon Dioxide (CO ₂) emissions by sectors in Malaysia (GreenTech Malaysia, 2014)	28

3.1	Typical low-voltage distribution network	50
3.2	Network topology of the laboratory-scaled experimental low-voltage distribution network	51
3.3	Test lab of the experimental low-voltage distribution network with energy storage system	52
3.4	Layout of the grid emulator	53
3.5	Grid emulator installed in the laboratory with (a) synchronous generator coupled with induction machine driven by (b) variable speed drive	53
3.6	Three-phase voltage profiles for (a) low-voltage grid emulator and (b) low-voltage distribution networks respectively	53
3.7	PV modules mounted on a 3.3 metres height metal structure at the University open space car park area. (a) Top view of the PV panels (b) Bottom view of the PV panels.	55
3.8	Topology of a wind turbine emulation system	56
3.9	Block diagram of the load emulator	56
3.10	(a) Actual load consumption in the University tutorial block and (b) load emulation pattern	57
3.11	Load emulators installed in the laboratory	57
3.12	Data acquisition system at the measuring nodes	59
3.13	Components for the data acquisition system	59
3.14	Data acquisition system flow chart	60
3.15	Web based application to program the data logger	61
3.16	Frame structure of the Modbus message	62
3.17	Block diagram of reading data from Data Taker via LabVIEW™	64
3.18	Snapshot of the data acquisition front panel in LabVIEW™	65

3.19	Voltage test I, II and III with an increasing load at (a) phase A (b) phase B and (c) phase C respectively	67
3.20	Voltage test IV and V with (a) three phase balanced load condition and (b) unbalance load condition	68
3.21	(a), (b) and (c) Voltage unbalance factor under loading condition I, II and III respectively	69
3.22	(a) and (b) Voltage unbalance factor under loading conditions IV and V respectively	70
3.23	(a) PV power, load and voltage unbalance factor (b) Voltage and voltage unbalance factor of the load and generation power test	71
4.1	Topology of a three-phase low-voltage distribution network integrated with PV systems	74
4.2	Frequency occurrence of the global completely clear sky index	75
4.3	PV power outputs of the three random days as compared to a clear sky reference	76
4.4	Frequency of the occurrence of voltage magnitude at the PCC	78
4.5	Daily PV power output in kWh and probability counts for the voltage rise from 6th-24th March 2013	79
4.6	Relationship between the voltage unbalance factor and the PV power output on the 15th March 2013	80
4.7	Probability counts of the voltage unbalance factor with respect to different time period	81
4.8	Short-term flicker and long-term flicker indices at the point of connection with the PV systems	82
5.1	Flow chart of the energy storage system development	90
5.2	Setup of the energy storage system	91
5.3	Connection layout of the Sunny Island bi-directional inverter	92

5.4	Configuration of single-phase energy storage system with (a) one master unit and (b) one master and one slave unit	93
5.5	Configuration of three single-phase energy storage systems	94
5.6	Configuration of the master and slave units via Com Sync In and Com Sync Out port	94
5.7	Three sets of valve-regulated lead acid batteries install (a) inside the laboratory and (b) outside the laboratory	95
5.8	Depth of discharge for solar.bloc 135 based on C10	95
5.9	Configuration for communication module RS485/USB converter	97
5.10	Block diagram of the communication system flow between the supervisory computer and the energy storage system	98
5.11	LabVIEW™ block diagram for writing real and reactive power of energy storage system	101
5.12	LabVIEW™ block diagram reading from energy storage system and data are written to text file	101
5.13	Front panel of LabVIEW™ with grid and energy storage monitoring system, and current controller	102
5.14	Response of the energy storage system (a) in relation to the charging current control, (b) network voltage unbalance factor and (c) three-phase voltage	104
5.15	Response of the energy storage system in relation to (a) the discharging current control, (b) network voltage unbalance factor and (c) the three-phase voltage profile	105
5.16	Flow chart of the simple control algorithm	107
5.17	Screenshot of the front panel for the controller in LabVIEW™	107

5.18	(a) Voltage unbalance factor (b) voltage profile at node 1 of the experimental network with balance load condition	109
5.19	(a) Voltage unbalance factor (b) voltage profile at node 1 of the experimental network with unbalance load condition	110
5.20	Variation of the network voltage and voltage unbalance factor under the same load condition	111
5.21	Variation of the voltage unbalance factor and load profile on the experimental network	112
5.22	Variation of the network voltage and PV power output on the experimental network	113
5.23	Variation of voltage unbalance factor on PCC	114
5.24	Flow chart of the fuzzy logic control algorithm	120
5.25	Fuzzy logic control algorithm	121
5.26	Fuzzy logic input membership for voltage change (ΔV)	122
5.27	Fuzzy logic input membership for the battery state of charge (SoC)	122
5.28	Fuzzy output membership of instruction (ΔI) to bi-directional inverter	124
5.29	Screenshot of fuzzy system in LabVIEW™	125
5.30	Block diagram of fuzzy system in LabVIEW™	125
5.31	LabVIEW™ front panel after the second implementation	126
5.32	Example of fuzzification and defuzzification in the proposed fuzzy control method	127
5.33	PV power output, the load demand, voltage and voltage unbalance factor at the PCC of the experimental network	130
5.34	Voltage unbalance factor, load profile and the response of fuzzy controlled energy storage system.	131

5.35	Three-phase voltage profile and voltage unbalance factor of the experimental network	132
5.36	Voltage magnitude with intermittent PV power output and load consumption	133
5.37	Voltage unbalance factor with intermittent PV power output	133
5.38	Voltage at phase A, PV power output, Sunny Island 5048 power output and load demand of the experimental case study VII	135
5.39	Voltage magnitude at phase A with increasing PV power output	136
5.40	(a) Change of the instruction and battery <i>SoC</i> (b) voltage magnitude of the experimental case study	138
5.41	Voltage unbalance factor of the experimental network	139
6.1	Setup of the proposed three single-phase fuzzy controlled energy storage systems	144
6.2	Data acquisition between supervisory computer, three single-phase energy storage systems and Data Taker	145
6.3	Control hierarchy of the three-phase energy storage system	149
6.4	Voltage unbalance factor, PV power output and load demand at the PCC of the experimental network	152
6.5	Three-phase voltage magnitudes and the corresponding voltage unbalance factor of the experiment	153
6.6	Voltage unbalance factor, two PV outputs and load demand at the PCC of the experimental network	154
6.7	Three-phase voltage magnitudes and the corresponding voltage unbalance factor of the experiment case study	155

6.8	PV power output, three-phase loads, power outputs of the fuzzy controlled energy storage systems and the corresponding voltage unbalance factor of the experimental case study	157
6.9	Three-phase voltage magnitude and the corresponding voltage unbalance factor of the experimental case study	158
6.10	Power outputs of the two PV systems, fuzzy controlled energy storage systems and the corresponding voltage unbalance factor of the experimental case study	159
6.11	Three-phase voltage magnitude and the corresponding voltage unbalance factor of the experimental case study	160
6.12	Load profiles, PV outputs and the corresponding voltage unbalance factor of the experimental case study	161
6.13	Change of the power output for three single-phase fuzzy controlled energy storage systems and battery SoC of the experimental case study	162
6.14	Three-phase voltage magnitude at the PCC and the corresponding voltage unbalance factor of the experimental case study	163
7.1	Experimental setup	168
7.2	Setup of the energy storage system consists of Studer Xtender XTM 4000-48, remote control RCC-02, communication module Xcom 232i, supervisory computer and battery bank	169
7.3	Layout of the bi-directional inverter	170
7.4	Block diagram of the system control flow	172
7.5	Display of the command prompt executed from scom.exe	173
7.6	Reading parameters in LabVIEW™	174
7.7	Writing parameters in LabVIEW™	175

7.8	(a) Voltage variation and (b) voltage unbalance factor of the experimental low-voltage distribution network under the condition of increasing load at phase A	177
7.9	(a) Voltage variation and (b) voltage unbalance factor of the experimental low-voltage distribution network with and without fuzzy controlled energy storage system	179
7.10	Load, PV power output, performance of the fuzzy controlled energy storage system and network voltage unbalance of the experimental case study	180
7.11	Phase to neutral voltage at Phase A, PV power output and network voltage unbalance factor of the experimental case study	180
7.12	Total PV power output, response of the fuzzy controlled energy storage system, three-phase load demand and voltage unbalance factor of the experimental network	183
7.13	Voltage at phase A and total PV power output of the experimental network	183
7.14	PV power output, load demand at phase A, response of the fuzzy controlled energy storage system and voltage unbalance factor of the experimental network	185
7.15	PV power output, load demand at phase A and voltage at phase A of the experimental network	186

LIST OF SYMBOLS/ ABBREVIATIONS

CO ₂	Carbon dioxide
DSM	Demand side management
ESS	Energy storage system
FACTS	Flexible alternative current transmission system
FiT	Feed-in tariff
GBI	Green building index
GHG	Greenhouse gaseous
LV	Low voltage
MS IEC	Malaysian Standard International electro-technical commission
OLTC	On-load tap changer
PCC	Point of common coupling
PSCAD	Power system computer aided design
PV	Photovoltaic system
RE	Renewable energy
SEDA	Sustainable energy development authority
SoC	State of charge
SREP	Small renewable energy power program
SSEZ	Small scale energy zone
STATCOM	Static synchronous compensator
SVR	Static VAr compensator
TCP/ IP	Transmission control protocol/ Internet protocol
TNB	Tenaga Nasional Berhad
VRLA	Valve regulated lead acid

VI	Virtual instrument file format
VSD	Variable speed drive
VSI	Voltage source inverter
VUF	Voltage unbalance factor

CHAPTER 1

INTRODUCTION

1.1 Research Background

Today's climate change, increase in fossil fuel consumption and global warming issues have led to the emergence of sustainable technologies. The Intergovernmental Panel on Climate Change (IPCC) mentioned that the root cause of the climate change is the increase in greenhouse gas (GHG) emissions produced by human activities. Figure 1.1 shows the global temperature anomaly plotted by National Aeronautics and Space Administration, Goddard Institute for Space Studies (NASA/ GISS). It can be observed that the effect of global warming was started earlier in the 1970s where the temperature anomaly was recorded to be positive.

Various measures have been identified to promote the awareness to reduce GHG in the country. The utilisation of renewable energy sources is recognised as an alternative source of power to address the issues of environment and energy. The Malaysian government has set a target of reducing the GHG emission by 40% by the year 2020 as compared to 2005 levels. In order to meet the target, the Malaysian government has offered various remunerative

packages including feed-in tariff, tax exemptions for green technologies, incentives and subsidies to encourage the utilisation of renewable energies.

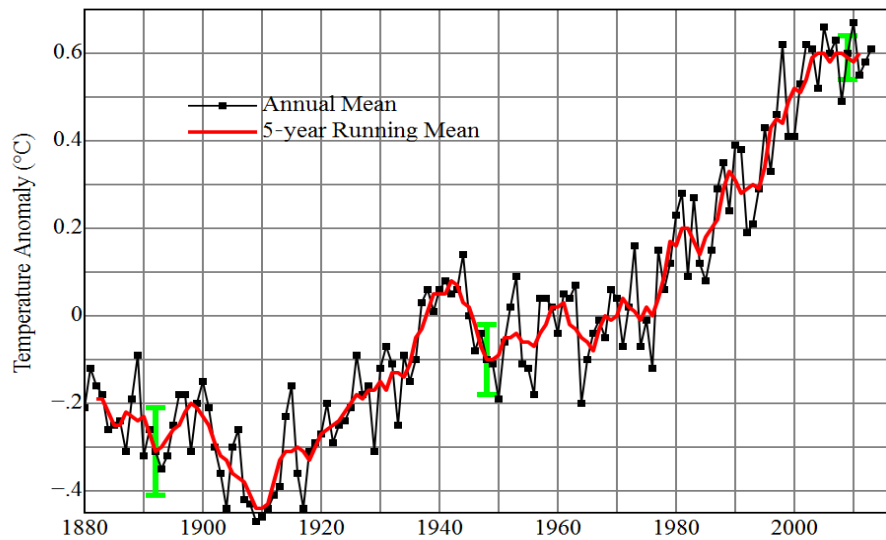


Figure 1.1 Global temperature anomaly from year 1880 to 2013 (NASA GISS, 2014)

Among all the renewable energy sources available in Malaysia, the outlook for solar energy has been positive and it is expected to increase significantly. The cumulative installed capacity from year 2012 to 2013 has risen up by 65 MW. However, one of the challenges in Malaysia is that most of the photovoltaic (PV) system installations are customer-driven and are non-centrally planned. Consequently, a large amount of grid-connected PV systems can cause severe power quality issues such as voltage rise, voltage unbalance, unnecessary neutral current circulation and reverse power flow. Figure 1.2 shows the conventional electrical power system. It is designed for unidirectional power flow from the generating units to the lower voltage levels at the customer's end. However, a large amount of renewable energy sources connected to the

distribution networks may cause reverse power flow within the electrical network as shown in Figure 1.3.

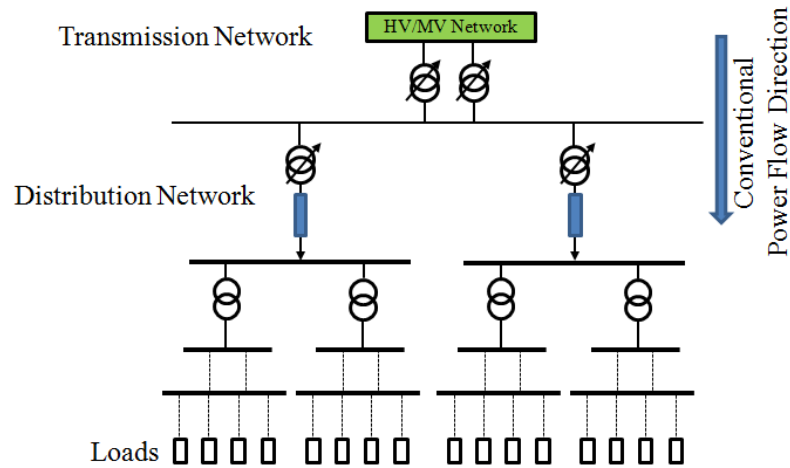


Figure 1.2 Conventional structure of the Malaysian electrical power system

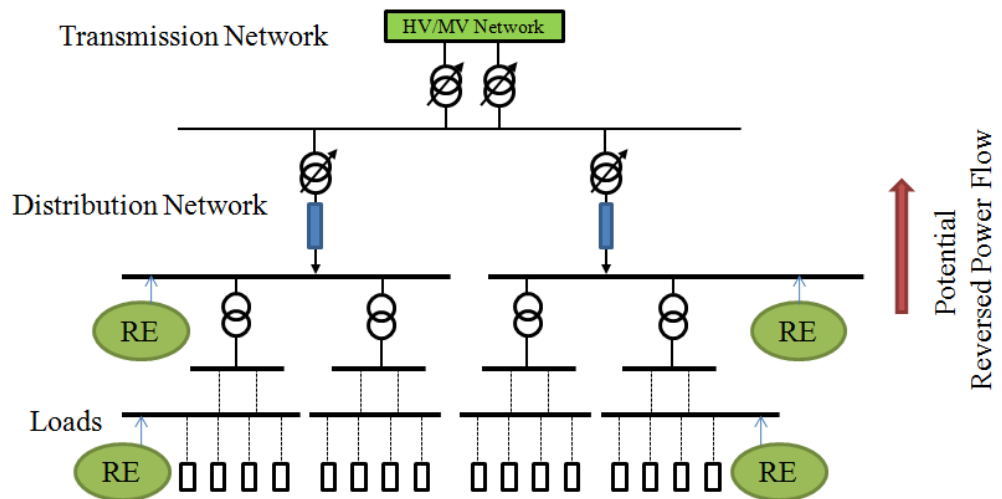


Figure 1.3 Structure of the electrical power system with the deployment of renewable energy sources on the Malaysian low-voltage distribution network

Among all the technical issues, voltage unbalance can be the most serious issue in Malaysia. This is due to fact that the installation and distribution of the single-phase renewable energy sources are rather arbitrary and not monitored by utility companies (Wong et al., 2011). Furthermore, the utility companies allow the single-phase customers to install the single-phase PV

systems freely up to 12 kW_p, whereas three-phase customers can install three-phase PV systems freely up to 425 kW_p at 11 kV (Abu et al., 2013).

A research has shown that the voltage unbalance factor can rise above the tolerance of 2.0% if the single-phase PV capacity installed on the low-voltage distribution network is greater than 12 kW (Wong et al., 2011). Several research works have proposed to use energy storage systems to accommodate a large amount of wind energy and mitigate voltage unbalance (Atwa and El-Saadany, 2010; Chen et al., 2011; Chua et al., 2012). So far, this approach is an effective means of mitigating any voltage issues on the distribution networks without curtailing any of the renewable energy. However, most of the existing energy storage systems are not designed to handle the voltage rises and voltage unbalances that fluctuate very rapidly throughout the day on the distribution networks with a large number of single-phase PV systems.

The fluctuation of voltage rises and voltage unbalances is caused by the large number of passing clouds over Malaysia. An effective control strategy is needed for the energy storage systems to mitigate the fluctuating voltage rises and voltage unbalances on the distribution networks with the PV systems. This research project is proposed to develop a fuzzy controlled energy storage system for mitigating voltage rise and voltage unbalance on the distribution network caused by intermittent PV power outputs. The traditional control methods are used to solve steady state voltage rises and voltage unbalances. The fuzzy control method is mainly used to deal with fluctuating voltage rises and voltage unbalances which happen predominantly in Southeast Asia or

other regions with cloudy skies. Therefore, this method will be the most appropriate choice when dealing with dynamic voltage rises and voltage unbalances. The fuzzy control provides the necessary pre-emptive action before the voltage excursion becomes too significant. This is to ensure that the voltage level and voltage unbalances are restored before it becomes severe. As a result, the voltage magnitude can be maintained well within the required tolerance under the high intermittency of PV systems.

1.2 Objectives

The objectives of this research work are as follows:-

- I. To design and develop a laboratory scale low-voltage distribution network with renewable energy sources.
- II. To evaluate technical impacts caused by the intermittent renewable energy and quantify the power quality issues on a low-voltage distribution network.
- III. To design a suitable control approach for an energy storage system on the low-voltage distribution network integrated with PV systems.
- IV. To evaluate the performance of the proposed energy storage system in mitigating voltage rises and voltage unbalance caused by renewable energy sources.

1.3 Research Methodology

This research aims to develop a suitable control algorithm for the energy storage system to mitigate voltage issues caused by the large deployment of PV systems on the distribution networks. The study was carried out using experimental approach. Figure 1.4 shows the flow chart of the methodology.

The research methodology is divided into 8 steps as follows:-

Step 1: Literature review

Various initiatives have been implemented by the Malaysian government to encourage the utilisation of renewable energy sources in the country. A brief introduction on these initiatives is given. Literature review is carried out to investigate the potential grid connected renewable energy sources and the deployment impacts on the low-voltage distribution networks. A discussion on the existing methods to overcome these technical issues caused by the integration of renewable energy sources will be done. A sensible solution is determined based on the literature review.

Step 2: Network design

The characteristics of the Malaysian distribution network are studied. These electrical characteristics are used to develop an experimental network emulator in the University laboratory. The network prototype is equipped with PV systems, load emulator and data acquisition system.

Step 3: Impact studies

This step is implemented to investigate and identify the potential voltage issues caused by single-phase PV systems in the University premises on the Malaysian distribution network.

Step 4: Energy storage system with simple control method

Energy storage system is one of the sensible solutions to overcome the voltage issues caused by PV systems. The performance of the energy storage system can be optimized if it is equipped with an appropriate control strategy. A simple control method is developed to manipulate the power flow of the energy storage system for voltage quality improvement.

Step 5: Single-phase energy storage system with fuzzy control

The nature of the PV power output is always intermittent. A fuzzy control algorithm is further implemented from *step 4* to address the rapid change of the voltage caused by PV power output.

Step 6: Performance assessment

Several case studies with various scenarios under different generations and loading conditions are performed to evaluate the performance of the single-phase energy storage system with fuzzy control to mitigate voltage issues particularly voltage rise and voltage unbalance due to PV systems.

Step 7: Controller Implementation

Most PV systems are single-phase and the installations are distributed non-uniformly on the Malaysian low-voltage distribution networks. Three single-phase energy storage systems are further implemented from *step 5* and they are coordinated and controlled by an improved control using fuzzy logic control and Park's transformation.

Step 8: Performance Assessment

Several scenarios with different generation and loading conditions are carried out to assess the performance of the improved version of the fuzzy controlled energy storage system.

Final Solution:

Using the above methodology, a fuzzy controlled energy storage system is proposed as a solution to improve voltage stability, mitigate voltage rise and voltage unbalance caused by intermittent PV power output.

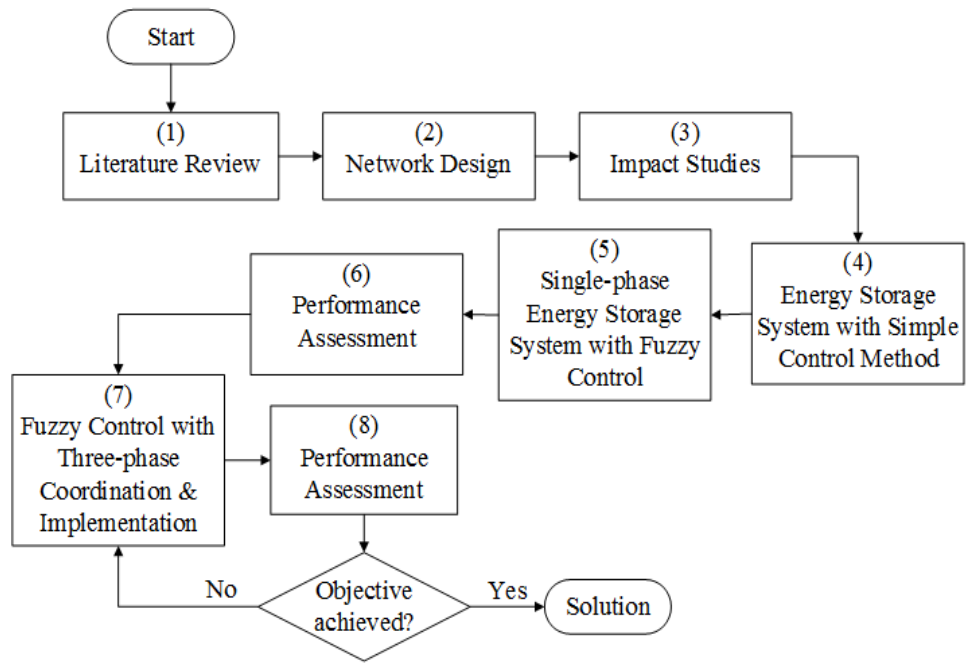


Figure 1.4 Flow chart of the methodology

1.4 Research Outline

The structure of the thesis is outlined in the following manner:-

Chapter 2 of this thesis summarises the literature review on the Malaysian regulatory framework for renewable energy. The potential grid-connected renewable energy sources are briefly discussed. It is followed by the literature review on the impacts of large deployment of renewable energy sources on the distribution networks and the existing methods to overcome these issues.

Chapter 3 illustrates the formation of the experimental low-voltage distribution network. The design and development of the electrical system,

emulation system, renewable energy sources and the data acquisition are outline clearly.

Chapter 4 presents the investigation of voltage impacts caused by the integration of PV system at the University premises on the distribution network. This chapter presents the characteristics of the PV power output and the impact of the voltage quality issues on the Malaysian low-voltage distribution network.

Chapter 5 describes the design and development of the single-phase energy storage system. The design objectives for the system are initially presented. It is followed by the description of the fuzzy control algorithm that is incorporated into the single-phase energy storage system. This chapter also presents the passive operation of the energy storage system with renewable energy sources.

Chapter 6 presents the implementation of the three single-phase energy storage systems. This chapter elucidates the approach to coordinate the three single-phase energy storage systems using the improved control with fuzzy logic control and Park's transformation. Several scenarios under different generation and loading conditions were considered to investigate the effectiveness of the proposed solution to reduce the voltage unbalance factor and restore the voltage level within the tolerance limit on the low-voltage distribution network.

Chapter 7 illustrates the validation work for the fuzzy control algorithm. The formation of single-phase energy storage system utilising a different brand of the bi-directional inverter is outlined in the chapter.

Chapter 8 draws a conclusion by summarising the key findings of the research and the potential future work that can be done.

1.5 Publications & Patent

Based on the research findings, a patent is filed and several papers have been published in peer review journals and international conferences listed as follows:-

No.	Title	Patent/ Journal/ Conference	Impact Factor
1	<i>Fuzzy control method on bi-directional inverter with energy storage for distribution networks with renewable energy</i>	Patent No.: PI2013002517	N/A
2	<i>Distributed energy storage systems with improved fuzzy controller for mitigating voltage unbalance on low-voltage network</i> http://dx.doi.org/10.1061/(ASCE)EY.1943-7897.0000260 (Published)	Journal: ASCE Journal of Energy Engineering	Thomps on ISI: 1.104
3	<i>Novel fuzzy controlled energy storage for low-voltage distribution networks with photovoltaic systems under highly cloudy condition</i> http://dx.doi.org/10.1061/(ASCE)EY.1943-7897.0000178 (Published)	Journal: ASCE Journal of Energy Engineering	Thomps on ISI: 1.104

4	<p><i>Grid-connected photovoltaic system in Malaysia: A review on voltage issues</i> http://dx.doi.org/10.1016/j.rser.2013.08.08 Z (Published)</p>	<p>Journal: Science Direct Renewable & Sustainable Energy Reviews</p>	<p>Thomps on ISI: 5.510</p>
5	<p><i>Self-intelligent active management system for electrical distribution networks with photovoltaic systems</i> http://dx.doi.org/10.1049/cp.2013.1743 (Published)</p>	<p>Conference: IET Renewable Power Generation Conference 2013</p>	<p>N/A</p>
6	<p><i>Self-intelligent active management system for electrical distribution networks with ocean renewable energy sources</i> (Published)</p>	<p>Book chapter: Ocean Renewable Energy: The New Frontier in Malaysia, published by UTM</p>	<p>N/A</p>
7	<p><i>Impacts of centrally and non-centrally planned distributed generation on low voltage distribution network</i> http://dx.doi.org/10.12720/sgce.1.1.60-66 (Published)</p>	<p>Journal: International Journal of Smart Grid and Clean Energy</p>	<p>Inspec</p>
8	<p><i>Energy storage with fuzzy controller for power quality improvement on distribution network with renewable energy</i> (Published)</p>	<p>Conference: 2nd Edition of The World Sustainable Energy Forum 2014 (EnerSol)</p>	<p>N/A</p>

CHAPTER 2

LITERATURE REVIEW

2.1 Introduction

This research seeks to investigate the future challenges associated with the integration of renewable energy sources on the low-voltage Malaysian distribution networks. In order to proceed, a review related to the current prospect of renewable energy sources in Malaysia, particularly PV system is discussed. PV systems are very promising in Malaysia due to its abundant solar irradiance. As mentioned in chapter 1, the Malaysian government has committed to reduce 40% of the GHG emission in the country by year 2020 with respect to the level in year 2005. In order to achieve a low-carbon margin, various efforts and initiatives have been taken in the past 10 years by the Malaysian government.

Renewable energy has been adopted globally as one of the alternative solutions to overcome the energy and environment issues. However, the existing distribution networks are designed to operate without the consideration of large deployment of renewable energy sources. In a conventional power system, the power flow is unidirectional; a large amount

of grid connected renewable energy has the potential to change the power flow to bi-directional, creating a number of technical issues such as voltage rise, voltage unbalance, reverse power flow. These issues can cause equipment interruption, poor network efficiency and poor supply reliability. The objective of this chapter is to investigate the consequences and integration issues associated with the key constraints evaluated by the developed countries. An overview of the existing strategies to resolve these technical issues is also presented. Energy storage is seen as one of the viable solutions to accommodate the power quality issues associated with the integration of renewable energy sources and therefore a review of these technologies is also presented in the chapter. Finally, a conclusion is drawn from this review with regard to the investigation of potential solution in mitigating power quality issues caused by renewable energy sources.

2.2 Regulatory Frameworks in Malaysia

The developed countries have taken various initiatives to ensure the success of renewable energies implementation. Energy policies are conducted to provide stable regulatory frameworks for renewable energy producers. Renewable energies are recognized worldwide as clean and environmental friendly alternative source of power. The main strategies taken by the developed countries include feed-in tariff and eliminate or reduce fossil fuel subsidies. The European government also takes initiatives to encourage the installation of renewable energy sources by introducing tax exemption, incentives, loan,

rebates and subsidies (Klessmann et al., 2011; Şekercioğlu and Yılmaz, 2012; Fouquet, 2013; Mondol and Koumpetsos, 2013).

The regulatory framework enacted by the developed countries may not be suitable for developing countries. In Malaysia, various strategies and key policies are developed by the government to achieve the nation's policy in which to mitigate the issues of security, energy efficiency and environmental impact for the next 30 years (Muhammad-Sukki et al., 2012). The main Malaysian government ministries and agencies to overrun the energy efficiency improvement are the Energy Unit of Economic Planning Unit (EPU) of the Prime Minister's Office, the Ministry of Energy, Green Technology, and Water (Kettha), Energy Commission (EC) and the GreenTech Malaysia (GTM). Recently, the Malaysian government has aggressively put in enormous initiatives and efforts to promote renewable energy (RE) utilization.

The timeline in chronological order for the above mentioned initiatives is shown in Figure 2.1. The government has introduced a comprehensive policy in implementing renewable energy. Renewable energy was first introduced in the country through Fifth Fuel Policy in year 2001. In the same time, Small Renewable Energy Power (SREP) program was launched to encourage small power generation using renewable energies. These policies and projects are implemented under the 8th and 9th Malaysia Plan where the government planned to achieve a total capacity of 500 MW grid connected renewable

energies. However, the implementation of this plan received sluggish response.

In 2006, the National Bio-Fuel Policy was launched to support the Fifth Fuel Policy which was also aimed at reducing the dependency of fossil fuel in Malaysia. Later, the National Green Technology Policy 2009 was launched to promote green technology and sustainable development in power generation. It was then followed by the implementation of National Renewable Energy Policy 2010 (NREP 2010). The vision of NREP 2010 was to promote and enhance the utilisation of renewable energy within the country. The objectives of NREP 2010 are to facilitate the growth in renewable energy industry and increase public awareness on the importance and role of renewable energy.

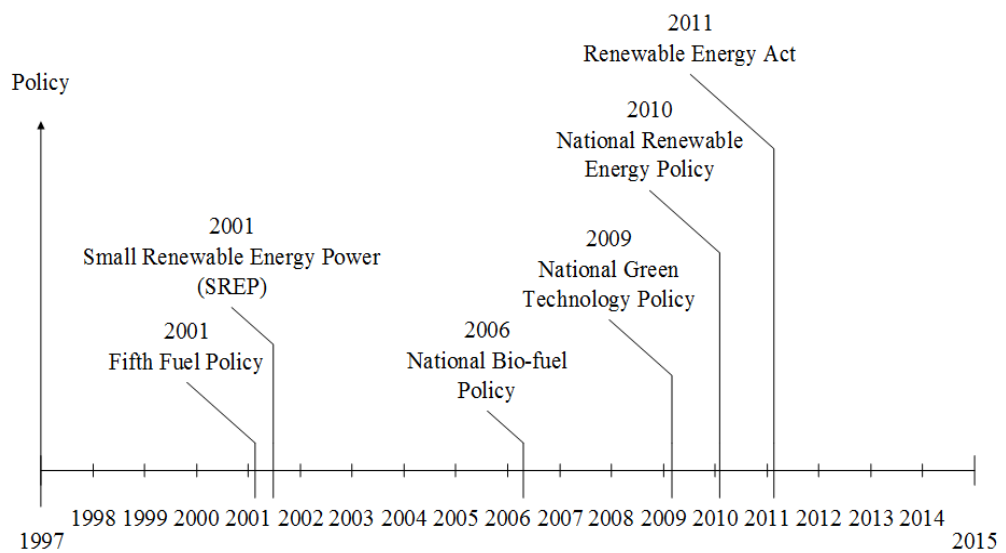


Figure 2.1 Timeline of the initiative taken by the Malaysian government

Presently, the total installed capacity of the renewable energy stands at less than 1.0% of the total power generation capacity nationwide as shown in Figure 2.2. However, the utilisation of renewable energy is expected to grow

with the implementation of feed-in tariff scheme under the Renewable Energy Act 2011, in which the individual can opt to sell the power generated to the utility company at a fixed premium rate.

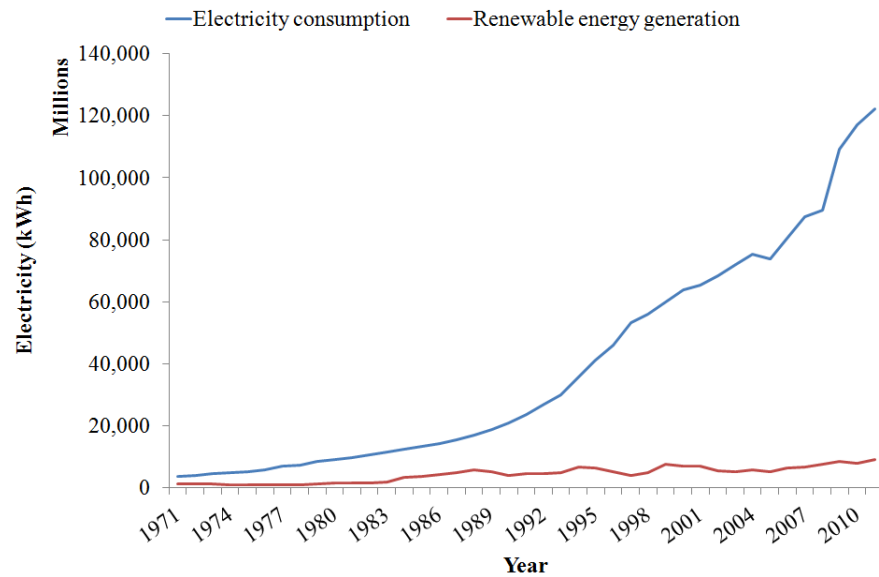


Figure 2.2 Electricity consumption and renewable energy generation in Malaysia from year 1971 – 2012 (The World Bank Data, 2014)

In the 10th Malaysian Plan, the government has targeted to achieve 985 MW by 2015, contributing to 5.5% of Malaysian’s total electricity generation mix. The Malaysian government introduced the feed-in tariff to foster RE because it was successfully implemented in over 40 countries including Germany, Spain, Italy and Thailand. Feed-in tariff are payments for those who generate electricity with RE sources.

Table 2.1 shows the details of feed-in tariff rate for solar, biomass, biogas and small-hydro in Malaysia. Renewable Energy (RE) fund, implemented by Sustainable Energy Development Authority Malaysia (SEDA) is used to pay for the users who sell their electricity under the feed-in tariff. An additional

tax of 1.6% will be imposed on the consumers' electricity bill towards the contribution of RE fund. However, domestic consumers who are utilizing less than 300 kWh will be exempted. These funds will be used to equalize between the renewable and non-renewable sources (Hashim et al., 2011). It is shown that the feed-in tariff for PV is the highest among all other technologies.

Table 2.1 Feed-in tariff (FiT) rate for solar in Malaysia

No.	Descriptions	Feed-in Tariff Rate (MYR/kWh)	Feed-in Tariff Rate* (USD/kWh)
Solar photovoltaic			
(a)	Solar photovoltaic installation with capacity of:		
i	Up to and including 4 kW	1.23	0.41
ii	Above 4 kW, up to and including 24 kW	1.20	0.40
iii	Above 24 kW, up to and including 72 kW	1.18	0.39
iv	Above 72 kW, up to and including 1 MW	1.14	0.38
v	Above 1 MW, up to and including 10 MW	0.95	0.32
vi	Above 10 MW, up to and including 30 MW	0.85	0.28
(b)	Solar photovoltaic installation (a) with criteria as follows entitle to have additional bonus:		
i	Use as installations in buildings or building structure	+0.26	+0.09
ii	Use as buildings materials	+0.25	+0.08
iii	Use of locally manufactured or assembled solar photovoltaic modules	+0.03	+0.01
iv	Use of locally manufactured or assembled solar inverters	+0.01	+0.003
Biomass			
(a)	Biomass installation with capacity of:		
i	Up to and including 10 MW	0.31	0.10
ii	Above 10 MW, up to and including 20 MW	0.29	0.10
iii	Above 20 MW, up to and including 30 MW	0.27	0.09
(b)	Biomass installation (a) with criteria as follows entitle to have additional bonus:		
i	Use as installation for gasification	0.02	+0.01
ii	Use as installation for steam generation >14% efficiency	0.01	+0.003
iii	Use of locally manufactured or assembled parts	0.01	+0.003
Biogas			
(a)	Biogas installation with capacity of:		
i	Up to and including 4 MW	0.32	0.11

ii	Above 4 MW, up to and including 10 MW	0.30	0.10
iii	Above 10 MW, up to and including 30 MW	0.28	0.09
(b)	Biomass installation (a) with criteria as follows entitle to have additional bonus:		
i	Use as installation for gas engine > 40% efficiency	0.02	+0.01
ii	Use of locally manufactured or assembled parts	0.01	+0.003
iii	Use for landfill or sewage gas	0.08	+0.03
Small-hydro			
(a)	Small-hydro installation with capacity of:		
i	Up to and including 10 MW	0.24	0.08
ii	Above 10 MW, up to and including 30 MW	0.23	0.08

*Feed-in Tariff rate in US Dollar (USD)/kWh are converted based on a conversion rate of USD 1.00 = MYR 3.00

PV system, being one of the most promising renewable energy sources in Malaysia, has the possibility to grow tremendously on the public low-voltage distribution networks. The introduction to feed-in tariff has brought to an average annual growth of 81% of the grid connected PV. Figure 2.3 shows the feed in tariff prices for PV systems and electricity retail prices for different countries. Among these countries, Malaysia has the lowest electricity retail price due to the subsidies from the Malaysian government. Although the Malaysian government has developed an effective policy on renewable energy to reduce the dependency of fossil fuel and mitigate the effect of climate change, the guidelines for the PV systems installation are limited. The technical issues are apparent in Malaysia where the frequency of passing clouds is possibly the highest in the world.

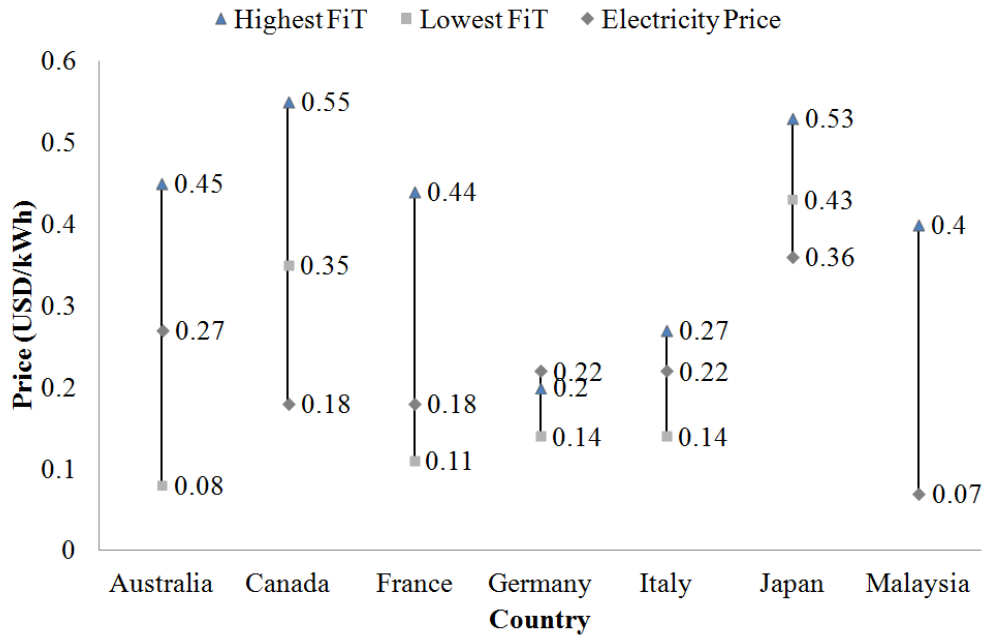


Figure 2.3 Feed-in tariff prices and retail electricity prices for different countries

2.3 Current Prospect of Renewable Energy in Malaysia

There are several potential renewable energy sources available in Malaysia, such as solar, biomass, biogas, mini-hydro, and municipal solid waste (Ahmad et al., 2011). According to SEDA database, there is approximately 166.49 MW in biomass and 29.53 MW in biogas under construction as of Jan 2014. The potential capacity of both biomass and biogas can become 1,340 MW and 410 MW respectively by 2028. The current small hydro generation is approximately 130.99 MW in Jan 2014 and should reach 490 MW by 2020. As for the waste power generation, the total capacity was 5.5 MW as of August 2009 and can be 360 MW by 2020.

Figure 2.4 shows the cumulative installed capacity of the renewable energy sources under the feed-in tariff scheme. It can be seen that 62% of the installed capacity comes from the installation of PV systems. Hence, the solar energy outlook in Malaysia is very promising and it is expected to surpass all other renewable energy sources by year 2050 (Chua et al., 2012). One of the reasons for this positive outlook is that Malaysia is a tropical country where high solar irradiance is available throughout the year. Furthermore, various remunerative packages have been introduced by the Malaysian government to promote the utilisation of PV systems among the domestic users. Malaysia is likely to be one of the largest solar power producers in the world in the near future (Mekhilef et al., 2012).

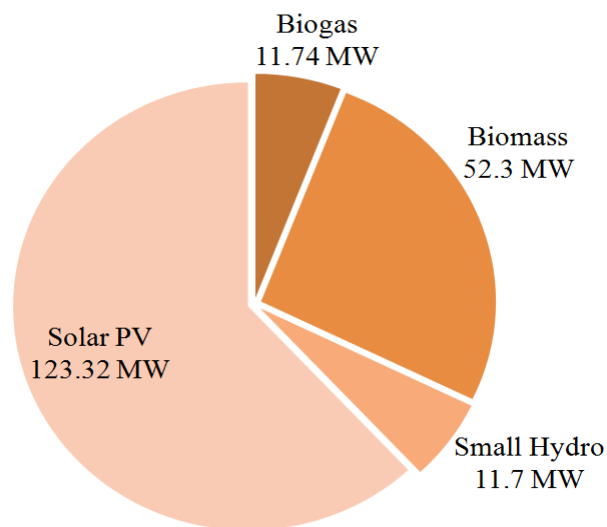


Figure 2.4 Cumulative installed capacity of commissioned renewable energy sources under the feed-in tariff as of May 2014 (SEDA, 2014a)

2.3.1 Photovoltaic (PV) system in Malaysia

PV cells consist of one or more semiconductor materials to convert solar energy to electrical energy. For higher capacity, PV cells are interconnected with each others to form a module. PV system utilises PV modules to convert solar irradiance into direct current (DC) and power electronics based inverter to regulate and convert the DC power generated from the PV module to 240 V AC power. PV system can be scaled to cover a small household requiring 1.0 kW_p to large farms requiring MW_p. Figure 2.5 shows the flow of power generation using PV system. Figure 2.6 shows the average solar radiation at various locations in the country (Mekhilef et al., 2012). It is noticed that the northern region in Peninsular Malaysia has an average solar radiation of 1650 kWh/m² whereas in East Malaysia, Kota Kinabalu in Sabah appears to have the highest solar radiation of 1900 kWh/m².

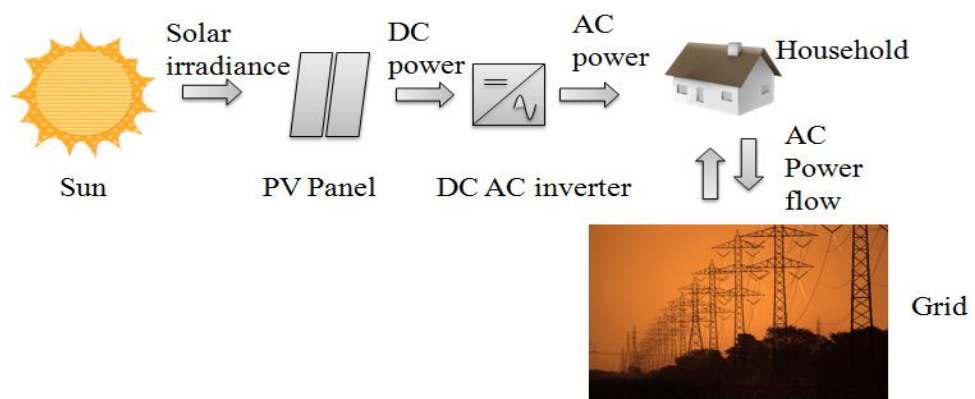


Figure 2.5 Power generations using PV system

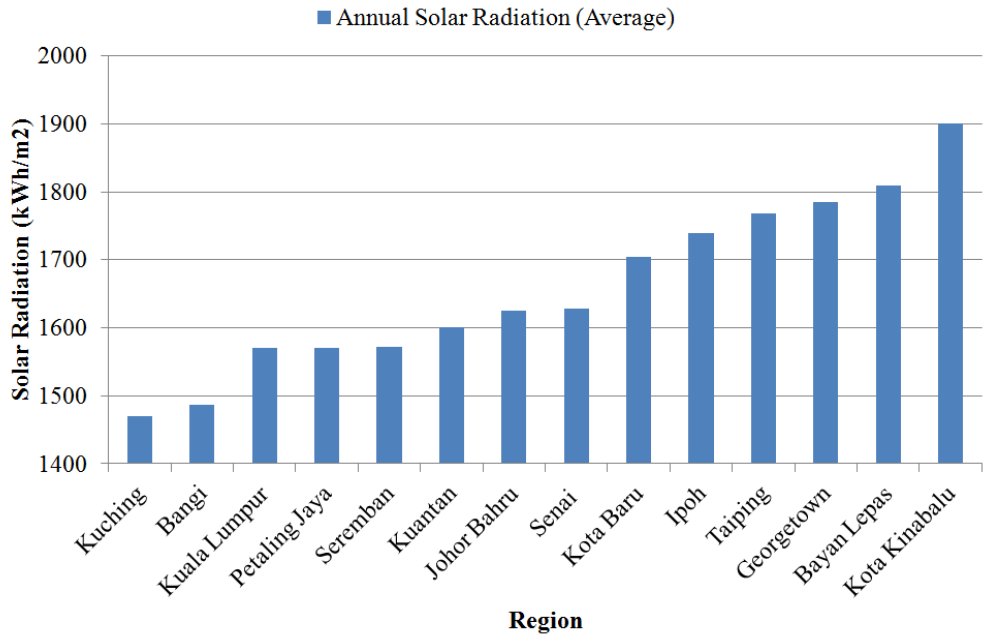


Figure 2.6 The annual average solar radiation on various regions in Malaysia

The current installed PV capacity up to year 2012 is approximately 20 MW as reported in the Trends in Photovoltaic Application survey report written by the International Energy Agency (IEA). Pusat Tenaga Malaysia (PTM) and IEA expected that solar energy has the potential to reach more than 6,500 MW by 2030 (Augustin et al., 2012).

Various research and development on inverters, PV concentrators, solar cell fabrication and characterization studies have been carried out by many local research institutions. These include research work on grid-connected inverters, development of solar cell, PV concentrator and PV power systems. Figure 2.7 shows the global module price index, cumulative and annual installed PV power. It is observed that the global module price index for PV module dropped drastically from USD\$ 3.84/W in 2006 to USD\$ 1.37/W in 2011. The SEDA database has shown that the cumulative installed capacity from year

2012 to 2013 has risen up by 65 MW due to the launch of feed-in tariff (SEDA, 2014a).

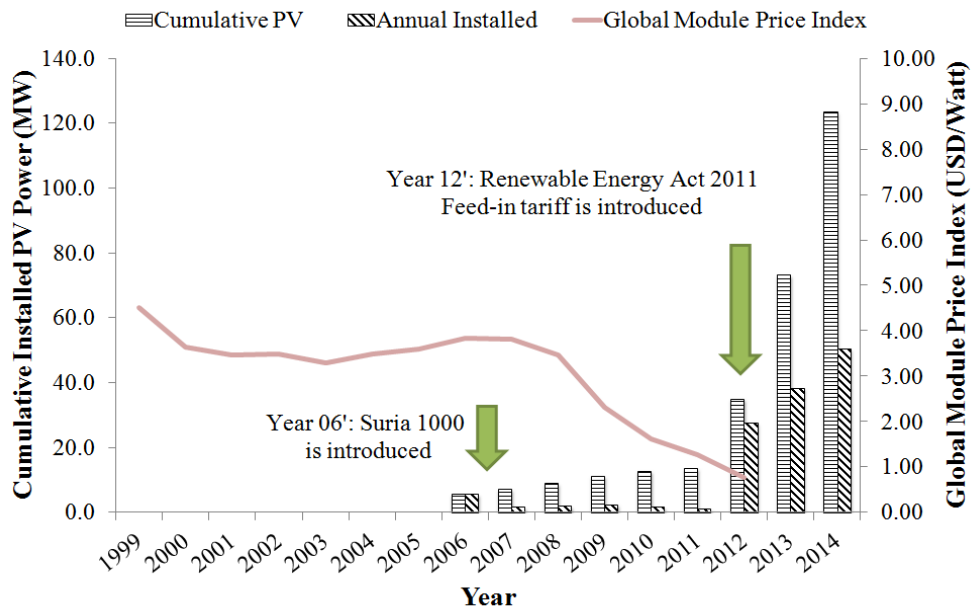


Figure 2.7 Global module price index, annual installed and cumulative installed grid connected PV capacity in Malaysia (SEDA, 2014a; NREL and LBNL, 2014)

2.3.2 Wind Energy

Wind energy is among the potential renewable energy sources available in Malaysia. The first wind farm in Malaysia was set up on Pulau Layang-layang which is located in Sabah. Research results compiled by University Kebangsaan Malaysia (UKM) in 2005 have shown a good wind generation profile. Nevertheless, harnessing wind energy in Malaysia very much depends on the location as Malaysia is geographically situated in the equatorial region and its climate is governed by the monsoons. Figure 2.8 illustrates the process flow of wind generation. Wind turbine is used to convert kinetic energy

generated by wind into electricity. A wind controller and an AC-DC converter is used to regulate and convert AC output from the wind turbine to a stable DC output. A DC-AC inverter is then used to convert the direct current to alternate current at 50 Hz.

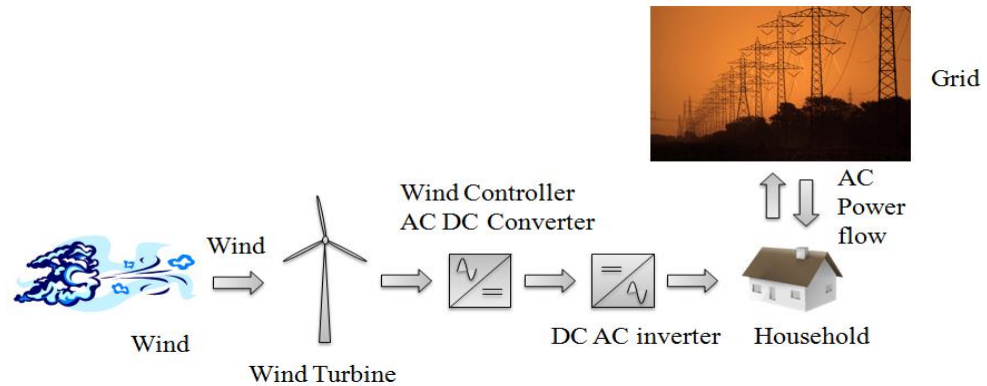


Figure 2.8 Wind generations

Research study has been carried out to assess wind energy in Malaysia with the installation of 16 stations covering east and west Peninsular Malaysia, Sabah and Sarawak (Mekhilef and Chandrasegaran, 2011). Figure 2.9 shows the wind speed study locations across Malaysia. Locations numbered with 1-3 cover Peninsular Malaysia that are facing South China Sea while locations numbered with 8-16 covers the Sabah and Sarawak coastline. Location 5-7 covers the coastline along the straits of Malacca. Figure 2.10 shows the average wind speed for the study locations as labelled in Figure 2.9. Research results show that locations facing South China Sea are the best choices for off-shore wind farm implementation due to the maximum potential during Northeast monsoon season from November to February (Mekhilef and Chandrasegaran, 2011).



Figure 2.9 Wind speed study location in Malaysia

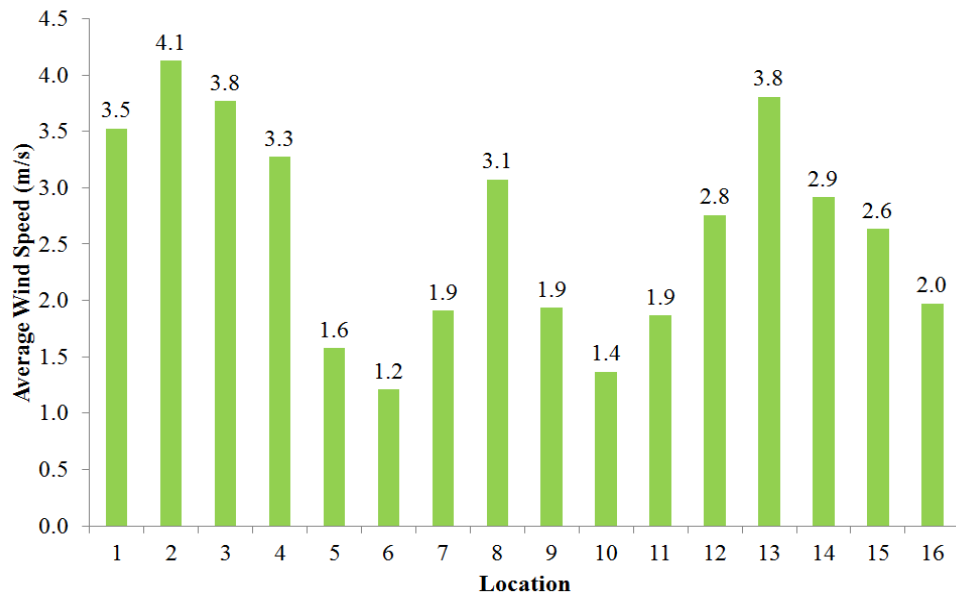


Figure 2.10 Average wind speeds at different locations in Malaysia (Chiang et al., 2003)

2.3.3 Small Hydro

Hydro generation projects are based on harnessing the power of flowing water from lakes, streams and rivers. Most of the hydro generation projects are located in remote areas. According to SEDA, the installed capacity of small

hydro power plants in Malaysia under the feed-in tariff program is approximately 11.7 MW while it is expected to have 206 MW by 2016 (SEDA, 2014b).

2.4 Potential Power Quality Issues Caused by Photovoltaic System

Global warming caused by excessive greenhouse gas (GHG) emission has brought to the attention of global leaders. Figure 2.11 shows the major sources contributing to CO₂ emissions in Malaysia. These sources including energy industries, transport sector, manufacturing, industries and construction, forest and grassland conversion, commercial and residential, soil emissions, mineral and metal production. Energy industries have been identified as the highest contribution in CO₂ emissions in the country. As a result, various programmes are launched to encourage the use of renewable energy in the country. Solar energy has an enormous amount of potential that can be utilised by various forms of technology, for example, PV system. At present, most PV systems are in single-phase and the installation to the premises is mainly customer driven and not centrally planned. Therefore, the growth of PV system on low-voltage distribution network has the potential to raise several technical issues including voltage fluctuation, voltage unbalance, voltage rise, reversed power flow and unnecessary neutral current flow (Wong et al., 2011).

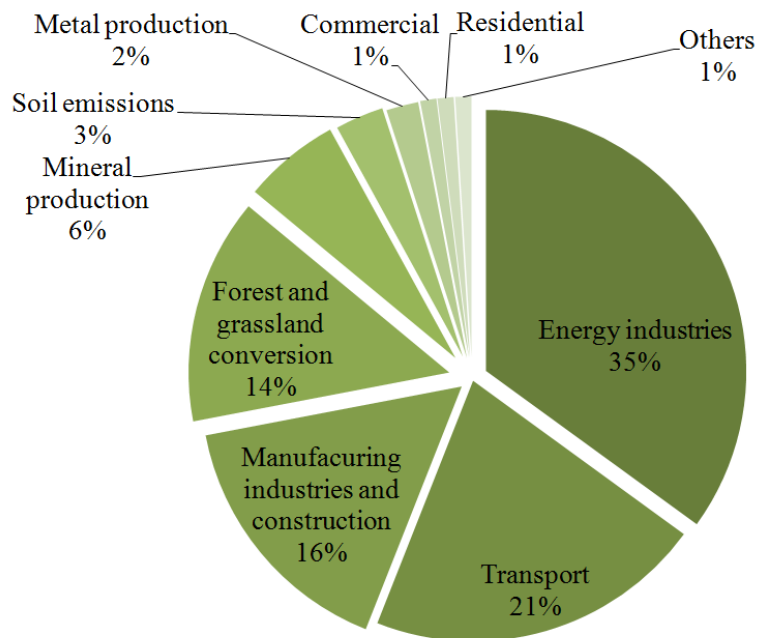


Figure 2.11 Major sources of Carbon Dioxide (CO₂) emissions by sectors in Malaysia (GreenTech Malaysia, 2014)

Research paper (Basso, 2008) has identified several technical issues caused by high penetration of large PV and wind turbine system on distribution network. Such technical issues include harmonics, flickers, load and generation imbalance. Global trends in sustainable energy investments for the year 2014 shows that the new investment in renewable energy projects has slightly slipped by 14% (McCrone et al., 2014). Nevertheless, this fall in 2013 was a reflection of reduction in costs of PV while the cumulative installed capacities of PV systems increased.

In Australia, distributed generators are predicted to meet 40% of the total energy required, with the main production contributed by grid connected PV systems (Lewis, 2011). In Singapore, PV array on the roof covers an area of 11,000 square meters with a generating capacity of 1.2 MW which can supply

at least 15% of the centre's electricity demand (Clover, 2013). Inline with the trend of increase in renewable energy sources on the electric networks, various research projects (Ingram et al., 2003; Yun Tiam, 2004; Lyons, 2010; Wong et al., 2011) were carried out to investigate the impacts of renewable energy sources on the distribution networks. The reliability of the electric network has become a major concern due to the integration of renewable energy sources.

Some of the efforts that have been implemented by the developed countries and the impacts of high penetration of renewable energy sources on the distribution networks have been widely studied. European laboratories at National Technical University of Athens (NTUA) in Greece, DeMoTec in Germany, SYSLAB in Denmark and the Small Scale Energy Zone (SSEZ) Laboratory in Durham University were setup to investigate the impacts of renewable energy sources and establish the active management system (Barnes et al., 2005; Barnes et al., 2007; Lyons, 2010). In the UK, voltage rise has been identified as one of the most serious power quality issues due to the high penetration of renewable energy sources (Lyons, 2010). Germany has implemented rules and regulations to limit the amount of renewable energy sources that can be fed into the grid.

A simulation model is developed at Helsinki University of Technology by using Decentralised System Simulation Tool for Optimized Generation (DESIGEN) to investigate large scale PV power integration on distribution networks. The results have demonstrated that the network model can handle PV without any significant issues if the PV power is the same or less than the

load. If the PV sizing is greater than the load, there is a tendency of significant voltage rise and the network losses are at least double that of a three-phase four wire distribution networks without PV integration (Paatero and Lund, 2007).

A field measurement is carried out on the 12 kW_p PV system located at a feeder in Florianopolis, Brazil. The results showed a small voltage rise at the point of connection. In order to further evaluate the impact of PV systems on the feeder voltage, a simulation program using Analise de Redes Eletricas (ANAREDE) is used to model a 4.2 MW_p distributed PV generator (Urbanetz et al., 2012). As a consequence, large deployment of PV systems on the distribution networks can cause severe voltage issues if coordination is not properly done.

2.4.1 Voltage Issues: Voltage Regulation and Voltage Rise

Distribution networks are designed without any PV integration and the installation of renewable energy sources on the distribution network has the potential to cause voltage rise at the feeder end (Barker and De Mello, 2000). Simulation has shown that voltage instability occurred in the IEEE 13 bus system by integrating 40% of the PV power to a heavily loaded network (Yan and Saha, 2012). In Japan, the density of grid connected PV systems is expected to increase in the urban area under the Japanese PV2030 roadmap. A typical size of 3-5 kW PV system will inject the generated power into the grid

during daytime. Under this circumstance, the reverse power flow can cause a voltage rise on the distribution network. This paper also describes the output power loss due to the grid voltage rise (Ueda et al., 2008).

Although PV integration with the distribution networks can reduce the transmission loss and peak load, improper coordination and implementation without regulatory framework can cause integration issues. A comprehensive analysis of the impacts on distribution networks with different penetration level (Chen et al., 2012) has shown that a small amount of PV penetration at the wrong location can produce unacceptable voltage profile. PV power output is solely dependent on the solar irradiance, PV systems tends to have peak generation during the middle of the day. Modelling approach using Power World simulation software shows that the increase in PV system penetration is likely to cause voltage level to increase (Lewis, 2011). The approximate voltage rise due to the renewable energy sources can be estimated using the equation as follows (Jenkins et al., 2000):-

$$\Delta V = \frac{PR + XQ}{V} \quad (2.1)$$

Where P and Q are the real and reactive power output from the renewable energy source respectively, R and X are the resistance and inductance of the system respectively. V is the nominal voltage of the system.

In Canada, Power System Computer Aided Design (PSCAD) software is used to evaluate the feeder voltage of a typical 240 V/ 750 kVA Canadian suburban radial distribution networks. Overvoltage is found to be one of the serious technical issues under low load condition is occurred. Cutting down the PV

capacity might be one of the solutions to overcome the overvoltage issues, however, with this solution, more power needs to import from the utility and this will also reduce the amount of CO₂ reduction (Tonkoski and Lopes, 2011).

2.4.2 Voltage Unbalance

The nature of balanced three-phase voltage is always to have equal magnitude and phase among all the three phases. It is possible to have balanced voltage at the generation and transmission level. However, it is unlikely to happen at the utilisation level due to non-linear load and uneven distribution of single-phase distributed generators. Voltage unbalance factor (*VUF*) is used to evaluate the degree of unbalance (Von and Banerjee, 2001). It is defined as follows:-

$$VUF(\%) = \frac{V^-}{V^+} \times 100\% \quad (2.2)$$

Where *VUF* is the voltage unbalance factor; *V-* is the negative sequence voltage; and *V+* is the positive sequence voltage. The negative (*V-*) and positive (*V+*) sequence voltages can be computed using the following equation:-

$$\begin{bmatrix} V_a \\ V_b \\ V_c \end{bmatrix} = \frac{1}{3} \begin{bmatrix} 1 & 1 & 1 \\ 1 & 1\angle 120^\circ & 1\angle -120^\circ \\ 1 & 1\angle -120^\circ & 1\angle 120^\circ \end{bmatrix} \begin{bmatrix} V_0 \\ V_+ \\ V_- \end{bmatrix} \quad (2.3)$$

Where V_a , V_b and V_c are the three phase line voltages at phase A, B and C respectively. V_0 , V_+ and V_- are the zero, positive and negative sequence voltage respectively.

Referring to the International Electrotechnical Commission (IEC) standard, a voltage unbalance of 1.0% can cause 6 to 10 times the current unbalance. A comprehensive analysis on the experimental case study is performed on a selected substation in Tehran. The assessment has verified that a relatively small amount of voltage unbalance can have a high amount of current unbalance. Large amount of current unbalance can contribute to network power loss (Bina and Kashefi, 2011). Similarly, a network will experience significant output energy loss due to the high grid voltage (Ueda et al., 2008). Unwanted current unbalance can produce unnecessary heat in the motor windings which will degrade the performance and reduce the lifespan of the induction motors (Jenkins et al., 2000).

2.4.3 Voltage Flickers and Fluctuation

PV power output is very much dependant on the solar irradiance. Region with cloudy skies may experience voltage fluctuation and flickers. Voltage fluctuation is defined as the changes in voltage magnitude for a period that is longer than the nominal voltage under consideration (J. Schlabbach and et. al., 2000). While voltage flicker can be defined as the repetitious variation in the electric voltage supply that result in a repetitious fluctuation in luminance of a

light source which is inconvenient to the human eyes (H. M. Al-Hamadi, 2012). Cloudy skies may become one of the barriers to the PV penetration. Undesirable voltage fluctuation on the distribution networks may lead to excessive use of on-load-tap-changer. A study was done to investigate the impact of 20% PV penetration on the feeder voltage under clear and cloudy skies. The results show that the tap changes during cloudy skies are 4 times more frequent as compared to the clear sky conditions (Ari and Baghzouz, 2011). As a consequence, a significant increase of tap changes will reduce the life span of the transformer.

The quality and safety of the electrical system can be seriously affected by voltage flickers and voltage fluctuations. It is the severe voltage quality issues that may affect the operation of machinery, process control equipment and malfunction of protection systems. It can propagate from downstream to upstream of the system or vice versa due to the propagation of currents (Elnady and Salama, 2007). A research study was carried out to investigate the power output fluctuations at 7 large PV plants located in Spain. These PV plants have power outputs ranging from 1 MW_p to 9.5 MW_p. It was observed from the results that the PV power fluctuation reduces as the plant size increased. As the plant size increased, there is a smoothing effect due to the geographical dispersion. The PV power output is also smoothed in relation to the irradiance variation for larger PV plants (Marcos et al., 2012).

Short-term and long-term flicker indices are normally used to quantify the severity of flicker. The short-term flicker index is calculated by integrating the

voltage fluctuations over a period of 10 minutes, while the long-term flicker index can be quantified by integrating the voltage fluctuations over 2 hours. The following formulas are used to calculate the short-term and long-term flicker indices (IEC 61000-3-3, 1994; Nambiar et al., 2010):-

$$d = \frac{V_{\max} - V_{\min}}{V_{\text{nom}}} \quad (2.4)$$

Where V_{\max} is the maximum voltage; V_{\min} is the minimum voltage and V_{nom} is the nominal voltage.

$$P_{ST} = P_{ST0} \times \frac{d}{d_0} \quad (2.5)$$

Where P_{ST} is the short term flicker; P_{ST0} is the relative short term flicker; d is the voltage change and d_0 is the relative voltage change. The long-term flicker is also known as the average of the short term flicker. It can be calculated as follows:

$$P_{LT} = \sqrt[3]{\sum_{i=1}^N \frac{(P_{ST}^i)^3}{N}} \quad (2.6)$$

where N is the total number of short-term flicker within the 2 hours and P_{ST}^i is the i_{th} short-term flicker.

2.4.4 Reversed Power Flow

The large deployment of renewable energy sources has the possibility to cause reverse power flow. An analysis showed that reverse power flow is likely to

occur during the period of small loads and high solar irradiance (Urbanetz et al., 2012). Investigation has also been done to analyze the ability of power transformer to facilitate the amount of power flow associated with high penetration of renewable energy sources. It is also identified that the reverse power flow occurs in the 11 kV and 33 kV power systems when the penetration of PV systems is more than 82.5% (Cipcigan and Taylor, 2007). The distribution networks are designed at a time when the power flow was towards the customers' load. The transformers are designed for step down operation.

Reverse power flow due to high penetration of renewable energy sources can be eliminated either by limiting the net power export to the higher voltage system, or it can be achieved using active local controller and energy storage system (Cipcigan and Taylor, 2007). This would allow the excess power generation to be stored into the storage system instead of flowing towards the higher voltage system.

2.5 Existing Methods for Power Quality Improvement

Voltage regulation, voltage rise and voltage unbalance are the common technical issues that pose a problem with the increase in the amount of PV penetrations. At present, several methods are proposed for voltage improvement in the distribution networks due to the integration of renewable energy sources:-

1. Renewable energy curtailment – Limiting the amount of active power exported from renewable energy sources.
2. Power electronic based devices – Flexible AC Transmission System, for example, Static synchronous compensator (STATCOM).
3. Energy storage – Store excess power generated by the renewable energy sources to reduce voltage rise.
4. OLTC control – Change the transformer tap position to lower the system voltage.
5. Load management – Demand side management to control the electricity usage of the customers.

The above mentioned methods are the existing techniques for power quality improvement on the distribution networks. In addition, some of these techniques can be operated in conjunction with each other in order to optimize the performance.

2.5.1 Renewable Energy Curtailment

Renewable energy sources connected at the remote end of a radial distribution networks have greater effects on voltage rise. Generation curtailment is a strategy that restricts the amount of real power flow into the distribution networks by shutting down some of the renewable energy sources. It has been widely investigated as an approach to ensure that the voltage is within the

acceptable limits (Shafiu et al., 2004; Zhou and Bialek, 2007; Noor Hidayat and Li, 2013). An investigation is carried out to determine the feasibility of implementing a solar neighborhood in a suburban residential area in Canada. It is found that active power curtailment is effective in preventing overvoltage during high generation and low load condition (Tonkoski and Lopes, 2011).

Generation curtailment is often used in the European countries to secure grid stability when there is a high risk of large amount wind energy during storms. At first sight, this could be a loss that should be avoided; however, a research paper argued that generation curtailment maybe an optimal solution with regard to total costs for providing electricity. Hence accepting generation curtailment can minimize the cost for network reinforcement (Klinge Jacobsen and Schröder, 2012). However, active power generation has higher economic value than reactive power import into the distribution networks. The owners of the renewable energy sources gain income from the feed-in tariff by exporting the power to the distribution network. Therefore, generation curtailment is not recommended as it limits the reduction of carbon footprint and reduces the revenue of the owners of the renewable energy sources. As a result, several research papers have proposed alternative solutions to mitigate the power quality issues caused by the high penetration of PV on the LV distribution networks. Among these solutions, the use of super-capacitor is proposed to mitigate the voltage flickers caused by the intermittent PV power output (Achim et al., 2003) and reactive power compensation is proposed for regulating and stabilizing the distribution voltages (Tran-Quoc et al., 2007).

2.5.2 Flexible AC Transmission System (FACTS) Devices: Static Synchronous Compensator (STATCOM)

Flexible AC Transmission System (FACTS) device is a power electronic based system that is used to control and increase power transfer capability of the network. An adaptive reactive power compensation facility such as a Static Synchronous Compensator (STATCOM) is one of the FACTS devices. It is a shunt compensator that is used to improve voltage flickers in industrial steel manufacturing where there is a dynamic change in large loads (Menniti et al., 2010).

Traditionally, a STATCOM without energy storage unit has no significant capability in providing active power to the grid. Research projects have been carried out to integrate STATCOM with an energy storage system to stabilize the system voltage and to provide active power support during the grid contingency (Svensson et al., 2006). It is also proposed to integrate the STATCOM with a supercapacitor based energy storage system for voltage regulation and voltage sag mitigation (Xi et al., 2008). D-STATCOM also known as Distributed Static Synchronous Compensator is a voltage-source inverter (VSI) based shunt compensation device that is used to solve power quality issues on the distribution network (Mitra and Venayagamoorthy, 2010). A new control algorithm generates a reference voltage for a D-STATCOM to ensure that the unity power factor is achieved at load terminal during nominal operation. The proposed system can inject currents on the distribution network to mitigate voltage sag (Kumar and Mishra, 2014).

D-STATCOM was integrated to a distribution network in Taiwan for reactive power compensation. Research has shown that the voltage control scheme of the proposed D-STATCOM is able to mitigate the system voltage violation that is caused by excessive PV power generation during peak solar irradiation (Chen et al., 2013). It is also proposed that the D-STATCOM to be installed at 2/3 of the feeder length in order to optimize the performance. The installed D-STATCOM maintains the voltage magnitude at the point of concern by manipulating the flow of reactive power between the network and the D-STATCOM (Shahnia et al., 2014). However, voltage control using reactive power is not as effective as active power on the low-voltage distribution networks due to the network resistance being greater than the reactance.

2.5.3 Energy Storage

Energy storage plays an important role in power management in the distribution networks with large deployment of renewable energy sources such as PV and wind turbine systems. Various research projects have identified that energy storage systems are capable of increasing network reliability during generation and demand fluctuations, maximize the net revenue of the investors by charging during off peak and discharging during peak hours (Fernandes and Philipp, 1977; Svensson et al., 2006). Research is carried out to investigate the use of energy storage for ancillary services and the feasibility of power quality improvement by utilizing energy storage system (Hajizadeh et al., 2010; Nguyen and Flueck, 2012).

A simple closed-loop control algorithm is proposed to coordinate the distributed energy storage systems with the on-load tap changer of the transformers to solve the steady-state voltage rises caused by PV systems while reducing the stress of the tap changers (Liu et al., 2012). Fuzzy logic was also used to develop a control algorithm to charge or discharge the energy storage system according to the online prices of electricity in every hour under the deregulated framework of electricity market (Darvishi et al., 2011).

Generally, energy storage can be integrated at various levels of the electrical systems. At the transmission level, it can be utilized for frequency control whereas at the distribution level, it can be utilized for voltage control and capacity support without limiting the capacity of the distributed generators. Subsequently, energy storage systems to be installed at the consumer level can provide peak shaving.

2.5.4 On-Load Tap Changer (OLTC) Control

On-load tap changer (OLTC) associated with voltage regulators are currently used for voltage control (Liu et al., 2012; Daratha et al., 2014). Adjusting the OLTC in the primary distribution transformers is one of the voltage control strategies (Crabtree et al., 2001). However, this approach is unable to address the voltage unbalance effectively because OLTC is not able to control the individual phase voltages on the distribution networks.

2.5.5 Load Management

Load management also known as demand side management (DSM), is widely used in the developed countries. In DSM, utility companies have the right to control, influence and reduce or increase the electricity demand of the customers with incentives. The main objective of the load management is to improve the quality of electricity by maintaining load generation balance, and stability of the power systems.

Research has been carried out to implement an algorithm for load control and a distribution management system controller (DMSC). The DMSC is used to estimate the state of the network and operate directly on controllable devices (Inigo, 2005). The author of (Tande, 2000) has suggested load management as an effective approach to mitigate voltage quality issues in wind power generation. One of the advantages of load management is that it can mitigate voltage rise issues with minimum network reinforcement and minimum constraints on the renewable energy sources. The load controller is used to modify and control the load curves in order to match the wind generation. However, suitable and controllable loads are not always available. Another paper also discusses that DSM as one of the potential approaches in solving voltage rise problems in power systems with large amount of renewable energy sources (Lim et al., 2005). This can be done by limiting the real power output of the renewable energy sources when it is likely to hit the statutory limits.

In Malaysia, DSM is not as popular as developed countries. A research paper outlined some DSM related projects lead by the utility company in Peninsular Malaysia. This research paper discussed the benefits of DSM from the aspect of utility company and the customers (Ibrahim et al., 1993). DSM can minimize the energy costs by shifting the load from peak to off peak times. This shifting can reduce the connection hours of peaking plants and hence reduce the GHG emission. However, the downside of the DSM is that the customers' acceptance of the control actions is still very low and is difficult to be improved (Luo et al., 2010).

2.6 Energy Storage System for Low-Voltage Distribution Networks

Energy storage system appears emerges to be an effective approach for mitigating the voltage issues without curtailing any renewable energy (Yan and Saha, 2012). The increasing penetration of renewable energy sources on today's distribution networks has led to the growing trend of using energy storage system. It is also said to be helpful to create a balance between the generation and demand to improve the performance of the power grid (Koochi-Kamali et al., 2013).

2.6.1 Revolution of Energy Storage System

Energy storage systems are no longer used only for conventional applications such as energy storage/backup. A coordinated voltage control scheme integrating electrical energy storage (ESS) is proposed to solve voltage problems caused by PV, wind generation, and electric vehicles (P. Wang et al., 2014). Integration of energy storage systems into low-voltage distribution networks is a new concept for improving system capacity and stability (Kashem and Ledwich, 2007). The authors (Yang et al., 2014) have proposed an appropriate sizing method of the battery energy storage system to mitigate the risk of distribution companies with high penetration of renewable energy sources. Optimal allocation of energy storage systems can maximize the total economic benefits. It can also create a balance between generation and consumption, so that it can reduce the power exchange at the substation (Zheng et al., 2014). A research project in the UK has proposed to integrate energy storage systems for active network management with wind power (Carr et al., 2014). Wind power generation is likely to increase in the near future. The use of energy storage systems is one of the potential methods to accommodate a large amount of wind power deployment without limiting the generation.

Various research projects have developed their own control strategy for peak load shaving using energy storage systems (Fernandes and Philipp, 1977; Oudalov et al., 2007; Y. Wang et al., 2014). During peak load periods, the control strategy conveys discharge commands to the energy storage system. On

the contrary, the control strategy enables charging during high PV power generation (Yang et al., 2014). With this control strategy, voltage rise due to high power generation can be eliminated.

A combination of PV system and energy storage units is proposed for reducing energy loss and enhancing voltage stability (Kashem and Ledwich, 2007; Hung et al., 2014). Any excess power generated by the PV system can be stored in the energy storage unit that is integrated with the PV system (Hung et al., 2014). However, energy storage without the management system does not optimize the performance to mitigate voltage unbalances on the distribution networks. This is due to its inability to control individual phase voltages on the distribution networks. The energy storage system also improves the efficiency and reliability of the utility grid by reducing the spinning reserve to meet peak power demands and also to provide support to the distributed network operator in case of plant failure.

2.6.2 Advantages and Limitations of Different Storage Technologies

Energy storage systems can be used to improve network stability, feeder voltage and supply quality and reliability (Wade et al., 2010). Most energy storage technologies are expensive, especially those that use lithium ion battery. At present, lead acid batteries are the most commonly used and cost effective storage device. However, lead acid batteries have short lifespan and the shelf life will be reduced if the charging and discharging rates are high.

Table 2.2 illustrates a list of energy storage technologies with their advantages and limitations. Due to cost constraint, lead acid battery is the most appropriate type of energy storage device for our application.

Table 2.2 Summary of energy storage technologies that market available for low-voltage distribution networks

Energy Storage Technology	Advantages	Disadvantages
Lead acid batteries	- Low costing - Efficiency approximately 80-90%	- Short lifespan - Deep discharge shorten lifespan
Lithium ion batteries (Li-ion)	- High energy density - High power and durable - Low self discharge	- High costing
Redox flow batteries	- Low self discharge	- Low efficiency approximately 60-70% - Limited temperature range, approximately 5°C to 45°C
Nickel Cadmium (NiCd)	- High charging cycle - Fast charging time - Durable	- Environmental unfriendly - Low energy density
Nickel –metal hydride (NiMH)	- Reliable - Durable - Higher energy density as compared to NiCd	- High self discharge - High maintenance - Performance degrades if stored at elevated temperature
Flywheel	- High efficiency	- High self-discharge rate
Supercapacitor	- Long shelf life (more than 20 years)	- High self-discharge rate - Low energy density

2.7 Summary

Future distribution networks are likely to have high penetration of distributed renewable energy sources. Significant developments have been made to create a flexible supply and demand chain, as well as in the area of network technologies and energy information networks. In European countries, when the intermittency of the renewable energy sources exceed 20-25% of the

demand, renewable energy curtailment is necessary in order to avoid grid disturbance unless the excess power generated is stored in the energy storage system. Active network management system has been emerged to be one of the solutions to accommodate and overcome technical issues caused by distributed renewable energy sources.

The intention of the Malaysian government is to increase the utilisation of renewable energy in the country for reducing the GHG emission by 40% from the 2005 levels by the year 2020. Introducing feed-in-tariff scheme has promoted the installation roof-top PV systems among domestic users and industrial players. As the share of renewable energy sources in the electricity sector increases, the energy storage system becomes increasingly important. With the drop in the price of the batteries and the increase in the life cycle, energy storage has become viable solution in active management. Table 2.3 shows that, the energy storage system can be integrated at different levels to have different impacts on the type of services provided. It is important to target the right application level as it involves different stakeholders of the electrical power systems. Energy storage system is essential to balance the power generation and demand, assimilation of excess power output from renewable energies and bridging low periods of regenerative power generation. Higher levels of the energy storage are required for grid flexibility and stability. Control strategy is important for the energy storage system to respond based on the network conditions. Hence, to integrate a high share of renewable energies, a system for controlling the real and reactive power flow is required.

Table 2.3 Application of energy storage system for different levels

	Transmission Level	Distribution Level	User Level
Application in Electrical Power System	- Ancillary services such as voltage and frequency regulation	- Ancillary services such as voltage and frequency regulation	- Stores excess energy generated by distributed generators
	Operating reserve	Peak shaving	End user peak shaving
		Demand side management	Reduce electricity bill by charging during off peak tariff and discharging during peak tariff
		Increase depth of renewable energy penetrations	

* Applicable to countries with off-peak and peak electricity tariff

Energy storage system is one of the sensible solutions to overcome the voltage issues caused by PV systems. Most of the existing energy storage systems do not solve the voltage rise and voltage unbalance issues that fluctuate throughout the day in the distribution network. The performance of the energy storage system can be optimized if it is equipped with an appropriate control strategy. An effective control strategy is needed for the energy storage systems to mitigate the fluctuating voltage rise and voltage unbalance on the distribution networks with PV systems that are available in the country with cloudy skies condition.

CHAPTER 3

ARCHITECTURE OF THE EXPERIMENTAL LOW-VOLTAGE DISTRIBUTION NETWORK

3.1 Introduction

The Malaysian transmission network voltages are 500 kV, 275 kV and 132 kV while the distribution networks are 33 kV, 11 kV and 415 V for three-phase systems. A laboratory scale experimental low-voltage distribution network is designed to investigate the effect of high penetration of PV systems on the distribution network and enable the development of suitable control system for the energy storage system to maintain satisfactory network operation. In this chapter, the design and details of each component for the experimental low-voltage distribution network are presented.

3.2 Review of the Malaysian Low-Voltage Distribution Network Topology

In order to develop a hardware platform to investigate the future challenges of PV systems and to investigate the active control techniques on the low-voltage

distribution network, it is necessary to review the existing distribution networks. The Malaysian low-voltage distribution network is a radial three-phase four wire system. Consumers are usually connected at the remote end of the feeders. Figure 3.1 shows the typical topology of a Malaysian low-voltage distribution network. The incoming grid is rated at 11 kV and is stepped down to 415 V via a step down transformer. Switchgears are normally placed at both high voltage and low-voltage side to isolate electrical equipment in the substation. The substation outgoings are branched out to four feeder pillars, namely FP3-1, FP3-2, FP3-3 and FP3-4 with a 300mm² four cores cross-linked polyethylene insulation aluminium underground cables (300MMP 4C XLPE AL) being used as the out-going feeders. The network shown in Figure 3.1 has 18 feeders in which the feeder ends with three-phase cables that serve the premises.

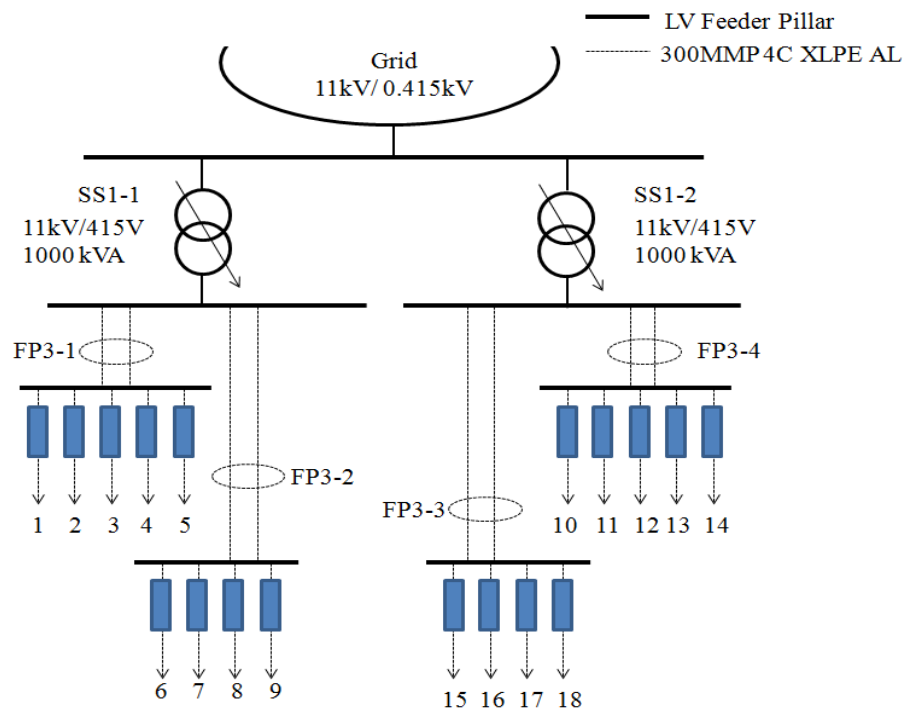


Figure 3.1 Typical low-voltage distribution network

3.3 Experimental Low-Voltage Distribution Network

The experimental low-voltage distribution network is designed to imitate the radial three-phase four wire system. The system is Terra-Terra (TT) earthing which is common practice in the Malaysian distribution network where both the transformer neutral and the installation frame are earthed. Figure 3.2 illustrates the placement of each device. The experimental low-voltage distribution network consists of two 3.6 kW_p single-phase PV systems, a 2.0 kW single-phase wind turbine emulator and a 9.0 kW three-phase controllable load bank. Three phase selectors are installed at the nodes for PV systems and wind emulator system so that the single-phase device can be switched freely to other phases. Miniature circuit breakers (MCB) are installed before each node to protect the nodes from overload and short circuit current. Figure 3.3 shows the test lab of the experimental low-voltage distribution network in the University. The details of the energy storage system will be discussed in Chapter 5. Meanwhile, each of the devices including PV system, wind emulator and controllable load will be further elaborated in the following sub-chapter.

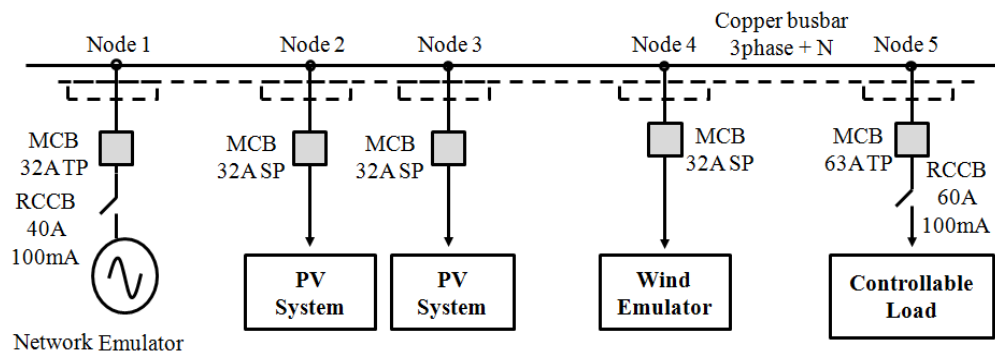


Figure 3.2 Network topology of the laboratory-scaled experimental low-voltage distribution network

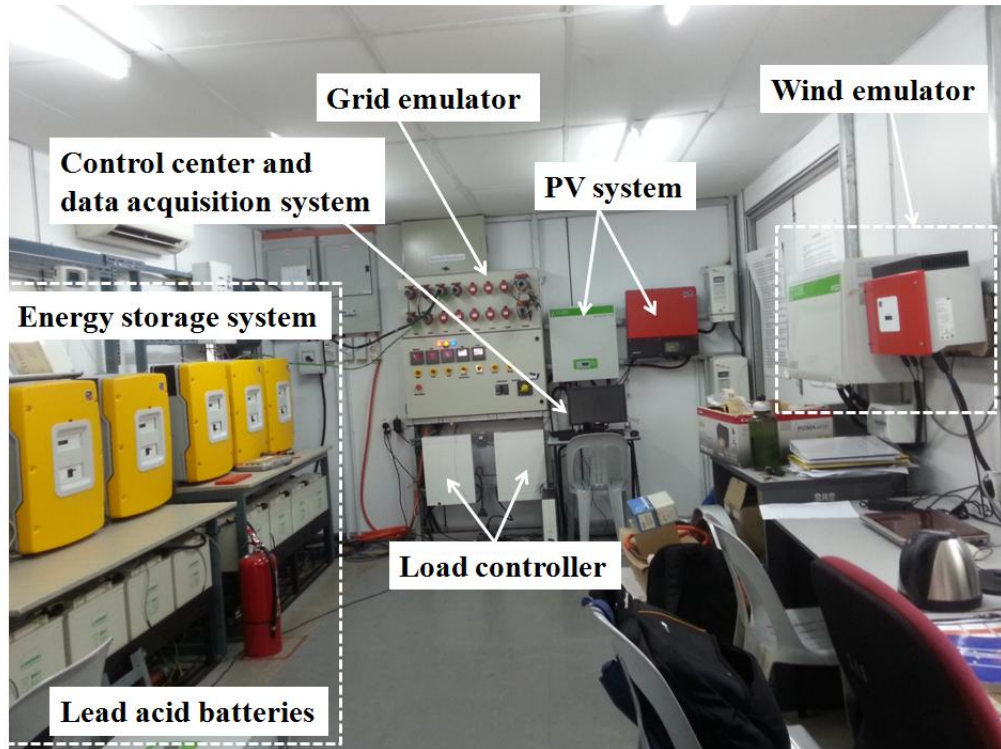


Figure 3.3 Test lab of the experimental low-voltage distribution network with energy storage system

3.3.1 Network Emulator

Network emulator is used to represent the Malaysian low-voltage distribution network. It consists of a 15 kVA synchronous machine coupled with an induction motor driven by a variable speed drive (VSD) as shown in Figure 3.4. In addition, VSD is used to regulate the system frequency at 50 Hz throughout the experiment. The synchronous machine varies the system frequency by changing the speed reference on the VSD.

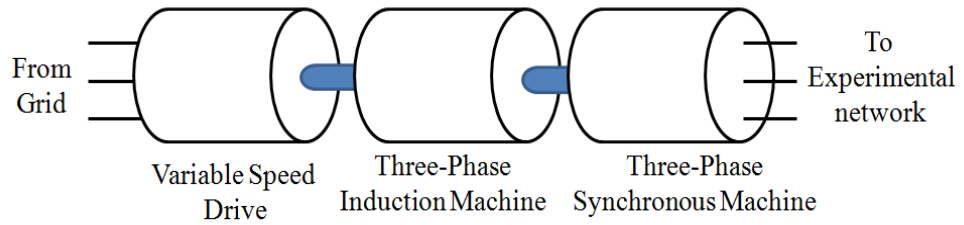


Figure 3.4 Layout of the grid emulator

The design of the grid emulator is developed to isolate the experimental network and the grid electrically. Figure 3.5(a) shows the setup of the grid emulator and (b) VSD installed in the laboratory. Figure 3.6 shows the voltage profiles of the (a) low-voltage grid emulator installed in the laboratory and the (b) low-voltage distribution networks taken from the utility grid.

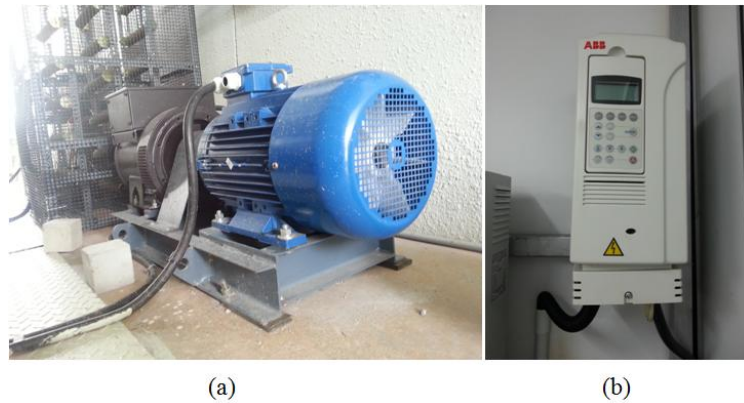


Figure 3.5 Grid emulator installed in the laboratory with (a) synchronous generator coupled with induction machine driven by (b) variable speed drive

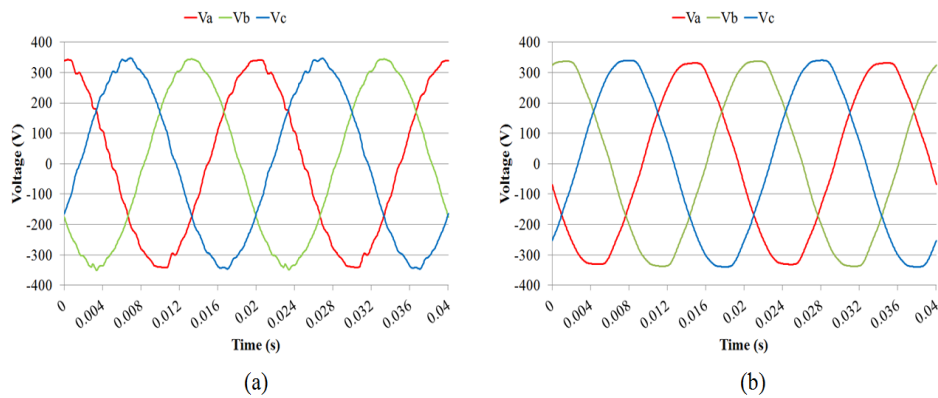


Figure 3.6 Three-phase voltage profiles for (a) low-voltage grid emulator and (b) low-voltage distribution networks respectively

3.3.2 Photovoltaic System

As discussed in Chapter 2, solar power has emerged to be one of the promising renewable energy sources in Malaysia. PV systems are most likely to achieve large deployment in the country in near future. In order to increase the accuracy of the research, two commercially available PV systems that comply with MS IEC 61727:2004 are installed on the experimental network. The use of actual PV systems will give a more accurate result in the experimental low-voltage distribution network. This is also to ensure that the reliability of the device and the AC output voltages are well within the permissible range. The two PV systems are installed on the experimental low-voltage distribution network. Each of the PV systems consists of 16 PV panels connected to a DC-AC inverter. A total of 32 panels contribute to a total of 7.2 kW_p. The PV inverter (model-Sunzet SP3) is rated at 3.0 kW and it is manufactured by Zigor, Italy.

The PV modules are manufactured by Panasonic, with model number VBMS230AE01. The type of the solar cells in the modules is polycrystalline. Table 3.1 shows the technical specification of the PV modules. Each module has a capacity of 230 W, hence making 3.68 kW_p for each PV system. In order to receive maximum amount of the sunlight, these PV modules are installed at the open space car park with the panels facing north and with a tilt of 5°, so that any dust trapped on the solar panels can be washed away by rains. Figure 3.7 shows the PV modules that are mounted on top of a 3.3 metres high metal

structure with a slight tilt angle located at the open space car park in the University.

Table 3.1 Technical specification of PV module

No	Characteristics	Specifications
1	Maximum power (P_{max})	230 W
2	Short circuit current (I_{sc})	8.42 A
3	Open circuit voltage (V_{oc})	37 V
4	Maximum power current (I_{pmax})	7.83 A
5	Maximum power voltage (V_{pmax})	29.4 V
6	Maximum system open circuit voltage	1000 V



(a)

(b)

Figure 3.7 PV modules mounted on a 3.3 metres height metal structure at the University open space car park area. (a) Top view of the PV panels (b) Bottom view of the PV panels

3.3.3 Wind Turbine Emulator

A three-phase induction motor coupled with a three-phase synchronous machine, a variable speed drive, a rectifier and single-phase inverter namely SMA Windy Boy 2500 is used to emulate a small-scale wind turbine as illustrated in Figure 3.8. The variable speed drive is used to vary the speed and torque to emulate the actual wind turbine speed and torque characteristics. The three-phase output is then rectified to supply a DC voltage to the Windy Boy

which will provide 50 Hz, 240 V single-phase AC voltage to one of the three phases in the experimental low-voltage distribution network.

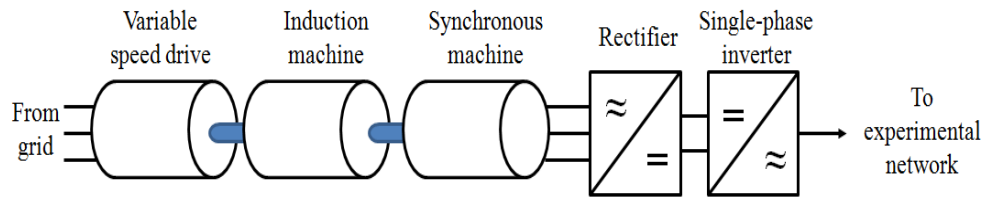


Figure 3.8 Topology of a wind turbine emulation system

3.3.4 Load Emulator

A three-phase variable load bank is designed to emulate the customer load. Figure 3.9 illustrates the topology of a load emulator. It consists of 18 power resistors with a rating of 500 W/ each. Six power resistors are lumped as one connected to one phase. Each resistor is controlled by a solid state relay which is operated by National Instruments 32 channels bi-directional digital input/output series module, NI9403. A control algorithm is developed by using LabVIEW™ to convert the load data to digital data. The digital data is then sent to the solid state relay to activate the resistor.

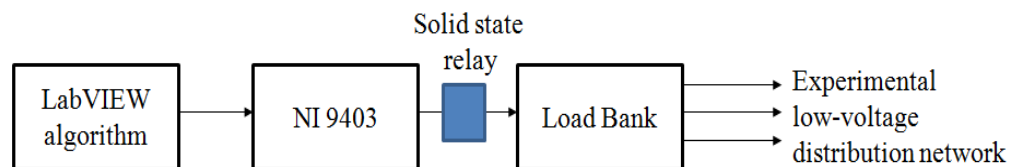


Figure 3.9 Block diagram of the load emulator

Each of the solid state relay controls a 500 W resistor in the load bank. Figure 3.10 shows the actual average daily load of a building at the University and the load profile of the three phase load emulator. The load at each phase can be varied by 500 W/step up to 3.0 kW at nominal voltage. Figure 3.11 shows two units of the load emulators installed in the laboratory.

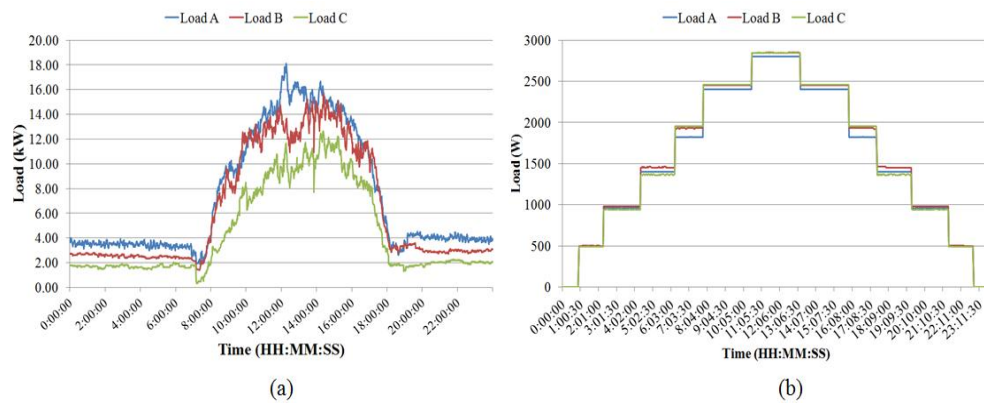


Figure 3.10 (a) Actual load consumption in the University tutorial block and (b) load emulation pattern



Figure 3.11 Load emulators installed in the laboratory

3.3.5 Data Acquisition System

A monitoring system is required to monitor the network conditions and measure the impacts of the PV and energy storage system on the experimental low-voltage distribution network. The measured voltages are used to determine whether the network conditions are satisfactory or not. In case of any voltage issues, these measured voltages are input into the control system to provide feedback to the bi-directional inverters. It is costly to measure all the parameters in every single point of the low-voltage distribution network. Therefore, a data acquisition system that measures voltage, current and power on five locations are setup on the experimental low-voltage distribution network. Several 40/ 5A current transformers and voltage transducer are used to measure current and voltage. Figure 3.12 illustrates the measuring points on the network. This is to ensure that all measurements from each system device are well monitored. PV systems connected at node 2 and 3 are assigned with the address of 002 and 003 respectively, while wind turbine and load are connected at node 4 and 5 and assigned with the addresses of 005 and 006 respectively.

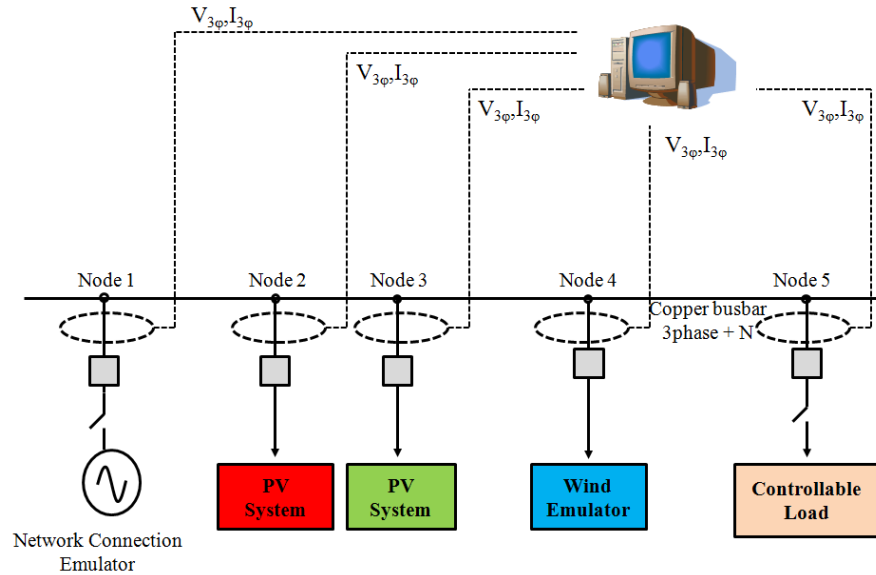


Figure 3.12 Data acquisition system at the measuring nodes

Figure 3.13 shows the components for the data acquisition system. Five units of Elcontrol STAR 3 power meters are connected via serial port connection to the data logger. Each of the power meters is installed at the node 1 to 5 as shown in Figure 3.12. These power meters are used to display the readings measured from the respective node. The data logger (Model: Data Taker 82 (DT82)) is connected via Ethernet port to the supervisory computer. It is used to acquire and compile the data from the Elcontrol STAR 3 power meters while a supervisory computer is used to record the data using a spreadsheet via LabVIEW™. This process is illustrated by using a flow chart in Figure 3.14.

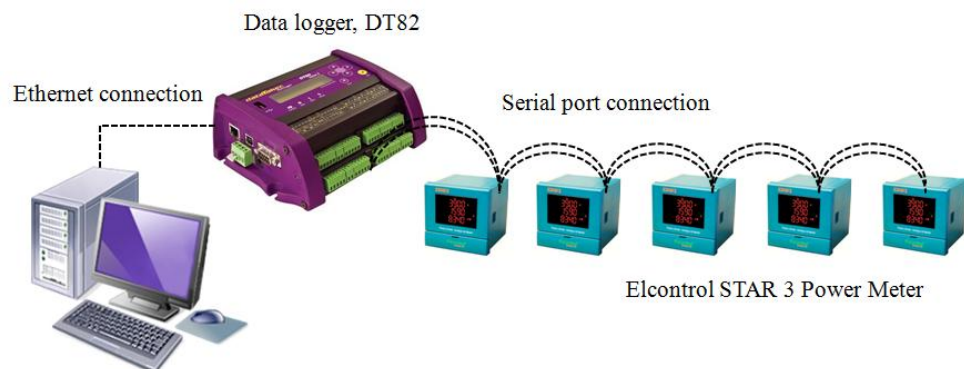


Figure 3.13 Components for the data acquisition system

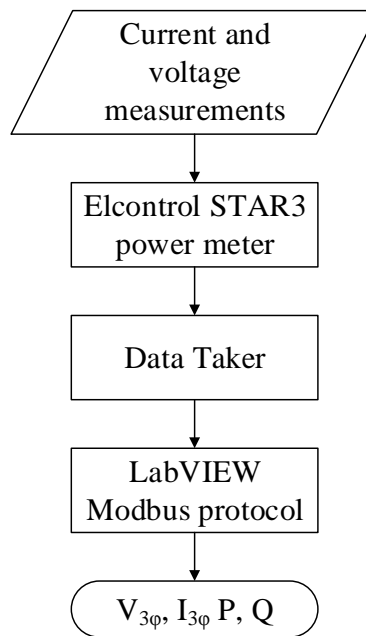


Figure 3.14 Data acquisition system flow chart

3.3.6 Data Taker, DT82

Data Taker DT82 is a data logger that records electrical parameters over a period of time. In this section, the detail of the data logging system is presented. Data Taker DT82 is used to measure, record and compile readings taken from the experimental low-voltage distribution network. The data logger is connected to the supervisory computer via Local Area Network (LAN) interface. A web based program developed by the manufacturer is accessed from any browser in the supervisory computer by using the Internet Protocol (IP) address assigned to the data logger. Figure 3.15 shows a program for the data logger being developed using the web based application. This program is

used to import the data taken from the power meters by the data logger.

Appendix A shows the program written in the Data Taker DT82.

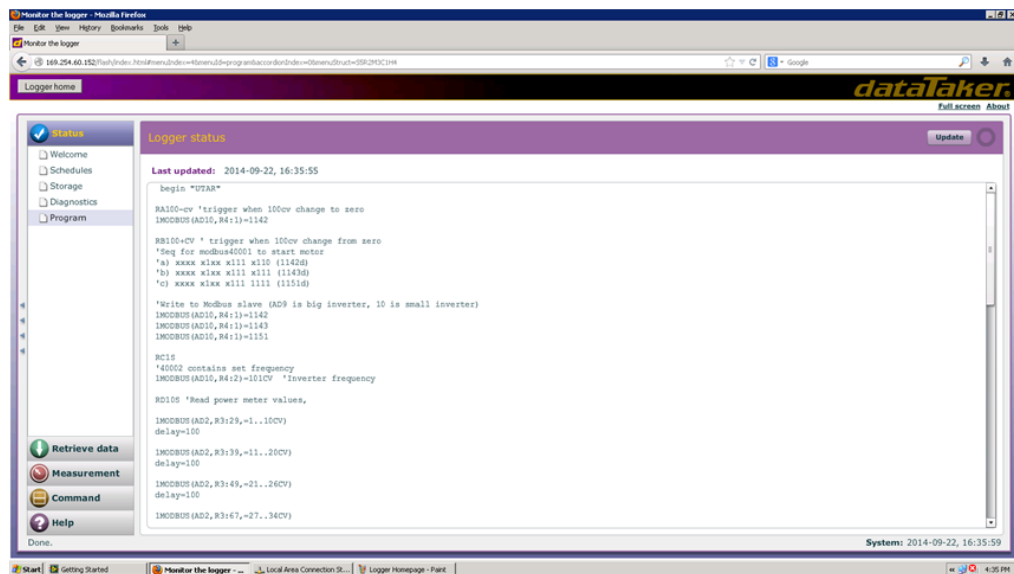


Figure 3.15 Web based application to program the data logger

The data logger receives data from the serial port. Before the data logger can receive the information from the power meter, the serial port parameters need to be initialised as follows:-

```
PROFILE SERSEN_PORT FUNCTION = MODBUS_MASTER  
PROFILE SERSEN_PORT BPS = 9600  
PROFILE SERSEN_PORT DATA_BITS = 8  
PROFILE SERSEN_PORT STOP_BITS = 1  
PROFILE SERSEN_PORT PARITY = NONE  
PROFILE SERSEN_PORT FLOW = NONE  
PROFILE SERSEN_PORT MODE = RS485
```

The DT82 uses Modbus as a serial communication protocol. The transfer rate in a communication channel is configured at a rate of 9600 bits per second.

Figure 3.16 shows the transferred bits including start bits, data bits, the parity bits (if used) and the stop bits.

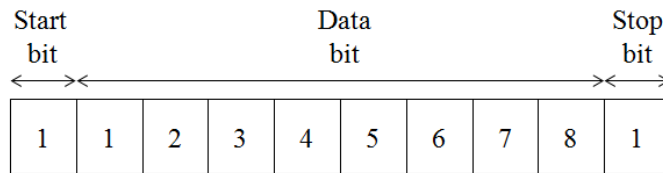


Figure 3.16 Frame structure of the Modbus message

The MODBUS_MASTER port function is used for receiving and processing incoming serial modbus requests using the 1MODBUS channel. Modbus is a communication protocol that is widely used in supervisory control and data acquisition (SCADA) system. It can provide an efficient and a standard way to transfer data values between the power meter and the supervisory computer. These configurations can be found in the user manual of Data Taker DT82. In order to read or write from a channel, the following commands are used.

To read from a channel:

1MODBUS (AD2, R3:29, 1..10CV)

Where AD is the address of the device, R3 is the instruction for reading the data stored in a particular register and CV is defined as channel variable. The above command indicates the modbus system reads the data stored in the register with the addresses of 0029 to 0038 from the device with the address of 002 and then store these values in the channel variable with the address of 1 to 10.

To write to a channel:

1MODBUS(AD10, R4:1)=1142

Where AD10 is the device with the address of 10 and R4 is the instruction for writing the data into a register with a particular address. The above command indicates the modbus system write the data with a value of 1142 into the register with an address of 0001. Appendix B shows the list of parameters to be written in the registers of the Data Taker DT82.

3.3.7 Setting Up Data Acquisition Program Using LabVIEW™

A LabVIEW™ control algorithm as shown in Figure 3.17 is developed in the personal computer to extract the data from the Data Taker via modbus protocol and display it in the graphical user interface. In order to establish a working connection between the supervisory computer and Data Taker, the IP address, 169.254.60.152 that has been assigned to the Data Taker must be initialised. Port 502 which is the standard port number for modbus is triggered to allow the data acquisition system for accessing the Data Taker modbus server. After the initialization, a modbus VI is used to extract the data recorded in the Channel Variables (CV) of the Data Taker to display in LabVIEW™. The starting address of the register and quantity of the parameters must be defined in the modbus VI to ensure the correct measurements are read from the Data Taker.

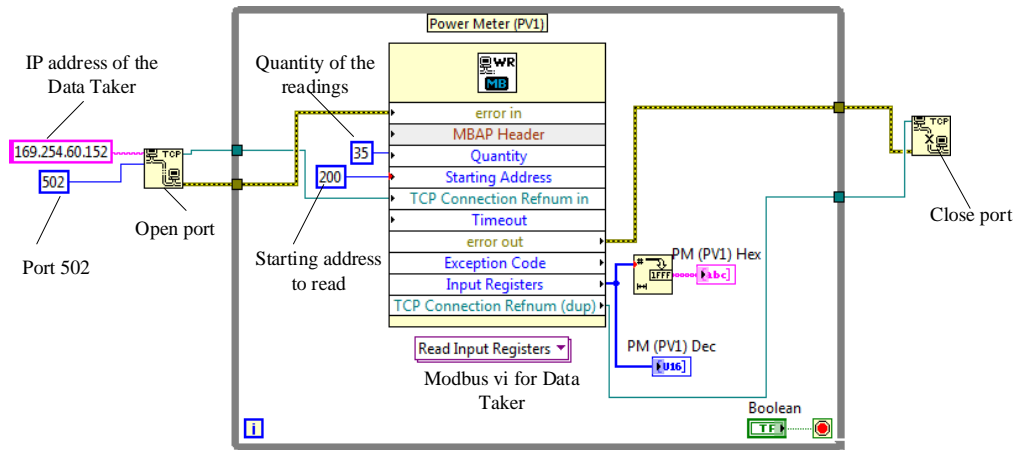


Figure 3.17 Block diagram of reading data from Data Taker via LabVIEW™

Figure 3.18 shows the graphical user interface of the data acquisition front panel taken from LabVIEW™. The power meters record each parameter in binary-coded decimal (BCD) format with two registers. The first register represents the mantissa while the second is the exponent. The mantissa is expressed with 3 BCD numbers on 12 bits while the exponent is in binary format and determines the position of the dot in the measurement (FFFFH = 10^{-1} ; 0000H = 10^0 ; 0001H = 10^1). For example (Elcontrol STAR 3, 2006): -

- Representation of current at line 1 = 53.3 A.

The value of the current is stored in Register with the addresses of 0035 and 0036. It is observed that Register 0035 and 0036 have the values of 0533H (Hexadecimal) and FFFFH (Hexadecimal) respectively. The final value of the current is represented by multiplying both Register 0035 and 0036 which gives the value of 533 x 10^{-1} .

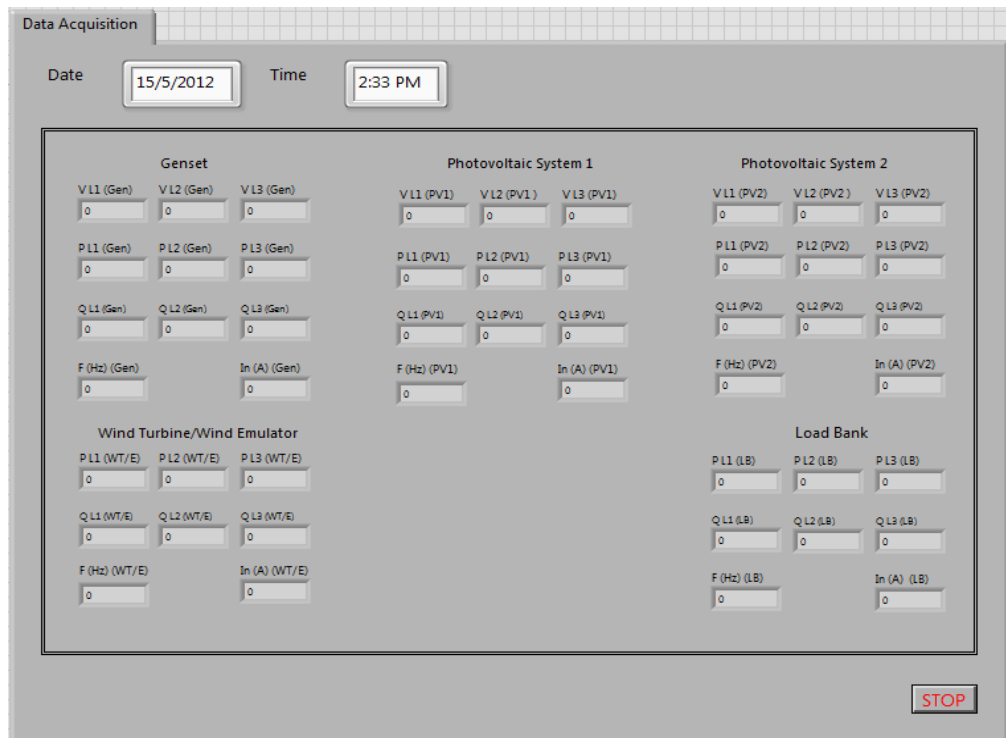


Figure 3.18 Snapshot of the data acquisition front panel in LabVIEW™

3.4 Evaluation of Experimental Low-Voltage Distribution Network

Under normal operation, the experimental low-voltage distribution network operates with the voltage within the permissible range. Table 3.2 shows that several tests have been carried out to investigate the performance of the experimental distribution network. Steady state voltage regulation and voltage unbalance are the two measured values to be studied in order to verify the operation of the experimental low-voltage distribution network.

Table 3.2 List of voltage and voltage unbalance tests under different scenarios

Scenario	Remarks
I	Voltage and voltage unbalance test under different load condition.
II	Voltage and voltage unbalance test with single load and single PV system.

(I) Scenario I: Changes in Voltage and Voltage Unbalance Under Different Loading Conditions

The nominal operating voltage for the experimental distribution network is defined as 240 V. With the reference to the International Electrotechnical Commission standard IEC 60038:2009, the statutory limit for voltage excursion is within the range of 216 V to 252 V which is equivalent to +10% and -6% with reference to 230 V on the low-voltage distribution network. A number of loading conditions are used to study the changes in voltage and voltage unbalance of the network. Voltage violation is caused either by an increment in load or by a reduction in generation. Either of the above can possibly cause a voltage violation on the statutory limit. Table 3.3 shows the different loading conditions being used in this Scenario I.

Table 3.3 Load conditions for voltage & voltage unbalance test

Loading Condition	Load A	Load B	Load C
I	Increasing	Zero	Zero
II	Zero	Increasing	Zero
III	Zero	Zero	Increasing
IV	Fixed load	Fixed load	Fixed load
V	Fixed load	No load	No load

The phase-to-neutral voltage is measured at output terminal of the network emulator and output terminal of the load bank throughout the study. Figure 3.19 shows the phase voltage under the loading condition for voltage test I, II and III. Figure 3.19 (a) shows that the voltages on phase A, B and C change together even though phase A is loaded. Similarly, Figure 3.19 (b) and (c) show the three-phase voltages change where only one phase is loaded.

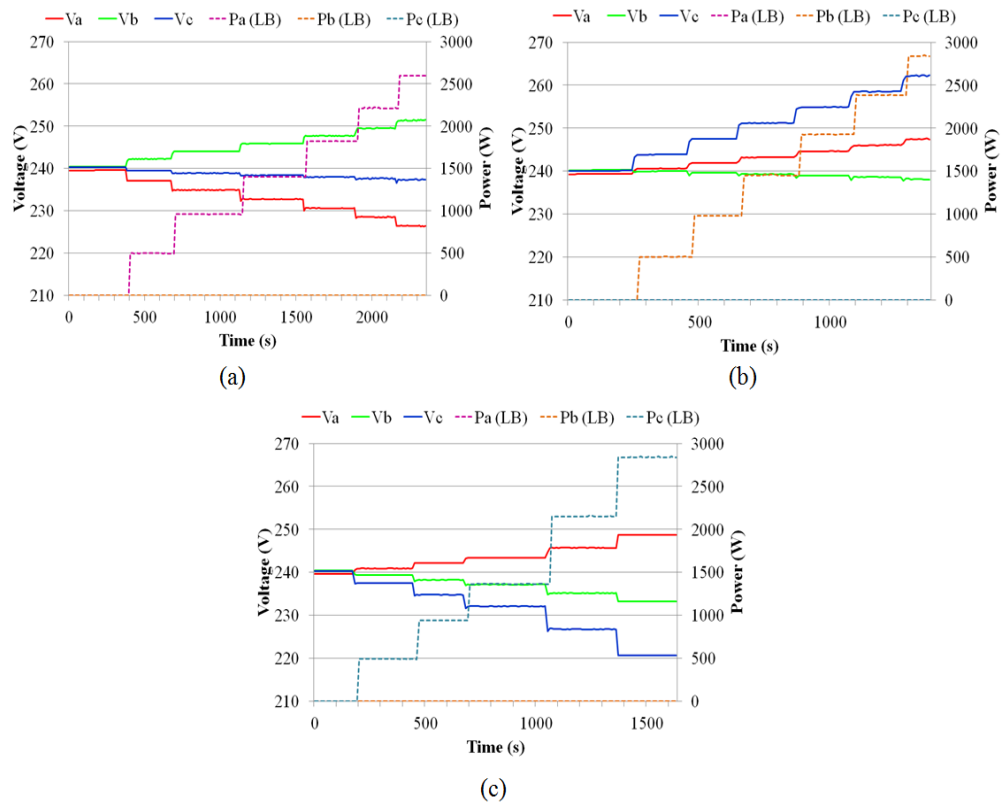


Figure 3.19 Voltage test I, II and III with an increasing load at (a) phase A (b) phase B and (c) phase C respectively

As for test IV and V, initially no load is connected until 650 s. Test IV introduces a balanced load condition with each of the phase being connected to a 500 W load. Similarly, test V introduces unbalanced load condition with only phase A being connected to a 500 W load, while phase B and C are not loaded. Figure 3.20 illustrates the voltage test comparisons between the balanced and unbalanced load condition. It is noticed that the phase to phase voltage difference is lesser for balanced load as compared to unbalanced load condition.

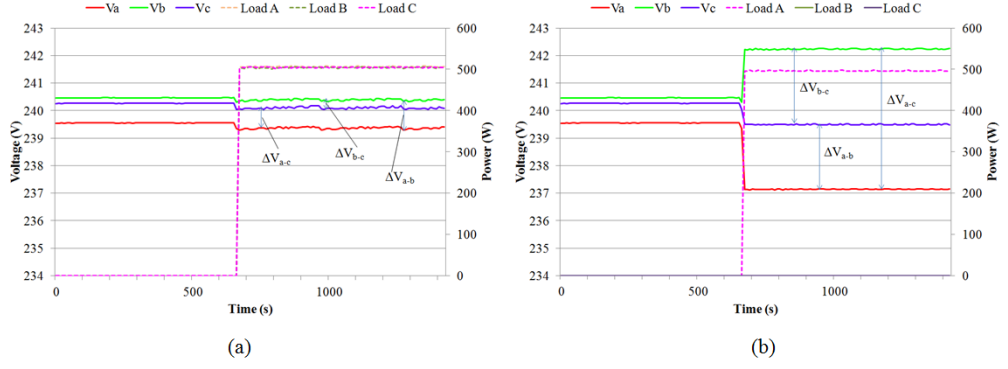


Figure 3.20 Voltage test IV and V with (a) three phase balanced load condition and (b) unbalance load condition respectively

If one particular phase-to-neutral voltage is changed due to unbalanced load condition, the neutral voltage is shifted away from the reference point because of the neutral current flows through the neutral line. As a result, the other two phases to neutral voltages will be changed as well. The voltage across the phase to neutral for each conductor can be represented as follows:

$$\Delta \bar{V}_{an} = \Delta \bar{V}_{ag} + \Delta \bar{V}_{ng} \quad (3.1)$$

$$\Delta \bar{V}_{bn} = \Delta \bar{V}_{bg} + \Delta \bar{V}_{ng} \quad (3.2)$$

$$\Delta \bar{V}_{cn} = \Delta \bar{V}_{cg} + \Delta \bar{V}_{ng} \quad (3.3)$$

Where $\Delta \bar{V}_{an}$, $\Delta \bar{V}_{bn}$, and $\Delta \bar{V}_{cn}$ are the phase to neutral voltage for phase A, B and C respectively. $\Delta \bar{V}_{ag}$, $\Delta \bar{V}_{bg}$ and $\Delta \bar{V}_{cg}$ are the phase to ground voltage for phase A, B and C. Whilst $\Delta \bar{V}_{ng}$ is the neutral to ground voltage. The shift in the neutral voltage is intensified because of the existence of the mutual couplings in between the three phases and the neutral line. The shift in the neutral voltage can be minimised if the line has multiple grounds. However, the distribution network with multiple grounding is not efficient and hence not

very common in Malaysia. Therefore, multiple grounding is not implemented in the experimental distribution network for this research work. As a result, any changes in one voltage can shift the neutral voltage and hence the other two voltages.

Voltage unbalance factor at the terminal of the network emulator is recorded every 10 seconds under the different loading conditions as specified in Table 3.3. Figure 3.21 illustrates the effect of network voltage unbalance factor when only one phase is heavily loaded under the loading conditions for test I, II and III. Figure 3.22 shows a comparison of the voltage unbalance factor for both balanced and unbalanced load condition for test IV and V respectively.

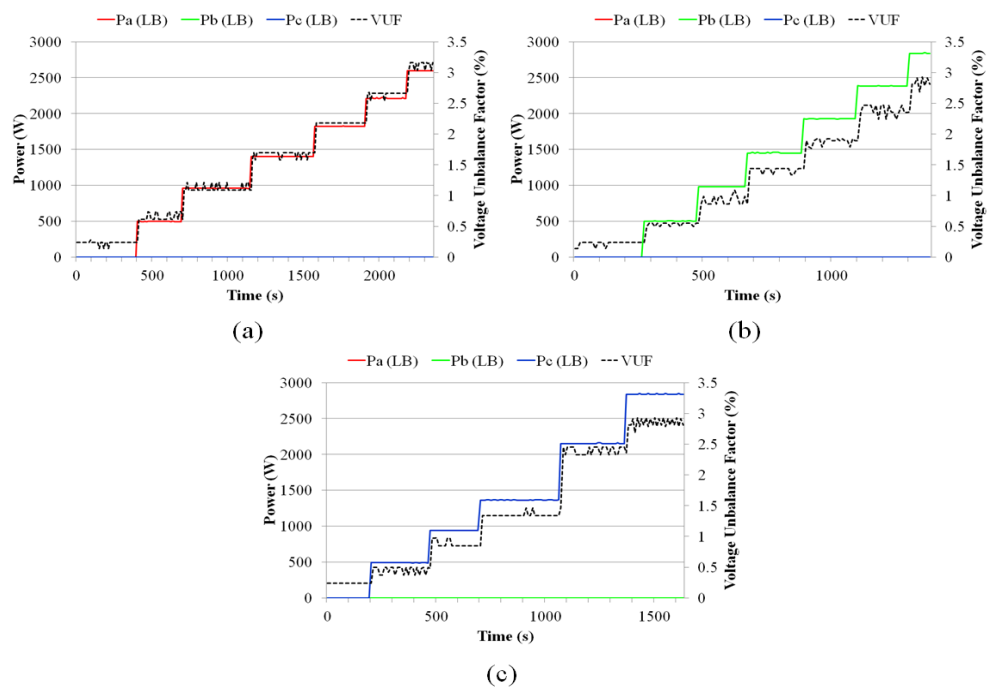


Figure 3.21 (a), (b) and (c) Voltage unbalance factor under loading condition I, II and III respectively

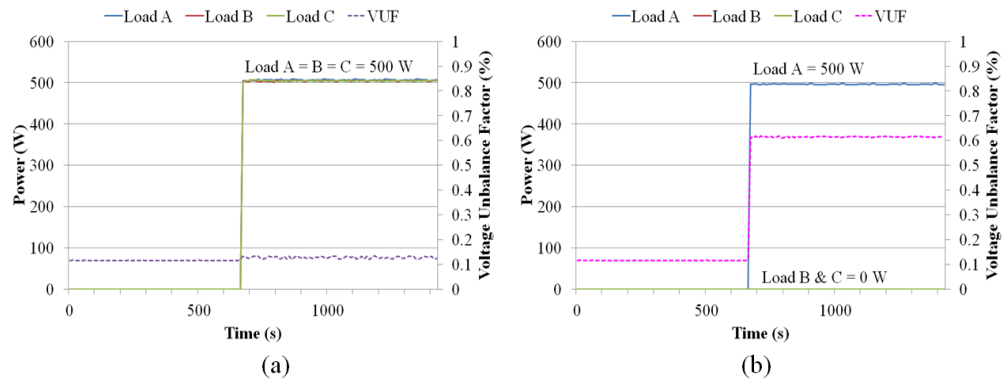


Figure 3.22 (a) and (b) Voltage unbalance factor under loading conditions IV and V respectively

The operation of the experimental low-voltage distribution network in Figure 3.21 has a voltage unbalance factor greater than 2.0% when one of the phases is loaded with more than 1.5 kW. These studies have demonstrated that an increase in the loading on one phase of the network resulting in asymmetrical sequence current flows will cause an increase in voltage unbalance factor. Initially, Figure 3.22(a) and (b) show the voltage unbalance factor is recorded at 0.1%. At 650 s, Figure 3.22(a) shows the voltage unbalance factor remained stable at 0.1% when a balanced load condition is introduced. Figure 3.22(b) recorded a hike in voltage unbalance factor from 0.1% to 0.6% when one phase is loaded with 500 W while the other two phases remained at no load.

(II) Scenario II: Changes in Voltage and Voltage Unbalance Factor under Different Loading and Generating Conditions

In this case study, single-phase load and single-phase PV system are connected at Phase A. Initially, the test begins with a 1.0 kW load connected at phase A. Figure 3.23 (a) shows the PV system starts to inject at 500 s

resulting in a reduction of voltage unbalance factor from 1.1% to 0.1%. Figure 3.23 (b) shows the voltage profile of the case study.

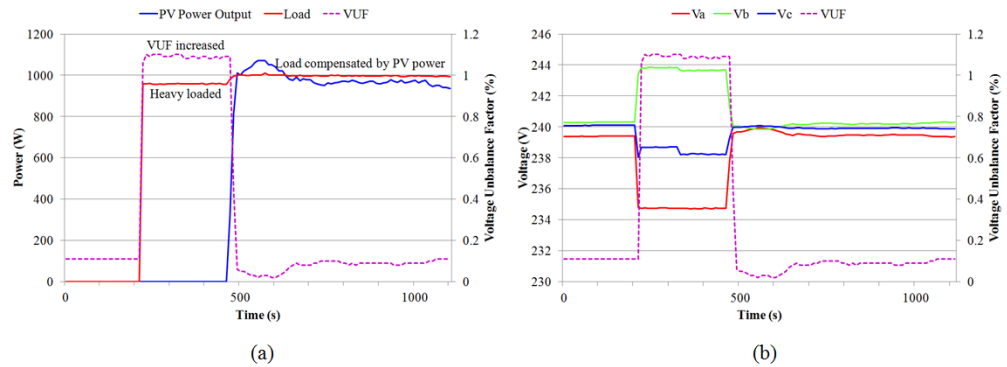


Figure 3.23 (a) PV power, load and voltage unbalance factor (b) Voltage and voltage unbalance factor of the load and generation power test

From 200 s to 500 s, the voltage at phase A drops due to the heavy load while the other two phases, phase B and C are affected due to the mutual coupling effect of a synchronous machine. At 500 s onwards, the three-phase voltages are back to its nominal after the load at phase A is compensated with an equivalent generation from the PV system. Renewable energy sources integrated to the distribution network has the effect to supply local loads and reduce consumption from the utility grid. At some periods, excess power generation from the renewable energy sources are exported to the grid resulting voltage rise on the LV networks.

3.5 Summary

The experimental low-voltage distribution network is set up to study the effect of loading and generation conditions on the voltage. The network has a

network emulator, load bank, PV systems and wind emulator. The network emulator is a 15 kVA synchronous machine coupled with an induction machine driven by a variable speed drive (VSD). The VSD is used to regulate the entire system at 50 Hz, 240 V. The network emulator is able to provide power balance over the three-phase system. The experimental low-voltage distribution network is a radial and TT earthing configuration. Two commercially available PV systems and a wind emulator are installed on the experimental low-voltage distribution network. All renewable energy sources are single-phase which would be the likely connection on the Malaysian low-voltage distribution networks. In addition, a 9.0 kW three-phase controllable load bank is developed. The load bank is purely resistive and does not feature inductive or capacitive loads. The data acquisition system is formed with several power meters, a data logger and a supervisory computer. This system is capable to measure, record and calculate the power quality quantities such as voltage rise, voltage regulation and voltage unbalance factor. The present system does not measure harmonics, but it is possible to do an extension by upgrading the power meters. The data acquisition program is developed by using LabVIEW™ to import and record the data stored in the data logger. Several tests were carried out to investigate the performance of the experimental low-voltage distribution network. The results have shown the suitability of the experimental network to represent the Malaysian low-voltage distribution networks.

CHAPTER 4

IMPACT OF GRID-CONNECTED PV SYSTEMS ON THE LOW-VOLTAGE DISTRIBUTION NETWORK

4.1 Introduction

Malaysia, a country that is geographically surrounded by the sea, maybe the cloudiest region in the world due to the vaporisation of the sea water associated with the seasonal winds that results in the large amount of passing clouds. The solar irradiation is highly scattered and fluctuating, hence causing the PV power output to be highly intermittent. Consequently, an enormous amount of voltage fluctuations and flickers are produced. The technical issues caused by the PV systems in Malaysia become unique because they are very dynamic instead of steady state. Hence, the dynamic voltage control is designed to counter check the voltage level from time to time to address the fast variation of voltage level due to the intermittent PV power output that causes voltage fluctuation. In this chapter, research study has been carried out to investigate the impact of a 7.2 kW grid connected PV system on a radial low-voltage distribution network. Two 3.6 kW_p single-phase PV systems are connected at Phase C of the low-voltage distribution network for a period of 19 days from 6th to 24th March 2013. A monitoring system has been set up as

shown in Figure 4.1. The monitoring system is to measure the three-phase voltage and power output of the PV systems. It consists of a supervisory computer integrated with National Instrument (NI) data acquisition chassis, a unit of NI9225 voltage module and a unit of NI9227 current module. LabVIEW™ is used to acquire and store readings obtained from the NI data acquisition chassis. Table 4.1 shows the resistance and reactance of the existing underground cable.

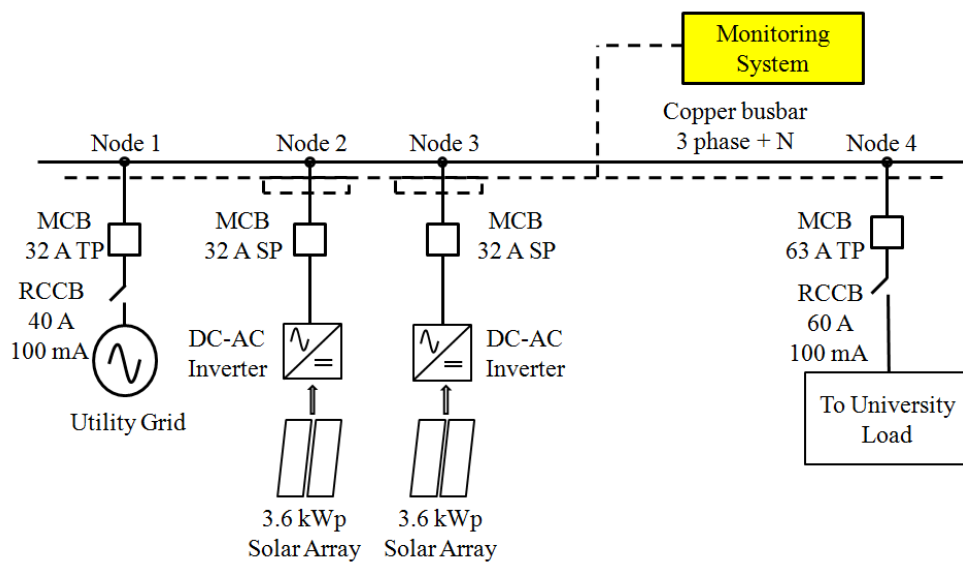


Figure 4.1 Topology of a three-phase low-voltage distribution network integrated with PV systems

Table 4.1 Parameters of the underground cables

Type of cable	Resistance (at 50 Hz at 90°C)	Reactance (at 50 Hz)
300MMP 4C XLPE Al	0.13 ohms/km	0.072 ohms/km
70MMP 4C XLPE Al	0.568 ohms/km	0.075 ohms/km

4.2 Characterization of Photovoltaic Power Output

Malaysia is located at the equatorial region that has a high irradiance level all year round. The level of irradiance in Malaysia is in the range of 1470 to 1700 kWh/m²/year (Lim et al., 2008). The vaporization of the sea water associated with the seasonal winds results in large amount of passing clouds, hence causing a low clear sky index in Malaysia as compared to other countries. Figure 4.2 shows the global climatology data of the clear sky index in the world. Under cloudy sky conditions, the solar irradiation is highly scattered and fluctuating, resulting in the substantial fluctuation of the power output of the PV systems (Marcos et al., 2012). Consequently, the intermittent power output from PV tends to generate an enormous amount of voltage fluctuations and flicker in the low-voltage distribution networks.

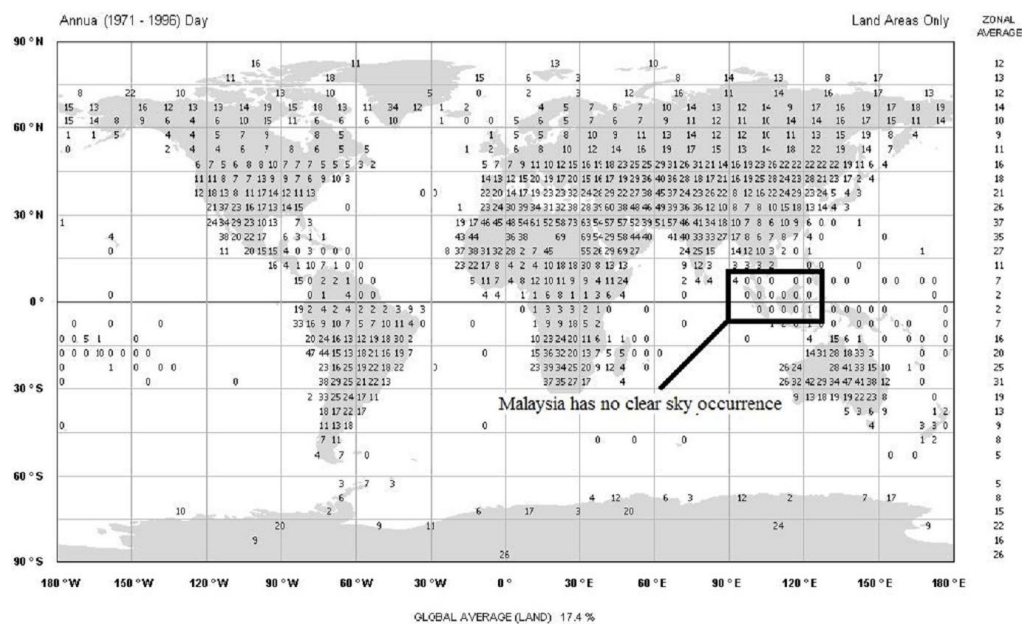


Figure 4.2 Frequency occurrence of the global completely clear sky index

Figure 4.3 shows the PV power outputs on 22nd, 23rd and 24th March 2013. It can be seen that the power output fluctuates frequently throughout the three days as compared to that of a clear sky reference. These reference values are the maximum PV power output at that particular period. The numerous fluctuation of the power outputs are caused by the high frequency of the passing clouds over the PV panels. It is also noticed that the high power output drops suddenly rather than gradually. This is because many of the passing clouds are very thick causing a sudden reduction in the total solar irradiation.

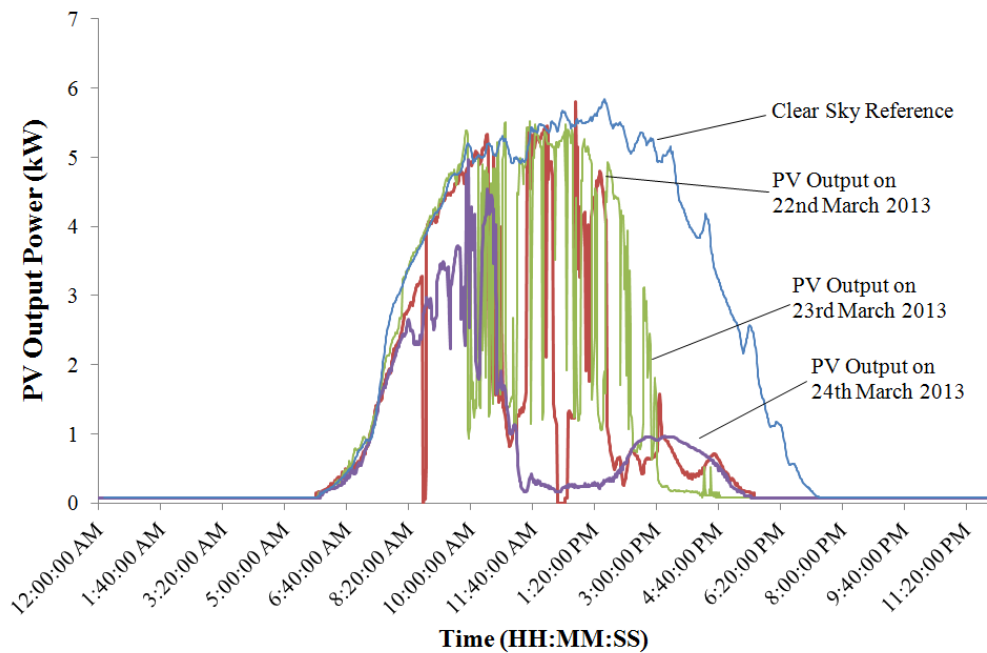


Figure 4.3 PV power outputs of the three random days as compared to a clear sky reference

4.3 Voltage Quality Issues

Voltage quality is increasing importance when widespread use of power electronic devices. In general, voltage quality issues, such as including voltage variation, voltage unbalance, voltage flickers and voltage fluctuations are

issues of major concern. In this chapter, voltage quality issues caused by the integration of PV systems are evaluated. Voltage at the point of the common coupling (PCC) is monitored over a period of 19 days and then characterized to show the probabilistic occurrence of voltage rises, voltage unbalance and flickers on the network.

4.3.1 Characteristic of Voltage Rises

Voltage rise characterization is carried out to determine the penetration effect of the grid connected PV system on the system voltage levels. The PV systems are installed in Phase C only. The three-phase voltage at the PCC is recorded on a regular basis. The frequency of occurrence of different voltage levels on phase A, B and C at the PCC are determined as shown in Figure 4.4. The frequency of occurrence of the voltage levels within the range of 247 V and 248 V are the highest on Phase A and B. The frequency of occurrence for the voltage levels to be within the range of 249 V to 250 V is the highest on Phase C. There are also some voltage magnitudes within the range of 251 V to 252 V which is at the border of the voltage tolerance. Furthermore, there are several voltage magnitudes greater than 252 V which is beyond the statutory limits. The installation of PV system onto a weak network can impact the overall voltage profile. In addition, voltage rise becomes a serious problem when the generation is greater than the demand.

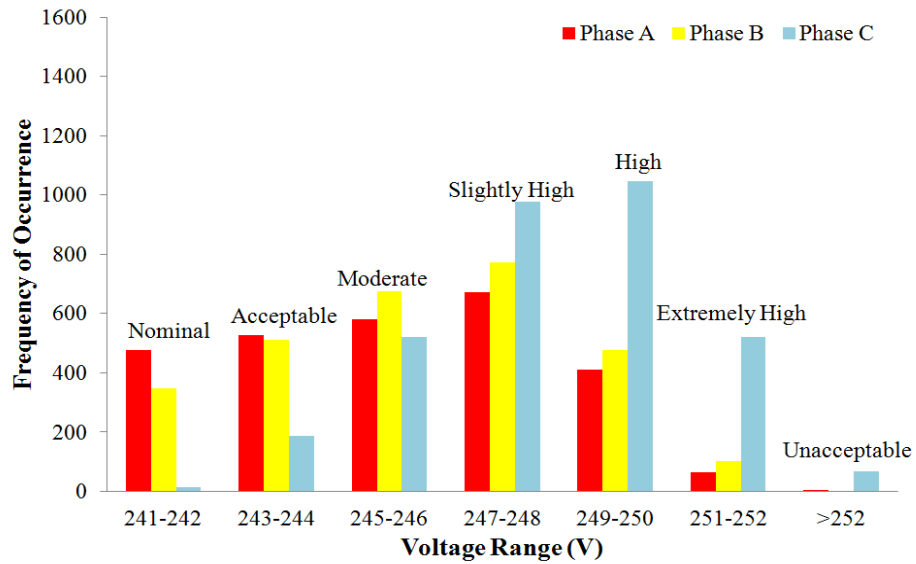


Figure 4.4 Frequency of the occurrence of voltage magnitude at the PCC

In this study, the upper voltage limit is set at 249 V. The probability of having voltage being greater than 249 V within a day is determined so that the likelihood of having voltage violation per day can be defined. Figure 4.5 shows the daily kWh generated by the PV system and the probability of having violation per day on Phase C. It is shown that the probability of having voltage violation per day is about 47% on average between 6th of March to 24th of March 2013. It is clearly illustrated that the violation of voltage is apparent in the future trend.

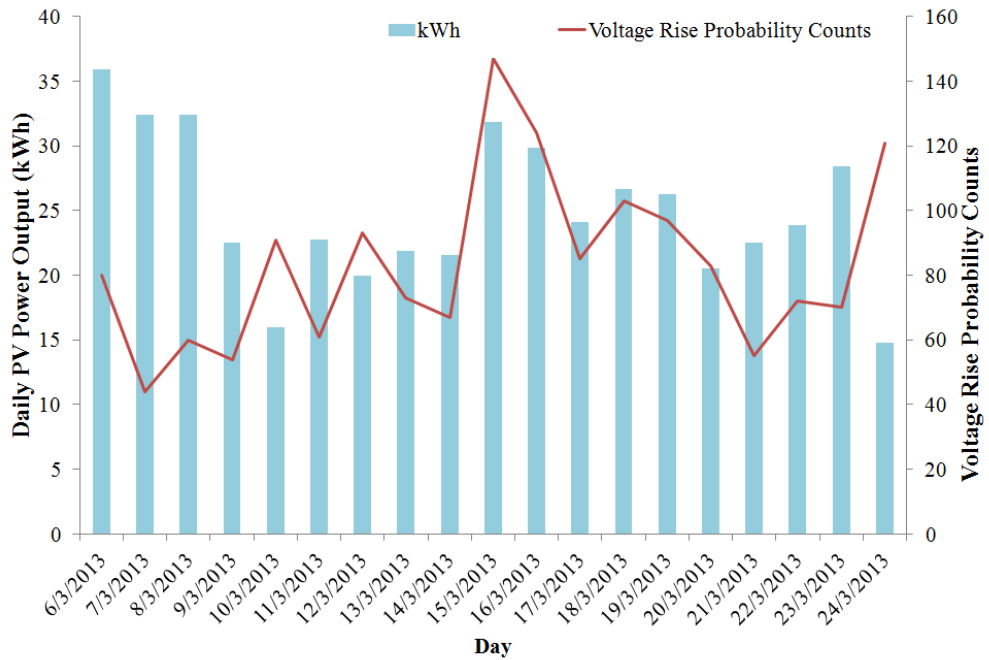


Figure 4.5 Daily PV power output in kWh and probability counts for the voltage rise from 6th-24th March 2013

4.3.2 Characteristic of Voltage Unbalance

The acceptable level of tolerance of the voltage unbalance factor is 2.0% in Malaysia. Figure 4.6 shows the relationship between the PV power output and the voltage unbalance factor as on 15th March 2012. The network voltage unbalance factor is approximately 0.5% when there is minimum PV power output from 12.00 am to 8.00 am. The voltage unbalance factor increases together with the PV power output. The voltage unbalance factor at the PCC hits beyond the acceptable tolerance of 2.0% during the peak PV power output which happens between 12.00 pm and 2.00 pm of the day. Eventually, the voltage unbalance factor drops to the minimum level when there is little PV power output starting from 6.30 pm.

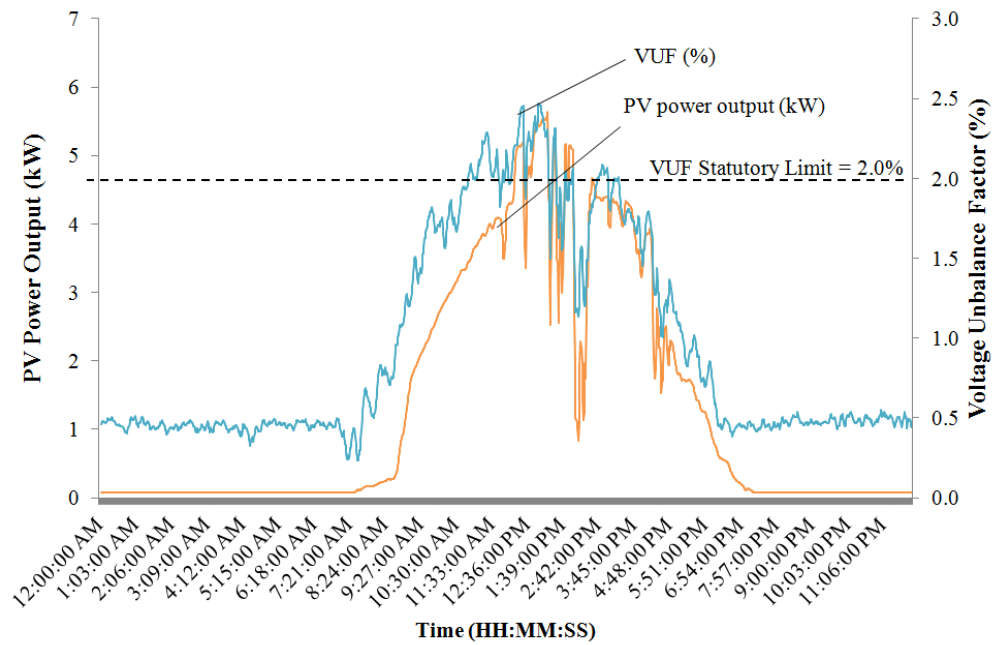


Figure 4.6 Relationship between the voltage unbalance factor and the PV power output on the 15th March 2013

A probability chart is plotted to show the probability of different range of voltage unbalance factor throughout the monitoring period. Figure 4.7 shows that the majority of the voltage unbalance factor happens between 1.0% and 2.0% and the corresponding durations are 60 seconds. However, it is also shown that the violation of voltage unbalance factor occurs for a duration of more than 60 seconds. Such violation is not acceptable by the utility companies. From the above, it can be proved that voltage unbalance factor violation occurs in Malaysia.

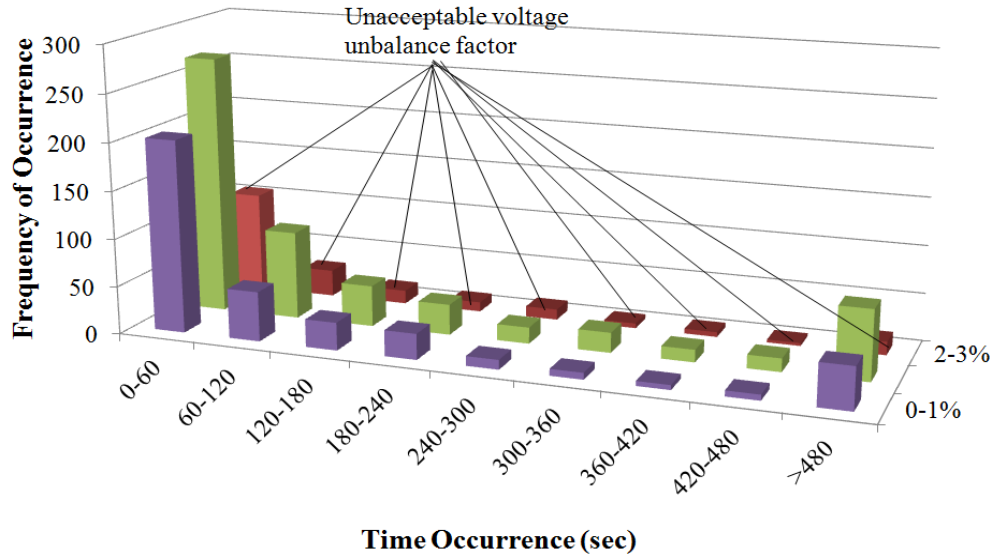


Figure 4.7 Probability counts of the voltage unbalance factor with respect to different time period

4.3.3 Quantification of Voltage Fluctuation and Flicker

The PV systems generate power from 8.00 am to 6.00 pm. Therefore, the values of voltage magnitude within this period are used to calculate the short-term and long-term flickers. Figure 4.8 shows the short-term and long-term flicker indices in Phase C where the PV systems are connected. The statutory limits for both the short-term and long-term flicker indices are 1.0 and 0.65 respectively. It is shown that the short-term flicker indices always rise above the maximum limit of 1.0.

The long-term flickers will rise above the limit of 0.65 for 65% of the time. It is also noticed that when there is minimum PV power output, the short-term flicker index is 0.38 while the long-term flicker index is 0.36. These values represent the background flicker indices and they are highly dependent on the

activities in the premise. It is clearly proved that the flickers on the network integrated with PV systems are very severe when the frequency of the passing clouds is very high.

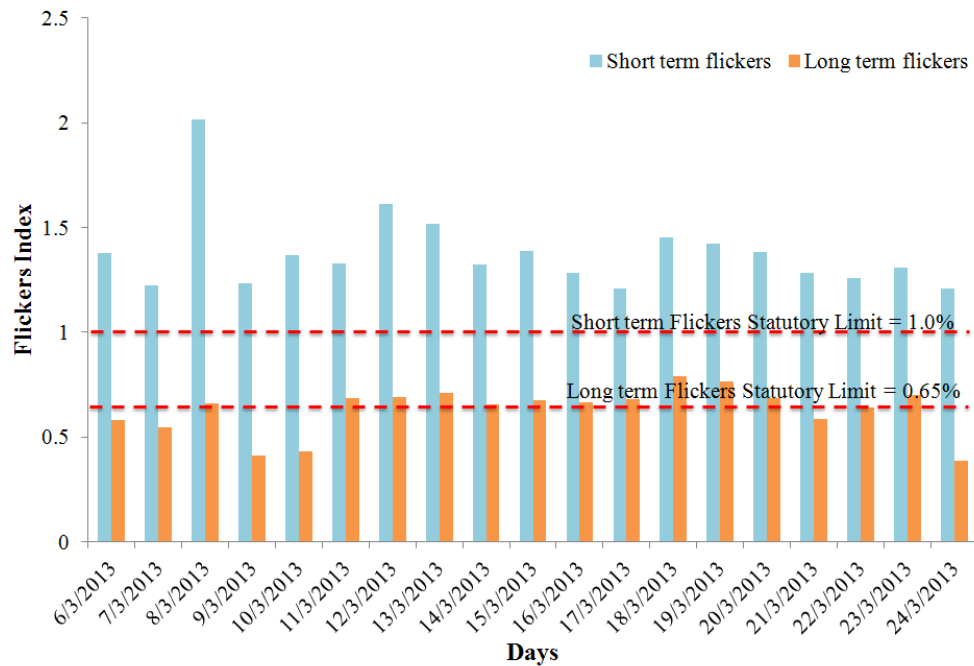


Figure 4.8 Short-term flicker and long-term flicker indices at the point of connection with the PV systems

4.4 Impacts of Voltage Issues on the low-voltage Distribution Networks

The nominal voltage supply in the Malaysian low-voltage distribution network is 230/ 400 V. In accordance with the International Electrotechnical Commission standard IEC 60038:2009, the statutory limit for voltage excursion on the low-voltage distribution network is +10% and -6% with reference to 230 V. Any unwanted voltage rise in the distribution network has the possibility to cause damage to the household equipment.

In a three-phase network, voltage unbalance takes place when the magnitude of each phase voltage is different or the phase angle between any two phase voltages differs from the balanced conditions. The fundamental principles of a three-phase four wire systems show that there should zero voltage unbalance factor if a balanced load condition is to be maintained. However, such a situation is hardly achieved because of the use of single-phase and non-linear loads such as switch-mode power supplies.

Table 4.2 shows a voltage unbalance of 1.0% can create 6 to 10 times the current unbalance. This current unbalance can create unnecessary temperature rise in the motor windings that degrade the performance and shorten the lifespan of the induction motors (McCoy and Douglass, 1996). The unbalanced condition could also deteriorate if a large amount of single-phase renewable energy sources are installed on the distribution networks (Jenkins et al., 2000).

Table 4.2 Voltage unbalance effects on a typical electric motor (Basso, 2008; Thomas, 2008)

No.	Characteristic	Performance		
1	Average voltage	230 V	230 V	230 V
2	Percentage of unbalance voltage	0.3	2.3	5.4
3	Percentage of unbalance current	0.4	17.7	40.0
4	Increased temperature rise (in Celcius)	0	30	40

Voltage fluctuation and flicker commonly happens on the high voltage (HV) and medium voltage (MV) networks (Dugan et al., 2012). This is because of machines like arc furnace, welding machines, rolling mills and mine winders are connected to the HV and MV networks (Deokar and Waghmare, 2010). However, flickers are not common on the low-voltage networks. If they

happen on the low-voltage networks, their durations are usually very short. This is because the low-voltage flickers are caused by the starting of large electrical motors, X-ray machines, pumps and refrigerators (Central, 1964). The impacts are not significant. However, if the occurrences of the flickers are too frequent, then electrical motors can exhibit a change in their starting torques and increase their power consumptions which create additional heat and reduce the efficiency of the machines. This can shorten the lifespan of the motors.

Voltage fluctuation and flicker can cause light sources to vary their luminosity. An individual can be affected by light flickers and may cause headaches, migraines and eye discomfort. In addition, unstable voltage supply causes electronic equipment malfunction, unwanted triggering of uninterruptible power supply (UPS) units to switch to battery mode and thus reducing the operational efficiency (IEC 61000-3-3, 1994)

4.5 Discussion

PV systems are likely to become the dominant type of the renewable energy sources in the Malaysian market due to its abundant solar irradiance. Although the Malaysian government has developed an effective policy on renewable energy to reduce the dependency of fossil fuel and mitigate the effect of climate change, none of these policies provide a detailed guideline on the installations of PV systems. The technical issues are apparent in Malaysia

where the frequency of passing clouds is possibly the highest in the world. Furthermore, most of the PV systems installations are customer driven and non-centrally planned. Therefore, improper coordination on the PV system installation may cause voltage unbalance due to non-uniform distribution. During low load condition, excess power injection may cause voltage rise.

Government and the utility company should establish the financial support scheme to enhance and mitigate the power quality issues caused by the PV systems. The funding can be created from the electricity bills, tax revenue, or a combination of both. The Malaysian government can imitate the feed-in tariff funding policy by including all system added cost for power quality mitigation system to the rate base and share among all electricity customers. However, the drawback of this option by spreading the cost may burden the society in large. Alternatively, the government can also allocate the tax revenue to implement the system. Other approaches such as to impose specific tax, for example, energy tax or carbon tax can be implemented as well. Funding generated from the tax has the possible risks because the stability of the policy environment can change with political and budgetary priorities.

National Renewable Energy Laboratory (NREL) suggests that this funding can be also generated through inter-utility cost sharing. Utility companies operate under high solar power district do not shoulder the full burden of any supplementary costs (Toby et al., 2010). Electricity distribution in Malaysia is very different from the deregulated market in the United States, United Kingdom and Singapore. There is no inter-utility cost sharing as the utility

companies in Malaysia monopolize the electricity market in Peninsular Malaysia, Sabah and Sarawak.

This chapter features the investigation of voltage severity of a 7.2 kW_p PV system connected on the electrical grid of the University. The voltage magnitude are measured and recorded on a regular basis over a period of time. Throughout the monitoring period, it is noticed that the voltage at the PCC are likely to violate its statutory limit. Furthermore, Malaysia is one of the countries with zero clear sky condition, and hence passing clouds can cause the PV power output to fluctuate.

The substantial fluctuation of PV power output can cause the voltage magnitude to vary. Nevertheless, installation of the renewable energy sources on the distribution network also play an important role in improving the reliability of the grid, reducing transmission loss and also provide voltage support. These can only be achieved if the installations are well planned. In general, the study has characterised the PV power output. The probability density of voltage rise and voltage unbalance factor is derived from the measurement data. Short-term and long-term voltage flicker indices are calculated to evaluate the severity of the flicker emission.

CHAPTER 5

**DESIGN AND DEVELOPMENT OF THE ENERGY STORAGE
SYSTEM**

5.1 Introduction

Energy storage system is one of the possible solutions for the technical issues caused by the integration of renewable energy sources with the low-voltage distribution networks. However, an energy storage system without appropriate control strategy does not solve the problems effectively. In this chapter, the physical architecture and the details of the control algorithm to control the proposed energy storage system are presented. Fuzzy logic is proposed to be part of the controller because it is different from the traditional Boolean as it can produce an appropriate output based on the changes in the input. The fuzzy control method employed in the energy storage system is able to manipulate the amount of its real power appropriately and effectively based on the changes in voltage magnitude at the point of concern. Figure 5.1 illustrates the process flow of the energy storage development. The physical development of the energy storage system can be divided into 8 stages as follows:-

Step 1: Setting up the bi-directional inverter, namely Sunny Island 5048

Sunny Island 5048 is mounted in an appropriate location before setting up the electrical connection, such as grounding, DC connection to the batteries and AC connection to the experimental distribution network. In this section, the details of all necessary connections are explained.

Step 2: Connecting to the battery bank

Sunny Island is powered up with 48 V lead acid batteries. Details of the lead acid batteries are illustrated in this section.

Step 3: Configure the Sunny Island 5048

After power up, Sunny Island is configured for the first time. A new system is configured according to the network parameters such as grid voltage, system description, and battery information.

Step 4: Configure the communication module

To enable the control strategy, it is necessary to configure the communication module in order to establish a link between the Sunny Island 5048 and the supervisory computer.

Step 5: Communication link with Supervisory Computer (LabVIEW™)

Once the hardware is ready, LabVIEW™ is used as a programming platform to monitor the energy storage system and network conditions. The program manipulates the power flow of the energy storage system in order to maintain the voltage quality without limiting the amount of PV systems.

Step 6: Stage I manual control

In this section, a manual control is established to communicate with the Sunny Island 5048 so that it can react according to the commands that are manually input by the supervisory computer.

Step 7: Stage II simple control

After the manual controller is set, a simple control algorithm is developed to monitor the network conditions and react based on the local voltage conditions. The controller is capable of performing simple process control to instruct Sunny Island to inject or absorb power in a single step change once at a time based on the measured voltage from the experimental network.

Step 8: Stage III fuzzy control

As mentioned earlier, the PV power output in Malaysia is fluctuating frequently. The simple controller is unable to cater the fast changing voltage levels due to the intermittent PV power. Therefore, a fuzzy logic controller is proposed to overcome the shortcoming of the simple controller. This section illustrates the fuzzy control strategy and the controller details.

Final step: Evaluation

Various scenarios under different generation and load conditions are considered to evaluate the performance of the fuzzy controlled energy storage system. Results show that the fuzzy control energy storage system is operated autonomously to reduce voltage rise and mitigate voltage unbalance in the distribution networks.

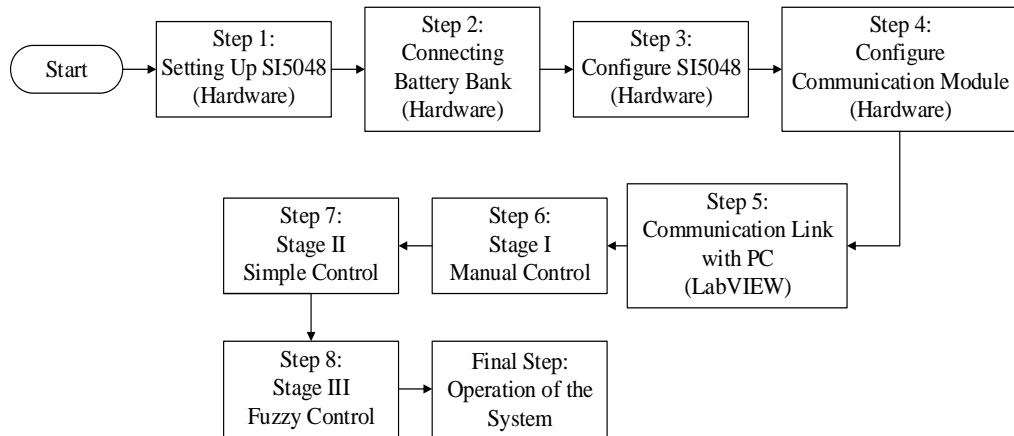


Figure 5.1 Flow chart of the energy storage system development

5.2 Energy Storage System

The physical architecture of the proposed energy storage system is developed with a bi-directional inverter, namely Sunny Island 5048 integrated with the battery bank as shown in Figure 5.2. It is designed and developed to mitigate the voltage rise and voltage unbalance caused by the intermittent PV power output on the distribution network. The battery bank is built with 16 units of valve-regulated lead acid (VRLA) batteries. A communication module, RS485/USB converter is used to establish a communication link between the bi-directional inverter and the supervisory computer.

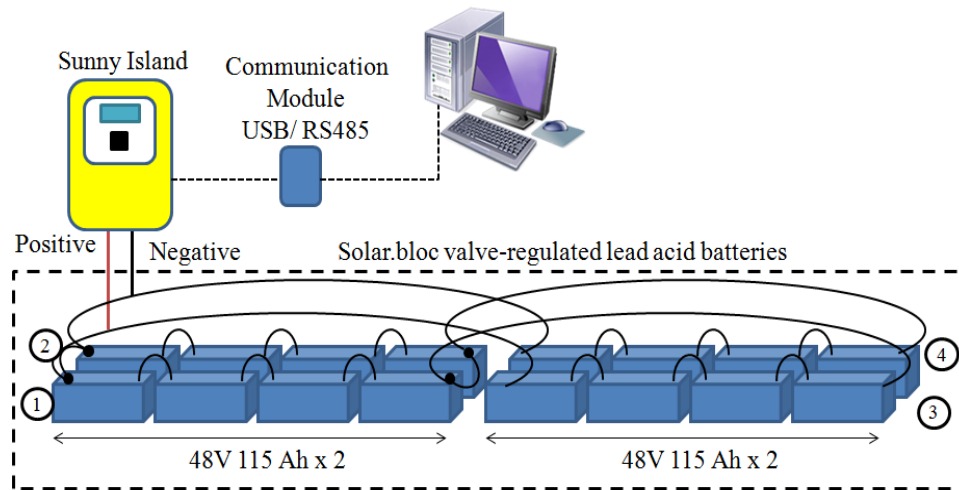


Figure 5.2 Setup of the energy storage system

5.2.1 Step 1: Setting Up the Bi-directional Inverter, namely Sunny Island 5048

Sunny Island 5048 is a bi-directional inverter manufactured by SMA GmbH from Germany. This Sunny Island is used in a standalone power system with renewable energy sources. The maximum rated power output of the bi-directional inverter is 5.0 kW. Sunny Island offers the highest flexibility where real time active and reactive power controls are possible. Furthermore, the parallel operation of 3 devices on a single-phase or three-phase network allows Sunny Island to supply the output power of 3 kW up to 300 kW. In this work, the Sunny Island 5048 integrated with batteries are controlled by the proposed fuzzy control algorithm to mitigate voltage rise and voltage unbalance caused by the intermittent PV power output on the low-voltage distribution networks.

Sunny Island 5048 operates with 48 V batteries. Figure 5.3 shows the Sunny Island connection layout. The VRLA batteries are connected to the battery cable connection labelled as (A) in Figure 5.3. While the AC output cables are connected with the connectors labelled as (B). In order to establish an external communication between the Sunny Island and the personal computer, a communication chipset namely piggy back PB-485-G2 needs to be added onto the communication interface labelled as (C) as shown in Figure 5.3.

The piggy back is an accessory to the bi-directional inverter, and it acts as a key to trigger the communication port in the bi-directional inverter. The ports (D) *Com Sync In* and (E) *Com Sync Out* are used to establish internal communication link between two bi-directional inverters to form a master and slave unit. An external RS485/USB converter, namely ICP CON I-7563 is connected in between the (F) *Com SMA In* port and the USB port to transfer the serial data to the personal computer while a terminating resistor should be plugged into the *Com SMA Out* port labelled as (G).

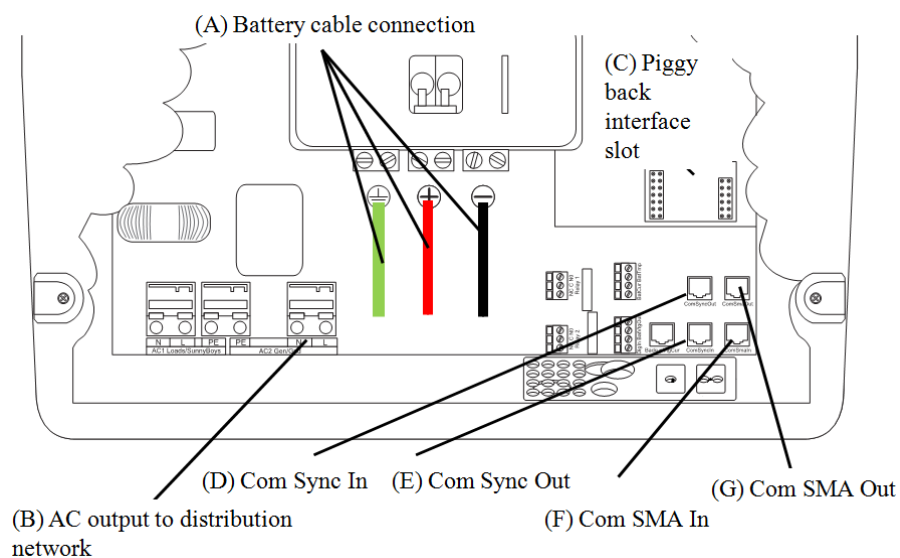


Figure 5.3 Connection layout of the Sunny Island bi-directional inverter

The Sunny Island 5048 can be connected in parallel with two or more units in order to increase the overall power output. Figure 5.4 (a) shows the configuration for single-phase energy storage system with one master unit and Figure 5.4 (b) illustrates the configuration for single-phase energy storage system with one master unit and one slave unit working in parallel to increase the overall power output.

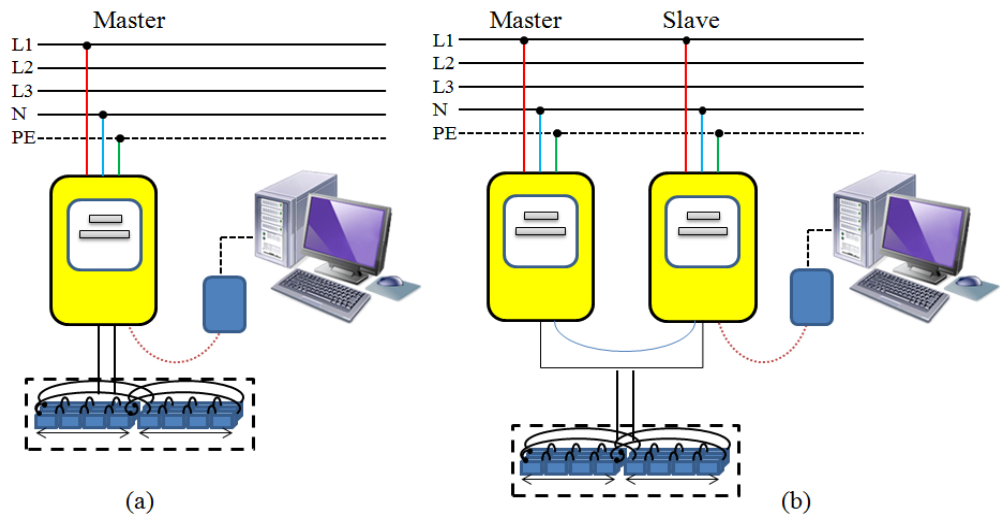


Figure 5.4 Configuration of single-phase energy storage system with (a) one master unit and (b) one master and one slave unit

Apart from these arrangements, three units of the Sunny Island 5048 can be arranged to have three single-phase energy storage systems in order to individually cater for each phase as shown in Figure 5.5. A RJ45 cable is needed to interconnect each Sunny Island in order to establish an internal communication bus between the Sunny Island modules. In each phase, up to 3 Sunny Islands can be interconnected to form a cluster system. Figure 5.6 shows the communication connection configuration for multiple devices working in parallel.

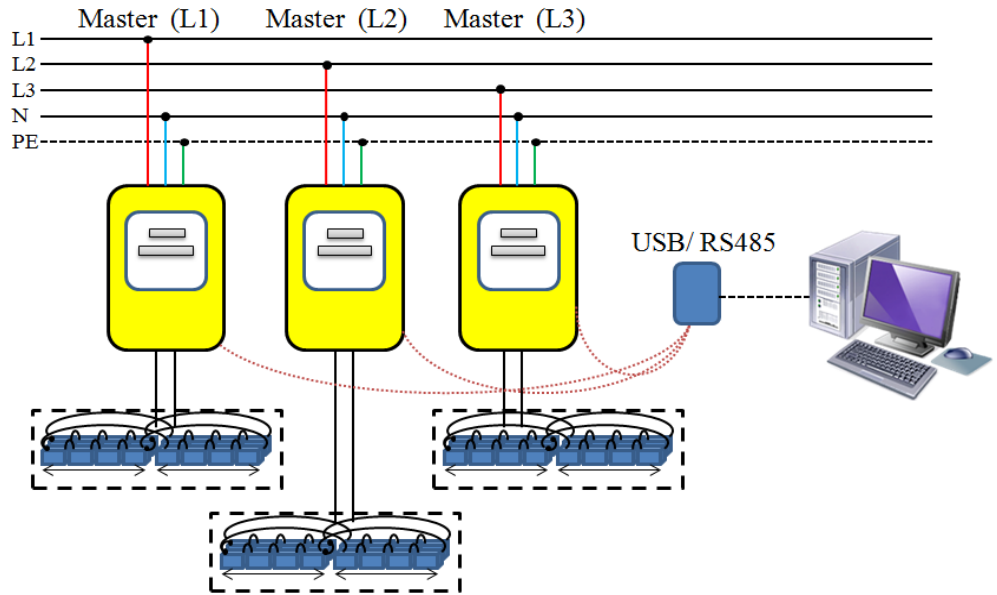


Figure 5.5 Configuration of three single-phase energy storage systems

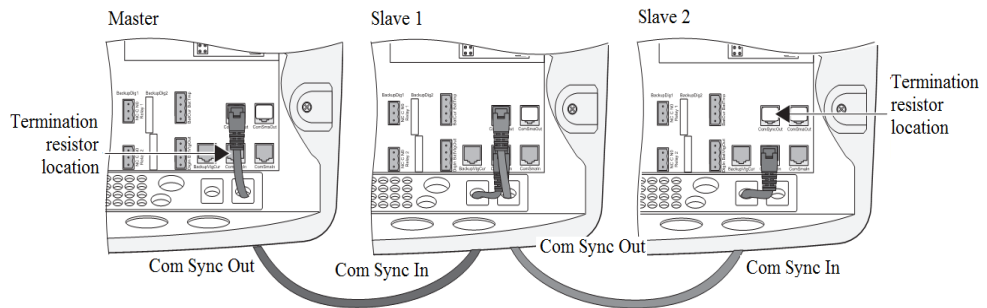


Figure 5.6 Configuration of the master and slave units via Com Sync In and Com Sync Out port

5.2.2 Step 2: Connecting to the Battery Bank

The battery bank is made up by 16 units of valve-regulated lead acid (VRLA) batteries. Each of the bi-directional inverter is integrated with four banks of batteries connected in parallel. Each bank consists of four units of Hoppecke solar. bloc VRLA batteries connected in series to have a capacity of 115 Ah at 48 V. These batteries are connected in parallel to have a greater capacity. The

total capacity for each Sunny Island 5048 is 460 Ah with an energy capacity of 5.52 kWh. The rated power for Sunny Island 5048 is 4.0 kW at 45°C and 5.0 kW at 25°C. Figure 5.7 shows the total units of batteries installed in the laboratory. Figure 5.8 shows the estimated life cycle of these batteries. It is observed that with a depth of discharge at 48%, it will result in 1,193 life cycles.

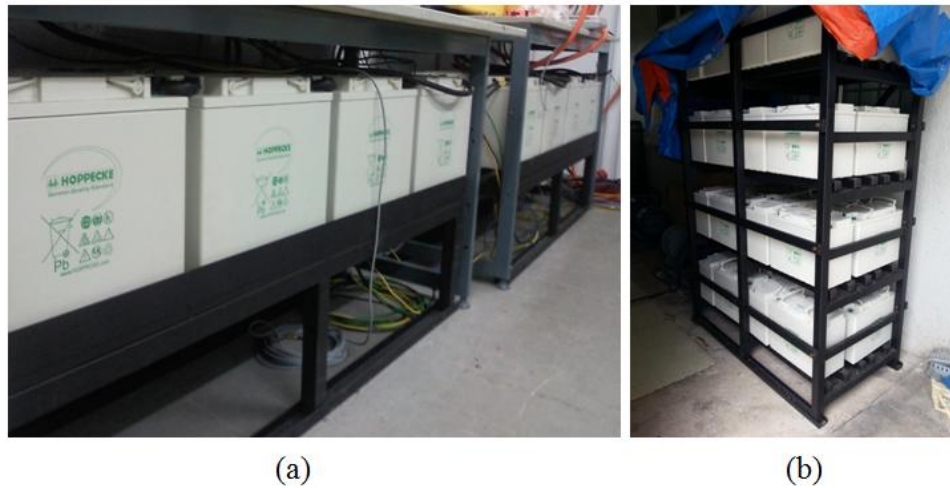


Figure 5.7 Three sets of valve-regulated lead acid batteries install (a) inside the laboratory and (b) outside the laboratory

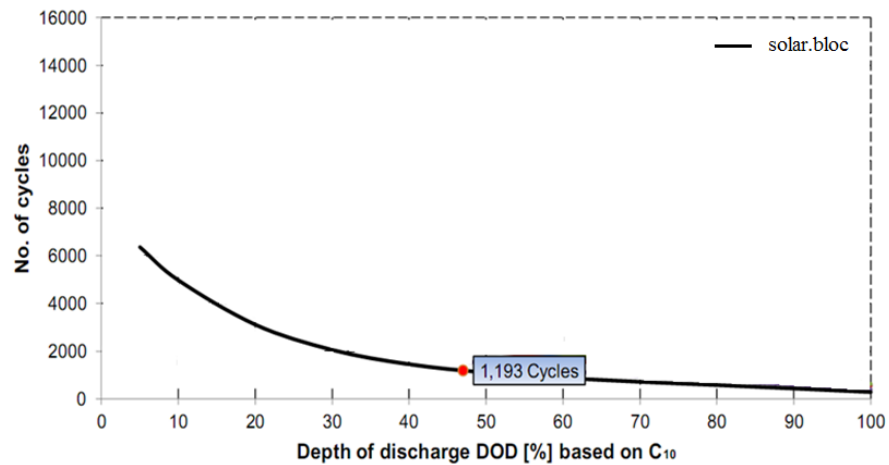


Figure 5.8 Depth of discharge for solar.bloc 135 based on C₁₀

5.2.3 Step 3: Configure the Sunny Island 5048

When Sunny Island 5048 is first powered up, Quick Configuration Guide (QCG) prompts the user for initial configuration. All the necessary parameters such as grid voltage, system configuration (e.g. three-phase system or single-phase) and battery configuration (e.g. the battery types, nominal voltage, charging current and battery capacity) need to be initialised for the first time. Sunny Island 5048 supports highest flexibility on real and reactive power control. This can be enabled by configuring several parameters as follows:

Step 1: Enter the installer password

(Password: Sum of digits of the operating hours)

Step 2: Select #600 to Direct Access

Step 3: Key in parameter number

#23801 FedInEna: Enable

#23802 FedInMod: Com

The parameter #23801 FedInEna is used to enable the ability to feed-in current from the Sunny Island to the grid. The parameter #23802 FedInMod is used to activate the communication between supervisory computer and the Sunny Island 5048. The real and reactive power can be controlled via the parameter #23807 FedInCurAt and #23808 FedInCurRt respectively. A positive value in the real power control indicates that the current is flowing out from the battery to the distribution network while a negative value indicates that the battery is being charged. Similarly for reactive power control, a positive value means capacitive reactive current while a negative value means an inductive reactive current.

5.2.4 Step 4: Configure the Communication Module

A communication module, RS485/USB converter is used to establish a communication link between Sunny Island 5048 and the supervisory computer. This communication module is manufactured by ICP Con from Taiwan with a model number I-7563 as shown in Figure 5.9. It is a cost effective module for transferring serial data over USB. The communication module comes with a self tuner that automatically tunes the baud rate and data format to the RS485 network.

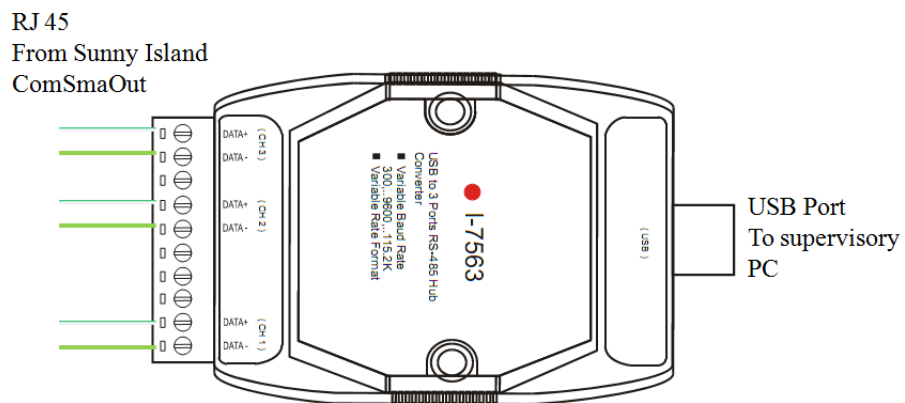


Figure 5.9 Configuration for communication module RS485/USB converter

5.2.5 Step 5: Communication Link with Supervisory Computer

A supervisory computer is used to communicate with the energy storage system via RS485/USB converter. The flow of data measurement and the instruction is represented in Figure 5.10. LabVIEW™ is used as a development environment to program a monitoring and controlling system for the distribution network and energy storage system. The data sent by the

supervisory computer to the data socket I/O interface are translated into a standard OLE process control (OPC) format. OLE is known as Object Linking and Embedding (OLE) for process control. The RS485/USB converter then changes the data from the OPC format into an appropriate format before sending to the energy storage system.

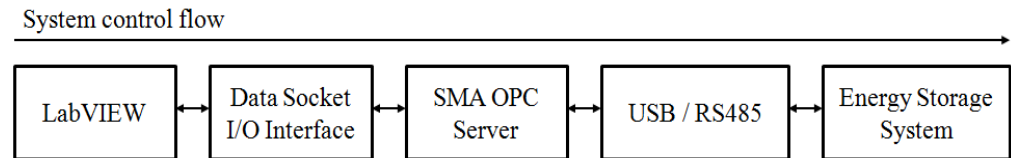


Figure 5.10 Block diagram of the communication system flow between the supervisory computer and the energy storage system

SMA OPC Server is functioning as a driver system to implement communication with SMA devices by using SMA data protocols via SunnyNet or SMANet. The standard filename of the initialisation file is named as “yasdi.ini”. To begin with, the configuration of SMA OPC Server can be customized through the file yasdi.ini.

Referring to the YASDI documentation (Prussing, 2006), Table 5.1 shows that the SMA data protocol can be initialized as follows:

Table 5.1 YASDI initialisation file formed with three sections.

Entry	Description	Define Value
(I) Driver Module		
Driver	- The interface driver to be loaded during runtime. (The file “yasdi_drv_serial.dll” provided by SMA for Windows operator)	yasdi_drv_serial.dll
(II) Communication Module		
Device	- Mandatory Entry. - Serial interface, “COM x” for Windows. While x can be 1, 2, 3... depending on the port location.	COM 3

Media	- Mandatory Entry. - RS232/ RS 485	RS232
Baudrate	- Mandatory Entry. - Speed of the serial interface in bits per second. - Value varies from 1200, 2400, 4800, 9600, 19200. Support up to 19200 bits/seconds in which is the fastest transport rate.	19200
Protocol	- Mandatory Entry. - SunnyNet/ SMA Net. - Newer device such as Sunny Island 5048 uses the protocol SMA Net.	SMANet
(III) Master Module		
ReadParamChanTimeout	Optional Entry. Timeout time in seconds for reading parameter channels.	4
ReadParamChanRetry	Optional Entry. Number of attempts to be retry for reading parameter channels.	3
WriteParamChanTimeout	Optional Entry. Timeout time in seconds for writing parameter channels.	4
WriteParamChanRetry	Optional Entry. Number of attempts to be retry for writing parameter channels.	3
ReadSpotChanTimeout	Optional Entry. Timeout time in seconds for reading spot value channels.	4
ReadSpotChanRetry	Optional Entry. Number of attempts to be retry for reading spot value channels.	3

The above is the configuration for communication with Sunny Island 5048. The device communicates through the serial interface, COM 3 of the respective PC. The speed of the serial interface is 19200 bits per second and the transport protocol uses SMANet. The timeout period for the reading and writing parameters from the device is set to 4 seconds. If the read/ write fails, it will attempt for 3 times. Similarly, the timeout period for reading spot value channels is defined as 4 seconds while the retry attempts is set to 3 should the reading failed. Appendix C shows the initialisation program for yasdi.ini.

As mentioned earlier, LabVIEW™ is used as a programming platform to develop the controlling and monitoring features for the energy storage system. LabVIEW™, also known as Laboratory Virtual Instrumentation Engineering Workbench is ideal for any measurement, data acquisition and instrument control system.

In LabVIEW™, data socket I/O interface is developed to allow easy data transfer over many protocols such as OPC (OLE Process Control), HTTP (Hypertext Transfer Protocol) and FTP (File Transfer Protocol). Table 5.2 shows the list of parameters that are readable from Sunny Island via the communication link established earlier. The appropriate format to subscribe to an OPC server in LabVIEW™ is written as follows:

opc://ServerName/OPCServer/DeviceAddress(Serial Number)\ChannelName

Table 5.2 List of parameters readable in Sunny Island

No.	Channel Name	Description
1	BatVtg	Battery voltage (V)
2	BatSoc	Battery state of charge (%)
3	InvVtg	Inverter voltage (V)
4	InvPwrAt	Inverter real power (kW)
5	InvPwrRt	Inverter reactive power (kVar)
6	Vac	Grid voltage (V)
7	Iac	Grid current (A)
8	Fac	Grid frequency (Hz)
9	TotBatCur	Total battery current (A)

Figure 5.11 shows the block diagram to manipulate the real and reactive power flow of the energy storage system using data socket I/O interface. The data socket is initialised in URL format before opening the connection. Once the connection is established, the data value of the parameter to be written is

updated before closing the connection. These steps will be repeated until the program is stopped.

Similarly, Figure 5.12 shows the LabVIEW™ block diagram that is used to read data from the Sunny Island. The list of parameters in URL format is used to initialise the data socket before opening the connection. Once the connection is established, these parameters values will be updated every seconds and will be written into the excel sheet for further analysis.

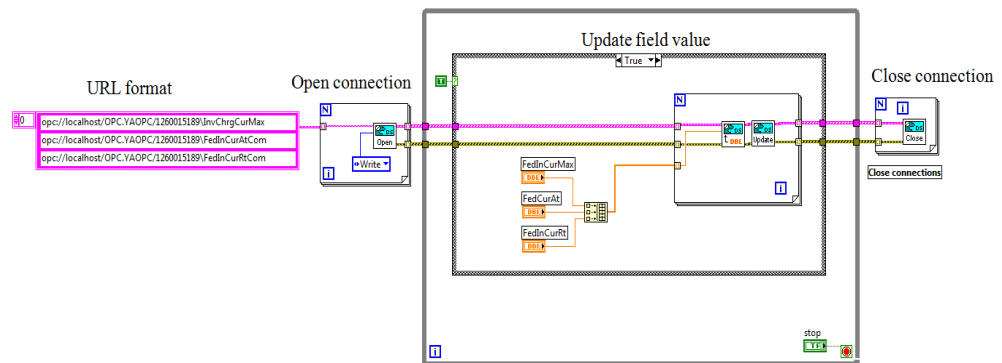


Figure 5.11 LabVIEW™ block diagram for writing real and reactive power of energy storage system

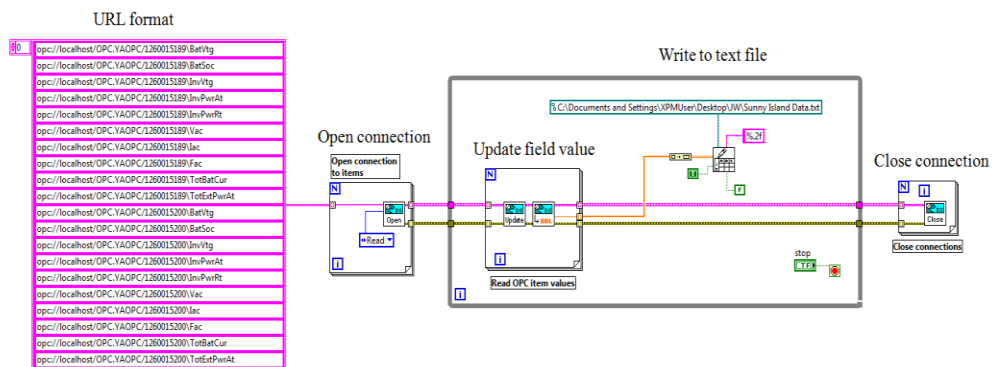


Figure 5.12 LabVIEW™ block diagram reading from energy storage system and data are written to text file

5.3 Step 6: Stage I Simple Controller

Centralised communication controllers have been implemented in the experimental low-voltage distribution network using LabVIEW™. As mentioned earlier, it is possible to control both the real and reactive power flow of the energy storage system. This can be achieved by manipulating the feed in current using the communication bus. Several tests were carried out to evaluate the performance and response of the Sunny Island 5048 as follows:-

- i) Scenario I: Charging energy storage system
- ii) Scenario II: Discharging energy storage system

Figure 5.13 shows the front panel of the controller in LabVIEW™. The front panel consists of grid and energy storage monitoring system that displays all the measuring data from the Power Meter and the energy storage system. The current controller is used to manipulate the real and reactive power flow import/ export from the energy storage system.

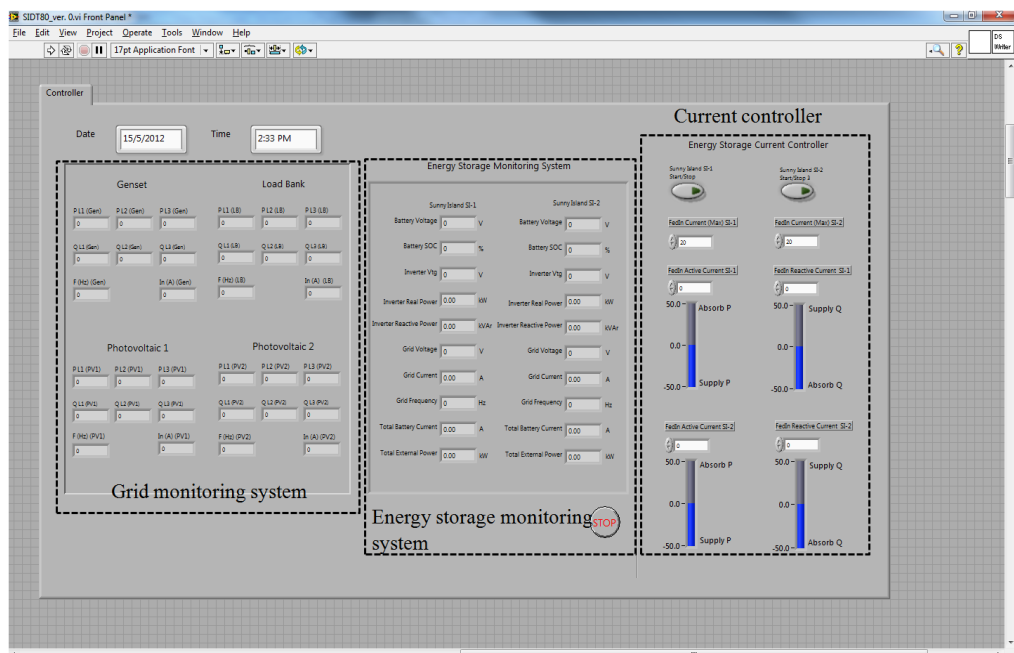


Figure 5.13 Front panel of LabVIEW™ with grid and energy storage monitoring system, and current controller

Scenario I: Charging

This test seeks to investigate the performance of Sunny Island 5048 in response to the charging instruction by manipulating the current control in LabVIEW™. In this test, the energy storage system in Phase A receives the instruction to charge the battery. Figure 5.14 (a) shows the charging power and the control current of the energy storage system. It can be observed that the control current is proportional to the charging power. Negative values indicate charging while positive values indicate discharging from the batteries. For example, the energy storage system is charging at 1.1 kW when receiving a -5A instruction from the current controller.

Figure 5.14 (b) and (c) show the voltage profile and voltage unbalance factor of the experimental network respectively when the energy storage system is charging at a different rate. This test is used to verify the response of the energy storage system in relation to the command received from the control algorithm. This test also shows the limitations of the experimental network with respect to the voltage unbalance factor and voltage profile. Figure 5.14 (b) also shows the network voltage unbalance has been increased above the statutory limit of 2.0% when the energy storage system is charging at 2.2 kW. Figure 5.14 (c) shows that even though the energy storage system is charging in Phase A, the voltage in phase B rises above the limit of 252 V due to the mutual coupling effect on the distribution network.

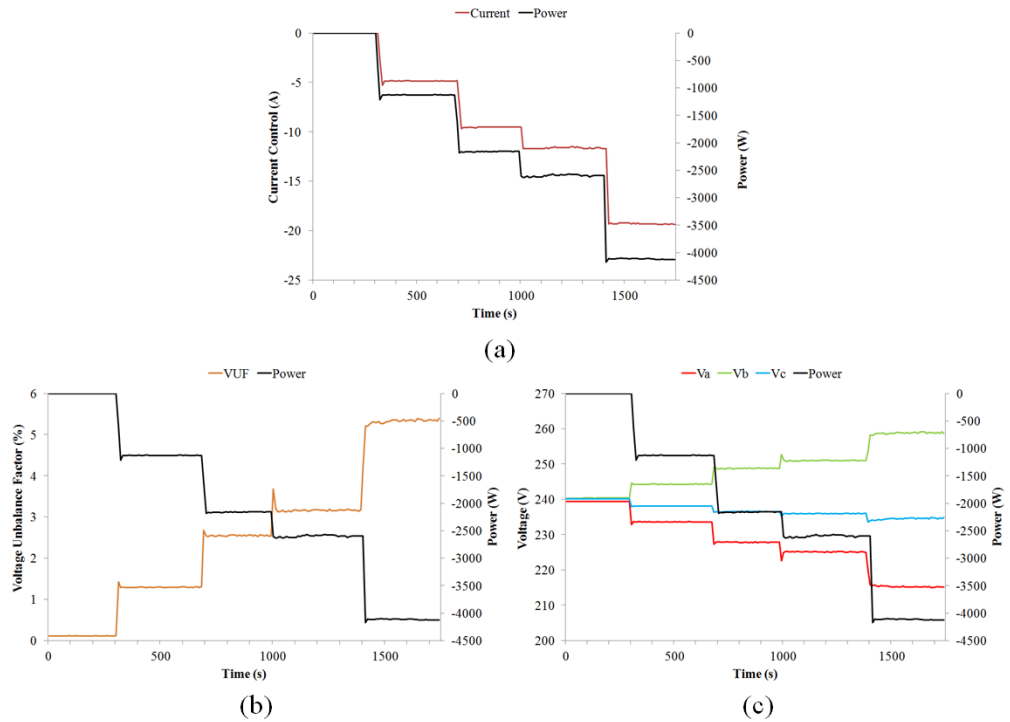


Figure 5.14 Response of the energy storage system (a) in relation to the charging current control, (b) network voltage unbalance factor and (c) three-phase voltage profile

Scenario II: Discharging

The performance of the energy storage system to export power to the experimental low-voltage distribution network in relation to the current control is studied using Scenario II. As mentioned earlier, positive value of the control current indicates discharging power from the batteries. Figure 5.15 (a) shows the energy storage power output and the control current. Figure 5.15 (b) shows the network voltage unbalance factor and load profile. Figure 5.15 (c) shows the voltage profile throughout the experimental case study.

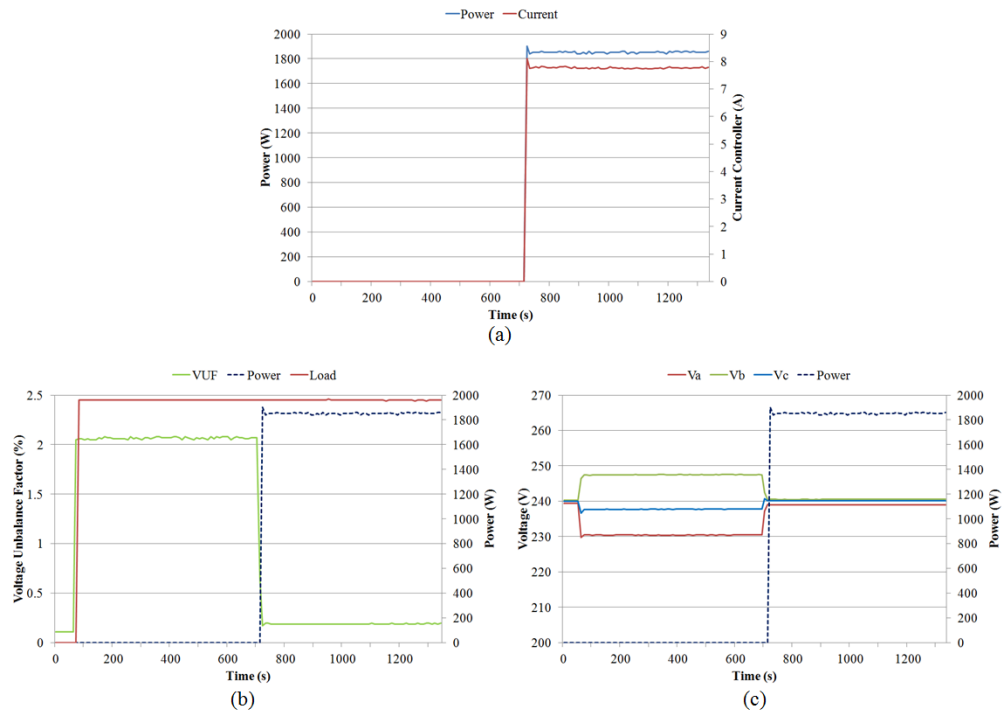


Figure 5.15 Response of the energy storage system in relation to (a) the discharging current control, (b) network voltage unbalance factor and (c) the three-phase voltage profile

At 100 s, a 2.0 kW load is introduced in Phase A of the experimental low-voltage distribution network while Phase B and C are at no load. It is observed that the voltage unbalance factor has been increased up to 2.0% with the unbalanced load condition. At 700 s, the energy storage system receives the instruction from the control algorithm to export power of 1.9 kW to the load. As a result, the voltage unbalance factor is reduced to 0.1%.

5.4 Step 7: Stage II Simple Automated Control

A simple control technique that can be used on the energy storage system has been outlined in the previous section. In this stage, a simple automated control

algorithm is further implemented from the simple control technique. This control algorithm is used to study the response of the energy storage system with respect to the network conditions.

5.4.1 Control Strategy

This section describes the development of the simple control method to maintain the voltage level by manipulating the power output of the energy storage system (Wong et al., 2013). Figure 5.16 shows the flow chart of the simple control algorithm where the system begins by initializing the $V_{ref} = 240$ V. The voltage level at the PCC is always compared with the lower and upper voltage limits to determine whether the network is within the tolerance or not. If the measured voltage is recorded outside the upper limit boundary due to excessive power generation from the PV, the control algorithm will instruct the energy storage system to store a fixed amount of energy.

Similarly, if the measured voltage falls outside the lower limit boundary, the energy storage system will dispatch power to the network. The simple control algorithm only allows the energy storage system to dispatch/ absorb power once at a time until the voltage condition in the network is within the tolerance value. Figure 5.17 shows the screenshot of the LabVIEW™ front panel for the simple controller. A switch is added to the program to take over the simple control to automated control.

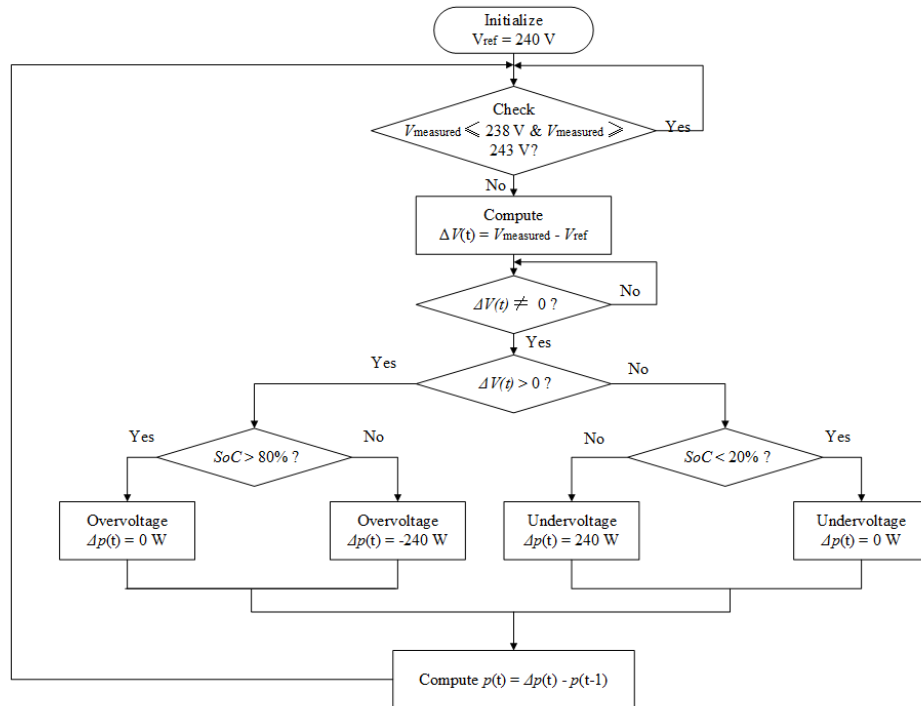


Figure 5.16 Flow chart of the simple control algorithm

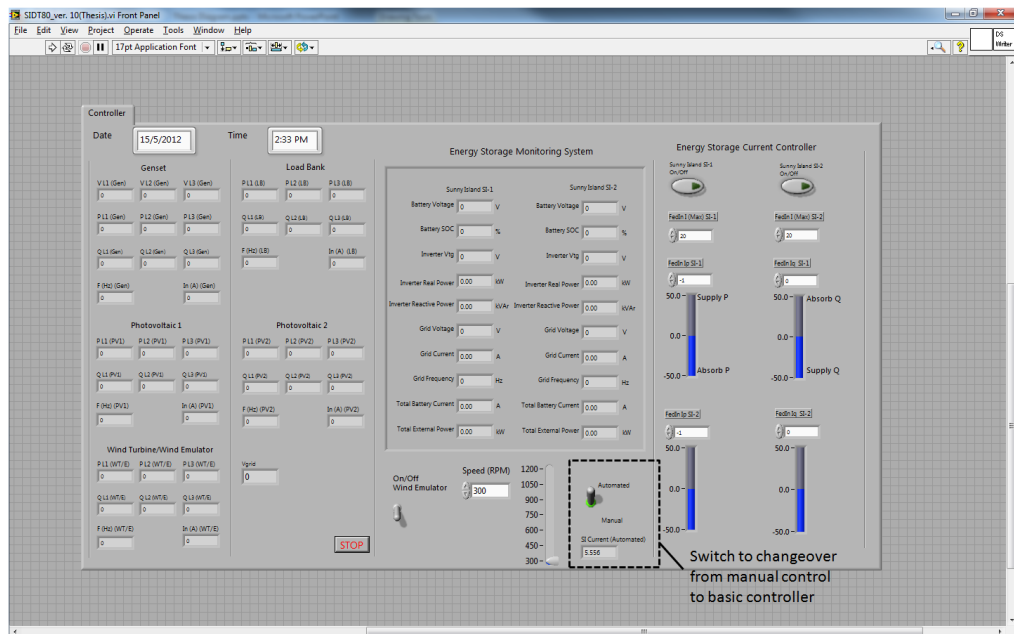


Figure 5.17 Screenshot of the front panel for the controller in LabVIEW™

5.4.2 Operation of the System

In this stage, a simple automated control algorithm is used to manipulate the real power flow of the energy storage system based on the network voltage condition. Several case studies are designed to investigate the performance of the simple control algorithm to reduce voltage rise and mitigate voltage unbalance under various generation and loading conditions. These case studies are listed as follows:-

Case Study I:

In this case study, the voltage profile of the experimental network is studied without the existence of the energy storage system. The case study varies the loading conditions (e.g. balanced load and unbalanced load) in order to investigate the voltage excursion.

Case Study II:

The simple automated control algorithm is first evaluated under unbalanced load variation. The effectiveness of the simple controlled energy storage system to mitigate voltage rise and voltage unbalance is recorded.

Case Study III:

The case study aims to study the performance of the simple automated controlled energy storage system under intermittency PV power output. The effectiveness of the proposed energy storage system to mitigate the voltage rise and voltage unbalance factor is presented.

5.4.3 Case Study I: Voltage Variation under Balanced and Unbalanced Load Condition without Controller

This case study is designed to provide a benchmark for the three-phase voltages and voltage unbalance factor of the experimental network without any correction from the energy storage system. The case study begins with a balanced load condition where each of the phases is connected to a 500 W load. Figure 5.18 (a) shows network voltage unbalance factor is recorded at 0.12% when the loads in all the three-phases are balanced. Figure 5.18 (b) shows the three-phase voltages recorded to be in between 239 V to 240.5 V.

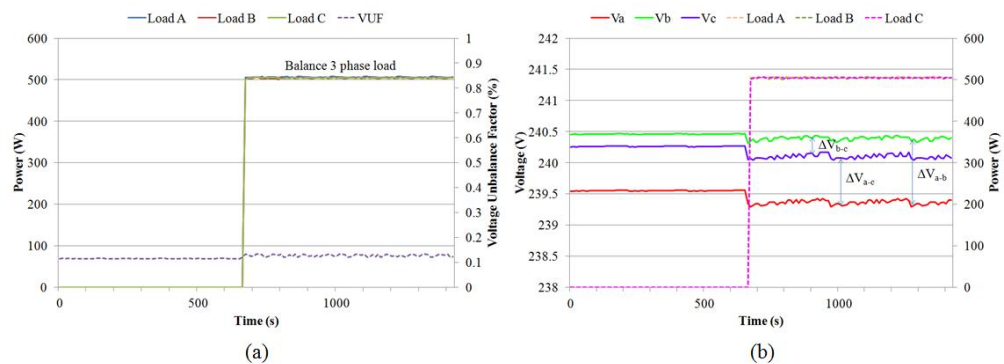


Figure 5.18 (a) Voltage unbalance factor (b) voltage profile at node 1 of the experimental network with balanced load condition

Later, the experimental distribution network is monitored under unbalanced load condition whereby a 500 W load is connected to Phase A while Phase B and C are not loaded. Figure 5.19 (a) shows the network voltage unbalance factor has been risen from 0.1% to 0.6% after Phase A is connected to a 500 W load. Figure 5.19 (b) shows the three-phase voltage values as 237 V, 240.5 V and 242.2 V for phase A, B and C respectively.

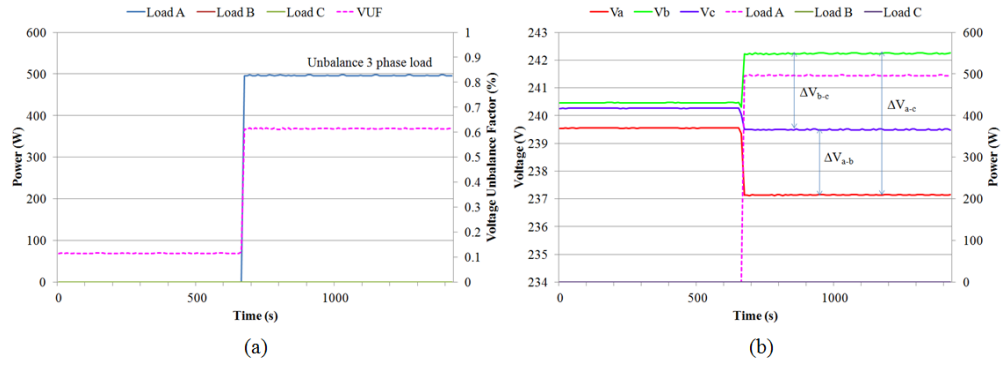


Figure 5.19 (a) Voltage unbalance factor (b) voltage profile at node 1 of the experimental network with unbalance load condition

5.4.4 Case Study II: Simple Controlled Energy Storage System under Unbalance Load Variation

This case study is used to investigate the performance of the simple control algorithm in response to the load variation. At 70 s, 1.0 kW loads are connected to each of the phase A, B and C respectively. After 200 s, an additional 1.7 kW load is added to phase A while phase B and C are kept at 1.0 kW.

Figure 5.20 shows the three-phase voltage profile and the network voltage unbalance of the experimental network. It is observed that the three-phase voltage unbalance factor remained balanced at 0.1% before the addition of 1.7 kW load to phase A. An increment of 1.7 kW load in phase A causes the voltage unbalance factor to rise from 0.1% to 2.0%. Figure 5.21 shows the voltage unbalance factor, the load variation and the response of the energy storage system throughout the experimental case study.

At 360 s, the energy storage system responds to the voltage excursion by supplying power to the experimental network. This is to compensate and relieve the stress of the generator in correcting the voltage drop in phase A, and further reduce the voltage unbalance factor of the experimental network. The total power supplied by the energy storage system continues to increase until 480 s. At this point, the network voltage unbalance is reduced to a minimum level of 0.1% while the three-phase voltages are back to nominal values.

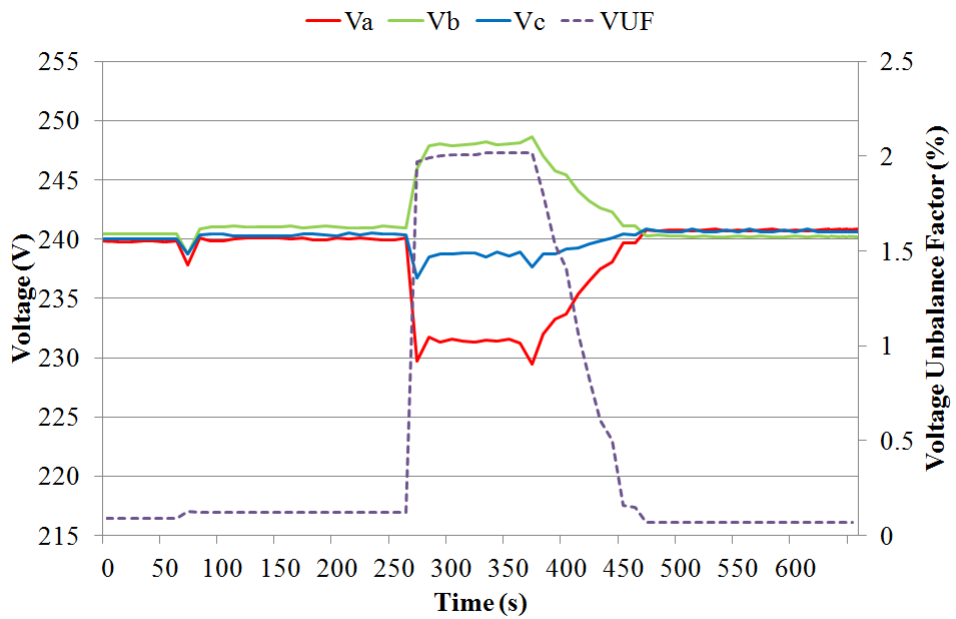


Figure 5.20 Variation of the network voltage and voltage unbalance factor under the same load condition

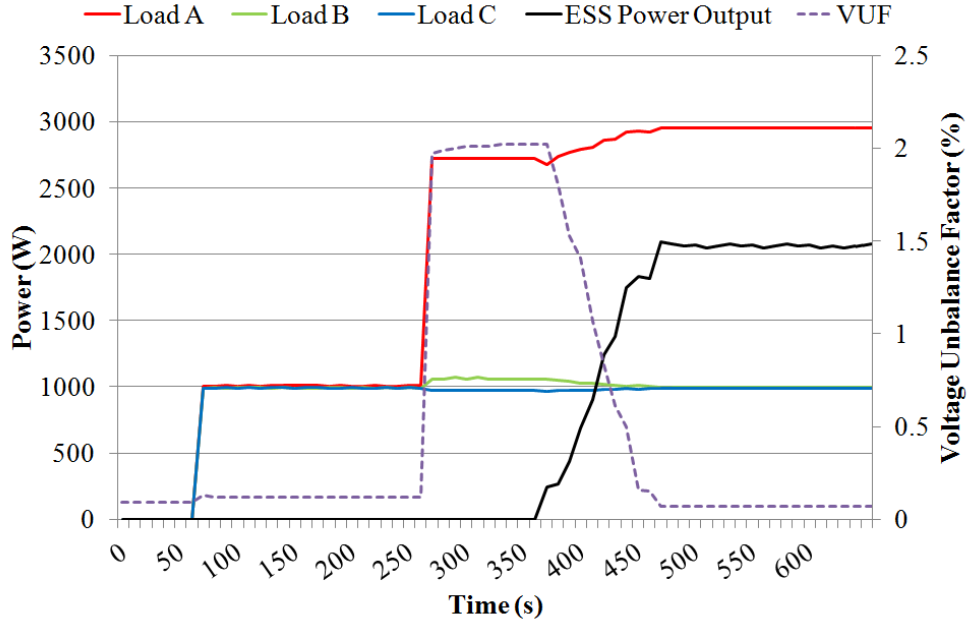


Figure 5.21 Variation of the voltage unbalance factor and load profile on the experimental network

5.4.5 Case Study III: Simple Automated Controlled Energy Storage System under Intermittency PV Power Output

The simple automated controlled energy storage system is further investigated under the condition of unbalanced load and intermittent PV power output. A 1.0 kW load and a 3.6 kW_p PV system are connected to phase A. The network voltage and voltage unbalance factor are recorded for analysis purposes. Figure 5.22 shows the voltage magnitude in phase A, PV power output and load consumption of the experimental case study. It is observed that there are two occasions where the network voltage increases above the maximum set point as shown in section I. The simple automated controlled energy storage system managed to restore the network voltage only after several seconds. At 620 s, voltage drop is recorded below the minimum set point in section II,

while the energy storage system only managed to restore the voltage drop after 150 s.

Figure 5.23 shows the variation of the network voltage unbalance factor (VUF) under the same generation and loading conditions as in Figure 5.22. It is shown that there are two occasions where the voltage unbalance factor rises above the statutory limit of 2.0%. The simple controlled storage system is not able to ensure that voltage unbalance is maintained below the required limit.

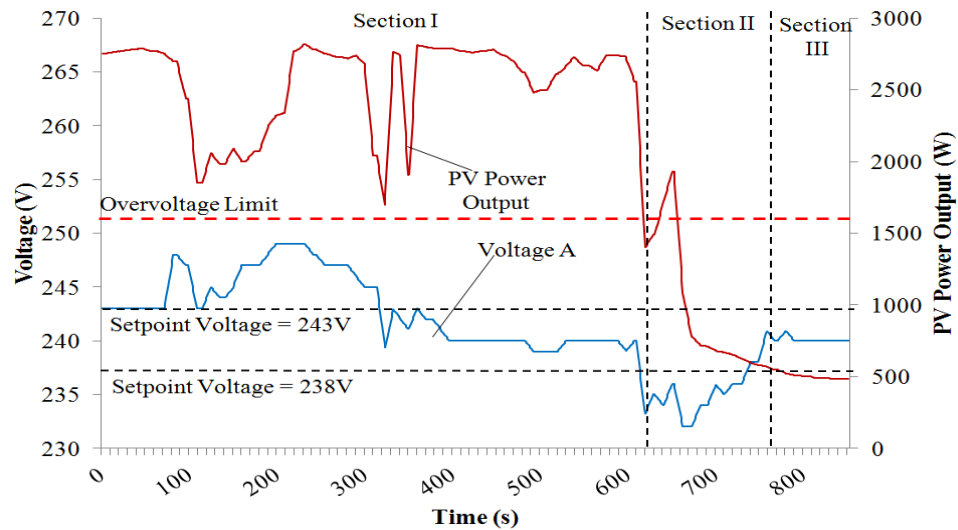


Figure 5.22 Variation of the network voltage and PV power output on the experimental network

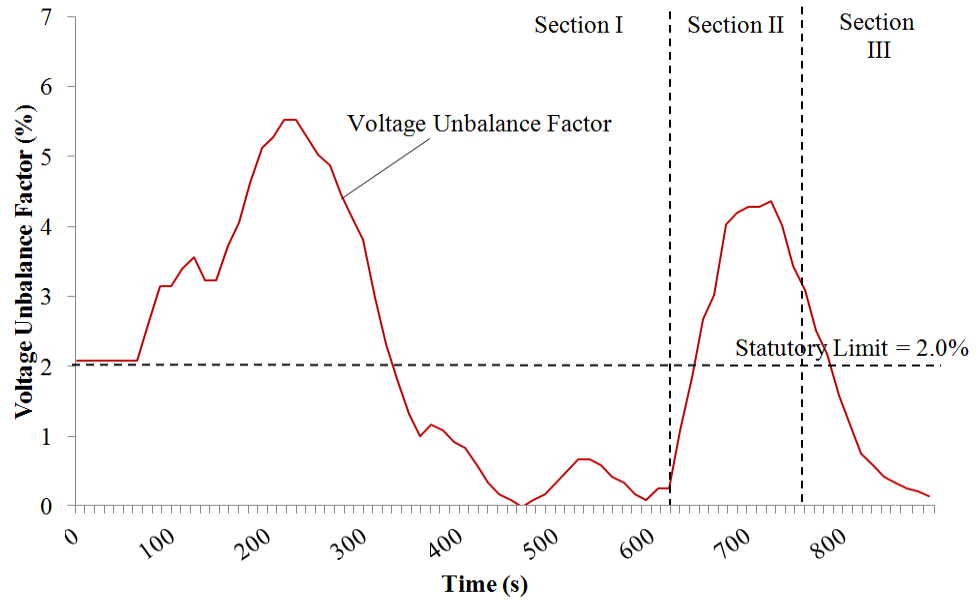


Figure 5.23 Variation of voltage unbalance factor on PCC

5.5 Step 8: Stage III Fuzzy Control

After a series of studies, it is noticed that the simple control algorithm does not effectively mitigate the voltage issues caused by the intermittent PV power output. Hence, a novel fuzzy control algorithm is developed and implemented in LabVIEW™ to manipulate the real power output of the energy storage system in order to maintain the voltage level on the distribution network. Generally, the fuzzy controlled energy storage system has an advantage over the simple control algorithm in which the fuzzy control algorithm is able to restore the voltage within the limit in shorter period as compared to the simple method.

5.5.1 The Reasons for Using Fuzzy Control

One of the reasons for developing the fuzzy control method is that the voltage rise and voltage unbalance fluctuates throughout the day. PID control was developed for single-phase energy storage and it was found to be effective to solve steady state voltage rises or drops (Chua et al., 2012). However, it is not able to solve the intermittent voltage fluctuations caused by the large amount of clouds passing over the PV systems because PID controller is too slow to respond to the rapid changes of voltage (Guo et al., 2011; Gaurav, 2012).

Several comparative studies have been performed to investigate the response time of a dynamic control by using conventional PID control approach and fuzzy control algorithm (Rahmat and Ghazaly, 2006; Essam and Khalid, 2010; Gaurav, 2012). It is found that the Fuzzy control system shows a good results in term of response time and settling time. Furthermore, it has the advantages of dealing with non-linear systems and incorporates more parameters to the rule base and membership functions. The research study also states that PID controller cannot be applied with the systems which have a fast change of parameters, because it would require the change of PID gain constants in the time. In this extend, the proposed fuzzy control algorithm incorporates the voltage changes caused by the intermittent PV power output as one of the membership function to generate the current instruction of the energy storage system in order to speed up the response time for mitigating voltage unbalance factor.

Therefore, the fuzzy control algorithm is developed due to its rapid response to the fast changing voltage. Also, the state of charge (*SoC*) can be part of the input parameters into the fuzzy control algorithm so that the amount of real power supplied or absorbed by the energy storage system is partly determined by the *SoC*. There are a number of publications showing that the fuzzy controller is always preferred because it is more effective than the PID controller (Rahmat and Ghazaly, 2006; Essam and Khalid, 2010; Gaurav, 2012).

Another reason for using the fuzzy control algorithm is that the load demand, the resistance and reactance of the distribution lines are usually unknown. The exact amount of real power that the energy storage system has to supply to or absorb from the network to maintain the voltage cannot be determined by the analytical approach (Wong et al., 2014). Therefore, the fuzzy control method is used to correct the voltage excursion. This can be explained in the following.

The variation of voltage magnitude at a point of the distribution network is expressed by (Jenkins et al. 2000):-

$$\tilde{V} = \tilde{V}_{nominal} + \frac{RP_{PV-L} + XQ_{PV-L}}{\tilde{V}_{nominal}} + j \frac{XP_{PV-L} - RQ_{PV-L}}{\tilde{V}_{nominal}} \quad (5.1)$$

Where

R and X are the line resistance and reactance respectively

$\tilde{V}_{nominal}$ is the rated voltage of the distributed grid at the PCC

P_{PV-L} and Q_{PV-L} are expressed as follows:

$$P_{PV-L} = P_{load} - P_{PV} \pm P_{inverter} \quad (5.2)$$

$$Q_{PV-L} = Q_{load} - Q_{PV} \pm Q_{inverter} \quad (5.3)$$

Whilst

P_{load} and Q_{load} are the real and reactive power of the load respectively
 P_{PV} and Q_{PV} are the real and reactive power output of PV respectively
 $P_{inverter}$ and $Q_{inverter}$ are the real and reactive power output of the bi-directional energy respectively

Eq. (5.1) can be rearranged to give the following equation.

$$P_{inverter} = f(\tilde{V}, P_{load}, Q_{load}, P_{PV}, Q_{PV}, R, X) \quad (5.4)$$

With reference to Eq. (2.1), the cable resistance in a low-voltage distribution network is greater than the reactance. Hence, using real power to address the voltage control problems always has a more significant impact on the voltage level as compared to the reactive power. Eq. (5.1), Eq. (5.2) and Eq. (5.3) show the variation of voltage magnitude at a point of the distribution network. Several parameters including P_{load} , Q_{load} , P_{PV} , Q_{PV} , R and X are necessary to determine the amount of $P_{inverter}$ and $Q_{inverter}$. However, $Q_{inverter}$ are set to zero in this work so that unity power factor can be obtained. Furthermore, real power has significant impact on the low-voltage distribution network as compared to reactive power. Eq. (5.4) is used to determine the amount of real power output of the energy storage system ($P_{inverter}$) so that the voltage at PCC can be maintained within the required tolerance. The value of $P_{inverter}$ can only be determined if the parameters of V , P_{load} , Q_{load} , P_{PV} , Q_{PV} are known. However, R and X are usually unknown. P_{PV} varies at all times due to the frequent passing clouds over the PV panel. Therefore, the value of $P_{inverter}$ cannot be determined. Moreover, Eq. (5.4) is a non-linear equation and has to

be solved iteratively which can be time consuming. Hence, it is not practical to use Eq. (5.4) under an ever changing power flow condition.

As a result, the fuzzy control method is required to solve the fluctuating voltage issues on the network.

5.5.2 Control Strategy of Fuzzy System

Fuzzy control is a method that makes use of rule-based decision according to the input memberships. This fuzzy control method is used to develop necessary corrective action based on the voltage excursion and the battery state of charge (*SoC*). The reason for incorporating the battery *SoC* into the system is because the health of the batteries is important and it should be well maintained since they are one of the most expensive items in the energy storage system. If the battery *SoC* is reduced to 60 %, then the energy storage system will be instructed to reduce its real power output to the network. This can slow down the reduction of the state of charge. If the battery *SoC* is less than 40 %, then the energy storage system is instructed to terminate the supply of real power in order to avoid any over-discharging conditions. Figure 5.24 shows the flow chart of the overall algorithm of the fuzzy control method. The algorithm begins with the initialization of $V_{\text{ref}} = 240 \text{ V}$ and $t=1$ where V_{ref} is the reference voltage and t is time. The upper and lower voltage set points are specified to form a separate voltage range which stays well within the statutory limits. The separate voltage range is to trigger the energy storage

system to carry out the preemptive action before the voltage rise or voltage unbalance becomes too significant.

The fuzzy control system receives the measured voltage (V_{measured}) and the battery *SoC* in real time from the bi-directional inverter. V_{measured} is the measured voltage at the PCC. The measured voltage is then compared with the upper and lower voltage set points to determine whether the network voltage is within the specified range or not. If the measured voltage deviates from the specified range, then the voltage difference ΔV is calculated using $V_{\text{measured}} - V_{\text{ref}}$ where V_{measured} is the measured voltage at a point of concern and V_{ref} is the nominal voltage. The measured voltage is obtained directly from a power meter installed at the point of concern, while the battery *SoC* is provided directly from the bi-directional inverter itself. The bi-directional inverter has a built-in feature that can estimate *SoC* accurately. Input memberships, ΔV and *SOC* are used to generate the instruction for bi-directional inverter whether to absorb or supply power from/to the network.

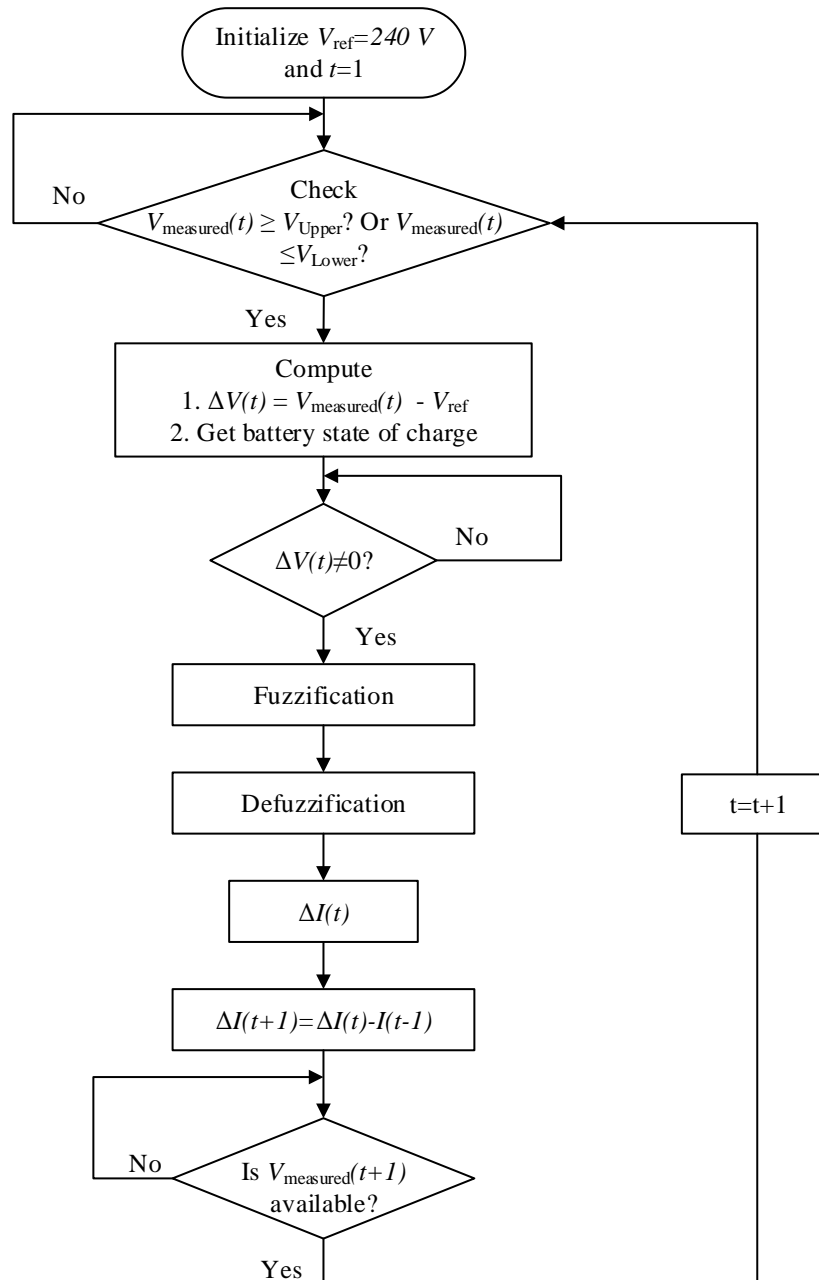


Figure 5.24 Flow chart of the fuzzy logic control algorithm

5.5.3 Fuzzy System in LabVIEW™

To begin with, a fuzzy system design toolbox by LabVIEW™ is used to define the pre-defined input and output fuzzy memberships. The fuzzy control

method uses ΔV and SoC as the two parameters to generate four linguistic outputs through fuzzification. The outputs are then used to produce one output (I) as the instruction to the bi-directional inverter through defuzzification. The inverter will then adjust its real power output according to the instruction. This whole process will continue until the voltage magnitude becomes satisfactory. Once the voltage magnitude on one phase is restored, then voltage unbalance factor will also be reduced. Figure 5.25 shows the fuzzification and defuzzification of the proposed fuzzy control method.

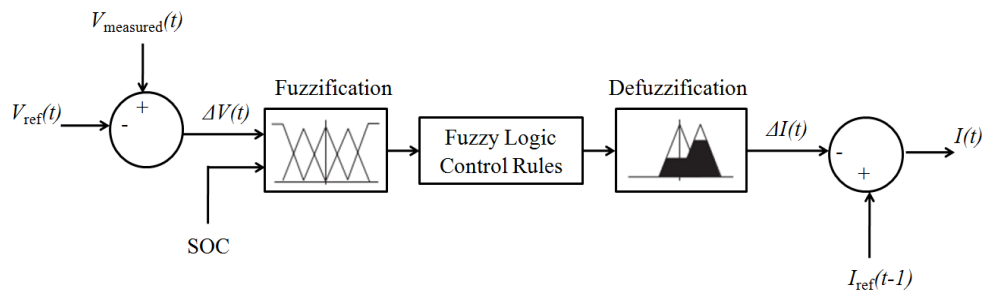


Figure 5.25 Fuzzy logic control algorithm

During the fuzzification, ΔV and SoC are used as the two input parameters to the two pre-defined fuzzy memberships. The pre-defined fuzzy membership for ΔV is enclosed by seven different envelopes of voltage conditions, namely extremely undervoltage (EUV), very undervoltage (VUV), undervoltage (UV), normal voltage (N), overvoltage (OV), very overvoltage (VOV) and extremely overvoltage (EOV) as shown in Figure 5.26. The input of ΔV to the fuzzy membership will generate two voltage conditions with their respective linguistic values. On the other hand, the pre-defined fuzzy membership for SoC is enclosed by seven different envelopes of SoC conditions, namely extremely low (EL), very low (VL), low (L), normal (N), high (H), very high (VH), extremely high (EH) as shown in Figure 5.27. The input of SoC to this

fuzzy membership will produce two battery state conditions with their respective fuzzy values. In total, there are four linguistic outputs generated from the fuzzification.

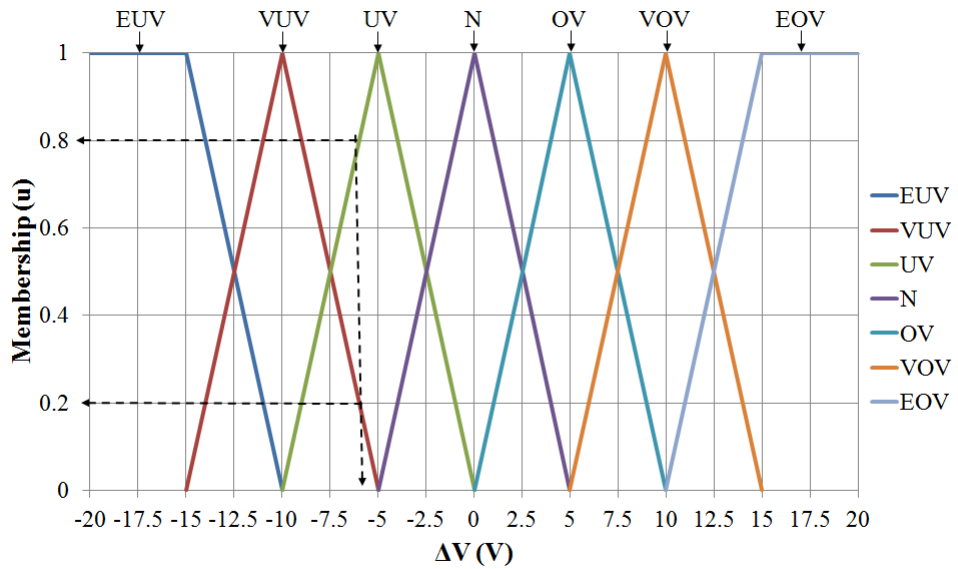


Figure 5.26 Fuzzy logic input membership for voltage change (ΔV)

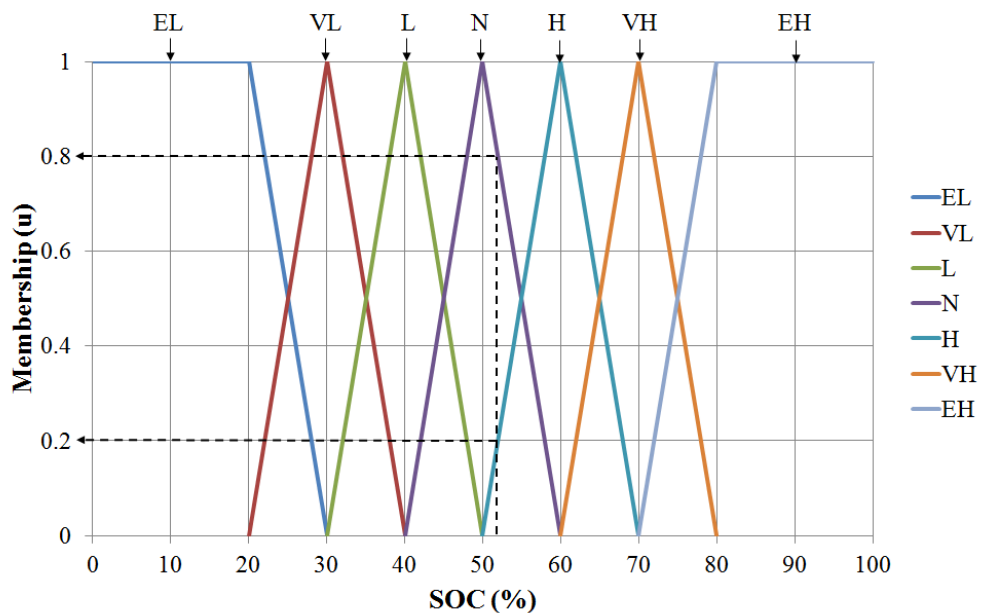


Figure 5.27 Fuzzy logic input membership for the battery state of charge (SoC)

During the defuzzification, the four linguistic outputs from the two fuzzy memberships are mapped with each other to determine the types of

instructions. There are seven pre-defined types of the instructions, namely extremely high supply power (EHSP), high supply power (HSP), supply power (SP), normal (N), absorb power (AP), high absorb power (HAP) and extremely high absorb power (EHAP) as shown in Table 5.3. The types and the degrees of the instructions are used to define the area enclosed in the fuzzy membership as shown in Figure 5.28. Through the centre of the area (CoA) defuzzification method, the required change in the real current (ΔI) is sent as the command to the bi-directional inverter.

The linguistic variable of ΔV can vary from -20 V to 20 V due to the voltage regulation of $\pm 10\%$ of the nominal value. SoC can also change from 0 to 100%. As a result, seven pre-defined linguistic terms are defined for ΔV and SoC to encompass the wide ranges of these two linguistic variables. This is to ensure that the outputs from the two linguistic variables are sensitive enough under the changes of ΔV and SoC . Similarly, there are seven types of the instructions being categorized to generate the output of ΔI based on the output values from ΔV and SoC . This is because the output of ΔI can be sensitive enough under the changes of the output variables.

Table 5.3. Definition of the instruction from the output variable

SoC	ΔV						
	EUV	VUV	UV	Normal	OV	VOV	EOV
EL	SP	N	N	N	HAP	EHAP	EHAP
VL	SP	SP	N	N	HAP	EHAP	EHAP
L	SP	SP	SP	N	HAP	EHAP	EHAP
Normal	HSP	HSP	SP	N	HAP	HAP	HAP
H	EHSP	EHSP	HSP	N	AP	AP	AP
VH	EHSP	EHSP	HSP	N	N	AP	AP
EH	EHSP	EHSP	HSP	N	N	N	AP

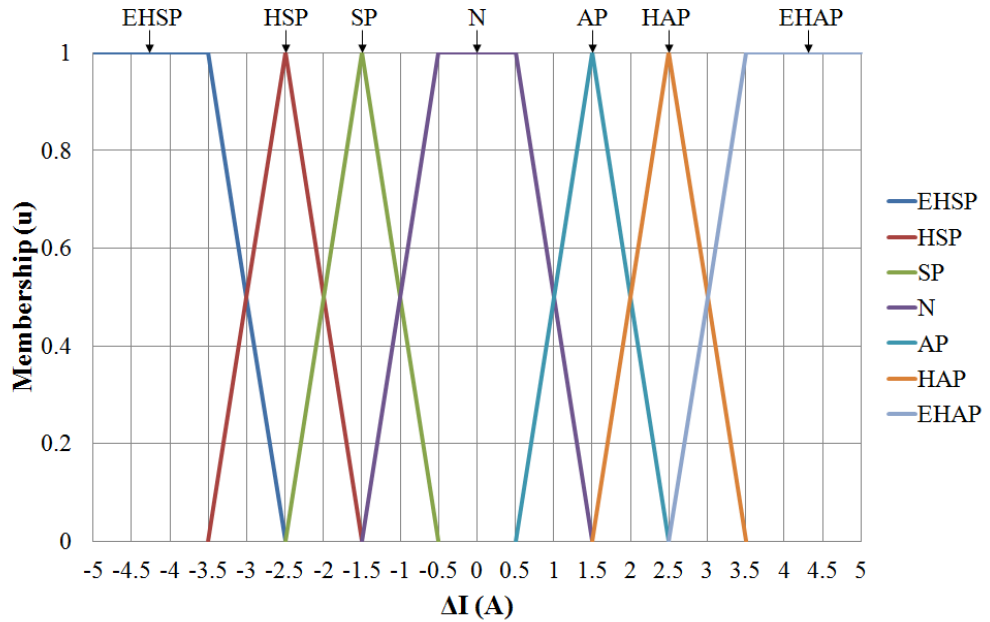


Figure 5.28 Fuzzy output membership of instruction (ΔI) to bi-directional inverter

LabVIEW fuzzy design toolbox is used to design the fuzzy system, a screenshot of the fuzzy design toolbox is shown as Figure 5.29. There are three tabs available in the toolbox and the functions of the toolbox are listed as follows:

- (i) Tab 1 –Variables: All the defined variables membership are displayed in this tab. In this case, ΔV and SoC are listed as the input variables while ΔI is listed as output variable.
- (ii) Tab 2 –Rules: The rules based corresponds to all possible combinations of the membership functions of the two input linguistic variables
- (iii) Tab 3 –Test system: Can be used to test the relationship between the input and output variables.

After a fuzzy system is designed, it is loaded to the .vi file before a fuzzy logic controller is used to calculate the output membership. Figure 5.30 shows a section of the block diagram to calculate ΔI in LabVIEW™. ΔV and SoC are input to the MISO (Multiple input single output) fuzzy controller to give an output of ΔI . Figure 5.31 shows the LabVIEW™ front panel of the data acquisition system for grid monitoring, energy storage monitoring and the simple control for energy storage system.

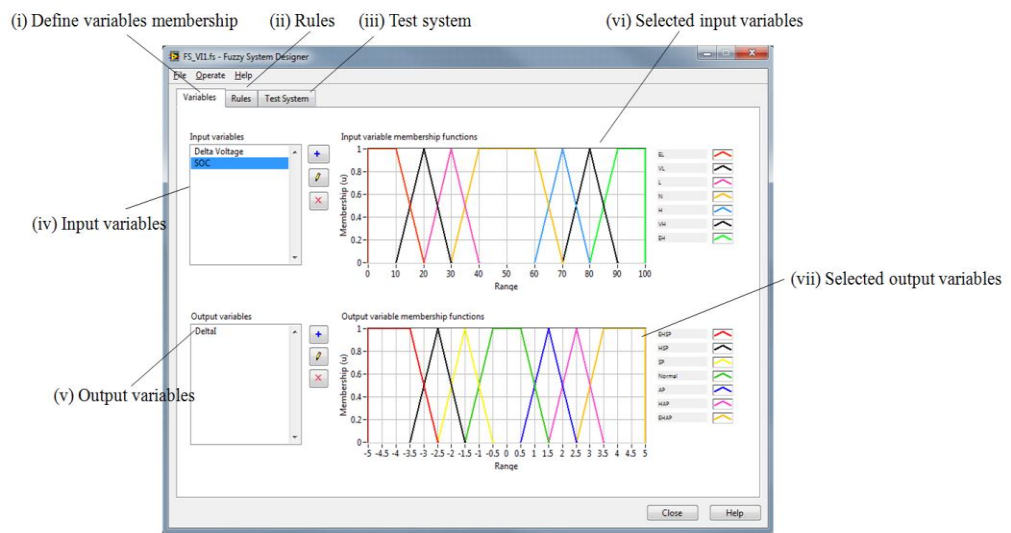


Figure 5.29 Screenshot of fuzzy system in LabVIEW™

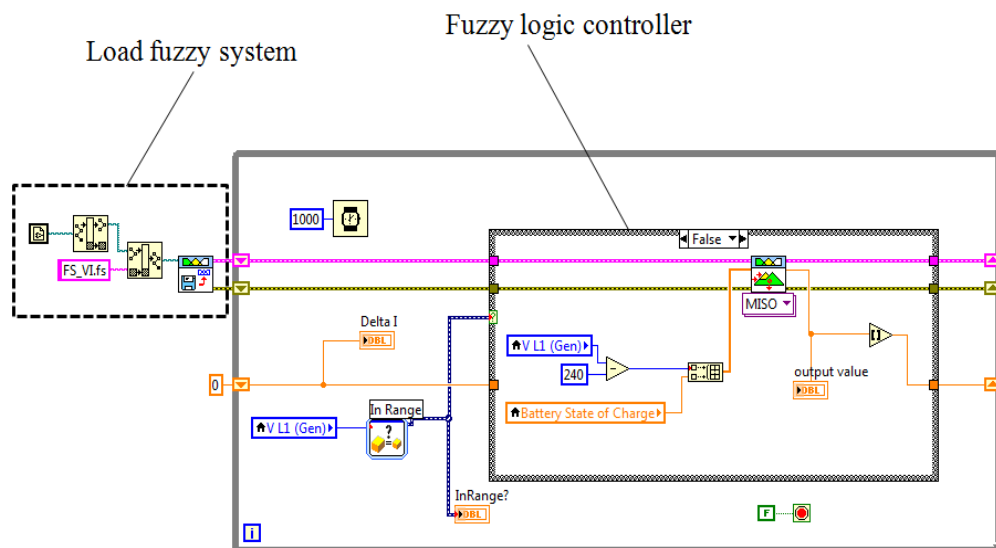


Figure 5.30 Block diagram of fuzzy system in LabVIEW™

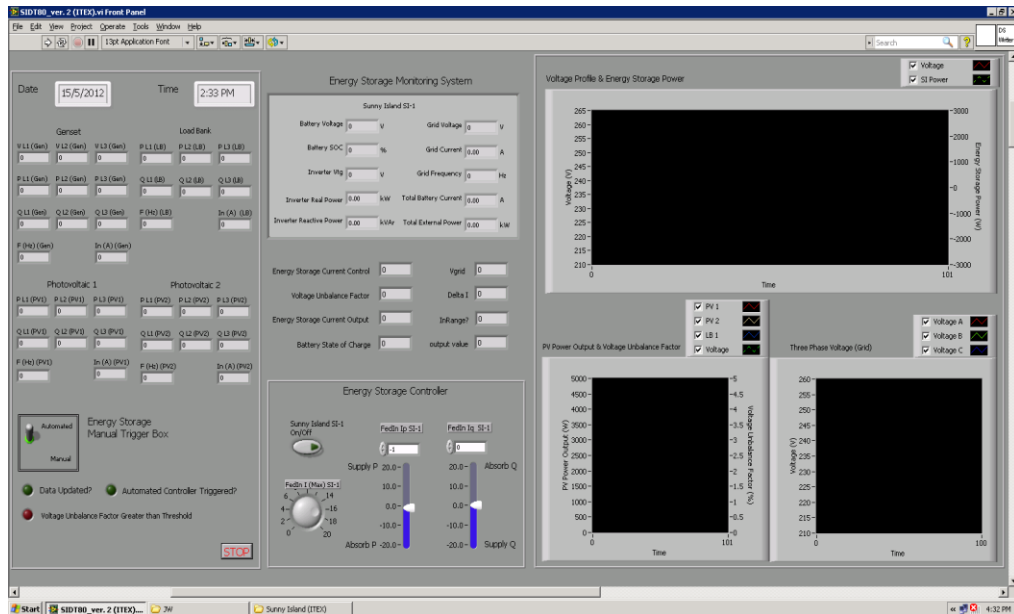


Figure 5.31 LabVIEW™ front panel after the second implementation

The fuzzy design toolbox comes with a test system which allows the testing of relationship between the input and output values of a fuzzy system to validate the rule base of the fuzzy system. Figure 5.32 shows an example of the fuzzification and defuzzification of the fuzzy control method using the LabVIEW™ fuzzy test system.

In the example, the input parameters ΔV and SoC are assumed to be $-6V$ and 53% respectively. A voltage difference of $-6 V$ to the respective input membership generates two outputs, i) 0.2 of very undervoltage (VUV) and ii) 0.8 of undervoltage (UV). Figure 5.26 shows that the input of $\Delta V = -6 V$ intersects with the lines of VUV and UV at values of 0.2 and 0.8 respectively.

SoC of 53% to the respective input membership produces two outputs; i) 0.2 of high (H) and ii) 0.8 of normal (N). Figure 5.27 shows that the input of $SoC = 53\%$ intersects with the lines of H and N at the values of 0.2 and 0.8

respectively. The AND (Minimum) antecedent is used as the antecedent connective where the smallest degree of the membership of the antecedents is chosen as the true value of the aggregated rule antecedent. Therefore, the smallest degree of any two linguistic terms is chosen as the true value and is shown below.

- If ΔV is 0.2 VUV AND SoC is 0.8 N, then ΔI is High Supply Power (HSP) with the membership value of 0.2
- If ΔV is 0.2 VUV AND SoC is 0.2 H, then ΔI is Extra High Supply Power (EHSP) with the membership value of 0.2
- If ΔV is 0.8 UV AND SoC is 0.8 N, then ΔI is Supply Power (SP) with the membership value of 0.8
- If ΔV is 0.8 UV AND SoC is 0.2 H, then ΔI is High Supply Power (HSP) with the membership value of 0.2

The instruction (ΔI) for the bi-directional inverter can then be calculated through center of area (CoA) defuzzification method. It is found to be -2.3 A.

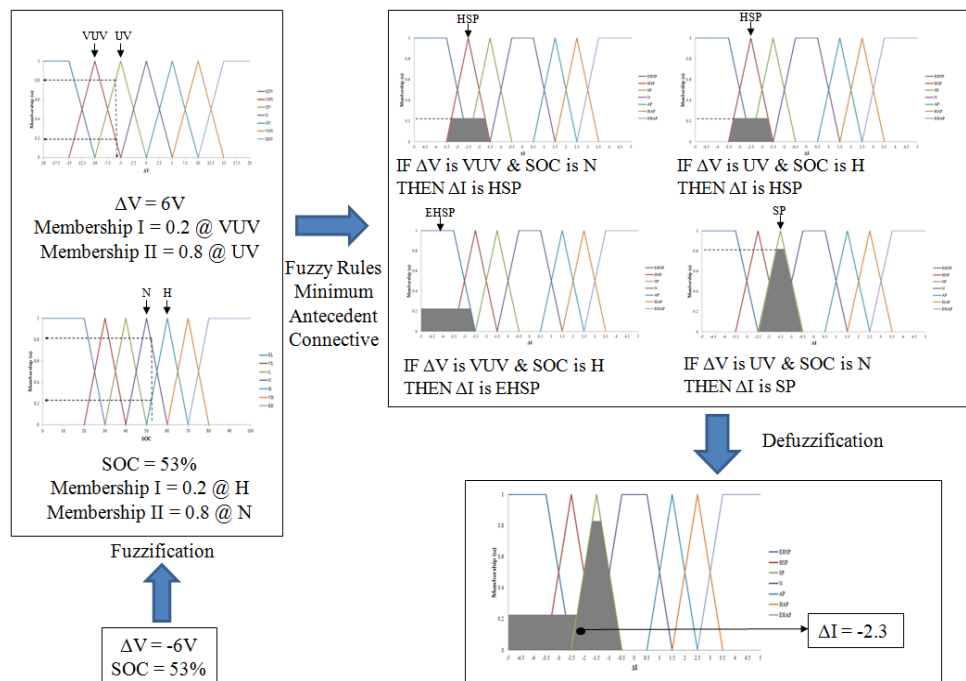


Figure 5.32 Example of fuzzification and defuzzification in the proposed fuzzy control method

5.6 Final Step: Operation of the System

As mentioned in Chapter 4, voltage rise and voltage unbalance have been identified as the most severe power quality issues due to the large amount of PV systems installation on the Malaysian low-voltage distribution networks. The effectiveness of the fuzzy controlled energy storage system to mitigate voltage rise and voltage unbalance issues is evaluated under various scenarios with different loading and generation conditions as follows:-

Case Study IV:

This case study is used as a benchmark for network voltage variation during high power output of PV without the energy storage system.

Case Study V:

The fuzzy controlled energy storage system is used to mitigate the voltage rise and network voltage unbalance under unbalance load variation.

Case Study VI:

This case study is designed to further verify the effectiveness of the fuzzy controlled energy storage system to improve the voltage issues caused by intermittency of PV power output.

Case Study VII:

In this case study, the effect on voltage using fuzzy controlled energy storage under sudden changes of generation and loading conditions is evaluated.

5.6.1 Case Study IV: Effects on Voltage Level during High Penetration from PV System without Fuzzy Controlled Energy Storage System

This case study is designed to show the effect of high PV power output on the voltage magnitude of the experimental network. Initially, a 2.0 kW load is connected to phase A while phase B and C remains at no load. The voltage magnitude at the PCC is measured and recorded on a regular basis. Figure 5.33 shows the PV power output, load consumption profiles, voltage and voltage unbalance factor of the experiment.

The voltage magnitude in phase A is approximately 240 V during the first 480 s when the PV power output is about 2.0 kW which is close to the load. However, from 540 s onwards, the PV system generates power greater than the load demand causing the network voltage to increase as well. As a consequence, voltage unbalance factor starts to increase as the PV power output becomes higher than the load demand. It is also observed that the voltage unbalance increases when the demand is greater than the generation. From 1020 s onwards, voltage drops to less than 240 V when the PV power generation no longer sufficient to supply to the load demand. In this case study, the pattern of the voltage unbalance factor is identical to the voltage magnitude in phase A. This is because the voltage unbalance factor is interrelated to the three-phase voltage.

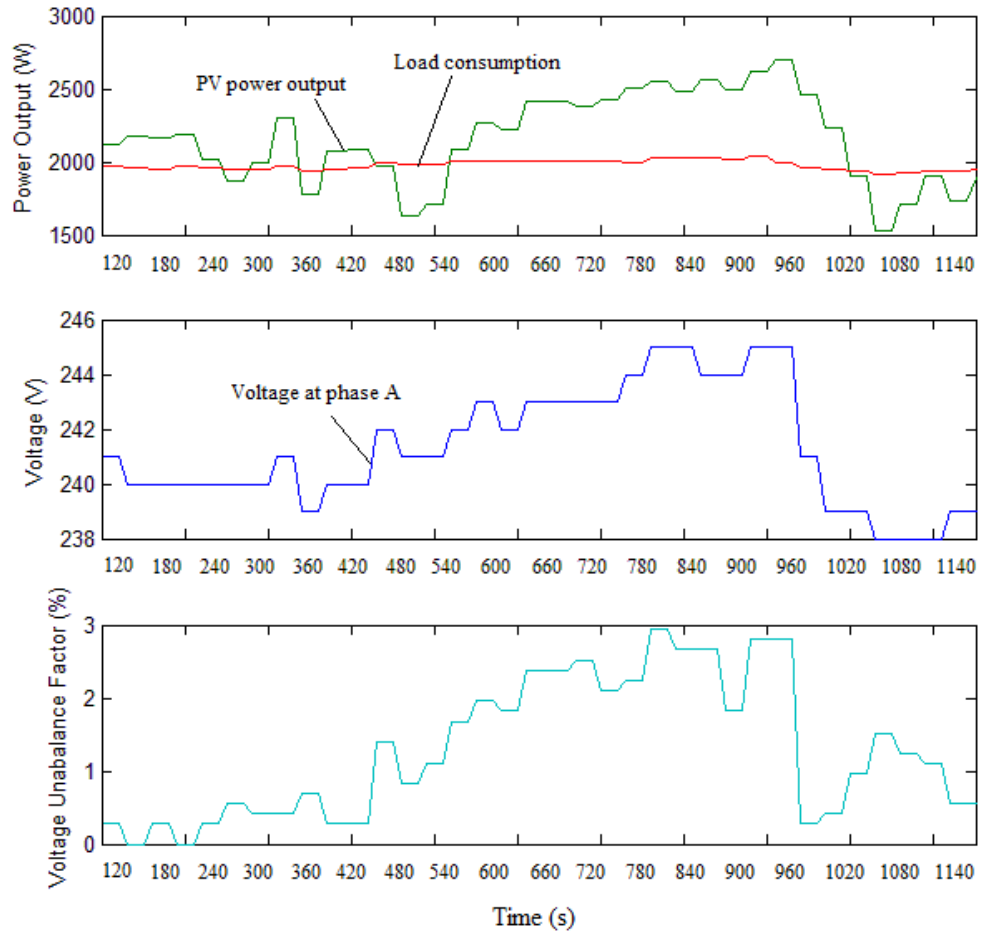


Figure 5.33 PV power output, the load demand, voltage and voltage unbalance factor at the PCC of the experimental network

5.6.2 Case Study V: Fuzzy Controlled Energy Storage System under Unbalance Load Condition

This case study is designed to study the response of the fuzzy controlled energy storage system under unbalanced load condition. Initially, each phase is connected with a 1.0 kW. The network voltage unbalance factor is recorded as minimum when the three-phase load is connected under a balanced condition.

At 370 s, the load in phase A has been increased from 1.0 kW to 2.8 kW causing the network to become extremely unbalanced. Figure 5.34 shows the network voltage unbalance factor, load condition and the power output response of the fuzzy controlled energy storage system. It is noticed that the three-phase voltages are corrected back to its nominal level while the voltage unbalance factor of the network is reduced from 2.0% to 0.1%. Figure 5.35 shows the voltage profile and voltage unbalance factor of the network throughout the experiment. The fuzzy controlled energy storage system continuously increases the power supplied to the experimental network until the three-phase voltage back is to its nominal value while the voltage unbalance factor is reduced to minimum.

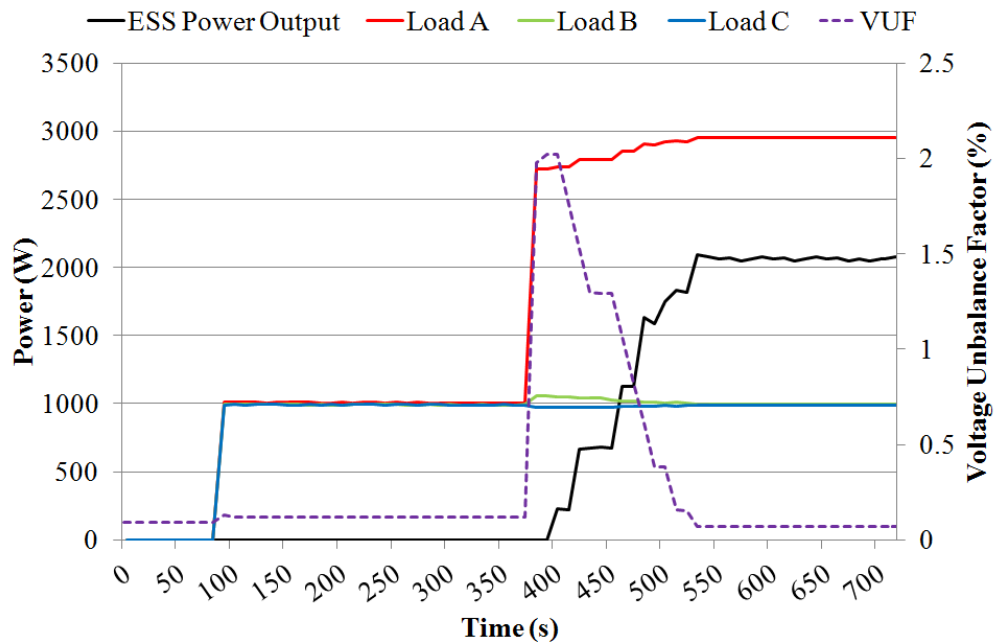


Figure 5.34 Voltage unbalance factor, load profile and the response of fuzzy controlled energy storage system.

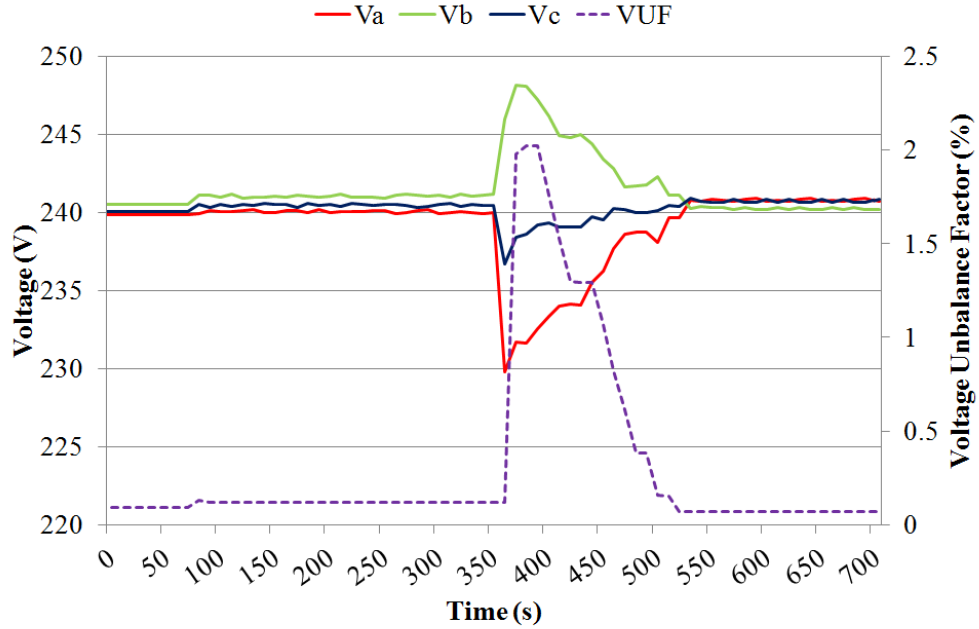


Figure 5.35 Three-phase voltage profile and voltage unbalance factor of the experimental network

5.6.3 Case Study VI: Fuzzy Control with Intermittency of PV Power Output

In this case study, a constant load of 1.0 kW is connected to the experimental network together with the 3.6 kW_p PV system in phase A. Figure 5.36 shows the voltage magnitude in phase A, PV power output and load consumption during the experimental case study when the fuzzy controlled energy storage is used. It is observed that the PV output fluctuates very rapidly in section I. The fuzzy control system is able to restore and maintain the voltage magnitude within the tolerance levels throughout the experiment. Figure 5.37 shows the voltage unbalance factor of the experimental network with the same loading and generation conditions as shown in Figure 5.36. It is observed that the voltage unbalance factor is always maintained below the limit of 2.0%.

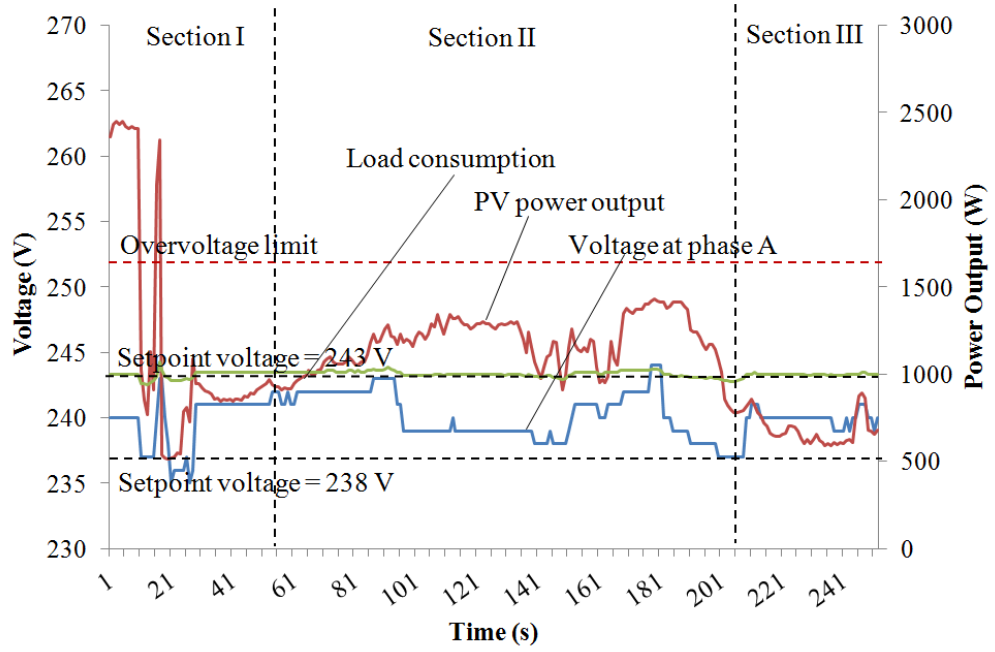


Figure 5.36 Voltage magnitude with intermittent PV power output and load consumption

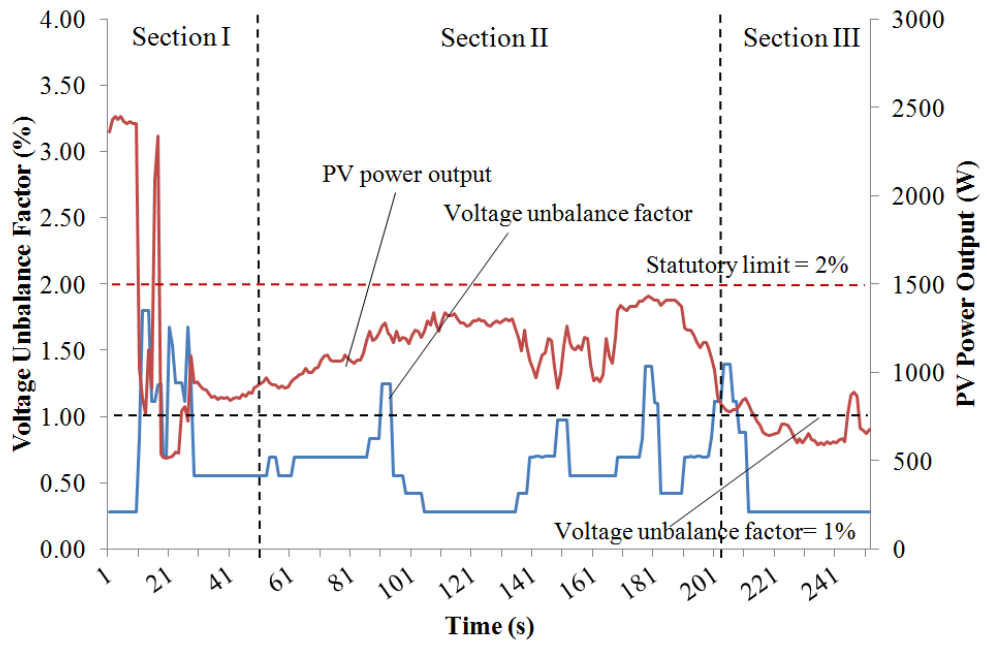


Figure 5.37 Voltage unbalance factor with intermittent PV power output

5.6.4 Case Study VII: Effect on Voltage using Fuzzy Controlled Energy Storage under Sudden Changes of Generation and Loading Conditions

This case study is designed to study the effectiveness of the proposed fuzzy control method to mitigate the fluctuating voltage rises under a sudden reduction of load demand with fluctuating PV power output. The maximum and minimum voltage set points are specified as 243 V and 238 V respectively in the fuzzy control algorithm. Figure 5.38 shows the network voltage, PV power output, power output of the fuzzy controlled energy storage system and the load profile. Initially, a fixed load of 500 W is introduced into the network and the PV system generates approximately 2.2 kW. Hence, an excess power of 1.7 kW is exported to the distribution network. The voltage magnitude increases to 248 V which is above the upper voltage set point of 243 V. The fuzzy control algorithm detects such a voltage excursion (ΔV) and hence instructs the fuzzy controlled energy storage system to increase the absorption of real power from the network starting from 0 kW to 1.5 kW over a period of 11 seconds. As a result, the network voltage drops from 248 V to 242 V.

At 38 seconds, the controllable load is purposely reduced to 0 kW. The network voltage increases to 245 V which is slightly above the upper voltage set point of 243 V. The fuzzy logic control algorithm detects the voltage change and then instructs the fuzzy controlled energy storage system to step up the absorption of real power from 1.5 kW to 1.6 kW. As a result, the voltage drops below the upper set point as shown in Figure 5.38. This result

shows that the fuzzy controlled energy storage is able to maintain the voltage magnitude within the required range under a sudden change of the load demand.

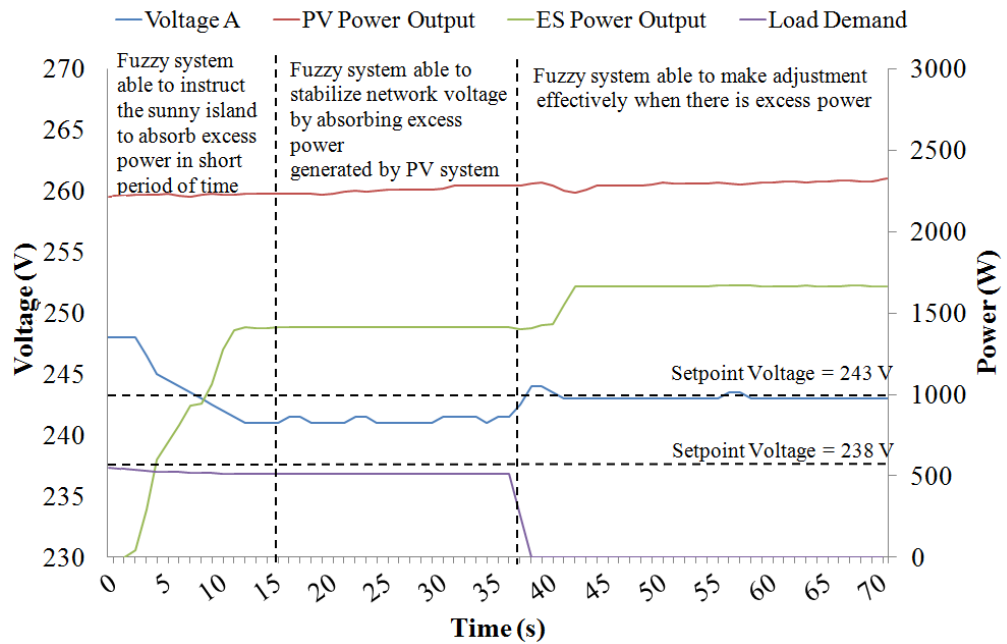


Figure 5.38 Voltage at phase A, PV power output, Sunny Island 5048 power output and load demand of the experimental case study VII

Another case study is designed to study the response of the proposed fuzzy control method to the sudden changes of PV power output and loading conditions. The three-phase load demand is set at 0.5 kW per phase throughout the experiment. The PV systems are connected to phase A of the network. Figure 5.39 shows the rapid fluctuation of the PV power output. The PV power output is about 2.22 kW in the beginning and then increases gradually to 2.3 kW from 13 to 39 seconds. At 15 seconds, the voltage magnitude rises above the upper set point. The fuzzy control system detects the change and hence instructs the bi-directional inverter to absorb the excess power from the network. As a result, the voltage drops below the upper set point. At 40 seconds, the PV power output drops suddenly, causing the voltage magnitude

to reduce immediately. However, the fuzzy control system restores the voltage magnitude shortly after the voltage reduction.

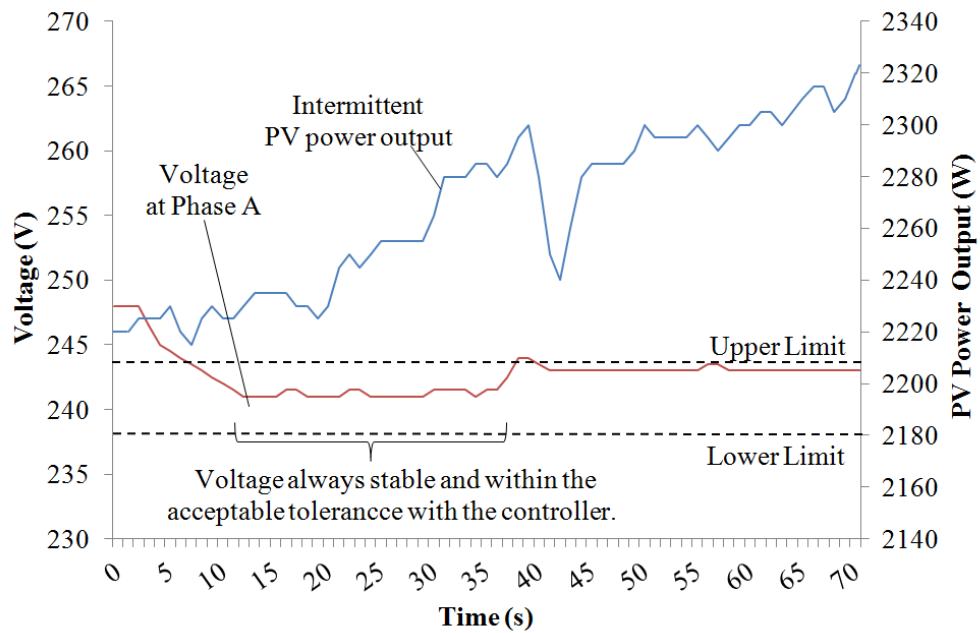


Figure 5.39 Voltage magnitude at phase A with increasing PV power output

Figure 5.40 shows the fluctuation of voltage magnitude caused by the change of loading condition and the changes in the instruction and battery *SoC* in response to the voltage changes. The loading and generation conditions of Figure 5.40 are different from that of Figure 5.39 because this study is to investigate the response of the fuzzy control system to the rapid changes of the loading condition. The PV power output fluctuates about 2.0 kW throughout the experiment. The load is fixed at 1.5 kW at the beginning.

At 13 seconds, the load is reduced to 1.0 kW causing the voltage to rise above the set point. However, the fuzzy control system is able to correct the voltage magnitude very rapidly. At 30 seconds, the load is increased to 1.5 kW making the voltage to drop below the set point. However, the fuzzy control system is

able to change the charging current, hence restoring the voltage magnitude very rapidly. At 50 seconds, the load is reduced to 0.5 kW resulting in the increase of voltage magnitude. However, the fuzzy control system again is able to correct the voltage magnitude promptly. It is noticed that *SoC* of the battery increases gradually from 55% to 60%. It does not change significantly because the experiment is conducted for a short period of time. A noticeable change in the battery *SoC* happens if the experiment is carried out for a long duration.

The total response time of the fuzzy control method encompasses the transmission time of data from the meters to the fuzzy control algorithm, the execution time of the algorithm to output a new instruction (ΔI) and the transmission time of the new instruction (ΔI) to the sunny island. The total response time is less than 0.5 s which does not create any issue. The fuzzy control method has been successful to correct the voltage within a short duration and accurately as proved experimentally.

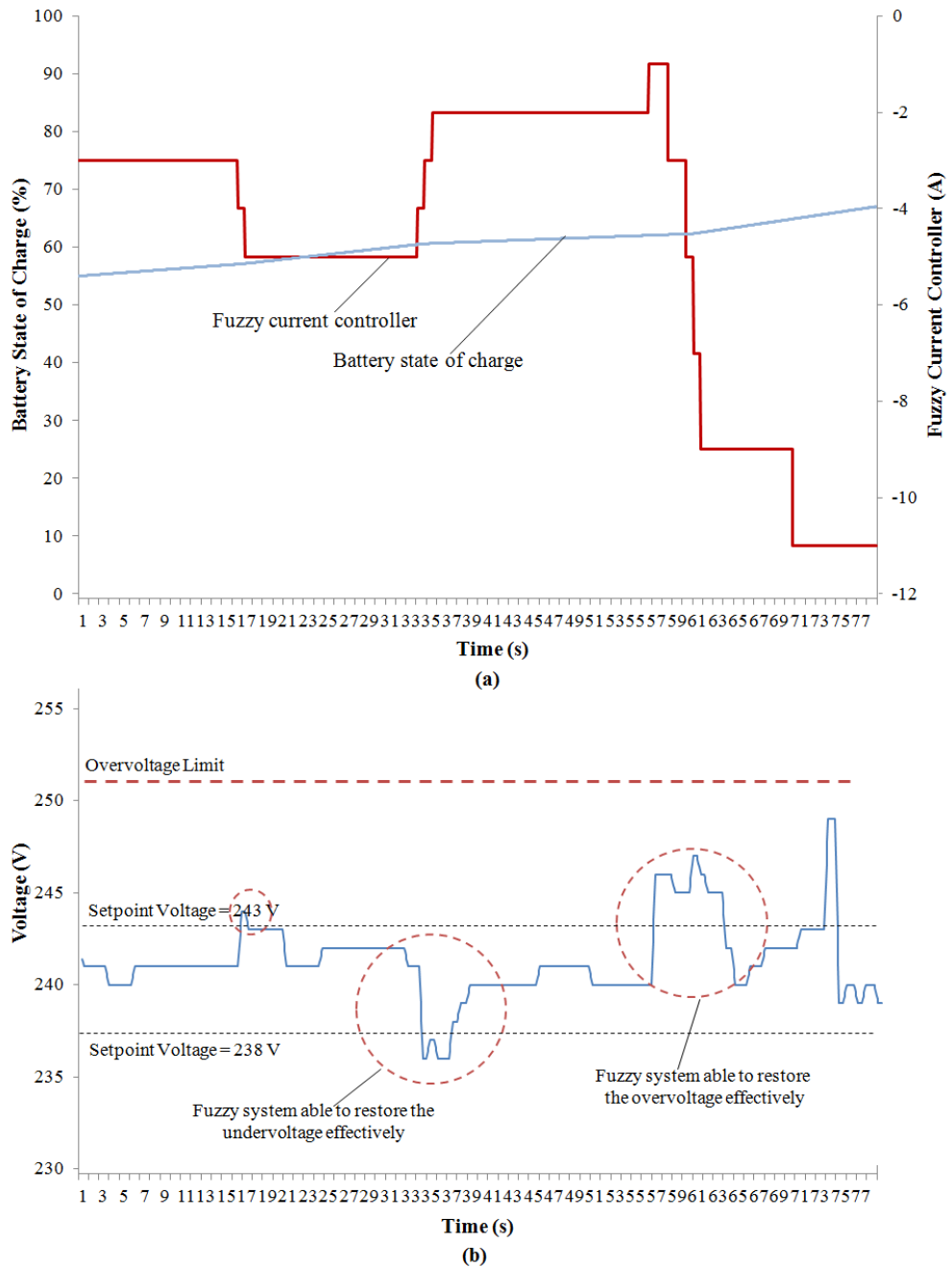


Figure 5.40 (a) Change of the instruction and battery *SoC* (b) voltage magnitude of the experimental case study

Figure 5.41 shows that the voltage unbalance factor of the experimental network under the same loading and generation conditions as that of Figure 5.40. It is observed that the fuzzy controlled system is able to maintain the voltage unbalance factor below the statutory limit. It is also worth noting that the correction of voltage level is carried out only on one phase. If the three-

phase voltages are corrected simultaneously, then the voltage unbalance factor will be reduced further.

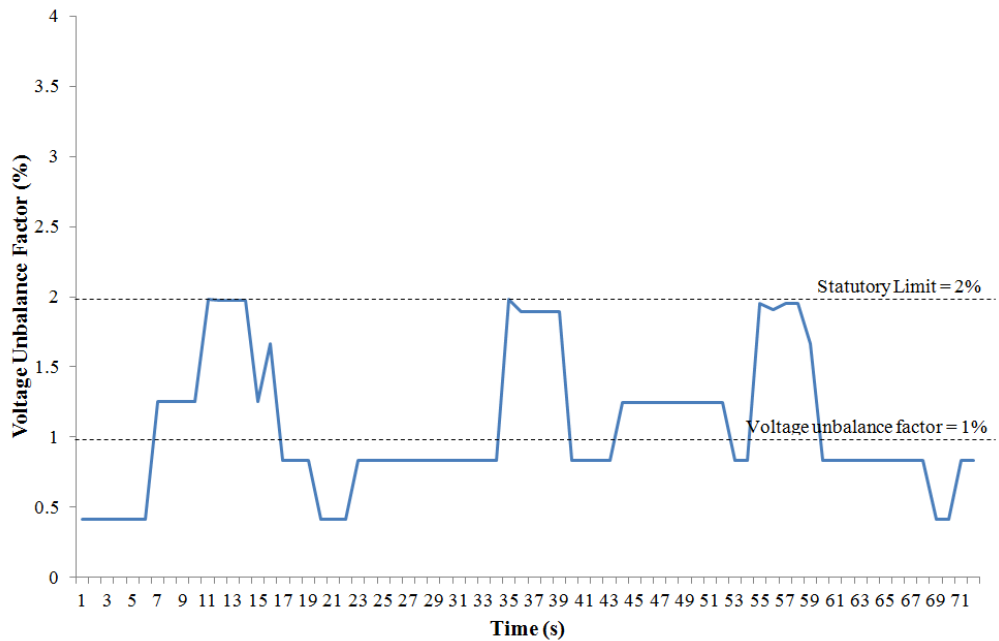


Figure 5.41 Voltage unbalance factor of the experimental network

5.7 Discussion

Several solutions have been made available to overcome various voltage issues caused by the growth of renewable energy sources on the distribution networks. Energy storage systems seem to be the most effective approach for mitigating voltage issues without wasting any additional renewable energy. However, most of the existing energy storage systems are not designed to solve the voltage rises and voltage unbalances that fluctuate throughout the day on the distribution networks with a large number of single-phase PV systems. The fluctuation of voltage rises and voltage unbalances is caused by the large number of passing clouds over a region. Therefore, an effective

control strategy is needed for the energy storage systems to mitigate the fluctuating voltage rises and voltage unbalances.

This chapter presents a fuzzy control method to be implemented in the energy storage system for mitigating any fluctuating voltage rises and voltage unbalances on the distribution networks integrated with the single-phase PV systems. The energy storage system consists of a bi-directional inverter, namely Sunny Island 5048, connected to a battery bank. The fuzzy control method is developed in a supervisory personal computer that communicates with the bi-directional inverter via RS485/USB converter. The fuzzy control module determines and sends the appropriate instruction to the energy storage system based on two input parameters: i) voltage excursion (ΔV) and ii) the battery SoC . The fuzzy control system then instructs the energy storage system to carry the necessary pre-emptive action before the voltage excursion becomes too significant. Such corrective action is necessary to ensure that any voltage rise or voltage unbalance is restored as quickly as possible. The renewable energy that is stored can be supplied to the customers at night to create extra capacity for the batteries to operate during the next day. This can ensure the continual operation of the energy storage system.

The performance of the fuzzy control method is verified by setting up the energy storage system on a low-voltage distribution network with two single-phase PV systems. A number of case studies have been performed to investigate the response of the fuzzy control system under various conditions of generation and demand. The experimental results show that the fuzzy

controlled energy storage system is able to restore the voltage magnitude as well as the voltage unbalance effectively under rapid changes of the PV power output and load demand. This fuzzy controlled energy storage system is found to be more capable than that of the basic controlled system.

CHAPTER 6

IMPLEMENTATION OF THE SYSTEM

6.1 Introduction

As mentioned in Chapter 4, the majority of the PV systems are single-phase while the installations are not centrally planned and are rather arbitrary. Therefore, the network voltage unbalance factor is likely to increase as the number of PV systems increases. Voltage unbalance factor is at its highest at the remote end of the distribution networks. In this chapter, an improved version of the control algorithm comprising of fuzzy logic control and the Park's transformation is implemented for the proposed energy storage system to control individual phase voltage in order to mitigate voltage unbalance.

The fuzzy logic based control algorithm is proposed to deal with fluctuating voltage rises and voltage unbalances that happen predominantly in Malaysia with highly intermittent PV power output. The Park's transformation is used to coordinate energy storage system on the three-phases to maintain the voltage balance effectively. The fuzzy logic control algorithm and Park's transformation work collaboratively to reduce voltage rise and mitigate voltage unbalance effectively. In addition, the performance of the fuzzy

control algorithm is validated by a series of experimental case studies. This chapter begins with the details of the proposed energy storage system, followed by an illustration of the conceptual design of the energy storage system and the control strategy of improving voltage quality. Various case studies under different generation and demand conditions are used to investigate the performance of the three single-phase fuzzy controlled energy storage systems. At the end of this chapter, a discussion of the results and conclusions are done.

6.2 Conceptual Design

This section describes the setup of the three single-phase energy storage systems to mitigate the voltage unbalance on the distribution network. It consists of three units of bi-directional inverters, namely SMA Sunny Island 5048. Each of the bi-directional inverter is integrated with 4 battery banks connected in parallel while each bank consists of four valve-regulated lead acid (VRLA) batteries connected in series to have a capacity of 115 Ah at 48 V. The total battery capacity for each single-phase energy storage system is 460 Ah.

Figure 6.1 illustrates the schematic diagram of three single-phase energy storage systems integrated on the experimental low-voltage distribution network, two units of 3.6 kW_p PV systems and a 9.0 kW three-phase

controllable load bank. The three single-phase energy storage systems are controlled and coordinated by a supervisory computer.

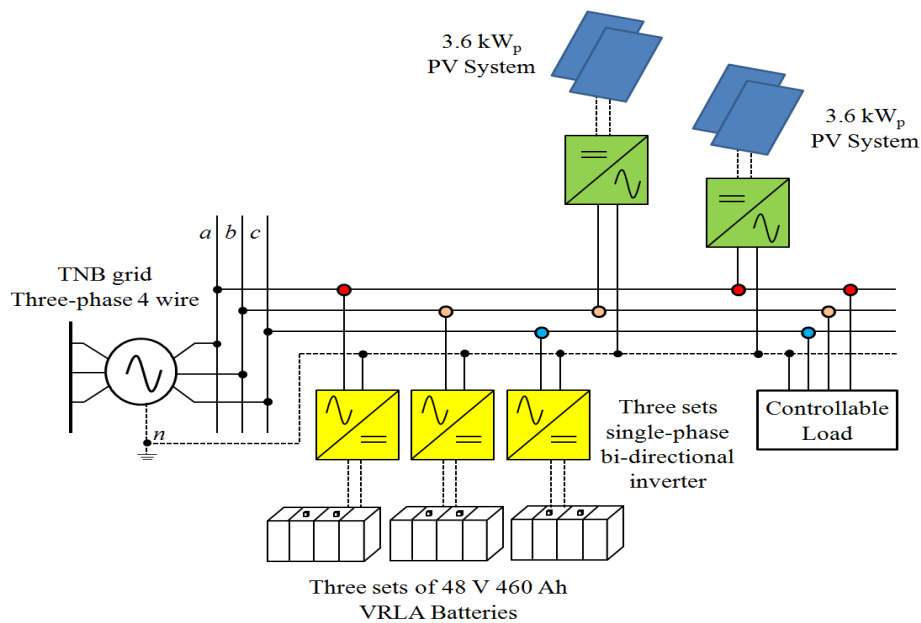


Figure 6.1 Setup of the proposed three single-phase fuzzy controlled energy storage systems

Elcontrol STAR 3 power meters are located at several points in order to measure the voltage, current and power at the generator, PV systems and load side. Several 40/5A current transformers are used to measure current. Data Taker DT82 is used to acquire and compile every data entry while a supervisory computer is used to record data and communicate with the three single-phase energy storage systems via RS485/USB converter. The data sent by the supervisory computer to the three single-phase energy storage systems are translated into a standard OPC format via YAOPC server that is under the SMA proprietary protocol. Figure 6.2 shows the flow of data measurements and the instruction between the supervisory computer and three single-phase energy storage systems.

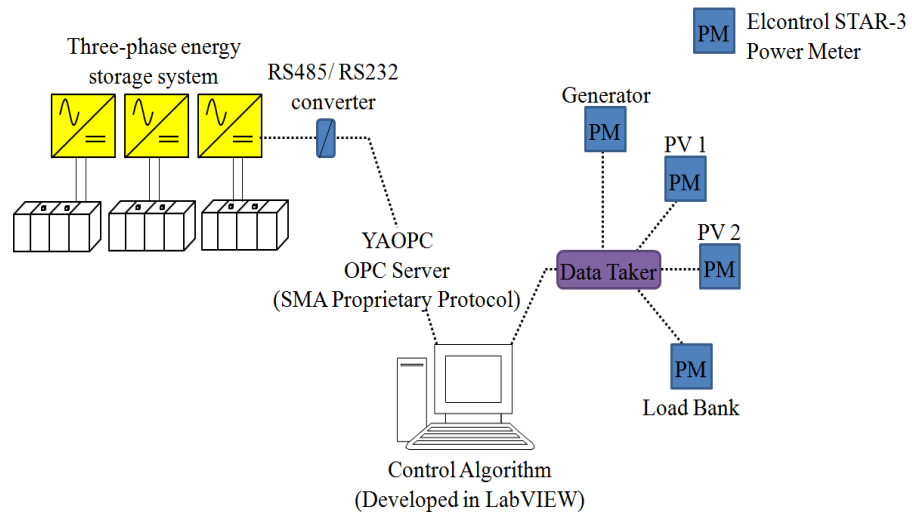


Figure 6.2 Data acquisition between supervisory computer, three single-phase energy storage systems and Data Taker

6.3 Strategy of Improving Voltage Quality

The nominal voltage for single-phase to ground is usually 230 V to 240 V while 415 V is for three-phase system. National standards IEC 60038:2009 has specified that the statutory limit for voltage excursion on the low-voltage distribution network is +10% and -6% with the reference of 230 V nominal voltage. The degree of a network unbalance is defined with voltage unbalance factor (*VUF*). The acceptable tolerance of the *VUF* is 2.0% in Malaysia and it shall not exceed 1.0% for 5 occasions within any 30 minute time period at the terminals at the customer's side. In this section, a fuzzy control strategy is proposed to mitigate the voltage unbalance factor and voltage level while concurrently allowing maximum power output of the PV systems. It is developed and implemented with LabVIEW™ to manipulate the real power output of the three single-phase energy storage systems.

The coordinated control of three-phase refers to a technique used to correct the voltage changes on the three phases simultaneously. This technique is effective if the voltage change at one phase is independent of that on the other two phases. However, there is a neutral line on the low-voltage distribution network. Each phase voltage, also known as the phase-to-neutral voltage, is measured from the phase to the respective point of the neutral line. If one particular phase-to-neutral voltage is changed due to the power injection from a PV system, then the neutral voltage can be shifted away from the reference because the unbalanced or harmonic current flows through the neutral line. As a result, the other two phase-to-neutral voltages will be changed instantly. Apart from that, moving one phase-to-neutral voltage will directly affect the voltages on other phases because of the mutual couplings in between the three phases and the neutral line.

In the proposed fuzzy controlled approach, the Park's Transformation is used to transform the three phase-to-neutral voltages into the sequence voltages in order to determine which phase should be corrected first. The correction must be carried out on one phase at a time before it can be moved to another phase. If one phase voltage is corrected, the changes on other phases due to the effects of the mutual couplings and harmonic currents can also be reduced. This approach can restore the balance of the low-voltage distribution networks under the influence of the mutual couplings and the circulation of the harmonic current.

In order to coordinate and identify the severe phase among all three phases, the well-known park transformation is used to estimate the sequence components of the voltage at a particular point of interest.

$$\begin{bmatrix} V_p \\ V_n \\ V_z \end{bmatrix} = \frac{1}{3} \begin{bmatrix} 1 & \alpha^2 & \alpha \\ 1 & \alpha & \alpha^2 \\ 1 & 1 & 1 \end{bmatrix} \begin{bmatrix} V_a \\ V_b \\ V_c \end{bmatrix} \quad (6.1)$$

where V_z , V_p and V_n are zero, positive and negative sequence voltage respectively. V_a , V_b and V_c are the phase A, B and C voltage respectively.

The voltage excursion ($dV_{a,b,c}$) between the phase voltage and the average phase voltage is calculated as follows:-

$$\begin{bmatrix} dV_a \\ dV_b \\ dV_c \end{bmatrix} = \left(\frac{1}{3} \begin{bmatrix} 1 & \alpha^2 & \alpha \\ 1 & \alpha & \alpha^2 \\ 1 & 1 & 1 \end{bmatrix} \right)^{-1} \begin{bmatrix} 0 \\ -V_n \\ -V_z \end{bmatrix} \quad (6.2)$$

This equation is equivalent to the differences between the phase voltage and the average voltage (Caldon et al., 2014). The correction will take place at the designated phase where the maximum voltage excursion is engaged,

$$d_m(\max) = \text{Max}\{dV_a, dV_b, dV_c\} \quad (6.3)$$

The fuzzy control will be triggered to control the real power output of the bi-directional inverter to maintain the voltage level and reduce the voltage unbalance factor. Figure 6.3 shows the control hierarchy. It consists of a supervisory system, phase selector, fuzzy control, storage control and dissipation control. The first level of the supervisory system determines the network conditions by measuring the three-phase voltages (V_a), (V_b) and (V_c), the generator power (P_{gen}) PV power output (P_{pvout}) and load consumption (P_{load}) of the experimental network. The second level supervises the conditions

of the energy storage system by measuring the battery SoC , DC-link voltage V_{dc} , and the output of the storage system.

The supervisory system will first identify the voltage unbalance factor of the distribution network. If the network unbalance factor is greater than 1.0%, the supervisory system will identify the voltage excursion (dV_m) based on eq. (6.2). This information will be dispatched to the phase selector in order to identify the most severe phase as shown in eq. (6.3). The reason for incorporating the phase selector into the control algorithm is because individual phase voltages are interrelated due to the mutual coupling and the voltage unbalance factor is affected by the individual phase voltages. The phase with highest voltage excursion is declared as the severe phase, and therefore, the bi-directional inverter that is connected on that particular phase will be triggered.

Simultaneously, the phase selector will dispatch the information of the phase voltage (V_m) and battery state of charge (SoC_m) of the chosen phase to the fuzzy control algorithm to compute the instruction ($\Delta I_m(t)$). Based on the output of the fuzzy control, the control algorithm will trigger either to store/dissipate the power to/ from the energy storage system. The energy storage system will absorb power from the network and store it in the batteries when the voltage is higher than the setpoint voltage. However, if the measured voltage is lower than the setpoint voltage, the energy storage system will supply power from the batteries to the network.

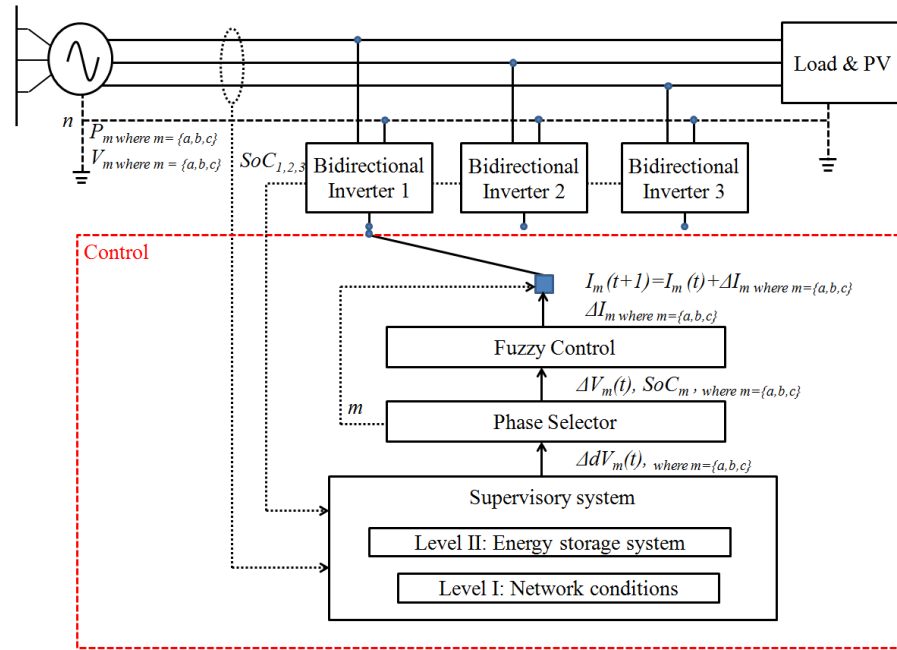


Figure 6.3 Control hierarchy of the three-phase energy storage system

In the existing fuzzy controller, the batteries' state of charge (SoC) is one of the input parameters. If the SoC is lower than a certain threshold, say 60%, then the fuzzy controller will immediately reduce the discharge current in order to avoid the rapid exhaustion of energy stored in the batteries. Similarly, if the SoC is higher than a certain threshold, say 95%, the control algorithm will limit the amount of the charging current to avoid the batteries being overcharged. The monitoring of the SoC is to maintain the lifespan of the batteries.

The details of the fuzzy control algorithm to compute the instruction (ΔI) to Sunny Island 5048 is shown in Figure 5.25. The fuzzy control system receives the measured voltage ($V_{measured}$) and the battery state of charge (SoC) in real time from the supervisory system. $V_{measured}$ is the voltage at the PCC. It is then

compared with the upper and lower voltage setpoints to determine whether the voltage is within its specified range. If the voltage deviates from the specified range, the voltage difference ΔV is calculated using $V_{measured} - V_{ref}$ where V_{ref} is the nominal voltage. The fuzzy control method uses ΔV and SoC to undergo the fuzzification and defuzzification steps, so to produce an instruction (ΔI) to the bi-directional inverter. The whole process will continue until the voltage unbalance factor is to be less than 1.0%. Once the voltage unbalance factor is restored, the voltage magnitude at each phase will be within the statutory limit.

6.4 Operation of the System

Previous section detailed the design and development of three single-phase energy storage systems with fuzzy control. In this section, three case studies were performed to evaluate the effectiveness of the energy storage system in mitigating the voltage rise, and voltage unbalance factor caused by the intermittent PV power output under different loading conditions. These case studies are listed as follows:-

Case Study I:

This case study is designed to present the voltage effects of non-uniform distribution of single-phase PV systems in the experimental network under balanced load condition. The experiment is divided to two sub-case studies, in which, one is evaluated with a single-phase PV system connected at one phase

while the second sub-case study is evaluated with two single-phase PV systems on two different phases.

Case Study II:

In this case study, the generation and condition are the same as case study I. The performance of the three single-phase fuzzy controlled energy storage systems for mitigating voltage rise and voltage unbalance factor is evaluated.

Case Study III:

In this case study, the performance of the three single-phase fuzzy controlled energy storage system is evaluated based on the extreme conditions where two PV systems are connected at different phases with unbalanced loading condition.

6.4.1 Case Study I: Network Condition with High Penetration of PV

6.4.1.1 Single PV Operation

The purpose of this case study is to evaluate the voltage effect with the integration of PV systems on the experimental low-voltage distribution network under balance load condition. The voltage magnitude at the PCC is measured and recorded on a regular basis. Voltage unbalance factor is calculated and recorded based on the measured three-phase voltage magnitude as shown in Eq. (6.1). In this case study, a fixed load of 1.0 kW is introduced to each phase respectively and a PV system is connected to phase C only.

Figure 6.4 shows the voltage unbalance factor, load profile and PV power output of the experimental low-voltage distribution network. At 140 s, PV system is synchronised with phase C of the network and generates 1.1 kW to the network. At 400 s, the PV system generates an output of 2.5 kW, hence causing the voltage unbalance factor to rise upto 2.3% which is above the statutory limit. From this experiment, it is noticed that an excess power of 2 kW can cause the network voltage unbalance factor to rise above 2.0%.

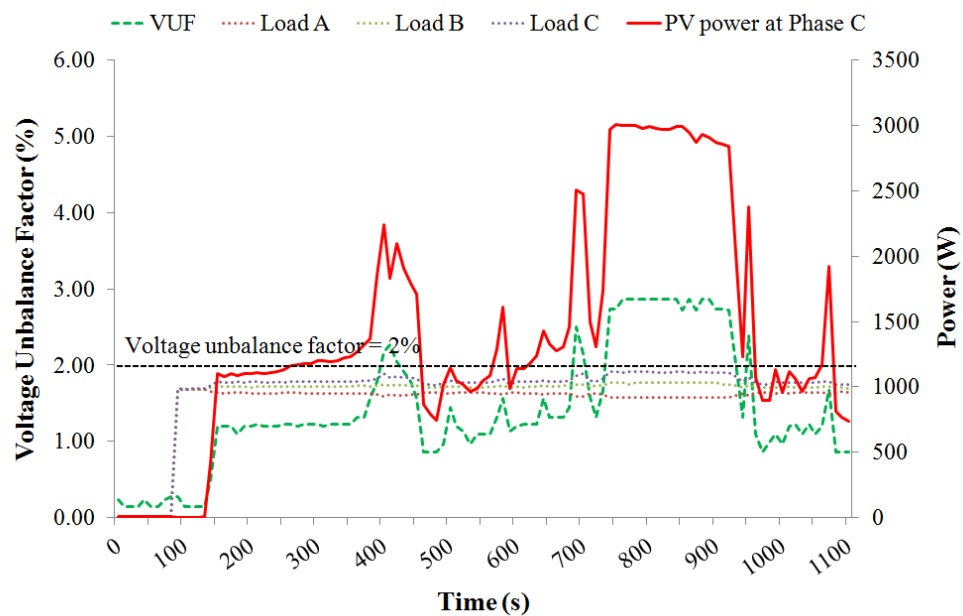


Figure 6.4 Voltage unbalance factor, PV power output and load demand at the PCC of the experimental network

Figure 6.5 shows the three-phase voltage magnitude and the voltage unbalance factor. The three-phase voltage magnitude is approximately 240 V when there is no PV connected to the experimental network. However, the network voltage unbalance factor starts to rise as the PV power output is higher than the load demand. At 750 s, an excess power of 2.0 kW is generated, hence causing the phase C voltage to increase to 255 V. At the same time, the

voltage on phase A and B are 247 V and 233 V respectively. The three-phase average voltage magnitude is calculated as 245 V. While the voltage excursion ΔV_a , ΔV_b , ΔV_c are calculated to be 2 V, -12 V and 10 V respectively. It is shown that the greater the voltage excursion, the greater the voltage unbalance factor of the network.

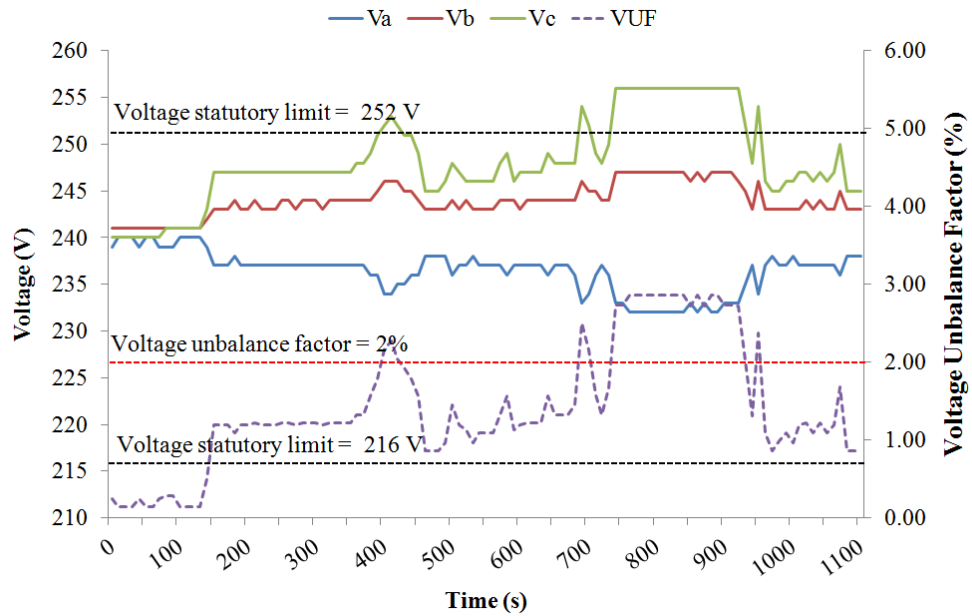


Figure 6.5 Three-phase voltage magnitudes and the corresponding voltage unbalance factor of the experiment

6.4.1.2 Two PV Operation

Another case study is carried out to investigate the impact of two PV systems on the voltage unbalance under balance load condition. Figure 6.6 shows the voltage unbalance factor, PV power output at phase B and C, and the load profile of the experimental case study. A fixed load of 1.0 kW is introduced to each phase respectively. At 300 s, the PV systems are connected to the network. From 301 s to 500 s, the PV systems connected at phase B and C

generate approximately 2.0 kW and 2.5 kW respectively, hence causing the voltage unbalance factor to hit higher than the statutory limit of 2.0%.

Starting from 700 s, PV power output are recorded to be close to the load. Hence, the voltage unbalance factor is reduced to approximately 1.5%. The voltage unbalance factor is often more than 1.0% although the PV power outputs at phase B and C are close to the load demand. This is due to the non-uniform distribution of PV systems has caused the network to become unbalanced. From 1150 s onwards, the PV power outputs are recorded to be very intermittent, hence making the voltage unbalance factor to rise above the statutory limit of 2.0%.

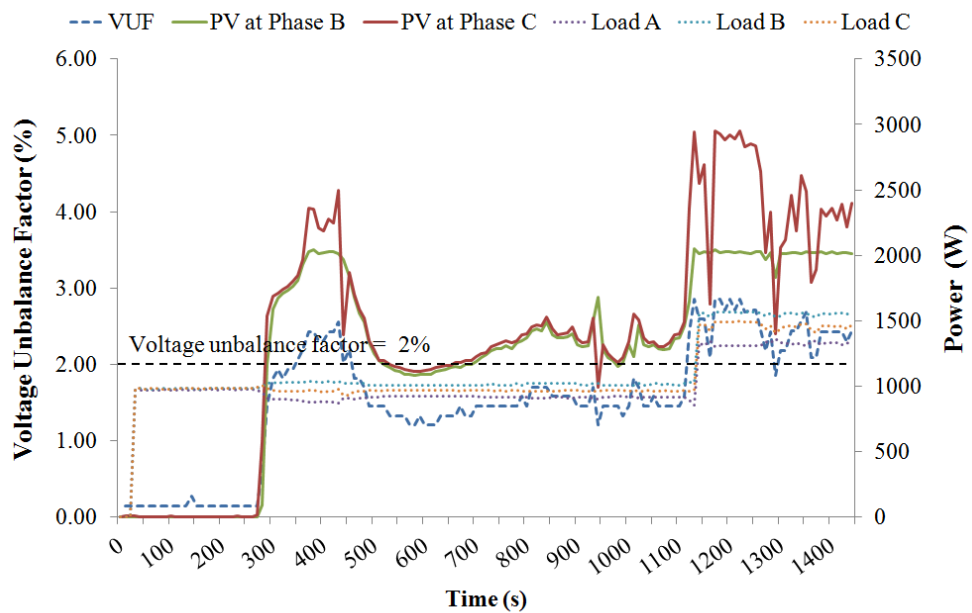


Figure 6.6 Voltage unbalance factor, two PV outputs and load demand at the PCC of the experimental network

Figure 6.7 shows the relationship between the three-phase voltage magnitude and the voltage unbalance factor of the experiment. At the first 300 s, the average voltage magnitude is calculated as 240 V while the voltage excursion

ΔV_a , ΔV_b , ΔV_c are calculated as -1 V, 1 V and 0 V. The three-phase voltage magnitudes do not differ far from each other, therefore the network voltage unbalance factor is recorded to be approximately 0.1%. However, starting from 301 s to 500 s, the three-phase voltage magnitude start to differ from each other due the unbalanced PV power generation. As a consequence, the voltage unbalance factor of the network is also increased.

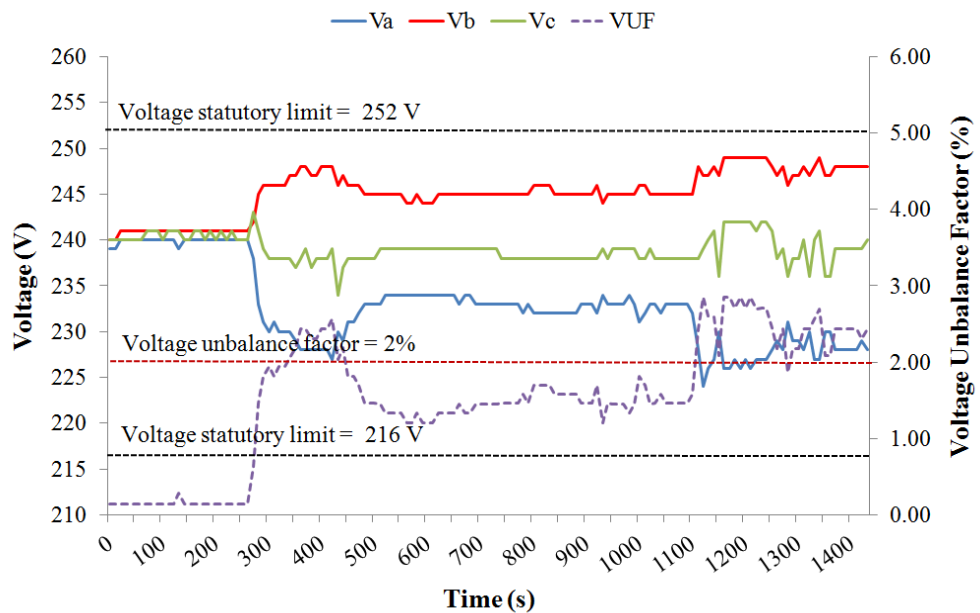


Figure 6.7 Three-phase voltage magnitudes and the corresponding voltage unbalance factor of the experiment case study

6.4.2 Case Study II: Performance of the ESS under Intermittent PV Power Output with Balance Load Condition

6.4.2.1 Single PV Operation

The control scheme is tested on the experimental low-voltage distribution network to evaluate the effectiveness of the control algorithm in mitigating the

voltage unbalance with one single-phase PV system under balanced load condition. Figure 6.8 shows the voltage unbalance factor, PV power output and power output of the energy storage throughout the experiment. Starting from 0 s to 1499 s, a fixed load of 1.0 kW is introduced to each phase. The network voltage unbalance factor is recorded at 0.5%. However, at 1500 s, PV is connected at phase A and it generates 3.8 kW. As a result, the voltage unbalance factor is increased from 0.5% to 1.9%. At 1740 s, the fuzzy controlled energy storage system at phase A starts to absorb the excess power, hence reducing the voltage unbalance factor to 0.9%.

A negative value of the energy storage power output indicates the fuzzy controlled energy storage system is absorbing surplus power from the network, while a positive value indicates the fuzzy controlled energy storage system is supplying power to the network. At 2240 s, the fuzzy controlled energy storage system at phase A further reduces the voltage unbalance factor to 0.5% by absorbing 2.9 kW from the network. In Section II, at 2640 s, PV power output is slightly increased to 3.96 kW causing the voltage unbalance factor to increase from 0.5% to 1.0%. At 3340 s, the voltage unbalance factor once again is reduced to 0.5% when the two fuzzy controlled energy storage systems connected to phase B and C have supply 1.1 kW and 1.2 kW respectively. The main advantage of the fuzzy controlled energy storage system is to create balance between the generation and demand.

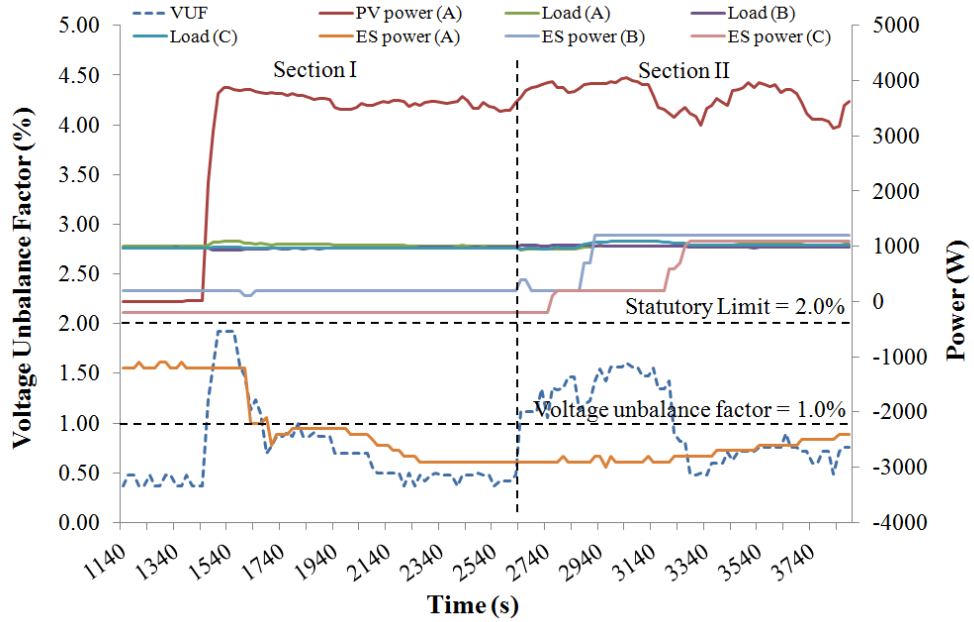


Figure 6.8 PV power output, three-phase loads, power outputs of the fuzzy controlled energy storage systems and the corresponding voltage unbalance factor of the experimental case study

Figure 6.9 shows the relationship between the three-phase voltage magnitude at the PCC and the voltage unbalance factor. At 1500 s, the average voltage magnitude is calculated as 241.67 V while the voltage excursion ΔV_a , ΔV_b , ΔV_c are calculated as 8.33 V, 7.67 V and 0.67 V respectively. Based on the calculation, phase A is selected for further corrective action. Hence, the fuzzy controlled energy storage system connected at phase A absorbs 2.4 kW from the network in order to reduce the voltage unbalance factor. As a consequence, voltage unbalance factor is reduced to less than 1.0%

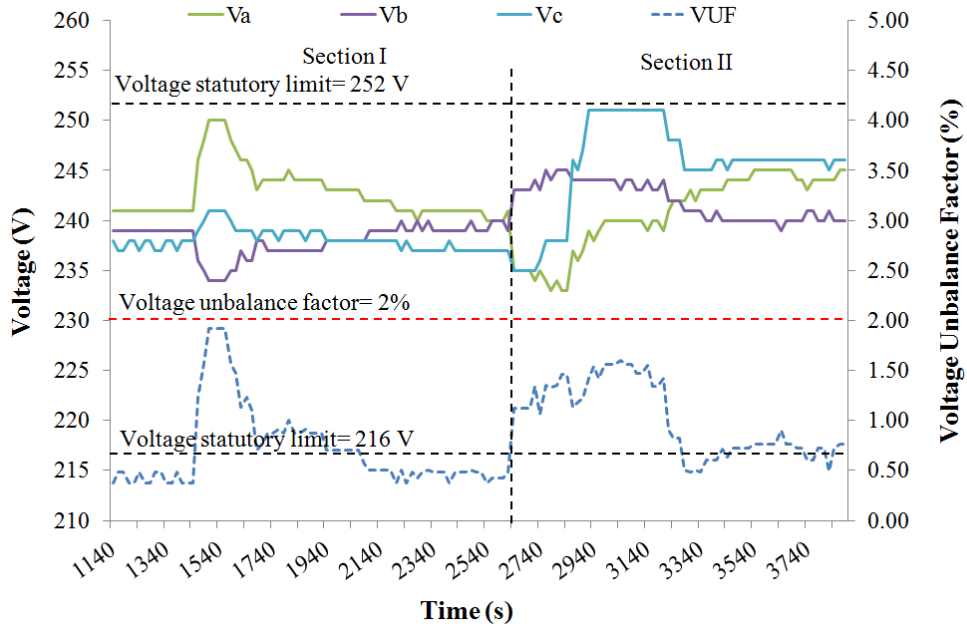


Figure 6.9 Three-phase voltage magnitude and the corresponding voltage unbalance factor of the experimental case study

6.4.2.2 Two PV Operation

The objective of this case study is to study the effectiveness of the proposed fuzzy control method to mitigate the voltage level and voltage unbalance factor with PV systems connected on two different phases under balance load condition. A fixed load of 1.5 kW is introduced to each phase of the experimental network and two 3.6 kW_p PV systems are connected to phase B and C respectively. Figure 6.10 shows the network voltage unbalance factor, PV power output and power output of the fuzzy controlled energy storage system. It is noticed that the PV power output fluctuates rapidly. In section I, starting from 520 s, the fuzzy controlled energy storage system connected on phase C gradually increases its power absorption from 0.2 kW to 0.5 kW and

up to 1.0 kW while the fuzzy controlled energy storage system on phase B gradually increases its power absorption from 0.2 kW to 1.2 kW. As a result, the voltage unbalance factor at 1300 s is reduced to 0.5%. In section II, it is noticed that PV power outputs drop suddenly and cause the voltage unbalance factor to increase from 0.5% to 1.5%. However the fuzzy control algorithm makes an appropriate corrective action at 2620 s. Therefore, the voltage unbalance factor is reduced to an acceptable value.

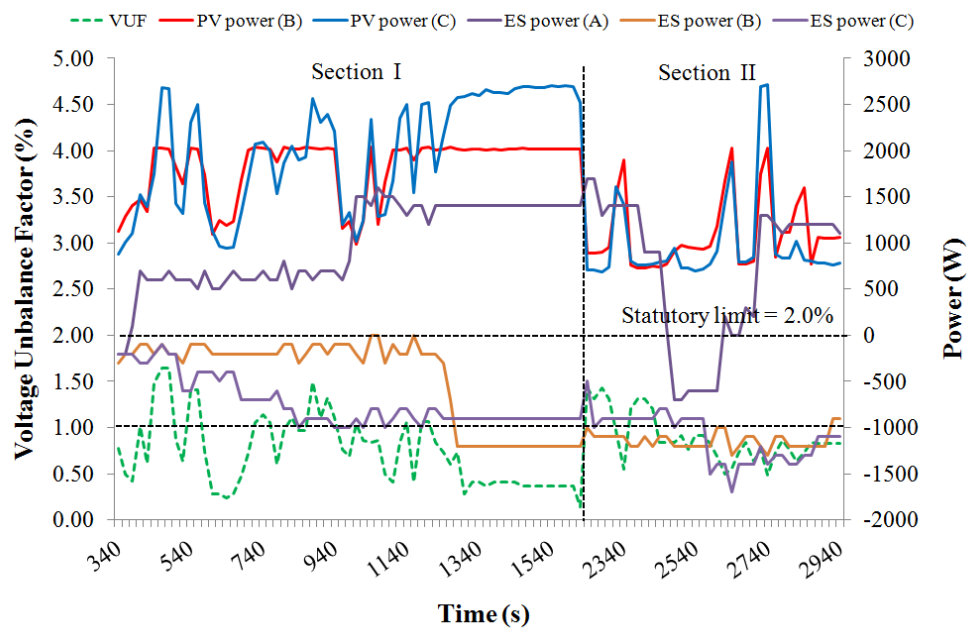


Figure 6.10 Power outputs of the two PV systems, fuzzy controlled energy storage systems and the corresponding voltage unbalance factor of the experimental case study

Figure 6.11 shows relationship between three-phase voltage magnitude and voltage unbalance factor. In Section I, at 520 s, the average voltage magnitude is calculated as 240 V while the voltage excursion ΔV_a , ΔV_b , ΔV_c are calculated as 2 V, 3 V and 1 V respectively. Therefore, fuzzy controlled energy storage system connected at phase B is selected to perform further corrective action. In Section II, at 2620 s, the average voltage magnitude is

calculated as 239.33 V while the voltage excursion ΔV_a , ΔV_b , ΔV_c are calculated as 1.67 V, 0.67 V and 2.33 V respectively. Hence, fuzzy controlled energy storage system connected at phase C is selected for further corrective action.

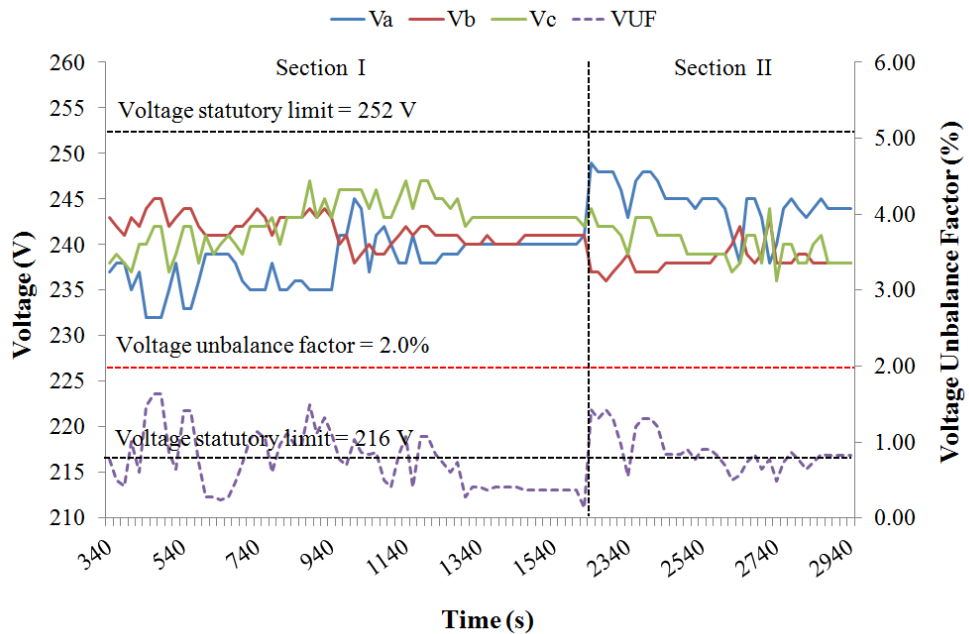


Figure 6.11 Three-phase voltage magnitude and the corresponding voltage unbalance factor of the experimental case study

6.4.3 Case Study III: Effectiveness of the Fuzzy Controlled Energy Storage System with PV under Unbalance Load Condition

The case study is designed to evaluate the response of the proposed three single-phase fuzzy controlled energy storage systems to a sudden change of PV power output under unbalanced load condition. The load profiles for phase A, B and C are set to 1.0 kW, 2.0 kW and 1.0 kW respectively. Figure 6.12 shows the voltage unbalance factor, three-phase load profile, and PV power

outputs at phase B and C respectively. At 450 s, the PV systems connected at phase B and C generate approximately 1.5 kW and 2.0 kW respectively, hence causing the voltage unbalance factor to rise above the statutory limit of 2.0%. However, it is noticed that under Section I, the fuzzy controlled energy storage systems connected at phase B and C have performed some corrective action to reduce the voltage unbalance factor from 2.0% to 0.5%. In Section II, the load at phase A is increased from 1.0 kW to 2.0 kW at 1350 s causing the voltage unbalance factor to rise above 1.7%. However, the fuzzy control system is able to correct the voltage magnitude very rapidly.

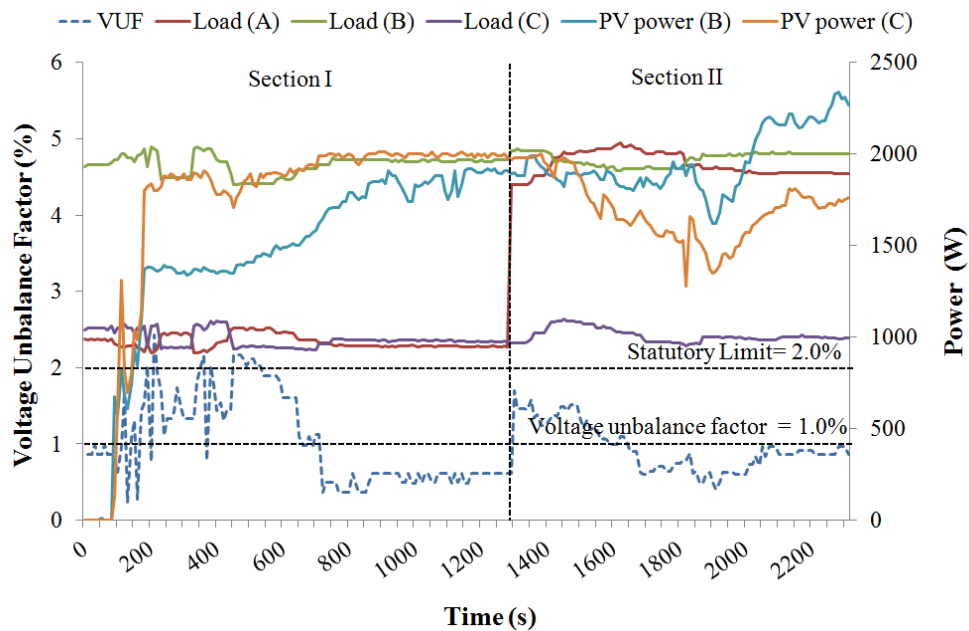


Figure 6.12 Load profiles, PV outputs and the corresponding voltage unbalance factor of the experimental case study

Figure 6.13 shows the change of the power output of the three single-phase fuzzy controlled energy storage systems and the battery state of charge (*SoC*). The responses of the energy storage system react accordingly to the voltage unbalance and network voltage level. Figure 6.14 shows the relationship

between three-phase voltage magnitude and the corresponding voltage unbalance factor of the experimental case study. In Section I, at 450 s, the average voltage magnitude is calculated as 244 V while the voltage excursion ΔV_a , ΔV_b , ΔV_c are calculated as 4 V, 3 V and 7 V respectively. Therefore, fuzzy controlled energy storage system connected at phase C is selected for further corrective action. The instruction to the fuzzy controlled energy storage system is calculated based on the voltage condition at phase C. At 1350 s, it is noticed that the voltage unbalance factor is increased due to the growth of the load on phase A. However, the three single-phase fuzzy controlled energy storage systems are able to correct the voltage unbalance factor promptly.

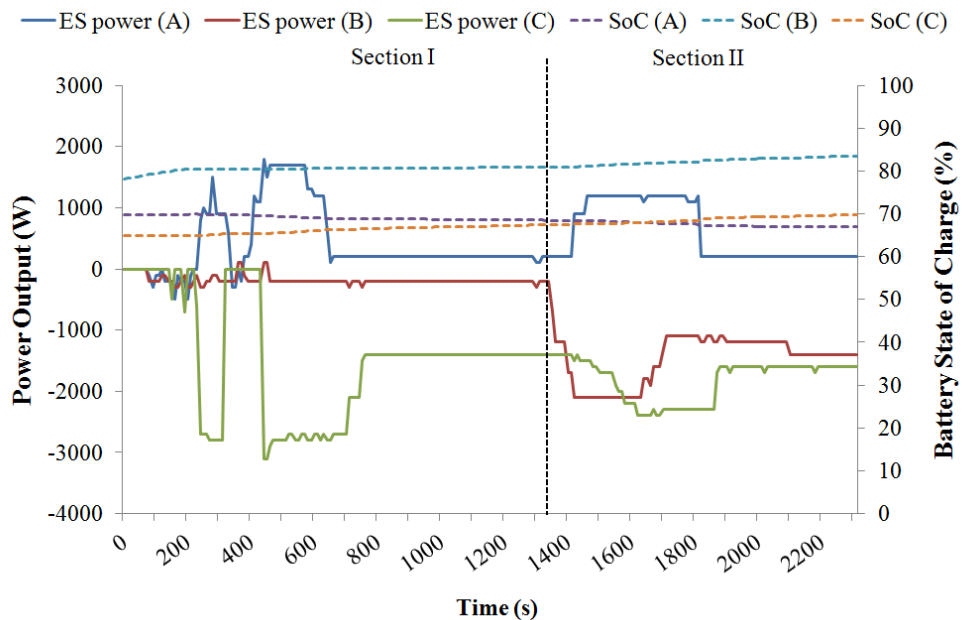


Figure 6.13 Change of the power output for three single-phase fuzzy controlled energy storage systems and battery *SoC* of the experimental case study

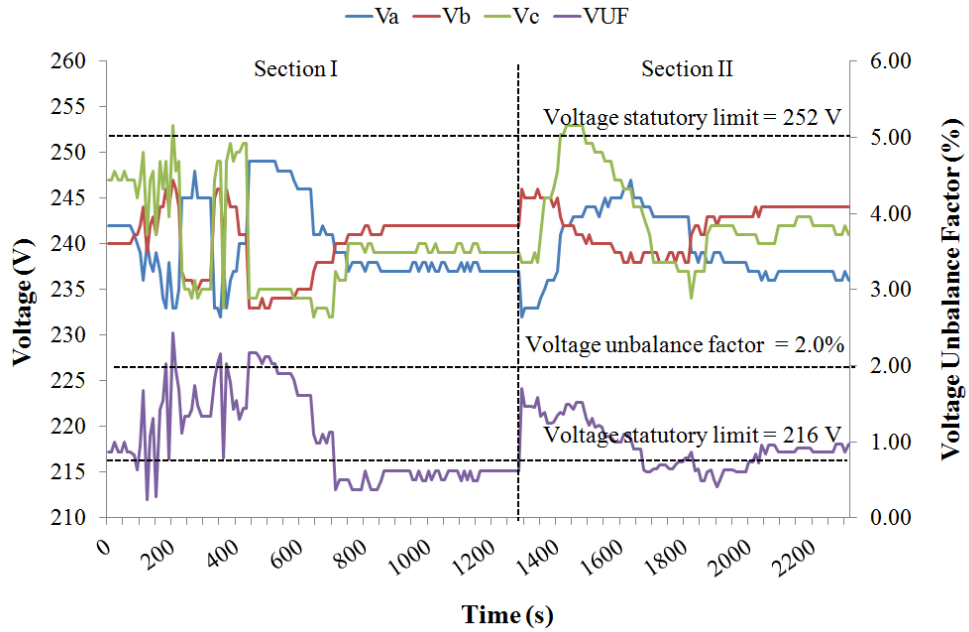


Figure 6.14 Three-phase voltage magnitude at the PCC and the corresponding voltage unbalance factor of the experimental case study

6.5 Discussion

This chapter presents an improved version of the control algorithm using fuzzy control and the Park's transformation to coordinate the three single-phase fuzzy controlled energy storage systems for mitigating voltage unbalances in the distribution networks integrated with two single-phase PV systems. The three single-phase fuzzy controlled energy storage systems consist of three units' bi-directional inverters. Each inverter is integrated with lead acid batteries. The fuzzy control algorithm is developed using LabVIEW™. The three single-phase fuzzy controlled energy storage systems are controlled by a supervisory computer.

The Park's transformation is used to calculate the positive, negative and zero sequence components of the three phase-to-neutral voltage at a particular point of interest. The sequence voltage is input to the phase detector in order to identify the affected phase that cause high degree of voltage unbalance factor and further coordinate the three-phase energy storage system so that it can address that particular phase to correct the voltage level back to its nominal and mitigate the voltage unbalance factor. In this extend, the Park's transformation is able to improve the performance of mitigating voltage unbalance factor to the minimum point.

The fuzzy control module calculates the voltage excursion (ΔV) and obtains the battery state of charge (SoC). Further instruction is given to the three single-phase fuzzy controlled energy storage systems in order to correct the voltage unbalance factor and maintain the voltage level at its statutory limit while ensuring no curtailment is involved. The performance of the fuzzy control algorithm is verified by setting up the three single-phase fuzzy controlled energy storage systems in a designed low-voltage distribution network with two single-phase PV systems.

The principles described earlier in this chapter were applied to various evaluation scenarios under several conditions with different generation and demands. These scenarios were outlined to verify the performance and effectiveness of the proposed control algorithm. In all the case studies, the developed control algorithm is found to satisfy the operational limit of the phase voltage and voltage unbalance factor with intermittent PV power output.

At the same time, unnecessary renewable energy curtailment was avoided. In addition, the fuzzy controlled energy storage system could provide significant benefits such as increase in the use of renewable energies without limiting the generation.

CHAPTER 7

EXPERIMENTAL VALIDATION OF FUZZY CONTROL ALGORITHM

7.1 Introduction

The fuzzy control method employed in the energy storage system is developed by using LabVIEW™. In this chapter, a bi-directional inverter manufactured by a different manufacturer, namely Studer Innotech is used to further verify the suitability of the fuzzy controlled energy storage system to mitigate voltage regulation and voltage unbalance of the distribution network caused by PV systems. Various scenarios with different generation and loading conditions are used to evaluate the effectiveness of the fuzzy controlled energy storage system. The physical development of the energy storage system can be categorized as follows:

Step 1: Setting up the Bi-directional Inverter

Different brands of the bi-directional inverter may have different setup procedures including different controlling parameters. Therefore, a brand new setup procedure is outlined.

Step 2: Control and monitoring in LabVIEW™

As mentioned earlier, different bi-directional inverter may have different control parameters. Therefore, necessary corrective action is needed to evaluate the suitable parameters for manipulating power flow of bi-directional inverter.

Step 3: Evaluation

A series of case studies under different loading and generating conditions are outlined to evaluate the performance of the energy storage system formed with a brand new bi-directional inverter manufactured by different manufacturer.

7.2 Experimental Setup

The experimental low-voltage distributed network as described in chapter 3 is used to perform the case studies. Figure 7.1 shows the experimental network consists of a network emulator, two units of 3.6 kW_p PV systems, a three-phase controllable load bank and an energy storage system.

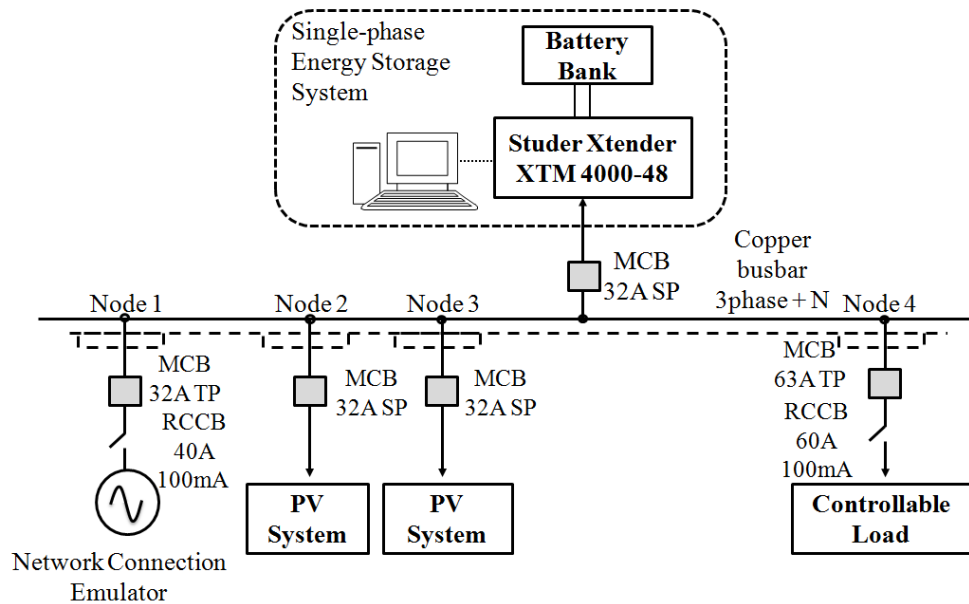


Figure 7.1 Experimental setup

7.3 Energy Storage System

The energy storage is designed and developed to mitigate voltage rise and voltage unbalance on the distribution network. Figure 7.2 shows the energy storage system consists of a different brand of the bi-directional inverter namely Studer Xtender XTM 4000-48 integrated with the battery bank. A communication module Xcom-232i and a remote control RCC-02 are used to establish a connection between the inverter and the supervisory computer. In this chapter, use of another alternative brand for setting up the energy storage system is discussed. The possibility of integrating the fuzzy control with a bi-directional inverter produced by other manufacturer is presented.

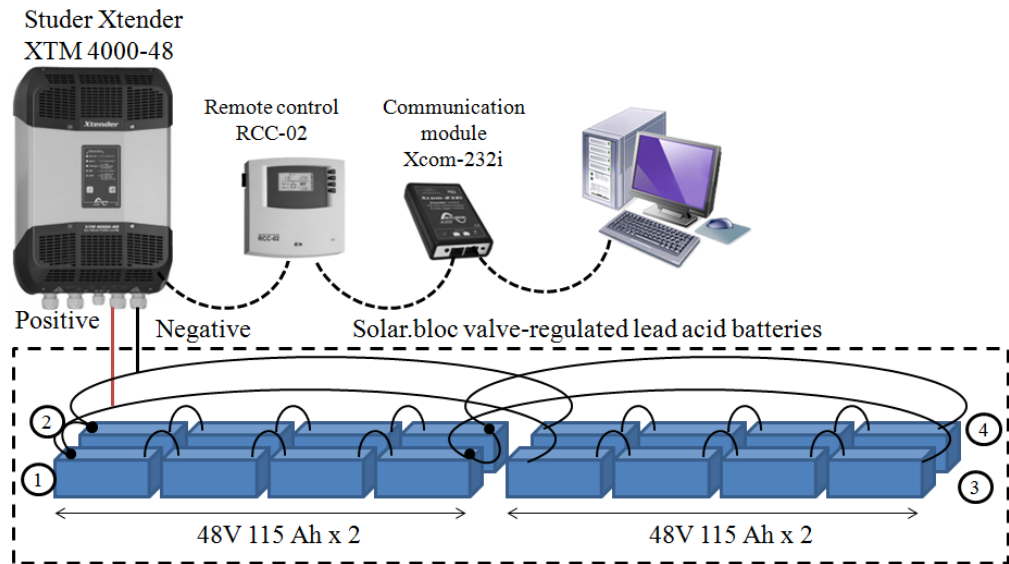


Figure 7.2 Setup of the energy storage system consists of Studer Xtender XTM 4000-48, remote control RCC-02, communication module Xcom 232i, supervisory computer and battery bank

7.3.1 Step 1: Setting Up the Bi-directional Inverter

A bi-directional inverter namely, Studer Xtender XTM 4000-48 is manufactured in Switzerland by Studer Innotec. The maximum rated power output of the inverter is 4.0 kW. Figure 7.3 shows the connection layout of the bi-directional inverter. A temperature sensor can be connected at port (1) as shown in Figure 7.3. It is used to measure the battery temperature in order to optimize the charging process. The XTM 4000-48 does not come with a display panel like Sunny Island 5048. Therefore, a remote control, RCC-02, is an add-on unit to display and program the bi-directional inverter. The remote control, RCC-02, is connected to the communication bus port labelled as (2) and shown in Figure 7.3. It enables the user to supervise the system and control the settings of parameters that are available on the bi-directional

inverter. The open/ terminator port labelled as (3) needs to be set at open position if 2 connectors are occupied. Alternatively, position T is chosen if only one port is occupied.

The bi-directional inverter is powered up by integrating with several units of VRLA batteries. These batteries are formed with 4 banks connected in parallel to have a higher capacity. Each bank consists of 4 units of VRLA batteries connected in series to have 48 V. The positive and negative terminals of the batteries are connected at port (4) and (5) respectively. While the AC output is connected at port labelled as (6). Once the bi-directional inverter is powered up, necessary parameters such as the nominal grid voltage, grid current and maximum charging currents need to be configured via the remote control RCC-02. Grid feed mode needs to be enabled before the bi-directional inverter can feed in current to the grid.

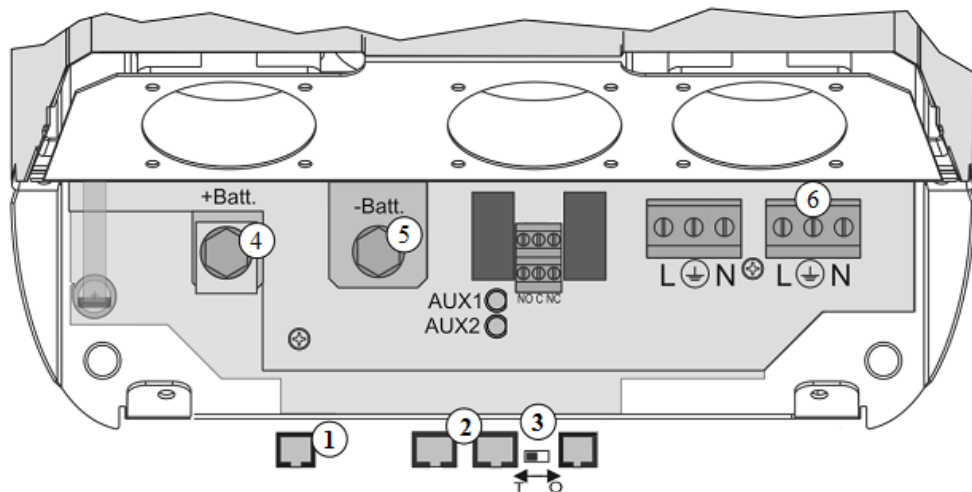


Figure 7.3 Layout of the bi-directional inverter

Unlike Sunny Island 5048, Studer Xtender XTM 4000-48 does not require a third party communication device to establish the communication link. The bi-

directional inverter comes with a communication module, Xcom-232i. It is used to establish a connection between the bi-directional inverter and a supervisory computer to control and monitor the system and network conditions.

Studer Xtender XTM 4000-48 appears to be another alternative inverter that can be used to reduce voltage rise and voltage unbalance factor. Manipulating the real power is possible for XTM 4000-48. However, unlike Sunny Island 5048, the XTM 4000-48 does not give an option to control its reactive power. Nevertheless, controlling reactive power is not a major concern at the moment, as the reactive power compensation is inefficient as compared to real power in the distribution networks as the network resistance is always greater than the reactance.

7.3.2 Step 2: Control and monitoring in LabVIEW

A supervisory computer is used to communicate with the bi-directional inverter. Figure 7.4 shows the system control flow. LabVIEW™ is used to control and monitor the condition of the bi-directional inverter. The company, Studer Innotec has developed an achieve file, scom.exe. It contains a command line tool to communicate through the serial port with the remote control, RCC-02. An achieve file execution interface that is available in the LabVIEW™ is used to execute the scom.exe. The commands are transmitted

via USB/ RS232 port to communication module, Xcom 232i before sending to the bi-directional inverter.

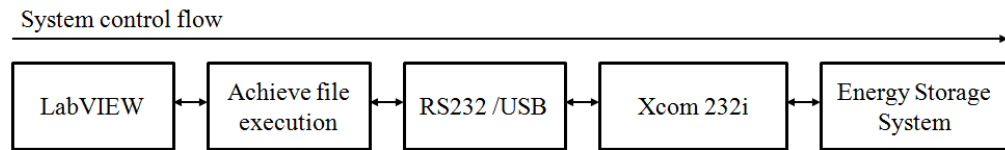


Figure 7.4 Block diagram of the system control flow

Table 7.1 shows the details of the command to be entered into the command prompt in order to read/write from the bi-directional inverter. Examples of read/ write command formats are listed as follows:

Reading:

```
> scom.exe --port=COM3 --verbose=3 read_property src_addr=1
dst_addr=101 object_type=1 object_id=3000 property_id=1 format=FLOAT
```

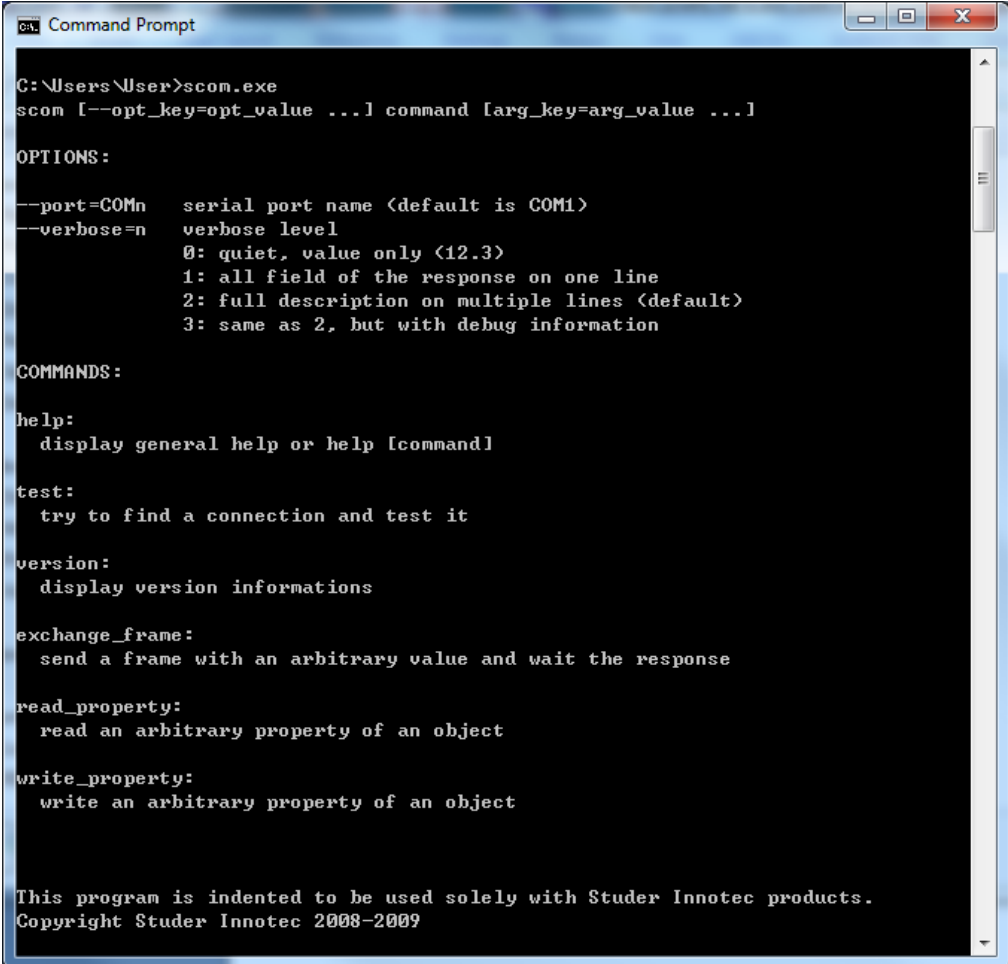
Writing:

```
> scom.exe --port=COM3 --verbose=3 write_property src_addr=1
dst_addr=101 object_type=2 object_id=1138 property_id=5 format=FLOAT
value=12.0
```

Table 7.1 Description of the command line written in the command prompt

No	Command	Description
1	port	Serial port name.
2	verbose	Verbose level. Refers Figure 7.5 for further description.
3	read_property	To read from inverter.
4	write_property	To write to bi-directional inverter.
5	src_addr	Source address. Default value is 1.
6	dst_addr	Destination address. Default value is 101.
7	object_type	User information = 1, Parameter =2.
8	object_id	Parameter ID. Refers Table 7.2.
9	property_id	Read only value = 1, Write value by user on installer level = 5.
10	format	Parameter format. Refers Table 7.2.
11	value	Data to be write to the inverter.

Figure 7.5 shows the command prompt after the execution from scom.exe. Table 7.2 shows the list of the parameter ID numbers and their format types. Only selected parameters are needed for the controlling and monitoring purposes. A full list of the parameters that can be controlled is available in the user manual of the remote control RCC-02.



```
C:\Users\User>scom.exe
scom [--opt_key=opt_value ...] command [arg_key=arg_value ...]

OPTIONS:
--port=COMn    serial port name (default is COM1)
--verbose=n    verbose level
                0: quiet, value only (12.3)
                1: all field of the response on one line
                2: full description on multiple lines (default)
                3: same as 2, but with debug information

COMMANDS:
help:
  display general help or help [command]
test:
  try to find a connection and test it
version:
  display version informations
exchange_frame:
  send a frame with an arbitrary value and wait the response
read_property:
  read an arbitrary property of an object
write_property:
  write an arbitrary property of an object

This program is indented to be used solely with Studer Innotec products.
Copyright Studer Innotec 2008-2009
```

Figure 7.5 Display of the command prompt executed from scom.exe

Table 7.2 List of parameters to be read/ write from/to the bi-directional inverter

No	Parameter ID	Parameter Description	Reading/ Writing Property	Writing Format
1	1127	Grid feeding allowed	Writing	BOOL
2	1138	Battery charging current	Writing	FLOAT
3	1523	Grid feed current	Writing	FLOAT
4	1524	Voltage target	Writing	FLOAT
5	3000	DC Voltage	Reading	NIL
6	3005	Battery current	Reading	NIL
7	3011	Input voltage	Reading	NIL
8	3012	Input current	Reading	NIL
9	3137	Input power	Reading	NIL
10	3138	Output power	Reading	NIL

Figure 7.6 shows the block diagram to monitor the parameters from the bi-directional inverter. Parameters ID as listed in Table 7.2 are updated every second and will be written to the excel spreadsheet for further analysis. An output indicator is added to show the value read from the bi-directional inverter. Similarly, Figure 7.7 shows the LabVIEW™ block diagram to control the bi-directional inverter by writing a value to the parameters. These steps will be repeated until the program is stopped.

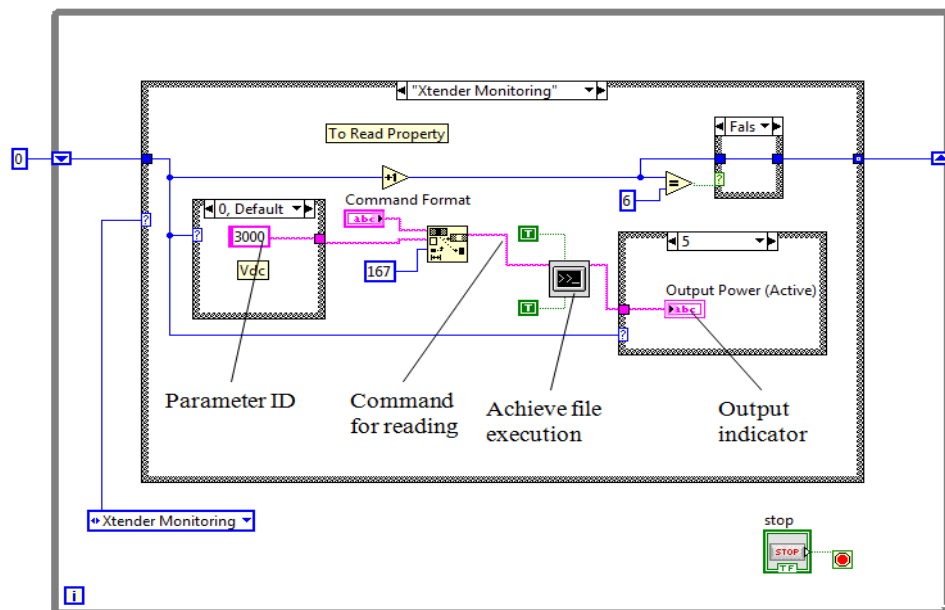


Figure 7.6 Reading parameters in LabVIEW™

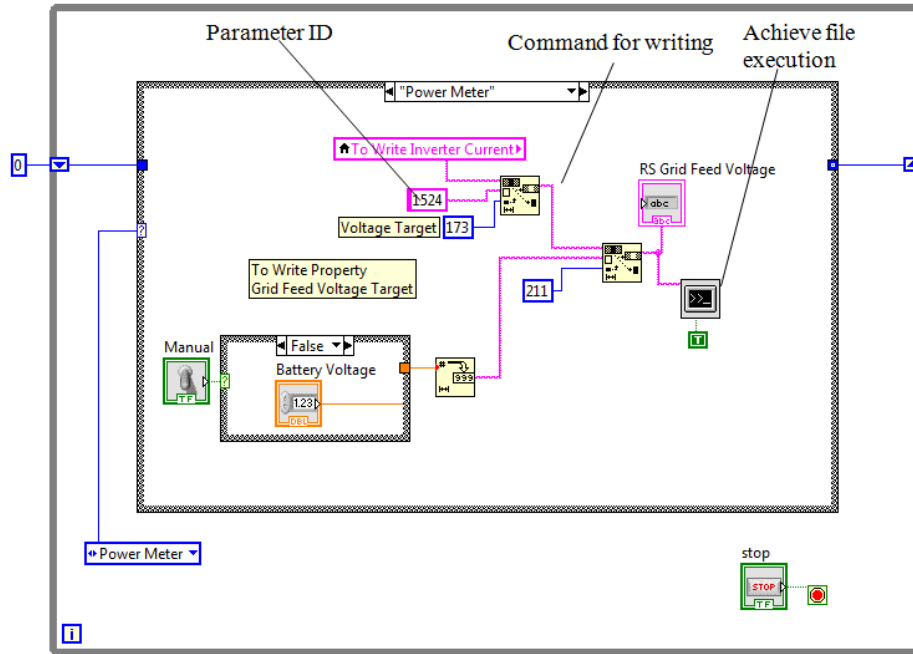


Figure 7.7 Writing parameters in LabVIEW™

7.4 Step 3: Evaluation

Centralised communication controllers have been implemented in the experimental low-voltage distribution network using LabVIEW™. This chapter proposes an alternative brand for developing the energy storage system and the suitability test for integrating the proposed fuzzy control algorithm. In this section, several case studies were carried out to evaluate the feasibility and performance of the energy storage system under different generation and loading conditions as follows:

Case Study I:

This case study investigates the voltage variation and voltage unbalance factor with increasing load at phase A. This is a benchmark study to evaluate the

voltage variation caused by the changing pattern of the load profile without the use of the use of the energy storage system.

Case Study II:

In this case study, the effectiveness of the proposed energy storage system to mitigate the voltage level and reduce the voltage unbalance factor of the experimental network with an increasing load at phase A.

Case Study III:

This case study is performed to investigate the performance of the fuzzy controlled energy storage system to mitigate the voltage level and voltage unbalance factor affected by two units of 3.6 kW_p PV systems under balanced load condition.

Case Study IV:

In this case study, the investigation is to study the performance of the fuzzy controlled energy storage system to mitigate the voltage level and voltage unbalance factor affected by two units of 3.6 kW_p PV systems under unbalanced load condition.

Case Study V:

This case study is designed to study the responses of the fuzzy controlled energy storage system under different generation and loading condition. The PV system attempts to connect and reconnect throughout the experimental case study while the load at phase A is varying.

7.4.1 Case Study I: Effects on Voltage Level under Load Variation without Energy Storage System

This case study is performed to evaluate the effect of increasing load at phase A on the experimental low-voltage distribution network. Figure 7.8 shows the load connected at phase A is increasing with a step of approximately 500 W while phase B and C remained at no load. Figure 7.8 (a) shows the load in phase A is increasing while the voltage at phase A is decreasing. Figure 7.8 (b) shows the voltage unbalance factor of the experimental low-voltage distribution network is increasing as the load at phase A is increasing. As one of the phase is heavily loaded, the network becomes increasingly unbalanced, hence causing the voltage unbalance factor to become severe.

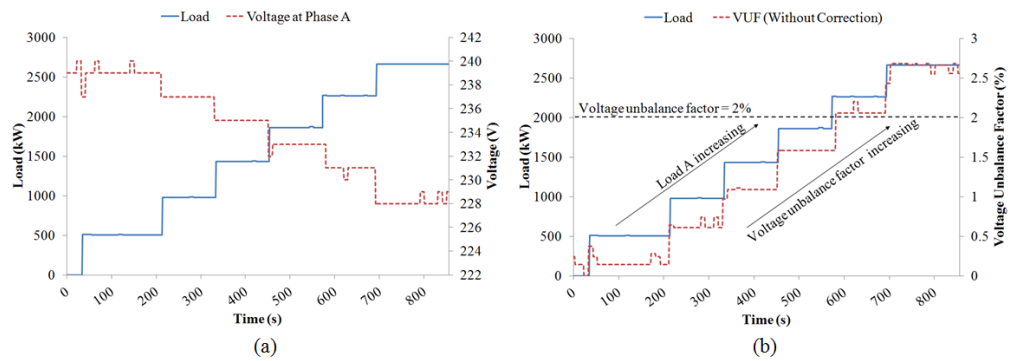


Figure 7.8 (a) Voltage variation and (b) voltage unbalance factor of the experimental low-voltage distribution network under the condition of increasing load at phase A

7.4.2 Case Study II: Effects on the Voltage Unbalance Factor under Load Variation with Fuzzy Controlled Energy Storage System

This case study is designed to compare the network voltage level and voltage unbalance factor under the same loading conditions with and without integrating the fuzzy controlled energy storage system. Figure 7.9 (a) shows the effect of voltage level at phase A with and without the fuzzy controlled energy storage system. It is noticed that voltage at phase A always remained within the tolerance range when the energy storage system is integrated to the experimental low-voltage distribution network. As the load in phase A is increasing, the voltage at phase A is decreasing, the fuzzy controlled energy storage system starts to support the network voltage when the voltage hits the threshold level. Consequently, the network voltage and voltage unbalance factor are kept within the tolerance range.

Figure 7.9 (b) illustrates the network voltage unbalance factor with and without fuzzy controlled energy storage system under the condition of increasing load at phase A. It is shown that the network voltage unbalance factor has violates its statutory limit of 2.0% when the load at phase A has increased up to 2.0 kW. The network voltage unbalance factor can increase up to 2.5% when the load at phase is increasing without the fuzzy controlled energy storage system. On the contrary, with the integration of fuzzy controlled energy storage system, the network voltage unbalance factor always remained below 1.0% even with the load at Phase A increased up to 2.5 kW.

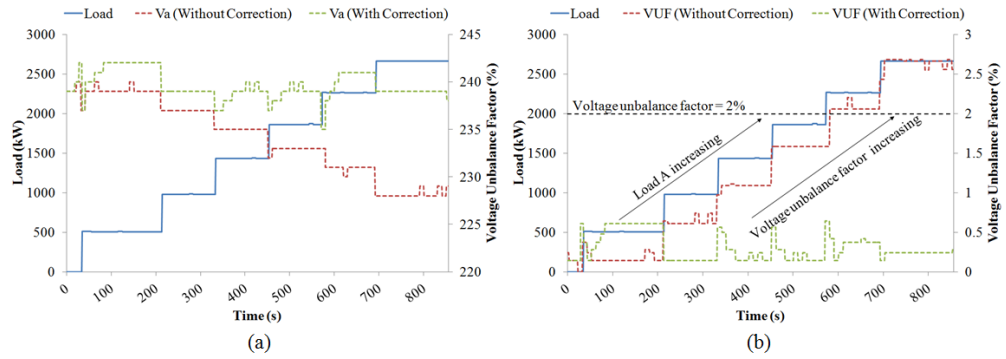


Figure 7.9 (a) Voltage variation and (b) voltage unbalance factor of the experimental low-voltage distribution network with and without fuzzy controlled energy storage system

7.4.3 Case Study III: Performance of the Fuzzy Controlled Energy Storage System with Single-phase PV System under Balanced Load Condition

In this implementation, the fuzzy controlled energy storage system is deployed in conjunction with PV systems under balanced load condition. Two units of 3.6 kW_p PV systems are connected to phase A. Figure 7.10 illustrates the voltage unbalance factor under PV power and load variation of the experimental distribution network. Figure 7.11 shows the network voltage level under the same generation and loading condition.

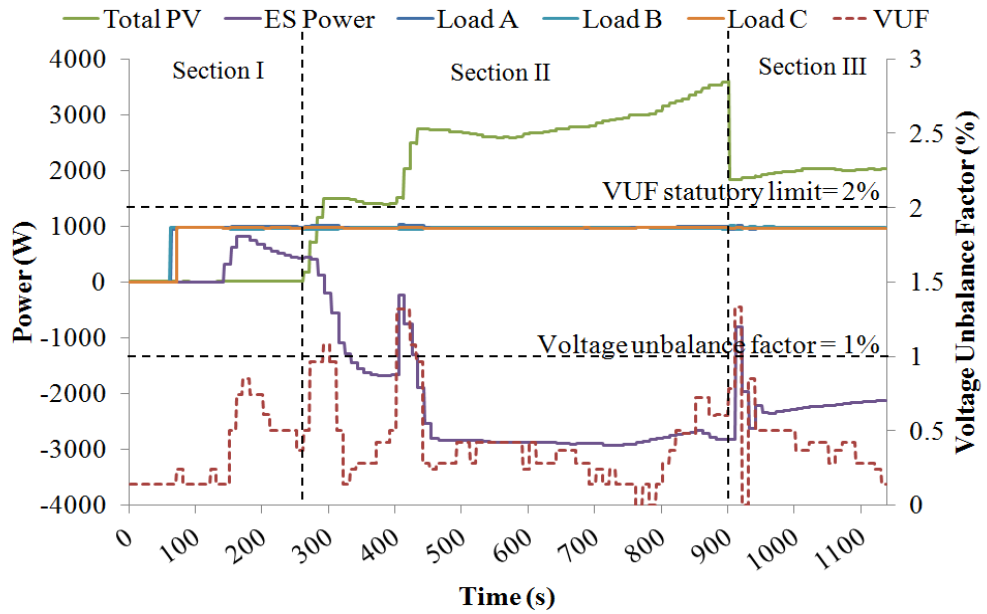


Figure 7.10 Load, PV power output, performance of the fuzzy controlled energy storage system and network voltage unbalance of the experimental case study

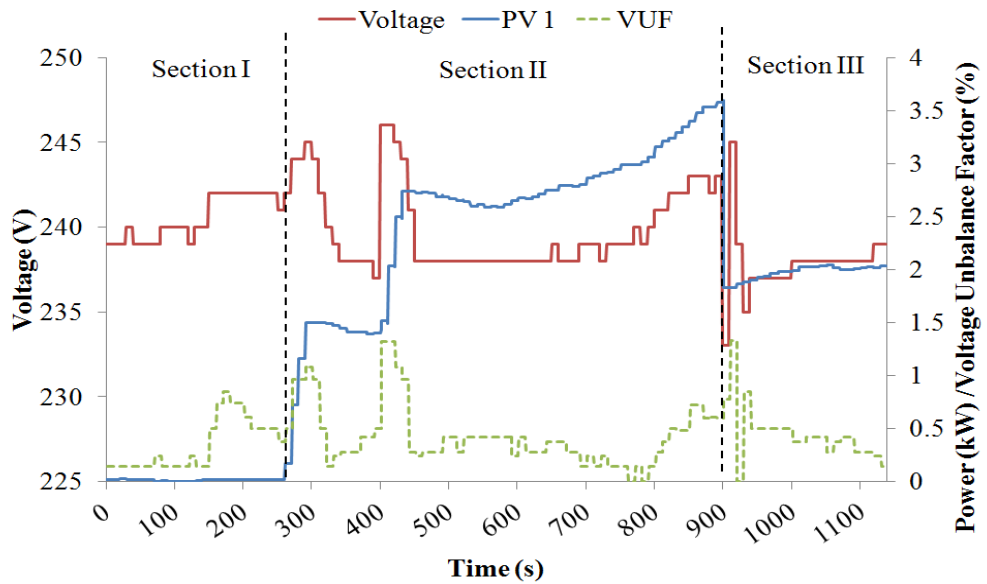


Figure 7.11 Phase to neutral voltage at Phase A, PV power output and network voltage unbalance factor of the experimental case study

Initially, the voltage unbalance factor is recorded at 0.12% before the load and PV systems are synchronised to the experimental network. In Section I, at 50 s, the experimental network is constantly connected to a balanced load of 1.0

kW for each phase respectively. The voltage unbalance factor is recorded to be minimum at this point while the voltage level is recorded in between 239 to 240 V. However, at 150 s, the fuzzy controlled energy storage system on phase A attempts to compensate the load at the same phase, hence causing the voltage unbalance factor to increase slightly from 0.12% to 0.8%, while the voltage magnitude at phase A is recorded at 242 V. This is because only load A is compensated, while load B and C remained at 1.0 kW.

In section II, the PV systems are connected to phase A. At 300 s, the generated power is greater than the load demand causing an excess power circulation in the network. As a consequence, the network voltage unbalance has increased from 0.5% to 1.1% while the voltage magnitude at phase A is recorded at 245 V. Under this circumstance, the control algorithm has feedback to the fuzzy controlled energy storage system to absorb the excess power. At 400 s, the PV power output is increased from 1.5 kW to 3.0 kW, causing the voltage unbalance factor to increase from 0.5% to 1.5%, and the voltage at phase A to raise to 246 V. The control algorithm immediately updates and instructs the fuzzy controlled energy storage system to further absorb more power. It is noticed that the voltage unbalance factor is always kept within 1.0% and the voltage level always maintained within 238 V to 242 V. Section III shows that there is a sudden drop from PV power output causing the voltage unbalance factor once again to hit beyond 1.0%. The control algorithm immediately adjusts the response to the fuzzy controlled energy storage system to reduce the voltage unbalance factor.

7.4.4 Case Study IV: Performance of the Fuzzy controlled energy storage system with Single-phase PV under Unbalanced Load Condition

This case study is designed to investigate the response of the fuzzy controlled energy storage system to mitigate voltage unbalance and voltage rise caused by the intermittent PV power output under unbalanced load condition. Initially, at 100 s, the three-phase unbalanced loads are constantly connected with 500 W, 1000 W and 1500 W to phases A, B and C respectively. Two PV systems are connected to phase A from 600 s onwards. Figure 7.12 shows the details of the network condition in this experimental case study. It consists of the total PV power output, the power output of the fuzzy controlled energy storage system, three-phase unbalanced load and the voltage unbalance factor. Figure 7.13 shows the network voltage at phase A and the total PV power output. Due to large amount of the passing clouds in the University region, the PV power output recorded is fluctuating. It is observed that the voltage unbalance factor is always kept within the statutory limit of 2.0% while the voltage at phase A is always kept within the statutory limit of 252 V with the integration of fuzzy controlled energy storage system on the experimental network.

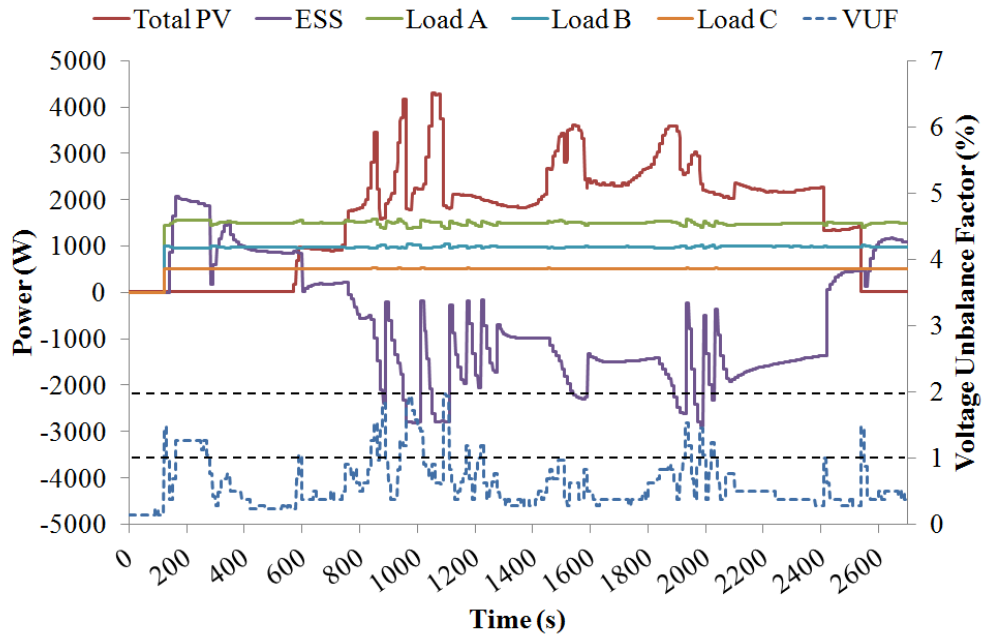


Figure 7.12 Total PV power output, response of the fuzzy controlled energy storage system, three-phase load demand and voltage unbalance factor of the experimental network

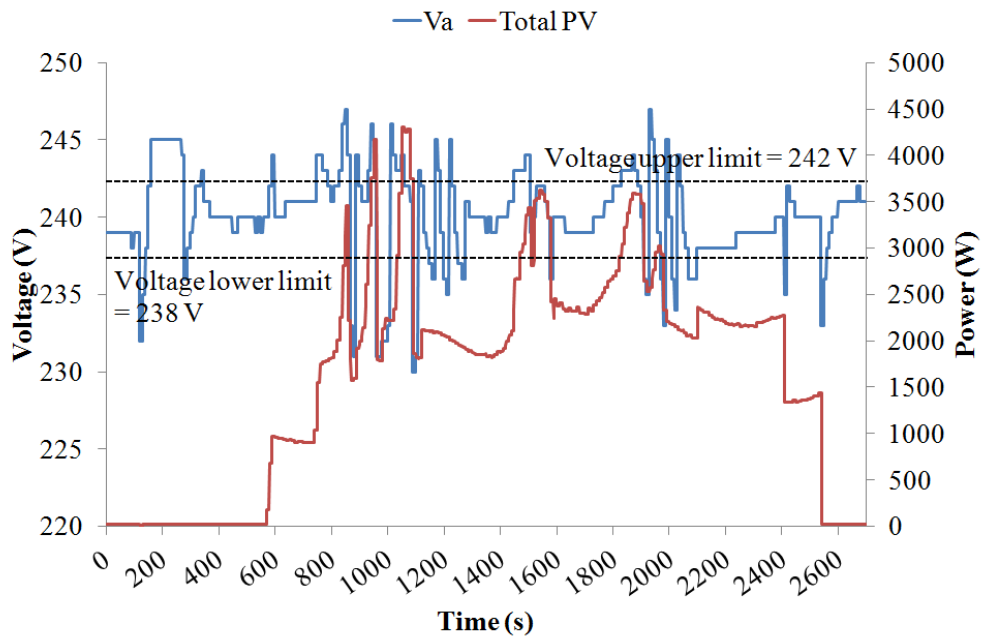


Figure 7.13 Voltage at phase A and total PV power output of the experimental network

7.4.5 Case Study V: Responses of the Fuzzy controlled energy storage system under Different Generation and Loading Condition

This case study is designed to evaluate the performance of fuzzy controlled energy storage system in response to different generation and loading conditions. In this case study, load A always varies while PV systems always connect and disconnect from the experimental network. Figure 7.14 illustrates the response of the fuzzy controlled energy storage system and voltage unbalance factor under different generation and load condition. In Section I, from 400 s to 1380 s, the load in phase A is always changing and the PV system is not connected. It is observed that the power output of the fuzzy controlled energy storage system is always changing to support the load in phase A and hence reduce the voltage unbalance factor. Figure 7.15 shows the network voltage, PV power output and the loading condition of the experimental case study. In Section I, the voltage in phase A is always kept within the tolerance range with the aid of the fuzzy controlled energy storage system.

Under Section II of Figure 7.14, from 1400 s to 1750 s, the PV system is connected to support the load on the experimental network. It is observed that the control algorithm has manipulated the real power of the fuzzy controlled energy storage system so that there is no excess power flowing in the network. From 1750 s to 2200 s, the PV system is purposely disconnected from the experimental network. It is observed that the rapid response of the fuzzy controlled energy storage system quickly supports the load in phase A to

reduce the network voltage unbalance factor. Similarly, the voltage level at phase A is always kept within the tolerance range. In Section III of Figure 7.14, from 2200 s onwards, the PV system is reconnected to the experimental network and at the same time, the load in phase A is changed, causing the voltage unbalance factor to strike beyond 2.0%. The fuzzy controlled energy storage system quickly adjusts its power output to reduce the voltage unbalance factor and keep the voltage in phase A within the statutory limit.

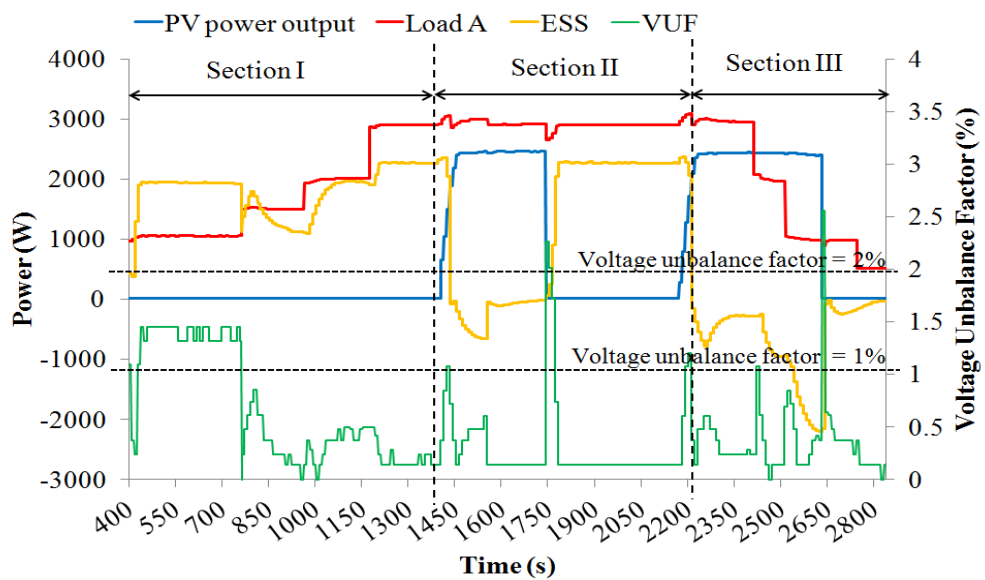


Figure 7.14 PV power output, load demand at phase A, response of the fuzzy controlled energy storage system and voltage unbalance factor of the experimental network

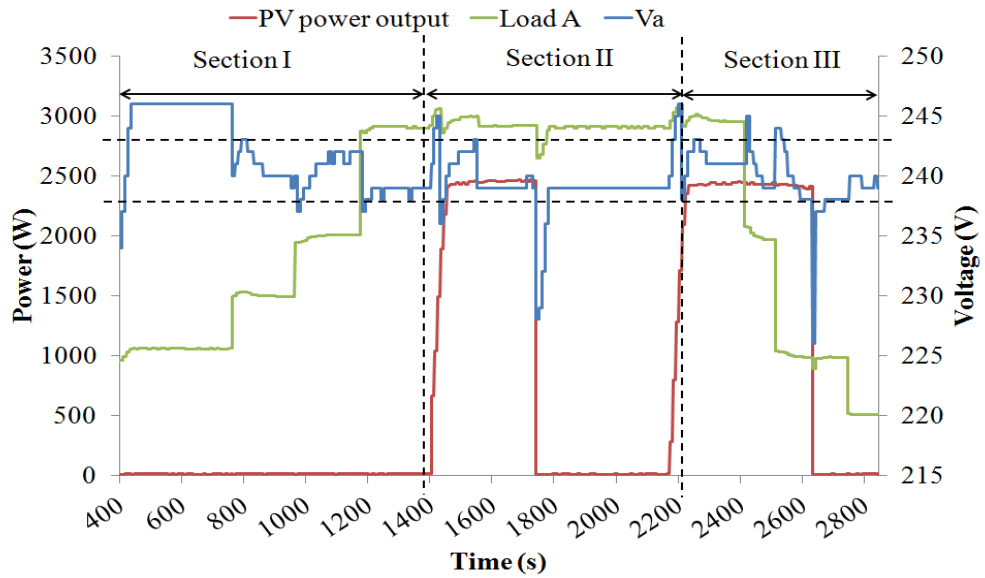


Figure 7.15 PV power output, load demand at phase A and voltage at phase A of the experimental network

7.5 Discussion

A fuzzy controlled energy storage system is developed using a different model of the bi-directional inverter, namely Studer Xtender XTM 4000-48 manufactured by Studer Innotec from Switzerland. This chapter has proven that the fuzzy control algorithm works well with a different setup of the fuzzy controlled energy storage system. In general, the performance of the control system will depend on the capability for active power control within the fuzzy controlled energy storage system. Table 7.3 shows the comparison of features between the Sunny Island 5048 and Studer Xtender XTM 4000-48.

Table 7.3 Comparison between Sunny Island 5048 and Studer Xtender XTM 4000-48

Description	Bi-directional Inverter	
	Sunny Island 5048	Studer Xtender XTM 4000-48
Communication Module	External accessories. RS485/USB converter	In-house accessories. Remote control, RCC-02 Communication module, Xcom 232i
Communication Protocol	Use OPC sever, SMA YAOPC	Use achieve file execution interface scom.exe
Display Panel	Integrated	Additional accessories. Remote control RCC-02
Features		
Control Flexibility	Able to manipulate both active and reactive power	Only able to manipulate active power
Maximum Power Output	Up to 300 kW with Multicluster box on three-phase	Up to 40 kW on three-phase
Battery Management System	Integrated	Additional accessories. Battery statue processor, BSP

In order to develop the control system, battery management and remote control system are mandatory accessories for Studer Xtender XTM 4000-48 whereas Sunny Island 5048 has a built-in display panel and battery management system. Sunny Island 5048 has the flexibility to manipulate both active and reactive power; however, Studer Xtender XTM 4000-48 does not offer such feature. Sunny Island 5048 maybe a suitable choice for developing a large scale energy storage system, this is because cascading Sunny Island 5048 can allow a maximum power output up to 300 kW in three-phase. Studer Xtender XTM 4000-48 only supports up to 40 kW in three-phase by cascading few units in parallel.

This chapter only emphasizes on the development of a single-phase fuzzy controlled energy storage system instead of three single-phase fuzzy

controlled energy storage systems as proposed in Chapter 6. Various scenarios were performed in order to assess the operation of the developed control system on the fuzzy controlled energy storage system built with a different bi-directional inverter. The fuzzy control system was found to be able to identify the voltage issues. At the same time, the proposed fuzzy controlled energy storage system is able to mitigate the voltage rise and voltage unbalance factor violation caused by the penetration of PV system.

CHAPTER 8

CONCLUSION & FUTURE WORK

8.1 Conclusions

The continuous growth of load demand has increased the fossil fuel consumption which in turn has increased the GHG emission in the country. The Malaysian government has put various efforts to reduce the GHG and promote the utilisation of renewable energy sources. The outlook for solar power has been positive due to the abundant amount of solar irradiance. The amount of grid connected PV systems is likely to increase in the near future. However, Malaysia is located at the equatorial region and has a low clear sky index. The solar irradiation under cloudy sky condition is highly scattered and fluctuating, hence making the PV power output to fluctuate substantially. At present, the electricity network is not designed to accommodate bi-directional flow. As the amount of grid connected PV systems increase, there is a tendency of reversed power flow in the electricity networks during low load and high power generation.

The objectives of this thesis are outlined in Chapter 1 while the conclusions are drawn as follows:-

I. To design and develop a laboratory scale low-voltage distribution network with renewable energy sources.

An analysis of the electrical characteristics on the Malaysian low-voltage distribution networks is performed. The experimental network is formed with a synchronous generator coupled with an induction machine. It is driven by a variable speed drive to regulate the experimental network frequency at 240 V, 50 Hz. Two commercial 3.6 kW_p PV systems are connected to the experimental network. Generation of electrical power using actual PV systems is believed to give more accurate results on the experimental low-voltage distribution network.

II. To evaluate technical impacts caused by the intermittent renewable energy and quantify the power quality issues on the low-voltage distribution network.

An investigation on the voltage issues caused by intermittent PV power output is carried out. The research work is conducted at a laboratory scale low-voltage distribution network to provide a comprehensive assessment on the impacts of PV system due to its intermittent power output. In addition, an analysis on the voltage issues of the grid connected PV system on the distribution networks is performed on the University premises. It is identified that the intermittent PV power output can cause significant technical issues particularly voltage rise, voltage unbalance, voltage flickers and fluctuations. In addition, voltage unbalance has been identified as the most severe issue that arises with large deployment of PV systems on the distribution networks. This is due to the lack of coordination for the PV system installation. Most PV

systems on the distribution networks are single-phase and the installations are customer driven with non-uniform distribution.

III. To design a suitable control approach for the energy storage system integrated to the low-voltage distribution network.

In order to overcome the voltage issues particularly voltage rise and voltage unbalance factor caused by the intermittent PV power output, a fuzzy controlled energy storage system is implemented. Three control strategies are considered over their suitability to satisfy the operational limits. The first control strategy implements a simple method to manipulate the real power flow of the single-phase fuzzy controlled energy storage system. The second control strategy implements a fuzzy logic control on a single-phase energy storage system. The decisions are made with two input parameters which are the battery state of charge (*SoC*) and the voltage excursion (ΔV) between the measured voltage and the reference voltage. The employment of the fuzzy logic on the control strategy is proposed due to its rapid response as the voltage can be fluctuating substantially. The third control strategy is implemented using the fuzzy logic and park transformation to coordinate a three single-phase fuzzy controlled energy storage system. These control strategies are implemented through LabVIEW as a programming platform. Fuzzy system toolkit is used to develop the fuzzy logic control system by defining the input and output membership functions. The fuzzy controlled energy storage system provides a grid interactive control strategy by manipulating the active power based on the specific control parameters. The network is categorised in two conditions, the normal operating condition and

the alert condition. During normal operating stage where the voltage unbalance factor is within the tolerance limit of 1.0%, the fuzzy logic control system is operated as standby mode. No correction will be done at this stage. During the alert stage where the voltage unbalance factor is greater than the tolerance limit of 1.0%, the fuzzy controlled energy storage system is deployed to manipulate the active power flow in order to mitigate the voltage rise and voltage unbalance factor.

IV) To evaluate the performance of the controlled energy storage system in mitigating voltage rise and voltage unbalance issues caused by renewable energy sources.

The control system is designed and developed to mitigate the voltage rise and voltage unbalance factor. Several case studies with different scenarios are performed to evaluate the performance of the fuzzy controlled energy storage system. In all the case studies, the control system that is developed is able to overcome the technical issues caused by intermittent PV power output.

This approach has the advantage to maximize the use of renewable energies without limiting the generation. This can be achieved by ensuring that the PV systems are operating at their maximum power output and thus avoid unnecessary power curtailment. The control strategy is able to identify the excess power flow in the network and feed it back to the fuzzy controlled energy storage system to absorb the power. Maintaining the generation and balance of the network can improve the power quality, increase stability, reliability and efficiency. By doing so, the utility company can avoid the

reinforcement cost of the distribution networks caused by large deployment of the grid connected PV system.

8.2 Limitation & Future Work

The research described in this thesis presents a fuzzy logic based approach to manipulate the active power flow of an energy storage system. At present, the experimental low-voltage distribution network is formed without the presence of a transformer. The additional transformer coupled to the network emulator would be a more accurate representation of a distribution network. The load system is purely resistive at the moment which is also a contrast to the real load on the low-voltage distribution network that import reactive power as a result of phase and harmonic distortion. In addition, the proposed fuzzy controlled energy storage system manipulates real power flow for improving voltage issues caused by intermittent PV power flow. Reactive power is not considered as voltage control because using reactive power is not effective as compared to real power. The main objective for this research is to develop an energy storage system and implement a suitable control algorithm to mitigate voltage issues caused by the intermittent PV power output. The future work can include real and reactive power as part of the control algorithm. This is because the reactive power also contributes to the power factor and phase angle correction.

Finally, the cost of the energy storage system is an important aspect to be considered for the widespread implementation of such system. Therefore, the

sizing of the energy storage system should be studied based on the load and the generation profile onsite to optimize the capacity of the fuzzy controlled energy storage system. Improvement to the communication rate can be enhanced by upgrading the hardware of the control system. As the PV power output is intermittent and fluctuating substantially, therefore, the performance of the hardware should be enhanced to avoid any lagging.

LIST OF REFERENCES

- Abu, H.A. et al., 2013. *TNB technical guidebook on grid-interconnection of photovoltaic power generation system to LV and MV networks*, Kuala Lumpur: Tenaga Nasional Berhad.
- Achim, W. et al., 2003. Power fluctuations in microgrids introduced by photovoltaics: Analysis and solutions. *2nd European PV-Hybrid and Mini-Grid Conference*. 25-26 September 2003 Kassel, Germany. Regensburg: Ostbayerisches Technologie-Transfer-Institut e.V. (OTTI), pp. 1–6.
- Ahmad, S., Kadir, M.Z.A.A. and Shafie, S., 2011. Current perspective of the renewable energy development in Malaysia. *Renewable and Sustainable Energy Reviews*, 15(2), pp.897–904.
- Al-Hamadi, H. M., 2012. Fuzzy logic voltage flicker estimation using Kalman filter. *Electrical Power and Energy Systems*, 36(1), pp. 60-67.
- Ari, G.K. and Baghzouz, Y., 2011. Impact of high PV penetration on voltage regulation in electrical distribution systems. *2011 International Conference on Clean Electrical Power (ICCEP)*. 14-16 June 2011 Ischia, Italy. Italy: IEEE Industrial Electronics Society, pp. 744–748.
- Atwa, Y.M. and El-Saadany, E.F., 2010. Optimal Allocation of ESS in Distribution Systems With a High Penetration of Wind Energy. *IEEE Transactions on Power Systems*, 25(4), pp.1815–1822.
- Augustin, M., Tom, M. and Luis, C., 2012. *Solar Cells: Materials, Manufacture and Operation*, 2nd Edition, United States: Academic Press.
- Barker, P.P. and De Mello, R.W., 2000. Determining the impact of distributed generation on power systems. I. Radial distribution systems. *Proceedings of the IEEE Power Engineering Society Summer Meeting 2000*. 16-20 July 2000 Seattle, Washington. United States: Power Engineering Society and Institute of Electrical and Electronics Engineers, Vol. 3, pp. 1645–1656.
- Barnes, M. et al., 2005. Microgrid laboratory facilities. *2005 International Conference on Future Power Systems*. 16-18 November 2005 Amsterdam, Netherlands. Netherlands: Institute of Electrical and Electronics Engineers and Benelux Section, pp. 1-6.
- Barnes, M. et al., 2007. Real-World MicroGrids-An Overview. *IEEE International Conference on System of Systems Engineering*, 2007. 16-18 April 2007 Texas, United States. United States: IEEE Aerospace and Electronics Systems Society, pp. 1–8.

- Basso, T.S., 2008. High-penetration, grid-connected photovoltaic technology codes and standards. *33rd IEEE Photovoltaic Specialists Conference*. 11-16 May 2008 San Diego, California. United States: IEEE Electron Devices Society, pp. 1–4.
- Bina, M.T. and Kashefi, A., 2011. Three-phase unbalance of distribution systems: Complementary analysis and experimental case study. *International Journal of Electrical Power and Energy Systems*, 33(4), pp.817–826.
- Caldon, R., Coppo, M. and Turri, R., 2014. Distributed voltage control strategy for LV networks with inverter-interfaced generators. *Electric Power Systems Research*, 107, pp.85–92.
- Carr, S. et al., 2014. Energy storage for active network management on electricity distribution networks with wind power. *IET Renewable Power Generation*, 8(3), pp.249–259.
- Central, S.E. of the W.E., 1964. *Electrical Transmission and Distribution Reference Book*, 4th edition, United States: Westinghouse Electric Corporation.
- Chen, C. et al., 2011. Optimal Allocation and Economic Analysis of Energy Storage System in Microgrids. *IEEE Transactions on Power Electronics*, 26(10), pp.2762–2773.
- Chen, C.-S. et al., 2013. Enhancement of PV Penetration With DSTATCOM in Taipower Distribution System. *IEEE Transactions on Power Systems*, 28(2), pp.1560–1567.
- Chen, P.-C. et al., 2012. Analysis of Voltage Profile Problems Due to the Penetration of Distributed Generation in Low-Voltage Secondary Distribution Networks. *IEEE Transactions on Power Delivery*, 27(4), pp.2020–2028.
- Chiang, E.P. et al., 2003. The potential of wave and offshore wind energy in around the coastline of Malaysia that face the South China Sea. *Proceedings of the International Symposium on Renewable Energy: Environmental Protection & Energy Solution for Sustainable Development*. 14-17 September 2003 Kuala Lumpur, Malaysia. Kuala Lumpur: Malaysia Institute of Energy and Malaysia Energy Centre, pp. 1–11.
- Chua, K.H. et al., 2012. Energy Storage System for Mitigating Voltage Unbalance on Low-Voltage Networks With Photovoltaic Systems. *IEEE Transactions on Power Delivery*, 27(4), pp.1783–1790.
- Cipcigan, L.M. and Taylor, P.C., 2007. Investigation of the reverse power flow requirements of high penetrations of small-scale embedded generation. *IET Renewable Power Generation*, 1(3), pp.160–166.

- Clover, I., 2013. *REC supplies Singapore's largest PV installation* [Online]. Available at: <http://www.pv-magazine.com/news/details/beitrag/rec-supplies-singapores-largest-pv-installation-100013563/#axzz3MnVSMnKh> [Accessed: 24 August 2014]
- Crabtree, J.D. et al., 2001. *Methods To Accommodate Embedded Generation Without Degrading Network Voltage Regulation*. United Kingdom: Harwell Laboratory, Energy Technology Support Unit.
- Daratha, N., Das, B. and Sharma, J., 2014. Coordination Between OLTC and SVC for Voltage Regulation in Unbalanced Distribution System Distributed Generation. *IEEE Transactions on Power Systems*, 29(1), pp.289–299.
- Darvishi, A., Alimardani, A. and Abdi, B., 2011. Optimized Fuzzy Control Algorithm in Integration of Energy Storage in Distribution Grids. *Energy Procedia*, 12, pp.951–957.
- Deokar, S.A. and Waghmare, L., 2010. Induction motor voltage flicker analysis and its mitigation measures using custom power devices: A case study. *International Journal of Engineering Science and Technology*, 2(12), pp.7626–7640.
- Dugan, R.C. et al., 2012. *Electrical Power System Quality*. India: McGraw-Hill Education Limited.
- Elcontrol STAR 3, 2006, *Modbus RS485 Serial Protocol* [Online]. Available at: http://www.elcontrol-energy.net/download/modbus_396_39din_dmm3_sirio_ed39din_star3_eng.pdf [Accessed: 11 April 2014].
- Elnady, A. and Salama, M.M.A., 2007. Mitigation of the voltage fluctuations using an efficient disturbance extraction technique. *Electric Power Systems Research*, 77(3-4), pp.266–275.
- Essam, N. and Khalid, A.B., 2010. Comparison between conventional and Fuzzy Logic PID Controllers for controlling DC Motors. *International Journal of Computer Science Issues*, 7(5), pp.128–134.
- Fernandes, R.A. and Philipp, H.D., 1977. Hydrogen cycle peak-shaving on the new york state grid using fuel cells. *IEEE Transactions on Power Apparatus and Systems*, 96(2), pp.467–477.
- Fouquet, D., 2013. Policy instruments for renewable energy – From a European perspective. *Renewable Energy*, 49, pp.15–18.
- Gaurav, A.K., 2012. Comparison between conventional PID and Fuzzy Logic Controller for liquid flow control: Performance evaluation of Fuzzy Logic and PID Controller by using MATLAB/Simulink. *International Journal of Innovative Technology and Exploring Engineering*, 1(1), pp.84–88.

- Greentech Malaysia, 2014. *Statistic: Major Sources of CO₂ Emissions* [Online]. Available at: http://www.greentechmalaysia.my/content.asp?zoneid=4&cmscategoryid=84#.VDS_eTFdpUQg [Accessed: 9 September 2014]
- Guo, L., Hung, J.Y. and Nelms, R.M., 2011. Comparative evaluation of sliding mode fuzzy controller and PID controller for a boost converter. *Electric Power Systems Research*, 81(1), pp.99–106.
- Hajizadeh, A., Golkar, M.A. and Feliachi, A., 2010. Voltage Control and Active Power Management of Hybrid Fuel-Cell/Energy-Storage Power Conversion System Under Unbalanced Voltage Sag Conditions. *IEEE Transactions on Energy Conversion*, 25(4), pp.1195 –1208.
- Hung, D.Q., Mithulananthan, N. and Bansal, R.C., 2014. Integration of PV and BES units in commercial distribution systems considering energy loss and voltage stability. *Applied Energy*, 113, pp.1162–1170.
- Ibrahim, M., Jaafar, M.Z. and Ghani, M.R.A., 1993. Demand-side management. *TENCON '93 Proceedings. Computer, Communication, Control and Power Engineering*. 19-21 October 1993 Beijing, China. China: Institute of Electrical and Electronics Engineers, Vol. 4, pp. 572–576.
- IEA International Energy Agency, 2011. Trends in photovoltaic applications – survey report of selected IEA countries between 1992 and 2011. IEA-PVPS T1-21:2012 [Online]. Available at: www.iaepvps.org/fileadmin/dam/public/report/.../tr_2009_neu.pdf [Accessed: 23 October 2013]
- IEC 61000-3-3 International Electrotechnical Commission, 1994. *Electromagnetic Compatibility (EMC) - Part 3: Limits - Section 3: Limitation of Voltage Fluctuations and Flicker in Low-Voltage Supply Systems for Equipment with Rated Current ≤16 A*. Switzerland: International Electrotechnical Commission [Online]. Available at: http://www.iec.ch/emc/emc_prod/prod_emission.htm [Accessed: 16 May 2013]
- IEC 61727 International Electrotechnical Commission, 2004. *Photovoltaic (PV) systems - Characteristics of the utility interface*. Switzerland: International Electrotechnical Commission [Online] Available at: <http://webstore.iec.ch/webstore/webstore.nsf/artnum/033529!opendocument> [Accessed: 16 May 2013]

- IEC 60038 International Electrotechnical Commission, 2009. *IEC Standard Voltages*. Switzerland: International Electrotechnical Commission [Online] Available at: http://webstore.iec.ch/Webstore/webstore.nsf/ArtNum_PK/43101!opendocument&preview=1 [Accessed: 16 May 2013]
- Ingram, S., Probert, S. and Jackson, K., 2003. *The impact of small scale embedded generation on the operating parameters of distribution networks* [Online], United Kingdom: Department of Trade and Industry (DTI) New and Renewable Energy Programme. Available at: http://webarchive.nationalarchives.gov.uk/20100919181607/http://www.ensg.gov.uk/assets/22_01_2004_phase1b_report_v10b_web_site_final.pdf [Accessed: 2 September 2013]
- Inigo, C., 2005. *Active control of distribution networks*. United Kingdom: The University of Manchester.
- Jenkins, N. et al., 2000. *Embedded Generation*, 1st edition, London: Cambridge University Press.
- Kashem, M.A. and Ledwich, G., 2007. Energy requirement for distributed energy resources with battery energy storage for voltage support in three-phase distribution lines. *Electric Power Systems Research*, 77(1), pp.10–23.
- Klessmann, C. et al., 2011. Status and perspectives of renewable energy policy and deployment in the European Union—What is needed to reach the 2020 targets? *Energy Policy*, 39(12), pp.7637–7657.
- Klinge Jacobsen, H. and Schröder, S.T., 2012. Curtailment of renewable generation: Economic optimality and incentives. *Energy Policy*, 49, pp.663–675.
- Koohi-Kamali, S. et al., 2013. Emergence of energy storage technologies as the solution for reliable operation of smart power systems: A review. *Renewable and Sustainable Energy Reviews*, 25, pp.135–165.
- Kumar, C. and Mishra, M.K., 2014. A Voltage-Controlled DSTATCOM for Power-Quality Improvement. *IEEE Transactions on Power Delivery*, 29(3), pp.1499–1507.
- Lewis, S.J., 2011. Analysis and management of the impacts of a high penetration of photovoltaic systems in an electricity distribution network. *IEEE PES Innovative Smart Grid Technologies Asia (ISGT), 2011*. 13-16 November 2011 Perth, Australia. Australia: Institute of Electrical and Electronics Engineers, pp. 1 –7.

- Lim, Y.S. et al., 2005. Additional applications of demand side management techniques in power systems integrated with distributed generation. *CIREN 2005 18th International Conference and Exhibition on Electricity Distribution*. 6-9 June 2005 Turin, Italy. Italy: IEE, pp. 1–5.
- Lim, Y.S., Lalchand, G. and Sow Lin, G.M., 2008. Economical, environmental and technical analysis of building integrated photovoltaic systems in Malaysia. *Energy Policy*, 36(6), pp.2130–2142.
- Liu, X. et al., 2012. Coordinated Control of Distributed Energy Storage System With Tap Changer Transformers for Voltage Rise Mitigation Under High Photovoltaic Penetration. *IEEE Transactions on Smart Grid*, 3(2), pp.897–906.
- Luo, T., Ault, G. and Galloway, S., 2010. Demand Side Management in a highly decentralized energy future. *2010 45th International Universities Power Engineering Conference (UPEC)*. 31 August – 3 September 2010 Cardiff, United Kingdom. United Kingdom: Institute of Electrical and Electronics Engineers, pp. 1–6.
- Lyons, P., 2010. *Experimental Investigation and Evaluation of Future Active Distribution Networks*. PhD Thesis. Durham University, United Kingdom. Available at: <http://etheses.dur.ac.uk/273/> [Accessed 30 October 2012].
- Marcos, J. et al., 2012. Power output fluctuations in large PV plants. *2012 International Conference on Renewable Energies and Power Quality*. 28-30 March 2012 Santiago de Compostela, Spain. Spain: European Association for the Development of Renewable Energy, Environment and Power Quality, pp. 1-6.
- McCoy, G.A. and Douglass, J.G., 1996. *Energy Efficient Electric Motor Selection Handbook*, United States: Department of Energy's Motor Challenge Program.
- McCrone, A. et al., 2014. *Global trends in renewable energy investment 2014, Germany: Frankfurt School UNEP Centre* [Online]. Available at: <http://fs-unep-centre.org/system/files/globaltrendsreport2014.pdf>. [15 March 2014]
- Mekhilef, S. and Chandrasegaran, D., 2011. Assessment of off-shore wind farms in Malaysia. *TENCON 2011 IEEE Region 10 Conference on Trends and Development in Converging Technology towards 2020*. 21-24 November 2011 Bali, Indonesia. Indonesia: IEEE Indonesia Section and Region 10 – Asia and Pacific, pp. 1351–1355.
- Mekhilef, S. et al., 2012. Solar energy in Malaysia: Current state and prospects. *Renewable and Sustainable Energy Reviews*, 16(1), pp.386–396.

- Menniti, D., Pinnarelli, A. and Sorrentino, N., 2010. An hybrid PV-wind supply system with D-Statcom interface for a water-lift station. *2010 International Symposium on Power Electronics Electrical Drives Automation and Motion (SPEEDAM)*. 14-16 Jun 2010 Pisa, Italy. Pisa: IEEE Industrial Electronics Society, pp. 1387–1392.
- Mitra, P. and Venayagamoorthy, G.K., 2010. An Adaptive Control Strategy for DSTATCOM Applications in an Electric Ship Power System. *IEEE Transactions on Power Electronics*, 25(1), pp.95–104.
- Mondol, J.D. and Koumpetsos, N., 2013. Overview of challenges, prospects, environmental impacts and policies for renewable energy and sustainable development in Greece. *Renewable and Sustainable Energy Reviews*, 23, pp.431–442.
- Muhammad-Sukki, F. et al., 2012. Solar photovoltaic in Malaysia: The way forward. *Renewable and Sustainable Energy Reviews*, 16(7), pp.5232–5244.
- Nambiar, A.J., Kiprakis, A.E. and Wallace, A.R., 2010. Quantification of voltage fluctuations caused by a wave farm connected to weak, rural electricity networks. *14th International Conference on Harmonics and Quality of Power (ICHQP)*. 26-29 September Bergamo, Italy. Bergamo: IEEE Power and Energy Society, pp. 1–8.
- National Aeronautics and Space Administration, Goddard Institute for Space Studies (NASA GISS), 2014. *Global Annual Mean Surface Air Temperature Change* [Online]. Available at: http://data.giss.nasa.gov/gistemp/graphs_v3/ [Accessed: 8 October 2014]
- National Renewable Energy Laboratory (NREL) and Lawrence Berkeley National Laboratory (LBNL), 2014. *Photovoltaic System Pricing Trends: Historical, Recent and Near Term Projections 2013 Edition* [Online]. Available at: <http://www.nrel.gov/docs/fy13osti/60207.pdf> [Accessed: 17 May 2014]
- Nguyen, C.P. and Flueck, A.J., 2012. Agent Based Restoration With Distributed Energy Storage Support in Smart Grids. *IEEE Transactions on Smart Grid*, 3(2), pp.1029 –1038.
- Noor Hidayat, M. and Li, F., 2013. Impact of distributed generation technologies on generation curtailment. *2013 IEEE Power and Energy Society General Meeting*. 21-25 July 2013 Vancouver, Canada. Vancouver: IEEE, pp. 1–5.
- Oudalov, A., Cherkaoui, R. and Beguin, A., 2007. Sizing and Optimal Operation of Battery Energy Storage System for Peak Shaving Application. *IEEE Power Tech 2007*. 1-5 July 2007 Lausanne, Switzerland. Lausanne: IEEE, pp. 621–625.

- Paatero, J.V. and Lund, P.D., 2007. Effects of large-scale photovoltaic power integration on electricity distribution networks. *Renewable Energy*, 32(2), pp.216–234.
- Prussing, 2006. *YASDI Documentation: Implementation of the SMA Data Protocol*. Kassel: SMA Solar Technology AG.
- Rahmat, M.F. and Ghazaly, M.M., 2006. Performance comparison between PID and Fuzzy Logic controller in position control system of DC servomotor. *Jurnal Teknologi*, 45(D), pp.1–17.
- Schlabach, J., Blume, D., and Stephanblome, T., 2000. *Voltage Quality in Electrical Power Systems*, London: The Institution of Engineering and Technology.
- Şekercioğlu, S. and Yılmaz, M., 2012. Renewable energy perspectives in the frame of Turkey's and the EU's energy policies. *Energy Conversion and Management*, 63, pp.233–238.
- Shafiu, A. et al., 2004. Active management and protection of distribution networks with distributed generation. *IEEE Power Engineering Society General Meeting, 2004*. 6-10 June Colorado, United States. Colorado: IEEE, pp. 1098–1103.
- Shahnia, F. et al., 2014. Voltage unbalance improvement in low voltage residential feeders with rooftop PVs using custom power devices. *International Journal of Electrical Power & Energy Systems*, 55, pp.362–377.
- Sustainable Energy Development Authority Malaysia (SEDA), 2014a. *Cumulative installed capacity of commissioned renewable energy sources under the feed-in tariff* [Online]. Available at: <http://seda.gov.my/?omaneg=000101000000010101010001000010000000000000000000&s=161> [Accessed: 3 August 2014]
- Sustainable Energy Development Authority Malaysia (SEDA), 2014b. *Cumulative installed capacity of renewable energy sources under progress* [Online]. Available at: <http://seda.gov.my/?omaneg=000101000000010101010001000010000000000000000000&s=538> [Accessed: 22 October 2014]
- Sustainable Energy Development Authority (SEDA) Malaysia, 2012. The renewable energy roadmap, National Energy Security 2012 Conference, Closing the energy supply – Demand Gap on 28th Feb 2012 [Online]. Available at: www.st.gov.my [Accessed: 10 October 2013]

- Svensson, J., Jones, P. and Halvarsson, P., 2006. Improved power system stability and reliability using innovative energy storage technologies. *8th IEE International Conference on AC and DC Power Transmission, ACDC 2006*. 28-31 March 2006 London, United Kingdom. London: IEEE, pp. 220–224.
- Tande, J.O.G., 2000. Exploitation of wind-energy resources in proximity to weak electric grids. *Applied Energy*, 65(1–4), pp.395–401.
- The Economic Planning Unit (EPU), Prime Minister's Department, 2010, *TENTH Malaysia Plan 2011-2015* [Online]. Available at: http://www.epu.gov.my/epu-theme/RMKE10/rmke10_english.html [Accessed: 15 April 2014]
- The World Bank Data- The International Bank for Reconstruction and Development (IBRD) and The International Development Association (IDA), 2014, *CO₂ Emissions (Metrics tons per capita) for Countries* [Online]. Available at: <http://data.worldbank.org/indicator/EN.ATM.CO2E.PC> [Accessed: 8 October 2014]
- Thomas, H.B., 2008. *Unbalanced Voltages and Electric Motors* [Online]. Available at: <http://www.pump-zone.com/topics/motors/unbalanced-voltages-and-electric-motors> [Accessed 5 June 2014].
- Toby, D.C. et al., 2010. *A Policymaker's Guide to Feed-in Tariff Policy Design*, U.S. Department of Energy, Office of Energy Efficiency and Renewable Energy: National Renewable Energy Laboratory [Online]. Available at: <http://www.nrel.gov/docs/fy10osti/44849.pdf> [Accessed April 23, 2013].
- Tonkoski, R. and Lopes, L.A.C., 2011. Impact of active power curtailment on overvoltage prevention and energy production of PV inverters connected to low voltage residential feeders. *Renewable Energy*, 36(12), pp.3566–3574.
- Tran-Quoc, T. et al., 2007. *Intelligent voltage control in distribution network with distributed generation CIGRE/CIREN* [Online]. Available at: http://www.cired.be/CIREN07/pdfs/CIREN2007_0727_paper.pdf [Accessed March 6, 2013].
- Ueda, Y. et al., 2008. Analysis Results of Output Power Loss Due to the Grid Voltage Rise in Grid-Connected Photovoltaic Power Generation Systems. *IEEE Transactions on Industrial Electronics*, 55(7), pp.2744–2751.
- Urbanetz, J., Braun, P. and R  ther, R., 2012. Power quality analysis of grid-connected solar photovoltaic generators in Brazil. *Energy Conversion and Management*, 64, pp.8–14.

- Von, J.A. and Banerjee, B., 2001. Assessment of Voltage Unbalance. *IEEE Transactions on Power Delivery*, 16(4), pp.782–790.
- Wade, N.S. et al., 2010. Evaluating the benefits of an electrical energy storage system in a future smart grid. *Energy Policy*, 38(11), pp.7180–7188.
- Wang, P. et al., 2014. Integrating Electrical Energy Storage Into Coordinated Voltage Control Schemes for Distribution Networks. *IEEE Transactions on Smart Grid*, 5(2), pp.1018–1032.
- Wang, Y., Lin, X. and Pedram, M., 2014. Adaptive Control for Energy Storage Systems in Households With Photovoltaic Modules. *IEEE Transactions on Smart Grid*, 5(2), pp.992–1001.
- Wong, J. et al., 2011. Optimal utilisation of small-scale embedded generators in a developing country – A case study in Malaysia. *Renewable Energy*, 36(9), pp.2562–2572.
- Wong, J., Lim, Y.S. and Morris, E., 2014. Novel Fuzzy Controlled Energy Storage for Low-Voltage Distribution Networks with Photovoltaic Systems under Highly Cloudy Conditions. *Journal of Energy Engineering*. Available at: <http://ascelibrary.org/doi/abs/10.1061/%28ASCE%29EY.1943-7897.0000178> [Accessed May 23, 2014].
- Wong, J., Lim, Y.S. and Morris, S., 2013. Self-intelligent active management system for electrical distribution networks with photovoltaic systems. *2nd IET Renewable Power Generation Conference (RPG 2013)*. 9-11 September 2013 Beijing, China. Beijing: IET, pp. 1–4.
- Xi, Z., Parkhideh, B. and Bhattacharya, S., 2008. Improving distribution system performance with integrated STATCOM and supercapacitor energy storage system. *IEEE Power Electronics Specialists Conference, 2008. PESC 2008*. 15-19 June 2008 Rhodes, Greece. Rhodes: IEEE PES, pp. 1390–1395.
- Yan, R. and Saha, T.K., 2012. Investigation of Voltage Stability for Residential Customers Due to High Photovoltaic Penetrations. *IEEE Transactions on Power Systems*, 27(2), pp.651–662.
- Yang, Y. et al., 2014. Sizing Strategy of Distributed Battery Storage System With High Penetration of Photovoltaic for Voltage Regulation and Peak Load Shaving. *IEEE Transactions on Smart Grid*, 5(2), pp.982–991.
- Yun Tiam, T., 2004. *Impact on the power system with a large penetration of photovoltaic generation*. PhD Thesis. University of Manchester Institute of Science and Technology, United Kingdom.
- Zheng, Y. et al., 2014. Optimal Allocation of Energy Storage System for Risk Mitigation of DISCOs With High Renewable Penetrations. *IEEE Transactions on Power Systems*, 29(1), pp.212–220.

Zhou, Q. and Bialek, J.W., 2007. Generation curtailment to manage voltage constraints in distribution networks. *IET Generation, Transmission and Distribution*, 1(3), pp.492–498.

APPENDIX A: Program Written In the Data Taker DT82

'Start with job "UTAR"

begin "UTAR"

'Trigger when 100cv change to zero

RA100-cv

1MODBUS(AD10,R4:1)=1142

'Write to Modbus slave (AD9 is big inverter, 10 is small inverter)

1MODBUS(AD10,R4:1)=1142

1MODBUS(AD10,R4:1)=1143

1MODBUS(AD10,R4:1)=1151

RC1S'40002 contains set frequency

1MODBUS(AD10,R4:2)=101CV *'Inverter frequency*

RD10S 'Read power meter values

1MODBUS(AD2,R3:29,=1..10CV)*'Read grid emulator*

delay=100

1MODBUS(AD2,R3:39,=11..20CV)

delay=100

1MODBUS(AD2,R3:49,=21..26CV)

delay=100

1MODBUS(AD2,R3:67,=27..34CV)

delay=100

1MODBUS(AD3,R3:29,=201..210CV)*'Read PVI*

delay=100

1MODBUS(AD3,R3:39,=211..220CV)

delay=100

1MODBUS(AD3,R3:49,=221..226CV)

delay=100

1MODBUS(AD3,R3:67,=227..234CV)

delay=100

1MODBUS(AD4,R3:29,=301..310CV)*'Read PV2*

delay=100

1MODBUS(AD4,R3:39,=311..320CV)

delay=100

1MODBUS(AD4,R3:49,=321..326CV)

delay=100

1MODBUS(AD4,R3:67,=327..334CV)
delay=100

1MODBUS(AD5,R3:29,=401..410CV)'*Read energy storage system*
delay=100

1MODBUS(AD5,R3:39,=411..420CV)
delay=100

1MODBUS(AD5,R3:49,=421..426CV)
delay=100

1MODBUS(AD5,R3:67,=427..434CV)
delay=100

1MODBUS(AD6,R3:29,=501..510CV)'*Read load bank*
delay=100

1MODBUS(AD6,R3:39,=511..520CV)
delay=100

1MODBUS(AD6,R3:49,=521..526CV)
delay=100

1MODBUS(AD6,R3:67,=527..534CV)
delay=100

END

APPENDIX B: List of Parameters Stored In the Registers of the DT82

No	Description	Register	Address for Readings in Power Meter				
			AD 2 (Grid Emulator)	AD 3 (PV 1)	AD 4 (PV 2)	AD 5 (WE)	AD 6 (Load Bank)
1	Voltage L1(<i>mantissa in BCD</i>)	29	0	200	300	400	500
2	Voltage L1(<i>binary exponent</i>)	30	1	201	301	401	501
3	Voltage L2	31	2	202	302	402	502
4	Voltage L2	32	3	203	303	403	503
5	Voltage L3	33	4	204	304	404	504
6	Voltage L3	34	5	205	305	405	505
7	Current L1	35	6	206	306	406	506
8	Current L1	36	7	207	307	407	507
9	Current L2	37	8	208	308	408	508
10	Current L2	38	9	209	309	409	509
11	Current L3	39	10	210	310	410	510
12	Current L3	40	11	211	311	411	511
13	Active power L1	41	12	212	312	412	512
14	Active power L1	42	13	213	313	413	513
15	Active power L2	43	14	214	314	414	514
16	Active power L2	44	15	215	315	415	515
17	Active power L3	45	16	216	316	416	516
18	Active power L3	46	17	217	317	417	517
19	Frequency	47	18	218	318	418	518
20	Frequency	48	19	219	319	419	519
21	Reactive power L1	49	20	220	320	420	520
22	Reactive power L1	50	21	221	321	421	521
23	Reactive power L2	51	22	222	322	422	522
24	Reactive power L2	52	23	223	323	423	523
25	Reactive power L3	53	24	224	324	424	524
26	Reactive power L3	54	25	225	325	425	525
27	Power factor L1	55	26	226	326	426	526
28	Power factor L1	56	27	227	327	427	527
29	Power factor L2	57	28	228	328	428	528
30	Power factor L2	58	29	229	329	429	529
31	Power factor L3	59	30	230	330	430	530
32	Power factor L3	60	31	231	331	431	531
33	Neutral current	61	32	232	332	432	532
34	Neutral current	62	33	233	333	433	533

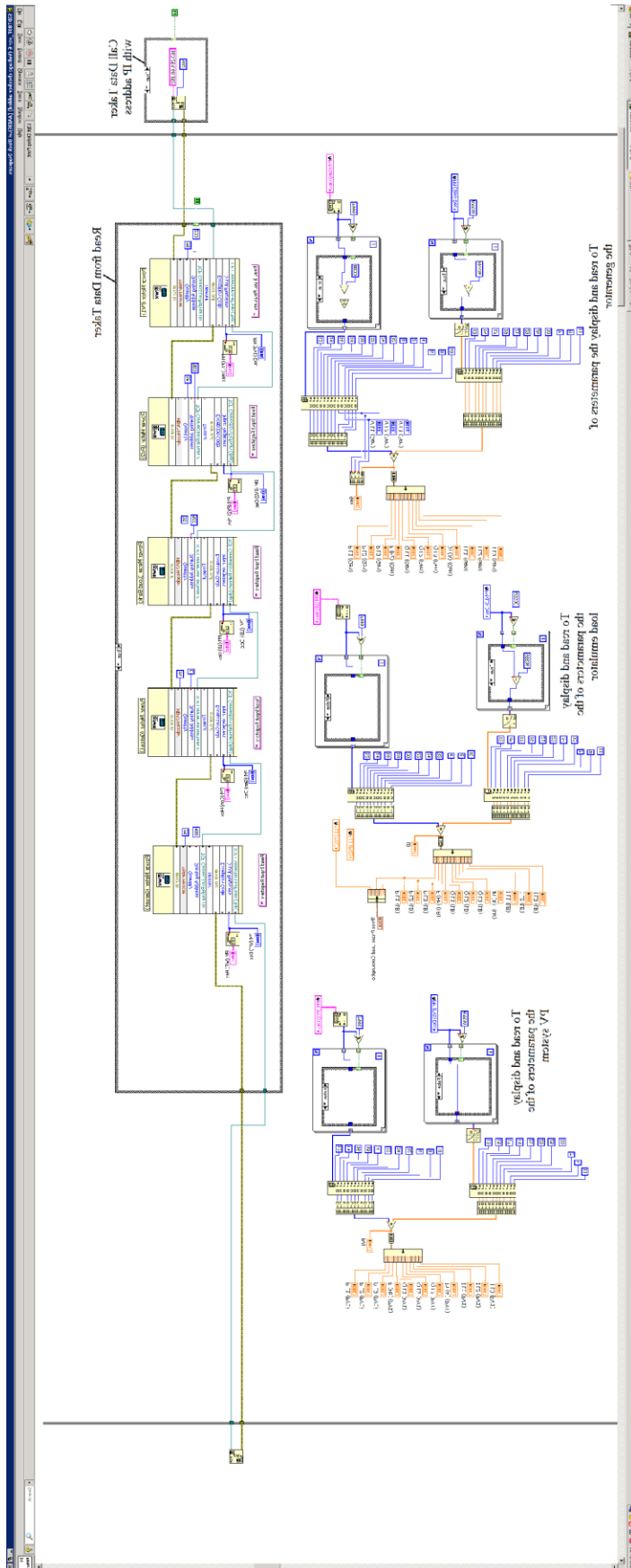
APPENDIX C: Initialisation Program For Yasdi.ini

```
[DriverModules]
Drive0=yasdi_drv_serial.dll
```

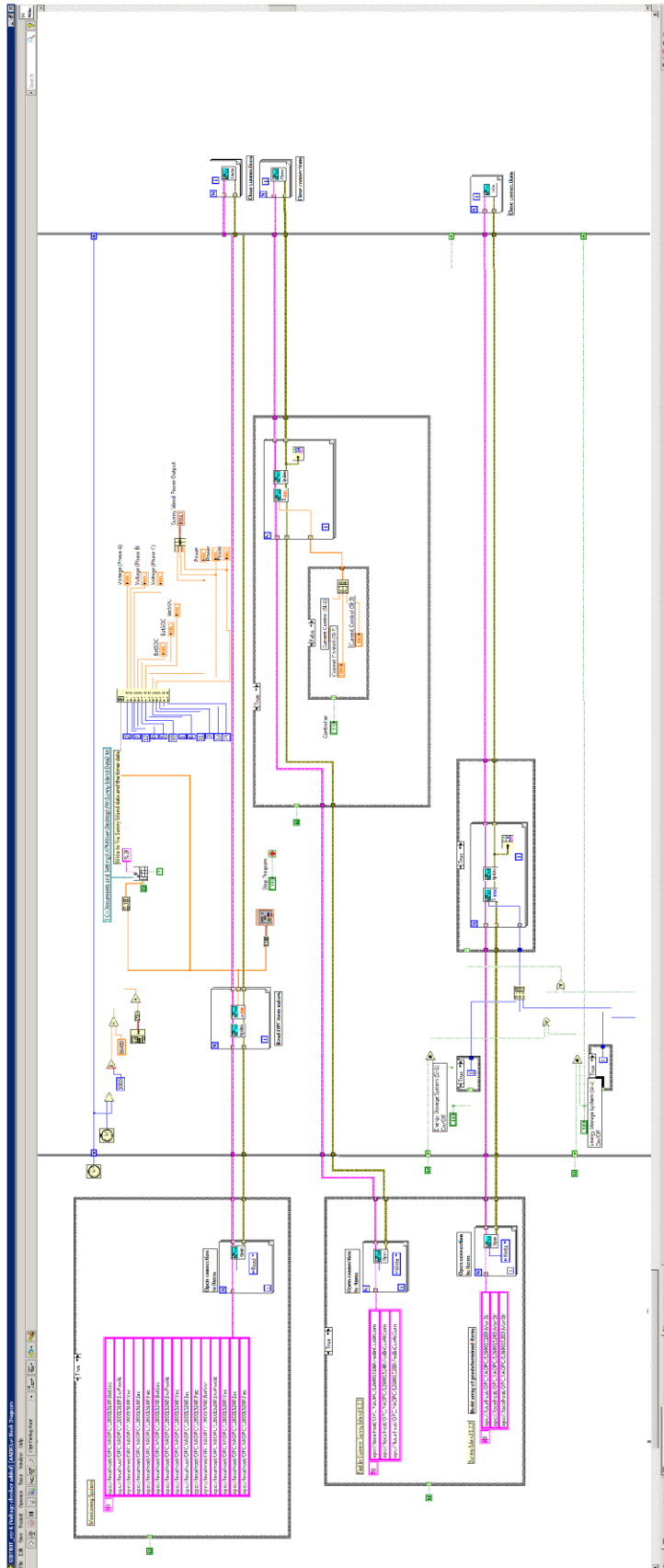
```
[COM3]
Device=COM3
Media=RS232
Baudrate=19200
Protocol=SMANet
```

```
[Master]
ReadTestChannels=0
ReadParamChanTimeout=4
ReadParamChanRetry=3
WriteParamChanTimeout=4
WriteParamChanRetry=3
ReadSpotChanTimeout=4
ReadSpotChanRetry=3
AutoReadOnlineChannels=1
```

APPENDIX D: Block diagram for Data Acquisition System



APPENDIX E: Block diagram for Read/Write from/to Energy Storage System



APPENDIX F: Block diagram of the Fuzzy Control Algorithm

